UNIVERSITY OF KWAZULU-NATAL

Adsorption of pharmaceuticals by nano-molecularly imprinted polymers (nano-MIPs) from wastewater: kinetics, isotherms, and thermodynamics studies

2024

Nonhlazeko Loveday Nxumalo

Adsorption of pharmaceuticals by nano-molecularly imprinted polymers (nano-MIPs) from wastewater: kinetics, isotherms, and thermodynamics studies.

Nonhlazeko Nxumalo

2024

A thesis submitted to the School of Chemistry and Physics, College of Agriculture, Engineering and Science, University of KwaZulu-Natal, Pietermaritzburg, for the degree of Doctor of Philosophy.

This thesis has been prepared according to **Format [2]** as outlined in the Information for the guidance of examiners of Higher degrees, which states:

Format 2: As a set of papers which are published, in press, submitted, or intended for submission.

As the candidate's supervisor, I have approved this thesis for submission.

[redacted]
…… …..

Supervisor: Date: 04/04/2024

Dr Precious Mahlambi

Co-Supervisors:

[redacted]

Dr Mphilisi Mahlambi Date: 04/04/2024

[redacted]

Dr Sihle Mngadi Date: 04/04/2024

[redacted]

Dr Tlou Chokwe Date: 04/04/2024

ABSTRACT

It has been reported that pharmaceuticals are not entirely removed or broken down during the wastewater treatment process, allowing them to escape into effluent water. This stems from the pharmaceuticals widespread use and the inefficient wastewater treatment methods. Therefore, the objective of this study was to develop more effective methods for removing pharmaceuticals from wastewater systems. Adsorption-based pharmaceutical removal is one of the most promising approaches because it is easily incorporated into current water treatment systems. The first part of this work reports on literature studies for recent advancements in the adsorption process involving the incorporation of an artificial molecularly imprinted polymer (MIP), that is an effective molecular receptor that can selectively recognize and remove pollutants. In magnetic solid-phase extraction, dispersive solid-phase microextraction, and solid-phase extraction, MIPs can be used as a selective adsorbent for analyte cleanup and preconcentration. Moreover, MIPs can be produced by combining nanoparticles to develop composite nanomaterials (nanoMIPs). In comparison to conventional bulk adsorbents, the enhanced selective adsorption capacity and kinetics are attributed to the large surface area per unit volume and specific functionality of nanomaterials. Nonetheless, some significant barriers to the application of nanomaterials are their dispersive qualities, difficulty in cycling, and secondary pollution from the loss of adsorbent during treatment. Another way to use nanoparticles for detectability enhancement is to modify the molecularly imprinted polymers chemical or physical characteristics. The nanoparticles' embedding in the MIP enhances the material's surface area or gives the adsorbent new features. This study describes a method for creating reusable, economical, and effective polymer-based silver nanoparticles-adsorbents. Notably, silver nanoparticles have a wide range of applications due to their unique properties which include their large surface area, shape and size. Plant-mediated synthesis plays a significant role in their synthesis. Remarkably, the synthesis of silver nanoparticles from plant extracts is inexpensive, easily scalable, and harmless for the environment. Plant extracts can be used to produce nanoparticles with controlled sizes and shapes. The molecular imprinting technique was used to create species-specific functionalities like carboxylic acid (-COOH) on a polymer surface. MIPs offer several advantages, including large surface area, targeted functionalities for high reactivity, and the ability to minimise nanoparticles from leaking into the surrounding environment when MIP-based adsorbents are being handled. To further comprehend the behaviour of adsorbents and the adsorption process, kinetics, thermodynamics, and isotherm models were explored.

The second part of the work involved synthesizing the MIPs for efficient and selective removal of pharmaceuticals from specific groups. All target compounds were employed as multiple templates in a bulk polymerization process carried out at 70 °C to synthesize MIPs. Additional reagents utilized in the synthesis included toluene as a porogenic solvent, ethylene glycol dimethacrylate as cross-linker, 1,1'-azobis-(cyclohexane carbonitrile) as an initiator and 2-vinyl pyridine as functional monomer, respectively. The synthesis of a non-imprinted polymer (NIP) was conducted without templates, using reaction conditions similar to those of MIP. Furthermore, following the synthesis, the polymers were characterized using X-ray diffraction, thermogravimetric analysis, differential scanning calorimetry, Fourier transform infrared spectroscopy, and scanning electron microscopy. Liquid chromatography-mass spectrometry (LC-MS) was successfully used to develop an analytical method for detection and quantification of the target pharmaceuticals. The method yielded quantification limits of 0.42 to 0.75 mg L^{-1} and detection limits of 0.14 to 0.25 mg L^{-1} for the target pharmaceuticals. The synthesized polymer attained maximum matrix-matched adsorption capacities of 3.89, 4.97 and 3.40 mg g^{-1} for sulfamethoxazole, nevirapine and ibuprofen, respectively within 10 minutes. Competitive adsorption of the target pharmaceuticals demonstrated a link between adsorption and the pharmaceuticals pKa, log Kow, and molecular size. Studies on batch adsorption and kinetics revealed that the binding of pharmaceuticals to the MIP particles suited the pseudo-second order kinetics, leading to various interactions through chemisorption. The data also fitted well in Langmuir isotherm which meant that the target pharmaceuticals adsorption occurred on the homogeneous binding sites of the MIP. Furthermore, the thermodynamic data demonstrated the adsorption process's endothermic and spontaneous nature. Notably, the synthesized MIP was highly selective and its application in environmental studies led to the development of a less expensive analytical method. Moreover, the MIP particles that had been generated were recovered to be reusable up to five cycles with removal efficiency >90%.

The third part involved incorporating silver nanoparticles (AgNPs) into MIPs using ibuprofen, nevirapine, and sulfamethoxazole as templates. In this part, starch (St) and macadamia nutshells (MCD) were employed in the synthesis of AgNPs as reducing and stabilizing agents. Following that, each of these AgNPs was incorporated with MIP, and the most effective combination was identified through comparison. The synthesized adsorbents were further optimized for the adsorptive removal of selected target pharmaceuticals. The % removal efficiencies were greater than 70%, indicating that the adsorbents are suitable for use in water

treatment processes. The material's adsorption mechanisms and performance were examined through the application of various kinetics and isotherm models. Both the St and MCD-AgNPs experimental data fit to Freundlich and Langmuir adsorption isotherms. However, based on the somewhat higher correlation coefficients, the Langmuir isotherm model provided a better fit. The St/MCD-nanoMIPs best suited the Freundlich model, indicating that the adsorption occurred on the multilayer heterogeneous surface. Further, both the St/MCD nanoMIP adsorbents underwent spontaneous, endothermic adsorption, as demonstrated by the thermodynamic data, whereas the behaviour of the kinetics was effectively anticipated by pseudo-second order model, which suggested adsorption through chemisorption. Accordingly, large internal surface area, greater loading capacity, thermal stability, and reusability were among the advantageous properties of the nanoMIPs adsorbent materials. Moreover, both adsorbents showed improved qualities and were highly selective and effective in removing the selected pharmaceuticals in wastewater. As a result, during the course of five adsorption/desorption cycles, the St/MCD nanoMIPs show a removal efficiency of more than 90%. As a result, they demonstrated proficiency in efficient application.

The fourth part involved the incorporation of MIP with Platanus acerifolia and Moringa oleifera silver nanoparticles. Using plants to synthesize AgNPs is a more cost-effective and low-maintenance method; in contrast, using other organisms requires a particular medium and a specific amount of time. Therefore, the leaves of both the platanus acerifolia (PL) and moringa oleifera (MO) served as stabilizing and reducing agents during the synthesis of AgNPs. Each optimized parameter that could influence the adsorption potential, such as temperature, adsorbate concentration, pH, adsorbent dose, and contact time, was examined in relation to the removal effectiveness of the MO/PL nanoMIP adsorbents. These evaluated parameters were optimum at pH 7, concentration of 0.2 mg/L and contact time of 10 minutes for both MO and PL-nanoMIPs, mass dosage of 30 mg and 20 mg, and temperature of 40 and 30 °C for MO and PL-nanoMIP, respectively. Further, the maximum removal efficiencies obtained at these optimum conditions were >97% for both MO-nanoMIP and PL-nanoMIP. The adsorption experimental data for both MO/PL-AgNPs and MO/PL-nanoMIPs nano-adsorbents fitted with the linear Langmuir model which suggests that the binding took place on the homogenous monolayer surface. Additionally, compared to MO/PL-AgNPs, the MO/PL-nanoMIPs adsorption capacities for the target pharmaceuticals were higher, suggesting that the nanoMIPs larger surface areas contribute to their enhanced adsorption capacity. The linear pseudo-second order kinetic model best fitted on MO/PL-nanoMIPs which implied adsorption through

chemisorption, whereas the thermodynamic data demonstrated that the adsorption process was endothermic and spontaneous. Moreover, the values of ΔH° for the MO/AgNPs were less than 40 kJ/mol and more than 40 kJ/mol for the MO/PL-nanoMIPs. This therefore confirmed that the MO/AgNPs was dominated by physical adsorption whereas the MP/PL-nanoMIPs was dominated by chemical adsorption. The MO/PL-nanoMIPs confirmed the high efficiency for the removal of target pharmaceuticals in wastewater. Upon recycling the adsorbents for five cycles, it was noted that the MO-nanoMIP adsorbent was effective continued to remove 86.7-88.8% and 97-98% for PL-nanoMIP even in the fifth cycle.

Indeed, the removal of sulfamethoxazole, nevirapine, and ibuprofen by nanoMIP adsorbents has demonstrated the importance of the surface area, structural stability, pore size and the electrostatic interactions brought about by the charges on the nanoMIPs surface. Consequently, among the investigated nanoMIP adsorbents, PL-nanoMIP demonstrated strong adsorption capacities for the targeted pharmaceuticals due to it large surface area and narrow size distribution as compared to the other nanoMIP adsorbents. The usability of plant leaves as a reducing and capping agent for nanoparticles as well as the recycling of nanoMIPs has the potential to transform waste that is no longer useful into valuable pollutants adsorbents. This would solve the problem of waste disposal and have beneficial impacts on the environment pollution and the economy. Notably, the nanoMIPs synthesized in this study are highly selective, reusable adsorbents that are cost effective and environmentally friendly. In contrast, as a substitute for more costly synthetic materials, these nanoMIPs are a promising material for the removal of different classes of pharmaceuticals in wastewater treatment plants and they can possibly be applied on a large scale.

ABBREVIATIONS

SMX	Sulfamethoxazole
Nvp	Nevirapine
Ibu	Ibuprofen
MIP	Molecularly imprinted polymer
NIP	Non imprinted polymer
AgNps	Silver nanoparticles
dSPE	Dispersive-solid phase extraction
SPE	Solid phase extraction
MSPE	Magnetic solid phase extraction
nanoMIP	nanoparticles molecularly imprinted polymer
St-nanoMIPs	Starch-nanoparticles molecularly imprinted polymer
MCD-nanoMIPs	Macadamia- nanoparticles molecularly imprinted polymer
PA-nanoMIPs	Platanus acerifolia- nanoparticles molecularly imprinted polymer
MO-nanoMIPs	Moringa oleifera- nanoparticles molecularly imprinted polymer
LC-MS	Liquid chromatography-mass spectrometry
UV-Vis	Ultraviolet-visible spectroscopy
TGA	Thermogravimetric analysis
DSC	Differential scanning calorimetry
TEM	Transmittance electron microscopy
XRD	X-Ray diffraction
FTIR	Fourier-transform infrared spectroscopy
WWTPs	Wastewater treatment plants
WHO	World health organizations
NSAIDs	Non-steroidal anti-inflammatory drugs
ARVs	Antiretrovirals
Qmax	Maximum adsorption capacity
Qe	amount of adsorbed adsorbate per unit weight of adsorbent
K_F	Freundlich constant
K_L	Langmuir equilibrium constant
$\Delta H°$	Enthalpy
$\Delta G°$	Gibbs energy
$\Delta S°$	Entropy

DECLARATIONS

DECLARATION 1 – PLAGIARISM

I, **Nonhlazeko Nxumalo** declare that:

1. The research reported in this thesis is my original research, and not been submitted for any degree or examination at any other university.
2. This thesis does not contain other persons' data, pictures, graphs or other information, unless specifically acknowledged as being sourced from other persons.
3. This thesis does not contain other persons' writing, unless specifically acknowledged as being sourced from other researchers. Where other written sources have been quoted, then:
   a. their words have been re-written, but the general information attributed to them have been referenced, and
   b. where their exact words have been used, then their writing has been placed in italics and inside quotation marks and referenced.
4. This thesis does not contain text, graphics or tables copied and pasted from the Internet, unless specifically acknowledged, and the source being detailed in the thesis and in the References section/s.

Signed [redacted]

Nonhlazeko Nxumalo

Signed [redacted]……

Dr PN Mahlambi (Supervisor)

Signed [redacted]……

Dr M Mahlambi (Co-Supervisor)

Signed [redacted]……

Dr S Mngadi (Co-supervisor)

Signed …….

Dr T Chokwe (Co-supervisor)

PUBLICATIONS AND CONFERENCES

Details of publications:

1. **Nxumalo, N.L**. and Mahlambi, P.N., 2023. Molecularly Imprinted Polymer-Based Adsorbents for the Selective Removal of Pharmaceuticals from Wastewater: Adsorption Kinetics, Isotherms, and Thermodynamics Studies. Industrial & Engineering Chemistry Research, https://doi.org/10.1021/acs.iecr.3c02096.
2. Removal of multiple classes of pharmaceuticals from wastewater using multi-template molecularly imprinted polymer (MIP) as an adsorbent: kinetics, isotherms and thermodynamic studies. (Under review by Journal of Applied Polymer Science)
3. Efficacy assessment of molecularly imprinted polymer incorporated with starch and macadamia capped silver nanoparticles for the removal of multi-class pharmaceuticals in wastewater. (Under review by Chemistry Select Journal)
4. Efficacy assessment of molecularly imprinted polymer incorporated with platanus acerifolia and moringa oleifera capped silver nanoparticles for the removal of multi-class pharmaceuticals in wastewater. (Formatted to be submitted to Polymer Science Journal)

Conferences contribution

- Pharmaceuticals adsorption by silver nanoparticles, molecularly imprinted polymers (MIP) and nanoparticles molecularly imprinted polymers (nano-MIPs) from wastewater. Oral presentation at the School of Chemistry and Physics postgraduate seminar session, 11 October 2023.
- Comparison of starch and macadamia capped nanoparticles for the removal of multi-class pharmaceuticals in wastewater. Flash presentation at UKZN's College of

Agriculture, Engineering and Science Postgraduate Research Innovation Symposium 02-03 November 2023.

- Comparison of platanus acerifolia and moringa oleifera capped nanoparticles for the removal of multi-class pharmaceuticals in wastewater. Poster presentation at the South African Chemical Institute's Postgraduate Symposium, 3rd place in the School of Chemistry and Physics, 23 November 2023.

DEDICATION

This work is dedicated to my mother, Mrs Nomusa Estansia Nxumalo. Your prayers provided light and direction for me as I was being carried through tumultuous times, my education journey is because of you. Lapho ungafikanga khona, mina ngizofika. My late father, Mr Mzikayise Joseph Nxumalo and my late brother, Sibonelo Nxumalo, this is for you. My two girls Naledi and Yandiswa, I dedicate this to you as a symbol of hard work and perseverance. May you be encouraged and always believe in yourselves. I love you girls so much.

ACKNOWLEDGEMENTS

- Almighty God, you have carried me throughout this journey that seemed impossible, and you made it possible. I am grateful for trusting me with the purpose You have embedded in me.
- To my mother, words can never express how much I love and appreciate you. You are my rock in life. I am grateful for your support, wisdom, and many sacrifices. I am also grateful for your unending love and patience. And lastly, I am grateful that you gave me the best gift of all: my education. All that I am, I owe to you.
- To my siblings, Sthembiso, Sphephelo, Nombulelo, Nondumiso, and Nonzuzo, bo Zwide kaLanga, thank you for your support. To my nieces and nephews, may this be a continuous source of inspiration to pursue your aspirations.
- My precious girls, Naledi and Yandiswa, you are my greatest blessings, I am particularly indebted for your constant support and understanding.
- To my supervisor, Dr Precious N. Mahlambi, without the supervision, guidance, patience, and care from you, none of this work would have been possible. I appreciate all of your time and feedback during this research. I am incredibly appreciative of the priceless knowledge you have shared with me.
- My co-supervisors, Dr Sihle Mngadi, Dr Tlou Chokwe and Dr Mphilisi Mahlambi, thank you for your contribution in this project and your assistance in proof-reading this research work.
- Dr Philisiwe Kunene and my colleagues in Analytical Chemistry group, I am eternally grateful for all your help, motivation and advice.
- Additionally, I am grateful for the chance to complete my PhD studies at the University of Kwa-Zulu Natal (UKZN, PMB), School of Chemistry. With particular gratitude to the National Research Foundation (NRF) for their financial assistance.

Table of Contents

Chapter 1

1.1 Introduction

1.1.1 Background and motivation

The increment of the worldwide populace and lack of sustainable water assets encourages the advancement of potential solutions for work on the waste's quality, potential for reuse and polluted water supplies (Bouwer, 2000, Metwally et al., 2021). Different types of water contaminants, including dyes, pharmaceuticals, endocrine disrupting compounds (EDCs), pesticides, and heavy metals, are produced by ongoing technological and industrial advancements that occur due to the growing population (Al Sharabati et al., 2021, Metwally et al., 2021). Thus, the remediation of water contamination, particularly pollution from freshwater, wastewater, environmental and human contamination, is one of the main environmental concerns globally (Morin-Crini et al., 2022, Okoro et al., 2022). Products used in daily life in high amounts, such as pharmaceuticals, are regarded as pollutants of rising concern (Khan et al., 2022, Ellis, 2006). Pharmaceuticals are synthetic or natural ingredients, used in the pharmaceutical, veterinary, and over-the-counter businesses (Al-Qaim et al., 2014). These are drugs that are used to identify, treat, or prevent illnesses as well as to restore, modify, or enhance organic processes. Moreover, pharmaceuticals are discharged into the aquatic environments via several pathways, such as sewage treatment plants leaks, discharges from facilities that manufacture pharmaceuticals, emissions from medical units, discharges of processed sewage effluent from sewage treatment facilities, the application of sewage sludge or animal manure to agricultural land, and disposal of unwanted pharmaceuticals (Waleng and Nomngongo, 2022, Martín et al., 2012, Čelić et al., 2019). Pharmaceuticals are mostly found in the environment due to inappropriate disposal of wastewater that has not been completely or sufficiently treated. (Vinayagam et al., 2022). Despite relatively low quantities, people can experience toxicological effects from hydrogenic sources as a result of pollution processes caused by heavy use of drugs (Ternes and Joss, 2007).

Depending on their physicochemical characteristics and method of action, pharmaceuticals are divided into several classes. Antidepressants, antiretroviral (ARV) medicines, non-steroidal anti-inflammatory drugs (NSAIDs), antibiotics, antiseptics, and other endocrine-disruptive substances are among the classifications (Hawash et al., 2023, Chaves et al., 2022). They have

been identified as a category of environmental pollutants, and they are becoming a greater threat as pollutants in surface or groundwater close to residential and commercial areas. (Kyzas et al., 2015). When they get into drinking water, they could be harmful to both aquatic life and humans. (Johnson et al., 2008, Cunningham et al., 2009, Sengar and Vijayanandan, 2022). As a result, pharmaceuticals have attracted substantial interest as a result of the potential health hazards connected to their exposure to human, aquatic, and terrestrial life when they enter the environment. (Ebele et al., 2017, Khan et al., 2021, Rathi et al., 2021).

Around 90% of medications taken by mouth are excreted by the body unchanged or only slightly digested and are therefore present in sewage discharge (Jelić et al., 2012, Nannou et al., 2020). Hence, consuming contaminated water poses risks such as getting sick, experiencing pharmaceutical side effects, and eventually developing drug resistance (Serwecińska, 2020, Daughton, 2004). As a result, it is essential to remove residues of pharmaceuticals in wastewater and drinking water (Massima Mouele et al., 2021, de Andrade et al., 2018, González Peña et al., 2021). Furthermore, the advancements in analytical methods have made it possible to detect trace amounts from a variety of environmental matrices, including drinking water, sediments, waste effluents, surface and subsurface water, and biota. (Zare et al., 2022, Almeida, 2021). However, it appears that conventional wastewater and water treatment unit operations cannot completely remove all pharmaceuticals, therefore, a range of modern process treatment technologies may be required. Since conventional plants that treat wastewater are unable to effectively remove a wide range of emerging pharmaceutical pollutants, additional and alternative methods may need to be looked into with the goal of improving the water quality (Sathya et al., 2022, Villar-Navarro et al., 2018). Hence, one of the main challenges in the wastewater treatment industry is using low-cost technology while maintaining criteria for health and safety in treated wastewater that has been recycled.

Accordingly, the adsorption process is a potential technique for wastewater treatment and water pollution prevention because of its lower maintenance requirements, increased efficacy, simpler design, and lack of unwanted byproducts. (Ghorbani et al., 2020, da Silva et al., 2019). The inefficiency of current techniques used in water treatment plants to remove the contaminant essentially drives the development of effective solutions to address pollution from effluent. In order to overcome the drawbacks of the traditional techniques (commonly, biochar and activated carbon) for treating wastewater, this study proposes the use of molecularly imprinted polymers (MIPs) as an efficient technique for the removal of pharmaceuticals from

wastewater by selective adsorption. The research indicates that the synthesis of MIPs can be tailored to fulfil specific target criteria, making them an attractive material for application as a highly selective adsorbent in environmental sciences. (Villarreal-Lucio et al., 2022). The primary purpose of this research was to develop sample preparation methods for sample clean-up, and removal of pharmaceutical residues for three classes of pharmaceuticals, specifically antibiotics, non-steroidal anti-inflammatory drugs (NSAIDs), and antiretroviral drugs in wastewater matrices. This was achieved using three approaches, firstly by applying MIP as an adsorbent, secondly, by silver nanoparticles, lastly, by incorporating of MIP with silver nanoparticles.

1.2 Problem statement

The treatment of polluted wastewater is a major environmental problem. The primary environmental problem is treating water pollution, especially that which originates from freshwater, wastewater, and human and environmental pollutants. (Singh et al., 2020). Freshwater resources are contaminated by pollutants found in wastewater effluent, which are hazardous to the environment and to humans (Edokpayi et al., 2017). These pollutants were generated by a variety of chemical industries, including those that produce textiles, dyes, metal plating, paper, fertilizer, batteries, metallurgical products, pesticides, fossil fuels, tanneries, mining, and various polymers. Studies conducted in South Africa in recent years have consistently found pharmaceuticals in the nation's water bodies, which has raised concerns about the improper discharge of these drugs in water systems (Waleng and Nomngongo, 2022). Pharmaceuticals, industrial chemicals, insecticides, and other substances are examples of micropollutants, which are primarily found in wastewater (Pérez-Lucas et al., 2022). Pharmaceuticals have recently been identified as "emerging contaminants" that are seriously polluting water streams and endangering both humans and aquatic life (Samal et al., 2022). Pharmaceuticals are a diverse group of biologically active hydrophilic chemical compounds, and their derivatives exhibit a great deal of variation in their structure, behaviour, and activity (Bolong et al., 2009). Additionally, pharmaceuticals have found access to the environment as a result of increasing pharmaceutical usage and insufficient removal of those drugs by conventional wastewater treatment plants (WWTPs). Their release into the environment has negative consequences on how humans and other living things metabolize, necessitating the use of sophisticated remediation techniques (Zare et al., 2022, Kosek et al., 2020). They have increased life expectancy, healed millions of fatal diseases, and enhanced quality of life, but

this achievement has also given rise to a new class of environmental toxins, raising worries across the globe. The prevalence of pharmaceuticals in aquatic settings indicates the ineffectiveness of traditional wastewater treatment techniques, necessitating the development of greener, sensitive, accurate and reliable alternative methodologies for the most effective removal of pharmaceuticals.

1.3 Rationale

Pharmaceuticals are one of the most prevalent contaminants discovered in water systems. Their presence in water bodies presents a serious risk to human health and aquatic organisms. Wastewater treatment plants (WWTPs) are among the major cause of pharmaceuticals in the environment. Typically, the majority of pharmaceuticals cannot be completely removed from water using the current water treatment techniques used in most WWTPs, resulting in the discharge of these pharmaceutical compounds into aquatic environments. The consequences of releasing low-quality wastewater back into the environment are severe because they affect the health of aquatic ecosystems and human health. Notably, some pharmaceuticals are discharged into the aquatic environments at concentrations higher than their predicted no effect concentrations (PNECs), thus posing ecological risk to some aquatic organisms. Accordingly, the prevalence of pharmaceuticals in aquatic ecosystems demonstrates the ineffectiveness of traditional wastewater treatment procedures, necessitating the urgent need for pharmaceuticals to be removed as effectively as possible via alternative techniques.

1.4 Research questions

- Can pharmaceuticals be efficiently removed from wastewater using nanoMIPs, and what are the removal efficiencies?
- Which parameters can be optimized to improve the removal efficiency of the targeted pharmaceuticals at lower concentrations?
- In contrast to MIP and AgNPs alone, will the incorporation of nanoparticles with molecularly imprinted polymers enhance the adsorption capacity of pharmaceuticals in wastewater?
- Can the selected pharmaceuticals be detected in the wastewater treatment plants under investigation and at what concentrations?
- Are the pharmaceutical concentrations higher in the influent streams than in the effluent streams of WWTPs?

- Which nanoMIP-adsorbent is best suited to remove the selected pharmaceuticals from wastewater samples between starch and macadamia nutshell and between platanus acerifolia and moringa oleifera?

1.5 Hypothesis

There is high pollution with pharmaceuticals in the aquatic environments due to their inadequate removal during wastewater treatment work processes. The incorporation of silver nanoparticles with molecularly imprinted polymers is effective and has a greater potential for the adsorption of selected pharmaceuticals in wastewater in contrast to silver nanoparticles and MIP alone. Moreover, to confirm that the procedures used in the wastewater treatment plants are efficient at removing these pharmaceuticals, analytes of interest should not be present in effluent samples or should be present at significantly lower concentrations than in influent samples.

1.6 Aim

This research aimed to assess the adsorption efficacy of molecularly imprinted polymers, silver nanoparticles and silver nanoparticles incorporated with molecularly imprinted polymers (nano-MIPs) for the removal of multiple classes of pharmaceuticals in wastewater by conducting kinetics, isotherms, and thermodynamics studies.

1.7 Objectives

- To synthesise and characterise MIPs.
- To synthesize and characterize Ag nanoparticles.
- To synthesis Ag nanoparticles incorporated in MIP cavities
- To characterize the synthesized nanoMIPs
- To design and conduct batch equilibrium adsorption tests using MIPs and nanoMIPs and to study the effects of varying parameters for the selected pharmaceuticals (initial pH, concentration, mass dosage, temperature and time).
- To assess adsorption kinetics, isotherms and thermodynamics to understand the nature and extent of adsorption in MIP and nanoMIPs for the selected pharmaceuticals.
- To assess the selectivity and renewability of MIPs and nanoMIPs.
- Apply MIP and nanoMIPs for selective removal of pharmaceuticals in wastewater.

1.8 Thesis organisation

The following section provides a brief synopsis of the dissertation's contents. **Chapter 1:** gives an overview of the dissertation's background, including the introduction, problem statement, rationale, research question, aim, and objectives. **Chapter 2:** presents a thorough literature review on the variety of treatment procedures for pharmaceuticals and their adsorptive removal methods from aqueous environments using various isotherms and kinetic models (paper 1). **Chapter 3:** describes the removal of multiple classes of pharmaceuticals from wastewater by employing molecularly imprinted polymer (MIP) with multiple templates as an adsorbent: kinetics, isotherms and thermodynamic studies (paper 2). **Chapter 4:** this chapter describes the efficacy assessment of molecularly imprinted polymer incorporated with starch and macadamia capped silver nanoparticles for the removal of multi-class pharmaceuticals in wastewater (paper 3). **Chapter 5:** this chapter describes the efficacy assessment of molecularly imprinted polymer incorporated with platanus acerifolia and moringa oleifera capped silver nanoparticles for the removal of multi-class pharmaceuticals in wastewater (paper 4). **Chapter 6:** includes an overview of the discussion from chapters 3, 4, and 5 as well as a general conclusion on the results obtained. Finally, this section included suggestions for further research based on the study's summarized findings.

1.9 References

ABU-HASHEM, A. A. & YOUSSEF, M. M. 2011. Synthesis of new visnagen and Khellin furochromone pyrimidine derivatives and their anti-inflammatory and analgesic activity. *Molecules,* 16**,** 1956-1972.

AL-QAIM, F. F., ABDULLAH, M. P., OTHMAN, M. R., LATIP, J. & AFIQ, W. 2014. A validation method development for simultaneous LC-ESI-TOF/MS analysis of some pharmaceuticals in Tangkas river-Malaysia. *Journal of the Brazilian Chemical Society,* 25**,** 271-281.

AL SHARABATI, M., ABOKWIEK, R., AL-OTHMAN, A., TAWALBEH, M., KARAMAN, C., OROOJI, Y. & KARIMI, F. 2021. Biodegradable polymers and their nano-composites for the removal of endocrine-disrupting chemicals (EDCs) from wastewater: A review. *Environmental Research,* 202**,** 111694.

ALMEIDA, C. M. 2021. Overview of Sample Preparation and Chromatographic Methods to Analysis Pharmaceutical Active Compounds in Waters Matrices. *Separations,* 8**,** 16.

BOLONG, N., ISMAIL, A., SALIM, M. R. & MATSUURA, T. 2009. A review of the effects of emerging contaminants in wastewater and options for their removal. *Desalination,* 239**,** 229-246.

BOUWER, H. 2000. Integrated water management: emerging issues and challenges. *Agricultural water management,* 45**,** 217-228.

ČELIĆ, M., GROS, M., FARRÉ, M., BARCELÓ, D. & PETROVIĆ, M. 2019. Pharmaceuticals as chemical markers of wastewater contamination in the vulnerable area of the Ebro Delta (Spain). *Science of the Total Environment,* 652**,** 952-963.

CHAVES, M., KÜLZER, J., LIMA, P., CALDAS, S. S. & PRIMEL, E. G. 2022. Updated knowledge, partitioning and ecological risk of pharmaceuticals and personal care products in global aquatic environments. *Environmental Science: Processes & Impacts*.

CUNNINGHAM, V. L., BINKS, S. P. & OLSON, M. J. 2009. Human health risk assessment from the presence of human pharmaceuticals in the aquatic environment. *Regulatory toxicology and pharmacology,* 53**,** 39-45.

DA SILVA, R. C. S., SANTOS, M. N., PIRES, B. C., DINALI, L. A. F., SUQUILA, F. A. C., TARLEY, C. R. T. & BORGES, K. B. 2019. Assessment of surfactants on performance of molecularly imprinted polymer toward adsorption of pharmaceutical. *Journal of Environmental Chemical Engineering,* 7**,** 103037.

DAUGHTON, C. G. 2004. Non-regulated water contaminants: emerging research. *Environmental impact assessment review,* 24**,** 711-732.

DE ANDRADE, J. R., OLIVEIRA, M. F., DA SILVA, M. G. & VIEIRA, M. G. 2018. Adsorption of pharmaceuticals from water and wastewater using nonconventional low-cost materials: a review. *Industrial & Engineering Chemistry Research,* 57**,** 3103-3127.

EBELE, A. J., ABDALLAH, M. A.-E. & HARRAD, S. 2017. Pharmaceuticals and personal care products (PPCPs) in the freshwater aquatic environment. *Emerging contaminants,* 3**,** 1-16.

EDOKPAYI, J. N., ODIYO, J. O. & DUROWOJU, O. S. 2017. Impact of wastewater on surface water quality in developing countries: a case study of South Africa. *Water quality,* 10**,** 66561.

ELLIS, J. B. 2006. Pharmaceutical and personal care products (PPCPs) in urban receiving waters. *Environmental pollution,* 144**,** 184-189.

GHORBANI, M., SEYEDIN, O. & AGHAMOHAMMADHASSAN, M. 2020. Adsorptive removal of lead (II) ion from water and wastewater media using carbon-based nanomaterials as unique sorbents: A review. *Journal of environmental management,* 254**,** 109814.

GONZÁLEZ PEÑA, O. I., LÓPEZ ZAVALA, M. Á. & CABRAL RUELAS, H. 2021. Pharmaceuticals market, consumption trends and disease incidence are not driving the pharmaceutical research on water and wastewater. *International journal of environmental research and public health,* 18**,** 2532.

HAWASH, H. B., MONEER, A. A., GALHOUM, A. A., ELGARAHY, A. M., MOHAMED, W. A., SAMY, M., EL-SEEDI, H. R., GABALLAH, M. S., MUBARAK, M. F. & ATTIA, N. F. 2023. Occurrence and spatial distribution of pharmaceuticals and personal care products (PPCPs) in the aquatic environment, their characteristics, and adopted legislations. *Journal of Water Process Engineering,* 52**,** 103490.

JELIĆ, A., GROS, M., PETROVIĆ, M., GINEBREDA, A. & BARCELÓ, D. 2012. Occurrence and elimination of pharmaceuticals during conventional wastewater treatment. *Emerging and priority pollutants in Rivers: bringing science into river management plans***,** 1-23.

JOHNSON, A. C., JÜRGENS, M. D., WILLIAMS, R. J., KÜMMERER, K., KORTENKAMP, A. & SUMPTER, J. P. 2008. Do cytotoxic chemotherapy drugs discharged into rivers pose a risk to the environment and human health? An overview and UK case study. *Journal of Hydrology,* 348**,** 167-175.

KHAN, A., AZIZ, H., KHAN, N., HASAN, M., AHMED, S., FAROOQI, I., DHINGRA, A., VAMBOL, V., CHANGANI, F. & YOUSEFI, M. 2021. Impact, disease outbreak and the eco-hazards associated with pharmaceutical residues: a critical review. *International Journal of Environmental Science and Technology***,** 1-12.

KHAN, S., NAUSHAD, M., GOVARTHANAN, M., IQBAL, J. & ALFADUL, S. M. 2022. Emerging contaminants of high concern for the environment: Current trends and future research. *Environmental Research,* 207**,** 112609.

KLAVARIOTI, M., MANTZAVINOS, D. & KASSINOS, D. 2009. Removal of residual pharmaceuticals from aqueous systems by advanced oxidation processes. *Environment international,* 35**,** 402-417.

KOSEK, K., LUCZKIEWICZ, A., FUDALA-KSIĄŻEK, S., JANKOWSKA, K., SZOPIŃSKA, M., SVAHN, O., TRÄNCKNER, J., KAISER, A., LANGAS, V. & BJÖRKLUND, E. 2020. Implementation of advanced micropollutants removal technologies in wastewater treatment plants (WWTPs)-Examples and challenges based on selected EU countries. *Environmental science & policy,* 112**,** 213-226.

KYZAS, G. Z., FU, J., LAZARIDIS, N. K., BIKIARIS, D. N. & MATIS, K. A. 2015. New approaches on the removal of pharmaceuticals from wastewaters with adsorbent materials. *Journal of molecular liquids,* 209**,** 87-93.

MARTÍN, J., CAMACHO-MUÑOZ, D., SANTOS, J., APARICIO, I. & ALONSO, E. 2012. Occurrence of pharmaceutical compounds in wastewater and sludge from wastewater treatment plants: removal and ecotoxicological impact of wastewater discharges and sludge disposal. *Journal of hazardous materials,* 239**,** 40-47.

MASSIMA MOUELE, E. S., TIJANI, J. O., BADMUS, K. O., PEREAO, O., BABAJIDE, O., ZHANG, C., SHAO, T., SOSNIN, E., TARASENKO, V. & FATOBA, O. O. 2021. Removal of pharmaceutical residues from water and wastewater using dielectric barrier discharge methods—A review. *International Journal of Environmental Research and Public Health,* 18**,** 1683.

METWALLY, M. G., BENHAWY, A. H., KHALIFA, R. M., EL NASHAR, R. M. & TROJANOWICZ, M. 2021. Application of molecularly imprinted polymers in the analysis of waters and wastewaters. *Molecules,* 26**,** 6515.

MORIN-CRINI, N., LICHTFOUSE, E., LIU, G., BALARAM, V., RIBEIRO, A. R. L., LU, Z., STOCK, F., CARMONA, E., TEIXEIRA, M. R. & PICOS-CORRALES, L. A.

2022. Worldwide cases of water pollution by emerging contaminants: a review. *Environmental Chemistry Letters,* 20**,** 2311-2338.

NANNOU, C., OFRYDOPOULOU, A., EVGENIDOU, E., HEATH, D., HEATH, E. & LAMBROPOULOU, D. 2020. Antiviral drugs in aquatic environment and wastewater treatment plants: a review on occurrence, fate, removal and ecotoxicity. *Science of the Total Environment,* 699**,** 134322.

OKORO, H. K., PANDEY, S., OGUNKUNLE, C. O., NGILA, C. J., ZVINOWANDA, C., JIMOH, I., LAWAL, I. A., OROSUN, M. M. & ADENIYI, A. G. 2022. Nanomaterial-based biosorbents: Adsorbent for efficient removal of selected organic pollutants from industrial wastewater. *Emerging Contaminants,* 8**,** 46-58.

PÉREZ-LUCAS, G., EL AATIK, A., ALISTE, M., HERNÁNDEZ, V., FENOLL, J. & NAVARRO, S. 2022. Reclamation of aqueous waste solutions polluted with pharmaceutical and pesticide residues by biological-photocatalytic (solar) coupling in situ for agricultural reuse. *Chemical Engineering Journal,* 448**,** 137616.

RATHI, B. S., KUMAR, P. S. & VO, D.-V. N. 2021. Critical review on hazardous pollutants in water environment: Occurrence, monitoring, fate, removal technologies and risk assessment. *Science of The Total Environment,* 797**,** 149134.

SAMAL, K., MAHAPATRA, S. & ALI, M. H. 2022. Pharmaceutical wastewater as Emerging Contaminants (EC): Treatment technologies, impact on environment and human health. *Energy Nexus***,** 100076.

SATHYA, K., NAGARAJAN, K., CARLIN GEOR MALAR, G., RAJALAKSHMI, S. & RAJA LAKSHMI, P. 2022. A comprehensive review on comparison among effluent treatment methods and modern methods of treatment of industrial wastewater effluent from different sources. *Applied Water Science,* 12**,** 70.

SENGAR, A. & VIJAYANANDAN, A. 2022. Human health and ecological risk assessment of 98 pharmaceuticals and personal care products (PPCPs) detected in Indian surface and wastewaters. *Science of the Total Environment,* 807**,** 150677.

SERWECIŃSKA, L. 2020. Antimicrobials and antibiotic-resistant bacteria: a risk to the environment and to public health. *Water,* 12**,** 3313.

SINGH, J., YADAV, P., PAL, A. K. & MISHRA, V. 2020. Water pollutants: Origin and status. *Sensors in water pollutants monitoring: Role of material.* Springer.

TERNES, T. & JOSS, A. 2007. *Human pharmaceuticals, hormones and fragrances*, IWA publishing.

VILLAR-NAVARRO, E., BAENA-NOGUERAS, R. M., PANIW, M., PERALES, J. A. & LARA-MARTÍN, P. A. 2018. Removal of pharmaceuticals in urban wastewater: High rate algae pond (HRAP) based technologies as an alternative to activated sludge based processes. *Water research,* 139**,** 19-29.

VILLARREAL-LUCIO, D. S., VARGAS-BERRONES, K. X., DÍAZ DE LEÓN-MARTÍNEZ, L. & FLORES-RAMÍEZ, R. 2022. Molecularly imprinted polymers for environmental adsorption applications. *Environmental Science and Pollution Research***,** 1-20.

VINAYAGAM, V., MURUGAN, S., KUMARESAN, R., NARAYANAN, M., SILLANPÄÄ, M., DAI VIET, N. V., KUSHWAHA, O. S., JENIS, P., POTDAR, P. & GADIYA, S. 2022. Sustainable adsorbents for the removal of pharmaceuticals from wastewater: A review. *Chemosphere***,** 134597.

WALENG, N. J. & NOMNGONGO, P. N. 2022. Occurrence of pharmaceuticals in the environmental waters: African and Asian perspectives. *Environmental Chemistry and Ecotoxicology,* 4**,** 50-66.

ZARE, E. N., FALLAH, Z., LE, V. T., DOAN, V.-D., MUDHOO, A., JOO, S.-W., VASSEGHIAN, Y., TAJBAKHSH, M., MORADI, O. & SILLANPÄÄ, M. 2022.

Remediation of pharmaceuticals from contaminated water by molecularly imprinted polymers: a review. *Environmental Chemistry Letters*, 1-36.

Chapter 2

Molecularly imprinted polymer-based adsorbents for the selective removal of pharmaceuticals from wastewater: adsorption kinetics, isotherms, and thermodynamics studies

Abstract

Majority of pharmaceuticals are found in the environment as mixtures. However, a significant amount of these therapeutic compounds cannot be completely metabolized by the human body; thus, they are excreted through faeces and urine and end up in wastewater treatment plants (WWTPs). The presence of pharmaceuticals and the degree to which they can be removed during wastewater treatment are now important research topics. Despite the adoption of various alternative technologies for the treatment of wastewater, the adsorption process is still regarded as a promising method due to its high efficiency, increased simplicity, and lower costs. Recent developments in the adsorption process involve the incorporation of an artificial molecularly imprinted polymer (MIP), which is a potent molecular receptor capable of selectively recognizing and removing pollutants. The MIP has advantageous characteristics, which include high affinity, predetermination, high stability, ease of preparation, and low cost. Notably, MIPs can be applied to the cleanup and preconcentration of analytes as the selective adsorbent of solid-phase extraction (SPE), magnetic solid phase extraction (MSPE), and dispersive solid-phase extraction (dSPE). Furthermore, MIPs can be produced as composite nanomaterials by employing nanoparticles (nanoMIPs). The advancements of MIPs employed as sorbent materials for quantitative assessment and purification of pharmaceuticals in environmental water have been given most of the focus. Therefore, this study not only aims to present the fundamental ideas about the application of MIPs as sorbents but also gives an overview of the considerable initiatives made in recent years to enhance the performance of MIPs. Considering this, various current approaches to the development of MIP-based extraction techniques are detailed in the present review. This review also demonstrates how kinetics, thermodynamics, and isotherm models can be used to better understand the behaviour of adsorbents and the adsorption process.

Keywords: pharmaceuticals, molecularly imprinted polymers, nanoparticles, adsorption

2.1 Introduction

Pharmaceuticals are one of the biggest environmental issues in the world because of how frequent they are used in the treatment of human and veterinary diseases, injuries, and illnesses. Consequently, pharmaceutically active compounds found in drugs and medicines are complex molecules having a variety of functions and physical characteristics to have particular biological activities. Pharmaceuticals are categorized into various classes based on their physicochemical properties and mode of action. Nonsteroidal anti-inflammatory drugs (NSAIDs), antidepressants, antibiotics, antiseptics, antiretroviral (ARV) medicines, etc., are among the classifications (Hawash et al., 2023, Chaves et al., 2022). The major sources of contamination are the pharmaceutical industry, hospital waste, farm livestock, unused medication disposal from various households, and the fate and transport of pharmaceuticals, their metabolites, and transformed products follow interdependent complex pathways, as shown in **Figure 2.1** (Anand et al., 2022). The threat of pharmaceutical pollutants in surface or groundwater close to residential and commercial areas is growing (Ortúzar et al., 2022). When they get into drinking water, they could be detrimental to humans as well as aquatic life (Sengar and Vijayanandan, 2022). Notably, pharmaceuticals are found in the aquatic environment in comparatively low concentrations (µg-ng L^{-1}). Excessive exposure to pharmaceuticals can cause unpleasant side effects like drowsiness, vomiting, stomach pain, fatigue, hepatic steatosis, pancreatis, heart diseases, etc (Serwecińska, 2020). Moreover, these effects may include impairment to fish and wildlife populations, decreased oxygen levels, closure of beaches and other limits on recreational water usage, limitations on the harvesting of fish and shellfish, and water contamination (Massima Mouele et al., 2021, González Peña et al., 2021). Furthermore, the ecosystem and human health could suffer if wastewater is not adequately treated. As a result of possible health effects related to exposure of human, aquatic and terrestrial life that pharmaceuticals have when they reach the environment, they have received a lot of attention (Khan et al., 2021, Rathi et al., 2021). Moreso, humans may be exposed to contaminants in the environment, even at comparatively low concentrations, as a result of drug consumption. (Patel et al., 2019).

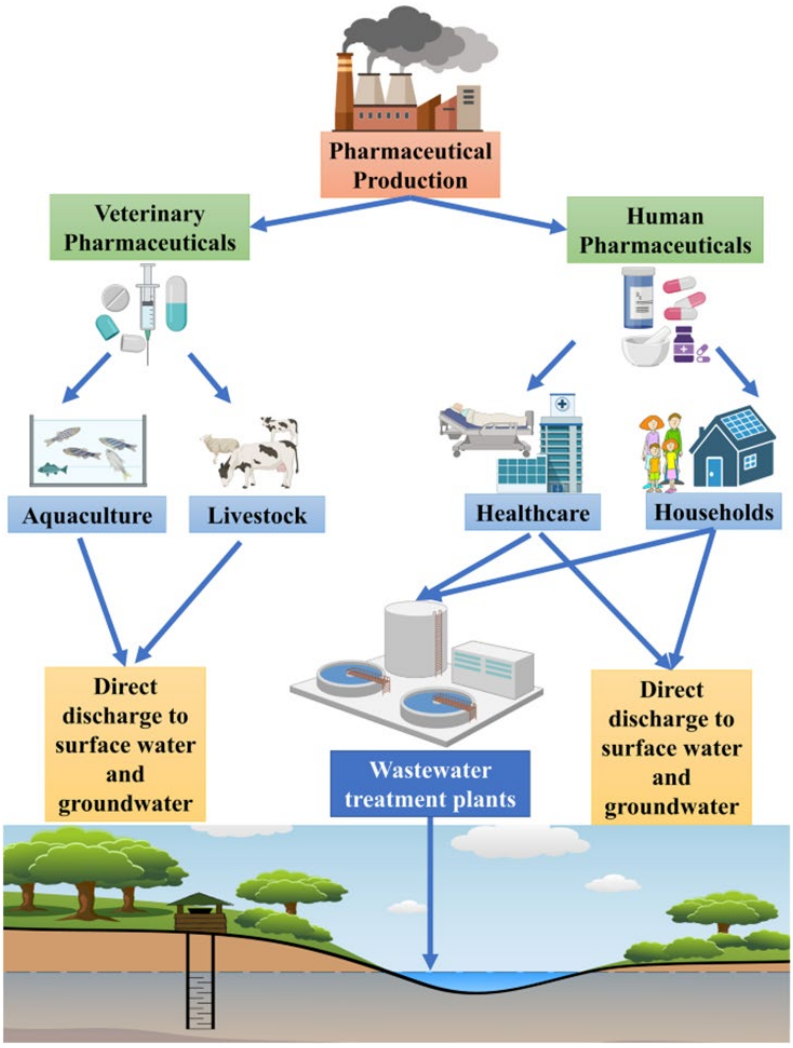

Figure 2.1: Sources and pathways for pharmaceuticals on the environment (Chauhan et al., 2023).

Extended use of nonsteroidal anti-inflammatory drugs (NSAIDs) by humans has been associated with a higher risk of side effects in various organs and systems, such as the digestive and cardiovascular systems. This has also adversely affected wild fish populations (Marmon et al., 2021). Fernandez and co-workers suggested that, the routine use of ARVs in aquatic environments may have unintended impacts on non-target animals, including fish development and growth abnormalities, liver damage, and general health deterioration (Fernández et al., 2022). Antibiotic-resistant genes and bacteria are therefore the greatest environmental health problem associated with antibiotics, as they reduce the efficiency of treatment against bacterial infections that affect both humans and aquatic animals (Ngqwala and Muchesa, 2020).

Numerous sources, such as discharges from pharmaceutical production facilities, emissions from medical units, treated sewage effluent discharges, and improper disposal of unwanted

pharmaceuticals, cause the release of pharmaceuticals into the aquatic environment (Nyaga et al., 2020, Waleng and Nomngongo, 2022). The primary source of pharmaceuticals in the environment is the discharge of wastewater that has not been sufficiently or completely treated (Vinayagam et al., 2022). It is important that unwanted medicines should be safely disposed of to mitigate the public and environmental health risks. Lack of general knowledge on how to dispose of unused pharmaceuticals leads to improper disposal resulting in accidental toxicity, rising healthcare costs, landfills pilfering/scavenging, water supply pollution, anti-microbial resistance, and death. Additionally, pharmaceuticals may enter the environment through the use of wastewater treatment plant sludge as manure and crop irrigation using river water from which the effluent is discharged. Pharmaceutical removal by WWTPs is crucial for lowering discharge to aquatic habitats. Nevertheless, traditional wastewater and water treatment unit operations do not really appear to be able to eliminate all kinds of pharmaceuticals., This might lead to the continued transfer of water-soluble pharmaceuticals into river water. Thus it is necessary to employ a variety of cutting-edge process treatment technologies to improve water quality (Sathya et al., 2022). Additionally, advances in analytical methods have made it possible to identify and eliminate traces of pharmaceuticals from a variety of environmental matrices, including drinking water, sediments, waste effluents, surface and subsurface water, and biota (Zare et al., 2022, Almeida, 2021).

Consequently, utilizing inexpensive technology while preserving safety and health standards in recycled treated effluents is one of the biggest difficulties in the field of wastewater treatment. In water pollution control and wastewater management, the adsorption process is a promising method because it has design and operational simplicity, higher efficacy, lower maintenance, and no undesirable by products (Ghorbani et al., 2020). The development of efficient technologies to remediate effluent contamination is driven by the ineffectiveness of existing methods employed in water treatment plants to remove the contaminant. In this study, molecularly imprinted polymers (MIPs) are discussed as an effective tool for the selective adsorption and removal of these pharmaceuticals from wastewater to get beyond the limitations of the traditional wastewater treatment facilities. According to the literature, the use of MIPs as a highly selective adsorbent material is a promising approach that can be employed in environmental sciences since they have a variety of synthesis methods that can be tuned to meet specific target requirements (Villarreal-Lucio et al., 2022).

Particularly, adsorption technologies are a low-cost alternative that are simple to utilize in developing nations where there is a shortage of complex technology, skilled labour, and available capital. Adsorption also seems to be the most widely applicable pharmaceutical removal technique. According to Rashed and co-workers, the method is useful for eliminating low concentrations of synthetic and natural organic pollutants from water and wastewater streams (Rashed, 2013). It is frequently used as a finishing step to get rid of a variety of low to medium molecular mass compounds without producing any by-products. Moreso, adsorption provides a number of benefits, including high removal efficiencies at low concentrations of pollutants. Also, the flexibility in design and operation, the ability to regenerate and reuse, the ability to be applied to batch and continuous processes, and dependable and straightforward operational methods (Quesada et al., 2019). According to studies on the use of adsorbents to extract pharmaceuticals from aqueous systems, hydrophobic pharmaceuticals have a higher affinity to the surface of the adsorbent than their hydrophilic counterparts (Khalil et al., 2020). Activated carbon, zeolite, clays, chitosan, etc, are the most utilized adsorbents in wastewater treatment (Ali et al., 2020, Biswas et al., 2021). These adsorption systems frequently fail to successfully remove even trace levels of pharmaceuticals from complex effluent due to their non-selective nature (Bilal et al., 2021, Shakoor et al., 2022).

As a result, improving the selectivity of adsorbents towards pharmaceuticals may present a viable substitute. In this sense, the synthesis of affinity materials might offer a flexible and reliable alternative. Molecularly imprinted polymers (MIPs) have gained more interest recently among affinity materials because of their unique features (Song et al., 2022). As a consequence, they are frequently utilized as adsorbents in solid phase extraction (SPE) techniques, stir bar sorptive extraction (SBSE), dispersion solid phase extraction (DSPE), and magnetic solid phase extraction (MSPE) (Sun et al., 2021). Furthermore, MIPs are a unique family of polymeric materials with built-in molecular identification properties and have enormous potential in a variety of fields, including environmental monitoring, food safety, and clinical diagnostics (Gu et al., 2022, Chadha et al., 2022). Notably, MIP approaches have undergone numerous improvements and developments for a variety of objectives (Fang et al., 2021, Ayankojo et al., 2022).

Molecularly imprinted polymer adsorbents have been extensively utilized in conventional solid-phase extraction (referred to as molecularly imprinted solid-phase extraction, or MISPE) techniques to extract an extensive range of compounds from water samples. (Turiel and Martín-

Esteban, 2019). At present, this is the most sophisticated technique available for preparing samples utilizing MIPs (Bosman et al., 2021, Wan et al., 2021). Following Sellergren and colleagues ground-breaking work in 1994 (Sellergren, 1994) for the extraction of pentamidine from human urine samples, molecularly imprinted solid-phase extraction (MISPE) has attracted significant interest for the detection of several pharmaceuticals in biological matrices (Hu et al., 2021, Wan et al., 2021). Consequently, solid-phase extraction (SPE) which uses stationary phases like nonpolar polymer or C18-bonded silica, is the most used technique for the extraction and clean-up of solutes of interest (Badawy et al., 2022). The term "sample cleanup" describes the enrichment or extraction of specified analytes from simple or complicated matrices (Suseela et al., 2023). This step is commonly followed by chromatographic techniques which then separate the extracted targeted analytes from the complex mixtures (Dugheri et al., 2021). The drawbacks of the SPE sorbent are it low selectivity, single-use nature, time-consuming due to many manual steps involved (sorbent conditioning and equilibration, sample loading, impurity removal and extract elution), may need to concentrate the extract prior to instrumental analysis (Chen et al., 2021). Dispersive solid phase extraction (d-SPE) is one of the SPE technique variations that significantly reduces the amount of time required and streamlines the extraction procedure (Manousi and Zachariadis, 2020). In this variation, the extraction procedure is carried out in a liquid sample using dispersed material rather than an SPE column, disk, or cartridge (Płotka-Wasylka et al., 2023). Particularly, d-SPE is a more recent improvement on the traditional SPE method that is gaining popularity because of its exceptional simplicity, quick extraction time, and minimal solvent expenditure requirements, as well as its high effectiveness and broad applicability (Sajid et al., 2021).

Magnetic solid-phase extraction (MSPE) is an additional interesting alternative to conventional SPE (Du et al., 2022). This useful technique for sample preparation enables the dispersion of solid sorbents in liquid sample matrices, followed by the adsorbent's magnetic retrieval (Yin et al., 2021). The MSPE sample pre-treatment method is also gaining popularity due to its exceptional adsorption effectiveness, speedy separation process, and ease of automated testing (Yin et al., 2021). Moreover, getting smaller polymer structures has been a recent area of emphasis. As a result, molecularly imprinted polymeric nanoparticle (nanoMIPs) development and improvement have opened up new avenues for nanotechnology research (Sullivan et al., 2021). The development of enhanced functional nanoMIPs, which have certain clear advantages over previously discovered MIPs with huge sizes and irregular shapes, has been a

major area of contemporary molecular imprinting research attention (Zhang, 2020). As a result of their enhanced functionality and simplicity in synthesis, nanoMIPs have started to replace traditional bulk MIPs (Sullivan et al., 2021). NanoMIPs have a high surface area to volume ratio because of their uniform size and shape due to their small particle size. When compared to a more conventional "bulk" material, these materials also naturally permit greater control over the reaction and easier incorporation of other (Shetty et al., 2022). In this context, the development of high affinity molecularly imprinted polymer (MIPs) sorbents have broadened the scope of applicability of these methods/techniques, significantly enhancing their selectivity (Contin et al., 2022).

Nonetheless, MIP techniques are extensively developed and used in a variety of sectors, including food analysis, analytical chemistry, therapeutics, drug administration, sensors, immunoassays, biological diagnosis, and environmental research (Suzaei et al., 2023). Although MIPs have made remarkable strides and will continue to be supported by developing technologies, getting MIPs with appropriate selectivity for aqueous applications is still a significant issue and is transforming into a research hotspot over time (Lowdon et al., 2020). This present study focuses on current advancements in MIPs, such as MIP-SPE, MIP-d-SPE, and nanoMIPs, as well as its applicability in the removal of pharmaceuticals from wastewater. Moreover, one of the 12 tenets of green analytical chemistry is the need for approaches that enable the analysis of various compounds as opposed to those that focus on a single analyte at a time. Hence, this work presents a molecularly imprinted polymer (MIP) synthesized for the selective and efficient extraction of selected pharmaceuticals belonging to three different classes, namely antiretrovirals (abacavir, nevirapine and efavirenz), non-steroidal anti-inflammatory drugs (ibuprofen, diclofenac, and naproxen) and antibiotics (sulfamethoxazole and ciprofloxacin). Accordingly, adsorption studies for determining the mechanisms and adsorption of MIPs, including adsorption isotherms, kinetics, and thermodynamics of the resultant polymer are also discussed.

2.1.1 Physicochemical properties of pharmaceuticals

The presence of mixtures of several pharmaceuticals with various physico-chemical properties in WWTPs complicates their removal process, and the rate at which they are removed depends on both the physiochemical properties of the pharmaceuticals and the treatment technique used by the plants (Papagiannaki et al., 2022). Pharmaceuticals are divided into various subclasses,

however the classes that are most frequently found in wastewater and urban water will be highlighted. These classes include antibiotics (e.g., sulfamethoxazole and ciprofloxacin, etc.), ARVs (e.g., nevirapine, abacavir, efavirenz, etc.) and NSAIDs (e.g., ibuprofen, naproxen, diclofenac, etc.). Physical and chemical characteristics of pharmaceuticals including hydrophobicity/hydrophilicity, molecular size and structure, charge, solubility, acid dissociation constant (pKa), and octanol-water coefficient (log Kow) seem to have a significant effect on their presence in various environmental matrices. The ability of a pharmaceutical compound to adsorb on solids or solubilise in aqueous media depends on whether it is hydrophobic or hydrophilic which relates to its octanol water coefficient (Kow). The hydrophobic (high log Kow) compounds often have a higher affinity for adsorption on solids while the hydrophilic (low log Kow) pharmaceutical has high affinity for aqueous media (Ambaye et al., 2021). **Table 2.1** shows the physicochemical properties of selected pharmaceuticals. However, pharmaceutical removal is made easier if they are less soluble in water, and thus, are expected to be removed faster from contaminated water compared to the highly soluble compounds. Notably, the degree of ionization is strongly influenced by pH, which may also have effects in aquatic systems containing pharmaceutical residues. The acid dissociation constant (or pKa) is a crucial element governing the therapeutic behaviour of pharmaceuticals. Due to the functional groups that some pharmaceuticals possess such as alcohol, amine, carboxylic acid and others, changing pH conditions will cause acidolysis, which will produce pharmaceutical molecules as anions, neutrals, and cations (Mangalgiri et al., 2022). Generally, at pH levels higher than the pKa, compounds dissociate into anionic forms, leaving just a small amount of neutral molecules. Compound hydrolysis causes poor adsorption from the solution; however, at pH levels below the pKa, compounds do not dissolve, improving the adsorption conditions.

Table 2.1: Classification of selected pharmaceuticals and their properties

Pharmaceutical	**Class**	**Chemical structure**	**Molecular weight (g/mol)**	**pKa**	**Log Kow**	**Water solubility (mg/mL)**	References
Nevirapine	ARVD	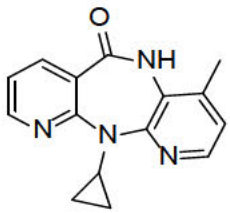	266.294	2.8	3.89	9.3×10^{-5}	(Adeola et al., 2021)
Efavirenz		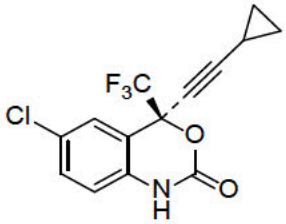	315.675	12.52	4.70	7.05×10^{-4}	(Adeola et al., 2021)
Abacavir		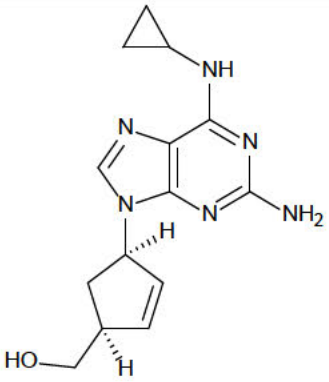	286.332	5.77	1.45	77	(Qwane et al., 2020)

Sulfamethoxazole	Antibiotic	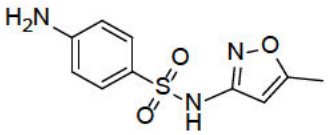	253.28	5.6	0.89	0.61	(Nas et al., 2021)
Ciprofloxacin		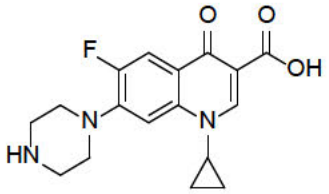	331.34	6.09	0.28	36	(Nas et al., 2021)
Ibuprofen	NSAID	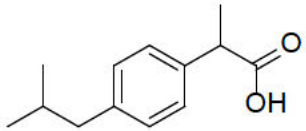	206.29	4.85	3.79	0.041	(Petrie and Camacho-Muñoz, 2021)
Naproxen		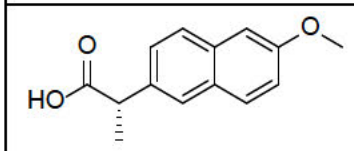	230.36	4.15	3.18	0.144	(Petrie and Camacho-Muñoz, 2021)
Diclofenac		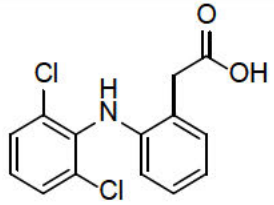	296.148	4.2	4.18	4.082×10^{-3}	(Rastogi et al., 2021)

2.1.1.1 Non-steroidal anti-inflammatory drugs

Recently, there has been a considerable growth in the production and usage of non-steroidal anti-inflammatory drugs (NSAIDs), which has led to a significant amount of these pharmaceuticals being released into the environment in original or metabolized form (Rastogi et al., 2021). Consequently, ibuprofen, diclofenac and naproxen are among the most popular pharmaceuticals that may be purchased over-the-counter without a prescription. They are used for the treatment of chronic illnesses, inflammation and have been extensively used by patients across the world since the outbreak of the COVID-19 pandemic (Oleszkiewicz et al., 2021). These drugs are frequently purchased in packs of several tablets, which are then stored and used when needed (Kołecka et al., 2022). Some pharmaceutical components may eventually expire and be improperly disposed of in sinks and toilets due to the unpredictable nature of pharmaceutical storage. Moreso, these pharmaceuticals are easily excreted from the consumer and transported into wastewater treatments plants (WWTPs). Hence, untreated or incompletely treated wastewater contains concentrations ($\mu g\ L^{-1}$) due to the widespread use of NSAIDs. They may be further transported into river water if they are not entirely eradicated by WWTPs during wastewater purification, as evidenced by their discovery in their effluents. These NSAIDs are among the medications on the World Health Organization's (WHO) list of Essential Drugs and are the most commonly administered pharmaceuticals for flu and cold symptoms. This reflects their high detection frequency and quantities in the environment and water supplies (Cao et al., 2021). Hence, removing them from the environment has become a top research goal since they are becoming micropollutants with substantial detrimental consequences on both the economy and the ecosystem. (Batucan et al., 2022, Bhatt et al., 2022). The NSAIDS (naproxen, diclofenac, and ibuprofen) were found in influent and effluent samples in South Africa (Hlengwa and Mahlambi, 2020, Mhuka et al., 2020), Egypt (Abdallah et al., 2019) and Nigeria (Ajibola et al., 2021), **Table 2.2**. High influent concentration of diclofenac was observed in Ijaiye wastewater treatment plants (Nigeria), whereas the amount of ibuprofen was higher in the effluent than the influent. This was due to ibuprofen conjugated metabolites being produced during wastewater treatment, which have the ability to revert to ibuprofen. Particularly, ibuprofen is typically found in higher amounts in South African water supplies among these NSAIDs resulting from its common usage in South Africa, its high consumption is associated with high amounts of the substance in wastewater. In a South African based study, the concentrations of ibuprofen recorded in WWTP influents were 38.1 $\mu g\ L^{-1}$ while the concentrations of naproxen and diclofenac did not exceed 21 $\mu g\ L^{-1}$ in

the influent (Hlengwa and Mahlambi, 2020). Ibuprofen, diclofenac, and naproxen maximum concentration of 3.6 and 0.089 μg L^{-1} were detected in Egypt effluent samples (Abdallah et al., 2019). Notably, pharmaceuticals are found in the aquatic environment in comparatively low concentrations (μg-ng L^{-1}).

Table 2.2: NSAIDs concentrations measured in African aquatic bodies.

Country	**Concentration (µg L^{-1})**						**Ref**
	Ibuprofen		**Naproxen**		**Diclofenac**		
	Inf	Eff	Inf	Eff	Inf	Eff	
South Africa	55-69	2.1-4.2	15-20	0.6-1.1	6.4-16	0.079-3.6	(Madikizela and Chimuka, 2017)
	76.4	Nd-7.65	0.0169-0.546	0.01309-0.3496	0.012-0246	0.0056-0.244	(Mhuka et al., 2020)
	31.8	9.45	2.89	Nd	21.1	Nd	(Hlengwa and Mahlambi, 2020)
Egypt	-	0.812-6	-	<LOQ-0.089	-	0.79-3.6	(Abdallah et al., 2019)
Nigeria	36	62	39	21	-	-	(Ajibola et al., 2021)

Nd=not detected. <LOQ = below method quantitation limit. Inf=influent, Eff= effluent

2.1.1.2 Antiretroviral (ARV) drugs

Pharmaceuticals of the antiviral medication class are used to treat viral infections by halting the development of pathogens (Yoon et al., 2020). Antiretroviral drugs (ARVDs) are medical treatments for retroviral infections, especially type 1 human immunodeficiency virus infections (HIV-1) (Adeola and Forbes, 2022, Kahilu et al., 2022). The ARVs vary from other drugs in that they combat a virus that can readily evolve into resistant strains if the patient does not follow the doctor's instructions. Notably, ARVs might cause resistant strains to emerge through persistent exposure to contaminated food and water, their presence in water bodies is therefore a serious concern. Notwithstanding, antiretroviral drugs are not completely metabolized by the body, therefore they are expelled as faeces and urine, which are then transported through the sewer to wastewater treatment facilities (Ngqwala and Muchesa, 2020). Their continuous emission and persistence in the receiving environment have raised concerns about potential ecological implications. Three kinds of antiretroviral medications-nucleoside or nucleotide reverse transcriptase inhibitors (NRTI), non-nucleoside reverse transcriptase inhibitors (NNRTI), and protease inhibitors are the emphasis of the World Health Organization's (WHO) ART guidelines (El Bouzidi et al., 2022). Nevirapine and efavirenz are the two NNRTIs that are most often prescribed first-line antiretroviral (ARV) medications for HIV/AIDS, while abacavir is one of the most common NRTI given as first-line treatment. Accordingly, South Africa uses more ARVs per person than any other country, which suggests that significant quantities of these substances will enter wastewater treatment plants that were not built to remove these medicines (Horn et al., 2022, Zhou et al., 2022). Notably, little research has been done on the existence of dissolved ARVs, their metabolic products, and removal methods in wastewater, even though multiple studies have demonstrated that ARVs are sterilized during wastewater treatment. However, ARVs have been found most frequently in water sources where they may pose serious issues, like the development of degradation products (Adeola and Forbes, 2022). In recent years, ARVDs have been found in the water resources of South Africa and Kenya. The results in **Table 2.3** shows that, among the detected ARVDs in African waters, efavirenz has been viewed as the prominent pharmaceutical that is mostly detected at higher concentrations of up to 140 μg L^{-1} recorded in a WWTP influent located in the city of Durban, South Africa (Mtolo et al., 2019). Moreover, these ARVDs are frequently detected in South African wastewater influent and effluent. Nevirapine was the most detected ARVD in the influent and effluent samples taken in Kenya (K'oreje et al., 2018). Efavirenz was detected in similar concentrations in both WWTP influent and effluent in South Africa. The detection of

these compounds in effluent water indicates the poor performance of the treatment plants processes (Abafe et al., 2018). Consequently, abacavir was sometimes not detected or detected in small concentration in South African effluent.

Table 2.3: ARVs concentrations measured in African aquatic bodies.

Country	Concentration (µg L^{-1})						References
	Nevirapine		Efavirenz		Abacavir		
	Inf	Eff	Inf	Eff	Inf	Eff	
South Africa	0.67-2.8	1.4	34	34	14	Nd	(Abafe et al., 2018)
	0.35	0.35	-	-	0.1	0.54	(Späth et al., 2021)
	0.681	0.658	1.42-15.4	0.982-9.15	-	-	(Mosekiemang et al., 2019)
	-	-	9.63-140	2.79-93.1	-	-	(Mtolo et al., 2019)
Kenya	3.3	2.11	-	-	-	-	(K'oreje et al., 2018)

Nd=Not detected, Inf=influent, Eff= effluent

2.1.1.3 Antibiotics

Antibiotics are a class of medications that are vital for the preservation of good health and a high quality of life (Chokshi et al., 2019). Antibiotics are used for a variety of purposes, including the treatment of illness, preventing infections in humans and animals, and boosting the immune system (Mangla et al., 2022). Sulfamethoxazole (SMX) and Ciprofloxacin (CIP) are two of the antibacterial substances that are most frequently found in aquatic environments (Nas et al., 2021). Due to its ability to combat multiple types of bacteria, ciprofloxacin and sulfamethoxazole has drawn a lot of attention. These antibiotics are effective in treating infections and illnesses brought on by both Gram-positive and Gram-negative aerobic bacteria (Jubeh et al., 2020). Moreso, CIP and SMX are two antibiotics from the sulfonamide and fluoroquinolone classes that are widely employed in the treatment of human urinary tract infections. Groundwater, surface water, and wastewater streams have all been shown to contain these antibiotics (Kaya et al., 2022b). Globally, there are now substantial issues due to the

significant increase in their consumption in recent years (Polianciuc et al., 2020). Worrisomely, the rising use of antibiotics has led to their detection in wastewater treatment plants effluent because of the WWTPs inability to completely remove them during treatment operations (Phoon et al., 2020). One of the greatest environmental issues affecting public health is the continued presence of antibiotics in the wastewater produced by the pharmaceutical industry. Consequently, through many direct channels, such as the discharge of untreated wastewater and unused and/or expired medication, the compounded mixtures of antibiotics and their metabolites are continuously released into the environment. In the event that antibiotics are released into the environment, they may result in the proliferation of genes that confer antibiotic resistance among environmental bacteria (Dai et al., 2021). Antibiotics have detrimental impacts on living things and may be hazardous to the ecosystem's balance since some fish and algae find them to be poisonous. Considering the potential risks antibiotics pose to human health and aquatic life, effective disposal methods are essential. Several countries investigated into the presence of antibiotics in African waters. Different antibiotics have been detected in Egypt (Abdallah et al., 2019), South Africa (Faleye et al., 2019, Nyamukamba et al., 2019, Mhuka et al., 2020, Mthiyane et al., 2023, Späth et al., 2021), Kenya (K'oreje et al., 2018), Zambia (Ngumba et al., 2020) and Tunisia (Moslah et al., 2018). Sulfamethoxazole had been detected in both influent and effluent with the highest concentration of 33 µg L^{-1} and 30.04 µg L^{-1} in Zambia (Ngumba et al., 2020). While ciprofloxacin was highest in South Africa with concentration of 1.3 µg L^{-1} influent sample and 1.6 µg L^{-1} in effluent sample, **Table 2.4** (Späth et al., 2021).

Table 2.4: Antibiotics concentrations found in different African water bodies.

Country	**Concentration (µg L^{-1})**				**References**
	Sulfamethoxazole		**Ciprofloxacin**		
	Inf	Eff	Inf	Eff	
South Africa	12	2.5	0.3	0.06	(Faleye et al., 2019)
	0.342	0.083	0.0772	0.0443	(Mhuka et al., 2020)
	0.342	0.383	1.3	1.6	(Mthiyane et al., 2023)
Egypt		13.4			(Abdallah et al., 2019)
Tunisia	0.0011	0.0032	0.0076	0.023	(Moslah et al., 2018)
Zambia	1.98-33.3	3.42-30.04	0.08-0.74	0.03-0.23	(Ngumba et al., 2020)
Kenya	14-112	0.5-10.8			(K'oreje et al., 2018)

Inf=influent, Eff= effluent

2.1.2 Removal of pharmaceuticals from WWTPs

The efficient removal of pharmaceutical compounds from wastewater treatment plants can be determined based on the concentrations detected in both influent and effluent daily loads (Bisognin et al., 2021, Khasawneh and Palaniandy, 2021). Under the assumption that the influent and effluent flow rates at the WWTP are constant, equal to the average daily flow rate, and that the influent and effluent concentrations correspond to the average daily values, equation 2.1 estimates the removal efficiency of pharmaceuticals from the WWTP, based on 24-hour combined water sample analysis.

$$\%\ Removal\ efficiency = \left(\frac{C_{influent} - C_{effluent}}{C_{influent}}\right) X\ 100 \qquad \text{Eq 2.1}$$

where $C_{influent}$ and $C_{effluent}$ are the concentrations (mg L^{-1}) measured in the WWTP influent and effluent, respectively. The removal efficiency for the selected pharmaceuticals from wastewater varies widely. These findings demonstrate that pharmaceuticals are not entirely eliminated during wastewater treatment, causing substantial quantities of them to infiltrate surface water bodies with WWTP effluent. Pharmaceuticals are occasionally successfully removed from wastewater, but they are also common and present in significant amounts in aquatic bodies receiving effluents from WWTPs. This might possibly be a result of the substantial amount present in the influent. There have been numerous reports in the literature describing various pharmaceutical removal efficiency during the wastewater treatment process (**Table 2.5**). The low pharmaceutical removal efficiency reported for efavirenz (Ngwenya and Mahlambi, 2023) in Amanzimtoti and ibuprofen (Ajibola et al., 2021) in Nigeria WWTPs is described as being caused by variations in the WWTP designs or pharmaceutical desorption from particulate matter during the wastewater treatment process which could lead to their frequent detection in the effluent water. Accordingly, literature reported values for the removal efficiency of nevirapine in Dewats WWTP were above 100% (Abafe et al., 2018). The removal efficiency in WWTPs depend on a number of variables, including compound physicochemical characteristics, the climate conditions, the type of treatment method used, and the conditions of operation of the treatment process. As a result, removal efficiency varies greatly between plants and within a single plant at different times. Notably, the findings did not clearly demonstrate that removal efficiencies were influenced by the class of compounds, as removal rates of compounds from various classes varied. Moreover, the data collected from literature in **Table 2.5** demonstrated that the majority of the compounds found in the WWTPs were reduced rather than completely eliminated by the wastewater treatment process, highlighting

the well-known fact that conventional wastewater treatment systems are ineffective at removing pharmaceuticals. This therefore calls for additional research into the remediation techniques that may be used to clean up the water bodies. Aiming to overcome the limits of the conventional wastewater treatment plants, molecularly imprinted polymers (MIPs) is a valid tool for selective adsorption and removal of pharmaceuticals from wastewater.

Table 2.5: Removal efficiencies of pharmaceuticals from various wastewater treatment processes.

Pharmaceutical	**Removal efficiency (%)**	**WWTP**	**Region**	**Ref**
Nevirapine	44 -87	Amanzimtoti	KwaZulu-Natal (South Africa)	(Ngwenya and Mahlambi, 2023)
	103-120	Dewats	KwaZulu-Natal (South Africa)	(Abafe et al., 2018)
	62	MBBR Pretoria	South Africa	(Mokgope et al., 2022)
	100	Daspoort	Pretoria, South Africa	(Mhuka et al., 2020)
Efavirenz	6-53	Amanzimtoti	KwaZulu-Natal Province (South Africa	(Ngwenya and Mahlambi, 2023)
	98-103	Dewats	KwaZulu-Natal (South Africa)	(Abafe et al., 2018)
	94	Pretoria	South Africa	(Mokgope et al., 2022)
	100	Daspoort	Pretoria, South Africa	(Mhuka et al., 2020)
Abacavir	67-74	Northern	Durban (South Africa)	(Qwane et al., 2020)

	75-91	Amanzimtoti	KwaZulu-Natal (South Africa)	(Ngwenya and Mahlambi, 2023)
	44-113	Dewats	KwaZulu-Natal (South Africa)	(Abafe et al., 2018)
Sulfamethoxazole	97-105	North-eastern	Tunisia	(Moslah et al., 2018)
	100	Daspoort	Pretoria, South Africa	(Mhuka et al., 2020)
	51-100	Durban metropolitan	KwaZulu-Natal (South Africa)	(Faleye et al., 2019)
Ciprofloxacin	65-84	North-eastern	Tunisia	(Moslah et al., 2018)
	18.8-96.4	Daspoort	Pretoria, South Africa	(Mhuka et al., 2020)
	87-100	Durban metropolitan	KwaZulu-Natal (South Africa)	(Faleye et al., 2019)
Ibuprofen	44-53	Nigerian	Nigeria	(Ajibola et al., 2021)
	99	Sewerage systems Ghana limited treatment plant (SSGL)	Ghana	(Kodom et al., 2021)
	79.5	Northern	KwaZulu-Natal (South Africa)	(Ngubane et al., 2019)
Naproxen	100	Daspoort	Pretoria (South Africa)	(Ngubane et al., 2019)

	82.3	Northern	KwaZulu-Natal (South Africa)	
	42-113	Umhlathuzana	KwaZulu-Natal (South Africa)	(Mlunguza et al., 2019)
Diclofenac	74	Sewerage systems Ghana limited treatment plant (SSGL)	Ghana	(Kodom et al., 2021)
	89.66	EL MENZAH	Tunisia	(Bessadok et al., 2023)
	65.5	Northern	KwaZulu-Natal (South Africa)	(Ngubane et al., 2019)
	76-98	Nigerian	Nigeria	(Ajibola et al., 2021)

2.1.3 Molecularly imprinted polymers (MIPs)

Molecularly imprinted polymers (MIPs) are adaptable materials that replicate natural antigen-antibody systems and permit the detection of analytes (Herrera-Chacón et al., 2021). The components of MIPs include templates, functional monomers, solvent, initiator, and cross-linker (Syed Yaacob et al., 2023). They are a class of smart adsorbents created by the directed polymerization of functional monomers around a target molecule (the template), which leaves a particular recognition site once the template is removed (Musarurwa and Tavengwa, 2022). Using synthetic polymers as a basis, the process of molecular imprinting allows for the fabrication of synthetic receptors for a specific target molecule (Bahrani et al., 2021). These materials are produced by polymerizing monomers and cross-linkers around the template molecules, resulting in a three-dimensional network polymer with a high degree of cross-linking (Hasanah et al., 2021). Following the removal of the template, the target molecule's molecular recognition properties are present at specific size and shape imprinted voids within the polymer network (**Figure 2.2**).

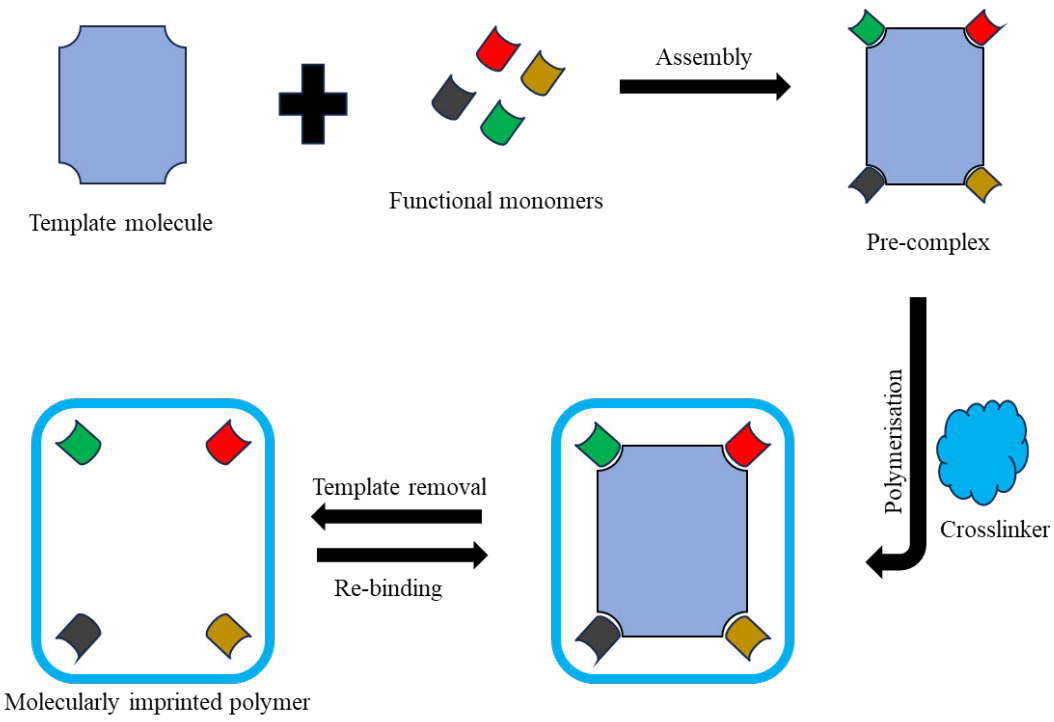

Figure 2.2: Schematic representation for the fabrication of molecularly imprinted polymers

MIPs that have been synthesized exhibit stability, tolerance to a wide variety of pH values, temperatures, and solvents, and selective interaction with the target molecule (Jamieson et al., 2021). Accordingly, MIPs offer excellent selectivity and affinity for the particular molecule

utilized in the imprinting process, are very simple to synthesize, and have slower rates of degradation, which prolong the duration that their recognition sites are active at room temperature (Pratama et al., 2020). The concept of MIPs and their potential application in various scientific fields has garnered significant attention (Akgönüllü et al., 2023). Due to their required selectivity, physical robustness, and thermal stability, as well as their affordability and ease of fabrication, MIPs have drawn a lot of attention and have been utilized extensively in various fields. MIPs were discovered to be highly suitable for use in chromatography, particularly liquid chromatography (Arabi et al., 2020). In the racemates resolutions of different molecules using high performance liquid chromatography (HPLC), MIPs have frequently been used as a stationary phase (Bouvarel, 2020). Accordingly, MIPs represent a viable alternative in the recognition systems landscape due to significant advancements in imprinting techniques and new synthetic procedures, as well as their superior recognition specificity and structural predictability (Jamieson et al., 2021). In addition, MIPs can be utilized in environmental research to clean up, prepare samples, and quantify the level of pollutants in wastewater. (Villarreal-Lucio et al., 2022). Recently, the idea of selectively removing novel chemicals utilizing MIPs has shown promise in environmental monitoring. However, most of the research on environmental monitoring has been directed toward designing MIPs that specifically target a particular drug or a class of pharmaceuticals. Nevertheless, pharmaceuticals do not exist in isolation in the environment; rather, they are mixed with various other compounds, some of which share physicochemical properties (Fernandes et al., 2021). Consequently, MIPs must be constructed with many compounds as templates to simultaneously remove most compounds in a group from water to overcome this restriction (Madikizela et al., 2022). The 8th of the 12 principles of green analytical chemistry emphasizes the necessity for methods that enable the analysis of several chemical compounds, as opposed to techniques that only analyse one analyte at a time (Nowak et al., 2021). This lowers analysis expenses even more.

2.1.3.1 Components of MIPs

2.1.3.1.1 Template

Templates play a major role in the spatial arrangement of functional monomers during polymerization. Various target compounds and templates with interests in the environment, biology, pharmaceuticals, chemicals, industry, and medicine have been used for developing MIPs. When choosing a compound to serve as a template for molecular imprinting, it is important to ensure that it will be chemically inert during polymerization and durable at

relatively high temperatures (>60 °C) or when exposed to ultraviolet light (Malik et al., 2019). Using a certain template molecule and a preferred polymerization process, a novel kind of polymer material is created, and the morphological and physicochemical characteristics of the resulting MIP are characterized. Unlike typical receptors, MIPs are selective because of the template molecule's memory. Therefore, in order for a template to be deemed ideal, the following criteria must be achieved: first, its functional groups must not prevent polymerization; second, they must exhibit exceptional thermal and chemical stability during the polymerization process; and third, their functional groups must be able to form complexes with functional monomers (Rahman et al., 2022).

2.1.3.1.2 Functional Monomer

Functional monomer is a compound that is responsible for the binding interactions in the imprinted binding site and for non-covalent molecular imprinting protocols (Rajpal et al., 2023). The selection of an appropriate functional monomer that can interact with the template molecule or ion to produce a complex in the pre-polymerization stage is a crucial element in the effective design of a MIP. The choice of monomer has a major impact on the final properties of the polymer. As a result, the functional monomer is selected with the goal of enhancing the template's functions by producing complexes. To maximize complex formation and, thus, the imprinting effect, it is unquestionably crucial to complement the functionality of the functional monomer with that of the template, for example, H-bond donor with H-bond acceptor (Sajini and Mathew, 2021). A crucial component of molecular imprinting technology is the selection of functional monomers that can interact non-covalently or covalently with template molecules, followed by polymerization with an excessive amount of crosslinking agent to create a certain template location. The monomers used in MIPs must be able to tolerate variations in temperature and chemical composition in addition to environmental stresses.

2.1.3.1.3 Cross-linker

In an imprinted polymer, the cross-linker fulfils three major functions. They serve crucial roles in (i) the management of the polymer matrix's shape, (ii) the stabilization of the imprinted binding site, and (iii) the addition of the polymer matrix mechanical stability (Boukadida et al., 2023). Through the use of a cross-linking agent, the functional monomer is fixed around the template. Cross-linking makes it possible to maintain a firm polymer structure even after the template is removed. Consequently, to attain a macroporous morphology, the crosslinking

agent is therefore often employed in far larger amounts than the functional monomer. Notably, the shape, selectivity, number of recognition sites, and adsorption capacity of MIP can all be impacted by the cross-linker used. The monomer structure surrounding the template will remain unchanged even if the template is removed if the MIP produced has a stiff structure. Therefore, the use of a crosslinker has a substantial impact on the stability of the MIP that is developed (Sajini and Mathew, 2021).

2.1.3.1.4 Initiator

Initiators are applied to trigger the polymerization. The selection of the initiator to start the polymerization depends on the reaction conditions. Thermal or photochemical activation of initiators can result in the production of free radicals, which initiate the polymerization chain reactions (Székely and Klussmann, 2019). The use of thermally and photochemically activated initiators would prevent the polymerization of thermally and photochemically unstable template molecules. Applying photochemically active initiators is necessary when low temperature polymerization is required (Elugoke et al., 2021). Peroxy compounds and azobis, which can be broken down by photolysis and thermolysis (50-70 °C), are substances that are frequently utilized as initiators (Murdaya et al., 2022).

2.1.4 Molecularly imprinted polymers used in sample preparation as highly selective adsorbents

The importance of sample preparation techniques has lately increased due to the increasingly complex experiments being undertaken in the extraction and determination procedures as well as the requirement for advanced outcomes (Kaya et al., 2022a). A number of sample preparation methods, including solid-phase extraction (SPE) and related processes, such as solid-phase microextraction (SPME) and magnetic solid-phase extraction (MSPE), offer analyte concentration, matrix effect elimination, sample medium stability, and sample clean-up (Kaya et al., 2022a). To improve the effectiveness of sample extraction, the right adsorbents are needed. Molecularly imprinted polymers are used to make extremely selective adsorbents because of their specially designed binding sites. The employment of MIPs as adsorbents during the preconcentration and clean-up phases of sample preparation has been rendered possible by their exceptional selectivity and recognition capabilities (Turiel and Martín-Esteban, 2019). MIP-based sorbents are reusable and cost-effective solutions that facilitate the rapid and facile separation of the target analyte from other molecules in the matrix. They are

mostly preferred in sample preparation procedures that rely on extraction. Additionally, one of the main advancements in sorbents for sample preparation is the use of nanoparticles. Application of nano-adsorbents for sample preparation purposes generally offers some benefits, including high adsorption capacity and preconcentration factors in addition to their easy functionalization and reusability, because nanomaterials have a high surface area to volume ratio compared to bulk and microscale materials. Consequently, nanomaterials can significantly increase the binding capacity of MIPs since they have a large surface area and more binding sites. Incorporating nanoparticles into the process of synthesizing unique MIPs results in a hybrid material with novel properties (Fresco-Cala et al., 2020).

2.1.4.1 Molecularly Imprinted Solid Phase Extraction (MISPE)

SPE is a flexible method that uses a sorbent bed and flow-through equilibrium to purify, separate, and concentrate analytes from a sample solution matrix. SPE is a vital approach for sample enrichment and clean-up of aqueous environmental materials (Hu et al., 2021). The first MIPs-related SPE application was published by Sellergren (Sellergren, 1994). After this effective application, numerous MIP-based SPE applications of diverse chemicals in various fields were performed and published in the literature (Yang and Shen, 2022). In order to improve the selectivity of extraction in SPE, MIPs are used as sorbent materials that have the ability to bind the target analyte in complex matrices with high loading capacity, great robustness, and easy preparation. MIPs have recently emerged as an intriguing study area for the creation of sorbents for SPE of chemicals in environmental and occupational samples due to their stability, affordability, and ease of fabrication (Fu et al., 2022, Kaya et al., 2022a). Based on the chemical and physical characteristics of a molecule, SPE is used to extract analytes of interest from other components in complex mixtures. Even though the SPE method is widely employed, it approaches can result in poor recovery, high costs, inconsistent extractions that interfere with the analyte's elution, impure extractions, and slow flow rates are all major problems with SPE (Kanu, 2021). These issues could lead to more difficulties in future, possibly necessitating the repetition of analysis and delaying the transmission of crucial data. Owing to these challenges, it is understandable why the SPE technique has been the subject of improvement and the development of even better, more cutting-edge, and environmentally friendly solutions for sample preparation (Abbasi and Haeri, 2021). Consequently, a number of green processes have been established and implemented. (Nouri et al., 2020). Molecularly imprinted polymer solid phase extraction (MISPE), a type of sorbent,

has exceptional absorption properties that make it possible to extract the target chemical at trace and ultra-trace levels (Tsalbouris et al., 2021). Recently, MISPE was used to analyse traces of target analytes, mostly pesticides, industrial pollutants, and pharmaceuticals (Mohiuddin et al., 2020), in actual waters (Zhu et al., 2019, Mohiuddin et al., 2021), drinking water (Li et al., 2019) and sediment extracts (Duan et al., 2013), and food extracts (Maragou et al., 2020). **Table 2.6** provides a summary of MISPE effectiveness in extracting pharmaceuticals from environmental samples. In particular, modern techniques that can identify target compounds to the nanogram per litre level or below, such as tandem mass spectrometry (MS/MS) or gas chromatography (GC), coupled to mass spectrometry (MS), or liquid chromatography (LC), are frequently used for the identification of pharmaceuticals in various water sources (Kulkarni and Miller, 2022). Liquid chromatography is the most used method because pharmaceuticals have polar properties (Hansen et al., 2020). Nevertheless, the use of liquid chromatography-mass spectrometry (LC-MS) as an environmental control method has quickly increased. Additionally, ultra-performance liquid chromatography (UPLC) has made it possible to create more accurate, quick, and environmentally friendly pharmaceutical analysis procedures in the field of liquid chromatography coupled to tandem mass spectrometry (Fernández-Fernández et al., 2022).

Table 2.6: Pharmaceuticals analysis in environmental samples using MISPE mode.

Matrix	**Class**	**Compounds**	**Mode**	**Technique**	**%Recoveries**	**LOD (µg/L)**	**References**
Ground water, river water, hospital wastewater, and sewage water sample	Tricyclic antidepressants	amitriptyline, nortriptyline, and clomipramine	Multi-template-MIP-SPE	HPLC-PDA	97.99 - 99.89	1-10	(Mohiuddin et al., 2021)
Wastewater samples	Antiretroviral drugs	abacavir, lamivudine, atazanavir, efavirenz, lopinavir, nevirapine and zidovudine	SPE	LC-MS/MS	75-104	0.002 - 0.02	(Abafe et al., 2018)
River water samples	Antibiotics	Raffinose , streptomycin sulfate, kanamycin sulfate, apramycin sulfate, gentamycin sulfate, tobramycin	Dummy MISPE	HPLC-MS/MS	70.8-108.3	0.006-0.6	(Zhang et al., 2020)
Wastewater samples	NSAID	Diclofenac	porous MIP-SPE	HPLC	95.41-124.14	12-20	(Mohiuddin et al., 2020)
Lake and river water samples	Antibiotics	Ciprofloxacin	MISPE	HPLC	87.33-102.50	1.47-2.9	(Zhu et al., 2019)

2.1.4.2 Magnetic solid phase extraction (MSPE)

In SPE methods that rely on magnetic separation phenomena, magnetic characteristics of the MIP have provided a suitable replacement for the conventional MIPs (Chen et al., 2022). It is particularly beneficial to use magnetic MIPs as sorbent materials since they may be used to extract MIPs with great selectivity while still allowing for a quick and easy separation due to the magnetic effect. They are often utilized in MSPE applications. In contrast to the traditional SPE process, MSPE does not require packing sorbent into cartridges, eliminating the drawbacks of column obstruction and high pressure. Scientists discovered that using MIP magnetism was a successful strategy for overcoming the drawbacks of MISPE (Wan et al., 2021). Safariková and co-workers coined the phrase "magnetic solid-phase extraction" (MSPE) for the first time in 1999 (Šafaříková and Šafařík, 1999). For the separation and preconcentration of organic molecules with planar molecular geometries, they employed magnetic charcoal and a reactive copper-phthalocyanine dye that was immobilized on thin silanized magnetite particles. This showed promise due to its user-friendliness, efficiency, and eco-friendliness. As a modified form of SPE, magnetic solid-phase extraction (MSPE) uses magnetic nanoparticles as adsorbents to separate and enrich target molecules in a sample matrix (Yu et al., 2019). MIPs gained even more popularity, in particular, when applied as a coating material for magnetic SPE (MSPE) (Jiménez-Skrzypek et al., 2021). Incorporating magnetic components into MIPs allows for the development of magnetic MIPs with the magnetic reusability property (Cui et al., 2022, Farooq et al., 2022). These magnetic MIPs can be readily extracted and repurposed from the sample solution by using a magnet (Hu et al., 2019). The core principle of MSPE is the use of a magnetic adsorbent, which permits adsorbent dispersion in a wide sample volume (Zhang et al., 2022). Magnetic separation can be used as a simple, cost-effective alternative to centrifugation and filtration by creating a controlled rebinding process by the use of magnetic components in MIP (Kaya et al., 2022a). Magnetic molecularly imprinted polymers are developed by directly forming polymers on the surface of a magnetic substrate (MMIP) (Ramin et al., 2023). The selection of the magnetic adsorbent for MSPE is crucial for attaining good extraction performance since it has a significant impact on the extraction efficiency, enrichment factor, selectivity, and anti-interference ability (Sajid et al., 2021). In a wide range of applications, especially in environmental, culinary, and biological studies, these materials have been widely employed to extract molecules from complicated matrices (Capriotti et al., 2019). Nevertheless, the main issue with MSPE is that the majority of the currently available adsorbents, which are often functionalized nanoparticles, are non-

specific and lack adequate selectivity for certain metal ions (Wang et al., 2022). Thus, demonstrating the immense potential of MSPE methods, which may be used for (ultra) trace measurements of various analytes in a variety of samples (Hagarová, 2020). Developing a novel adsorbent with superior selectivity and adsorption capability is crucial. Diverse synthesis approaches have led to the development of reusable functionalized magnetic adsorbents with enhanced adsorption capacities, which have been effectively employed in MSPE for the identification of pharmaceuticals in environmental samples. As indicated in **Table 2.7**, MSPE has been widely used for the extraction and determination of pharmaceuticals in a variety of matrices. Even though MSPE performs analytically well, more study and development are still needed to make this approach a competitive substitute for conventional SPE in routine analysis.

Table 2.7: Pharmaceuticals analysis in environmental samples using magnetic solid-phase extraction (MSPE) mode.

Class	**Matrix**	**Compounds**	**Technique**	**Recoveries (%)**	**LOD ($\mu g\ L^{-1}$)**	**References**
Antibiotics	Tap water and wastewater samples	sulfamethoxazole and trimethoprim	UV-Visible	95-98	30 - 80	(Mehrabi et al., 2020)
	Wastewater, surface, ground water samples	sulfaquinoxaline, sulfa diazine, sulfamerazine , sulfamethoxazole, su lfapyridine, and sulfathiazole	UHPLC-MS/MS	82-106.2	490-1590	(Guo et al., 2018)
NSAIDs	Groundwater, tap and river water	Naproxen, diclofenac and ketoprofen	HPLC-DAD	91.20 -101.13	0.2	(Li et al., 2019)
	River water samples	Ketoprofen, naproxen and diclofenac	HPLC	84.67 - 113.73	0.2-0.4	(Han et al., 2019)
	Wastewater samples	Naproxen, and triclosan	HPLC	81-89	0.5-0.8	(Li et al., 2018)

Emerging contaminants (ECs)	Wastewater samples	Carbamazepine, Diclofenac, Gemfibrozil, Sulfamethoxazole and, Triclosan	UHPLC-Orbitrap MS	58.4-102.6	11000-33600	(Kalaboka and Sakkas, 2023)

2.1.4.3 Dispersive solid phase extraction (DSPE)

Dispersive solid phase extraction (d-SPE), a more recent improvement on the traditional SPE method, is gaining popularity due to its exceptional simplicity, speedy extraction time, and reduced solvent expenditure requirements, along with its great efficacy and broad applicability (Büyüktiryaki et al., 2020). Dispersive solid phase extraction, or d-SPE, is a pre-treatment technique that has been applied and is thought to be a versatile, dependable, and selective technology with several uses (Jayasinghe et al., 2020). This approach is based on dispersing a solid sorbent in liquid samples to achieve the extraction, separation, and cleanup of different analytes from complex matrices (Jakubus et al., 2019). It is regarded as a micro- and macroscale method of extraction and cleaning (Ali et al., 2022). Target analytes are adsorbed to the surface of the adsorbent dispersion in the solvent in dispersive solid-phase extraction (d-SPE), which includes adding adsorbents to the sample solution rather than placing them inside the SPE column. With this method, the issue of conventional SPE's insufficient contact area is partially addressed, and the area of contact between targets and adsorbents is significantly increased. (Arabi et al., 2020). However, to ensure selectivity extraction, removal, or preconcentration of analytes contained in analytical matrices, the sorbent must be chosen carefully, considering chemical and physical features that allow for maximum interaction between the sorbent and the analytes (Maranata et al., 2021). The advantages of DSPE have led to numerous applications based on the use of relatively different adsorbents for pre-concentration and/or clean-up reasons, and some techniques have involved using MIPs as adsorbents (Zou et al., 2022, Lu et al., 2019). **Table 2.8** provides an executive summary that highlights the efficacy and efficiency of the DSPE approach in pharmaceutical analysis.

Table 2.8: Pharmaceuticals analysis in environmental samples using dispersive solid-phase extraction (d-SPE) mode.

Matrix	**Class**	**Compounds**	**Mode**	**Technique**	**Recoveries (%)**	**LOD (µg L^{-1})**	**References**
Tap water, lake water, river water, and waste water samples	NSAIDs	Ketoprofen, diclofenac, ibuprofen and mefenamic acid	DµSPE	HPLC-UV	85.1-106.4	0.21-0.51	(Abd Wahib et al., 2018)
Wastewater samples	Antibiotics	Ciprofloxacin, danofloxacin, and enrofloxacin	d-SPE	HPLC	90-99	0.05-0.2	(Dimpe and Nomngongo, 2019)
Wastewater, surface water samples	Multiclass pharmaceutical	Metronidazole, sulfamethoxazole, naproxen and diclofenac,	d-SPE with MWCNTs	LC-ESI-MS/MS	81 - 103	0.01-0.08	(Jakubus et al., 2019)
River water samples	Fluoroquinolones	Norfloxacin and enrofloxacin	dt-MIP-DSPE	HPLC	80.9-101.0	0.22- 0.67	(Lu et al., 2019)
Tap water, surface seawater and lake water samples	Antibiotics	Sulfadiazine, sulfamerazine, sulfamethazine, and sulfamethoxazole	MIP-DSPME	HPLC-DAD	90.5-101.9	<0.03	(Lu et al., 2020)

Surface water samples	Antifungal/antibiotic	Griseofulvin	surface molecularly imprinted polymers SMIP-DSPE	HPLC	91.6-98.8	10	(Bashir et al., 2020)
Wastewater samples	anticonvulsant drug	Carbamazepine	DSPE	HPLC-DAD	85.5-98%	0.51	(Hassan et al., 2021)
Wastewater and river water samples	ARVDs	Nevirapine and zidovudine	Dμ-SPE	HPLC-DAD	91.6 - 99.1%	0.20 - 0.23	(Akawa et al., 2021)

2.1.4.4 NanoMIPs

Due to their high selectivity, superior sorptive and adsorptive properties, improved thermal, chemical, and mechanical stability, and increased device longevity when used as adsorbents, nanomaterials are the key trends in sample preparation sorbents (Wen, 2020). As a result of their enormous specific surface areas, nanomaterials show great adsorption capabilities, reactivity, and free mobility in solution. It is commonly recognized that nanoparticles have properties that depend on their size and shape and that they can be used in a variety of scientific fields (Baig et al., 2021, Khan et al., 2022b). Compared to traditional approaches, MIP synthesis utilizing nanotechnology has received a lot of attention lately (Yadav et al., 2021). In comparison to traditional MIP, nanomaterials offer additional benefits including increased sensitivity and selectivity (Shah et al., 2021). Nanotechnology can be used to efficiently remove a range of pollutants from contemporary wastewater (Mondal et al., 2023). The use of nanomaterials is necessary for the development of more efficient water treatment and remediation systems to replace traditional techniques. During the imprinting process, nanoparticles have often been employed as signal-amplification agents to increase the effectiveness of MIP-based diagnostic systems. (Xu et al., 2020). As a result, MIPs display the inherent properties of polymers, including ease of production, affordability, resilience, and stability. Furthermore, incorporating nanoparticles to their polymeric structure can enhance some of these characteristics and offer new functions (Ramin et al., 2023, Sullivan et al., 2022). Notably, MIP nanoparticles (nanoMIPs) have attracted the most attention from researchers among all nanomaterial sorbents due to their potential for use in significant extraction procedures (Mazari et al., 2021). Moreso, nanoMIPs are a significant advancement in imprinting technology since they address several issues with bulk polymerized MIP, including uneven recognition site distribution, irregular shape, partial template removal, and delayed mass transfers (Rahman et al., 2022). The summary of nanoparticles application on the removal pharmaceuticals in water and wastewater is shown in **Table 2.9**. Novel analytical methods for the removal of pharmaceuticals with nanoMIPs combined ultraperformance liquid chromatography tandem mass spectrometry (UPLC–MS/MS), high Performance liquid chromatography (HPLC), gas chromatography (GC) etc.

Table 2.9: Pharmaceuticals analysis in environmental samples using nanoparticles.

Matrix	**Class**	**Mode**	**Technique**	**Recoveries**	**LOD (µg L^{-1})**	**Ref**
Wastewater samples	NSAIDs	Core-shell magnetic Fe_3O_4@MIL-100(Fe) nanoparticles	UPLC-MS/MS	75.2-105.2	0.1-30	(Liu et al., 2019)
Tap water samples	Nitroaromatic	nanoMIPs	Fluorescence	90-100.3	0.6-0.7	(Elbelazi et al., 2019)
Wastewater samples	NSAIDs	(nanoMIPs)	SPE–HPLC	42-100	3.7-15	(Altintas et al., 2016)
River water, tap water and municipal wastewater samples	NSAIDs	Fe_3O_4 nanoparticles - MSPE	HPLC	93.6-98.9	0.2 - 300	(Alinezhad et al., 2018)
Dam and river water samples	NSAIDs	Magnetic cellulose nanoparticles	HPLC	85 - 116	3.2-7.2	(Abujaber et al., 2018)
Ground water and wastewater samples	NSAIDs	Fe_3O_4@AgNPs	HPLC	89- 93	200	(Vicente-Martínez et al., 2020)

2.1.4.4.1 Synthesis of nanoparticles

Several nanomaterials have been developed to reduce the concentrations of hazardous pollutants in contaminated water because they have enhanced characteristics as a consequence of their nanoscale influence (Patil, 2020). As a result, it has been demonstrated that various forms of nanomaterials are efficient in eliminating organic contaminants, inorganic anions, heavy metals, and microbes (Roy et al., 2021). Metallic nanoparticles (NPs) are unique among the synthetic nanomaterials that have so far been created because of their electrical conductivity, catalysis, high chemical stability, and antibacterial capabilities (Ezeuko et al., 2021). Furthermore, metal nanoparticles are useful for adsorption because of their high adsorption capacity, effective surface area, catalytic activity, reactivity, and superior textural qualities. Additionally, they have the ability to bind negatively and positively charged contaminants (Sahoo and Prelot, 2020). Metallic nanoparticles such as silver nanoparticles (AgNPs), silica oxide nanoparticles (SiO_2 NPs), etc have demonstrated their potentials in application for removal of pharmaceuticals in wastewater (Remya et al., 2022). The most popular source of silver ions is silver nitrate ($AgNO_3$) because it easily and quickly produces nanoparticles and with a high yield of nanoparticles (Alzubaidi et al., 2023). Due to their exceptional plasmonic activity, a broad spectrum of antibacterial activities, chemical stability, high thermal and electrical conductivity, and catalytic capabilities, silver nanoparticles (Ag-NPs) have drawn a lot of attention among other types of metal nanoparticles (Panhwar et al., 2022). In the synthesis of nanoparticles (NPs), the reducing and capping agents play a key role (Al-Khattaf, 2021). In particular, numerous synthetic approaches have been established, especially for the synthesis of AgNPs (Arif and Uddin, 2021). Accordingly, the hazardous solvents, reducing agents, and surfactants employed, as well as some of the chemical processes used during the syntheses, have generated questions about the health and environmental risks they pose (Castillo-Henríquez et al., 2020). With the invention of an environmentally friendly method for synthesizing AgNPs employing appropriate selections of reductive, stabilizing, and solvents, environmental protection has become an increasing concern (Ahmed et al., 2022). Hence, a green strategy that is sustainable, cost-effective, and kind to the environment (using non-toxic chemicals or living organisms, for example) is essential for the synthesis of Ag NPs (Khan et al., 2022a, Mustapha et al., 2022). Notably, the concept of producing green nanoparticles (NPs) was initially introduced by Raveendran and co-workers, who used D-glucose as a reducing agent and starch as a capping agent to make starch silver nanoparticles (AgNPs) (Raveendran et al., 2003). The chemical reagents utilized in the production of NPs

have direct or indirect harmful effects on the environment (Tortella et al., 2020). Various reducing and capping agents have been used to stabilize the nanoparticles and stop them from aggregating (Sidhu et al., 2022). Moreover, several hazardous substances, including sodium borohydride, citrate, N, N-dimethyl formamide, and hydrazine hydrate, were employed as reducing agents in some processes to produce AgNPs (Zhu et al., 2020). Understanding the synthesis of nanoparticles by environmentally friendly methods, like using non-toxic or biological reagents, is therefore significant. Chemical reduction of silver salts is the most widely used method of producing Ag colloidal particles (Gahlawat and Choudhury, 2019). The ability to donate electrons for the reduction of Ag^{+} ions to Ag^{0} is possessed by chemical and biological agents. **Figure 2.3** depicts the formation of AgNPs by the reduction of Ag^{+} ion to Ag^{0}, and its stabilization by reducing/capping agent. Hence, the nanoparticles produced can be kept in storage for a long period without losing their stability. Notably, based on numerous investigations, nanomaterials show high promise for practical use in the treatment of industrial and water-based effluents (Ahmed et al., 2022).

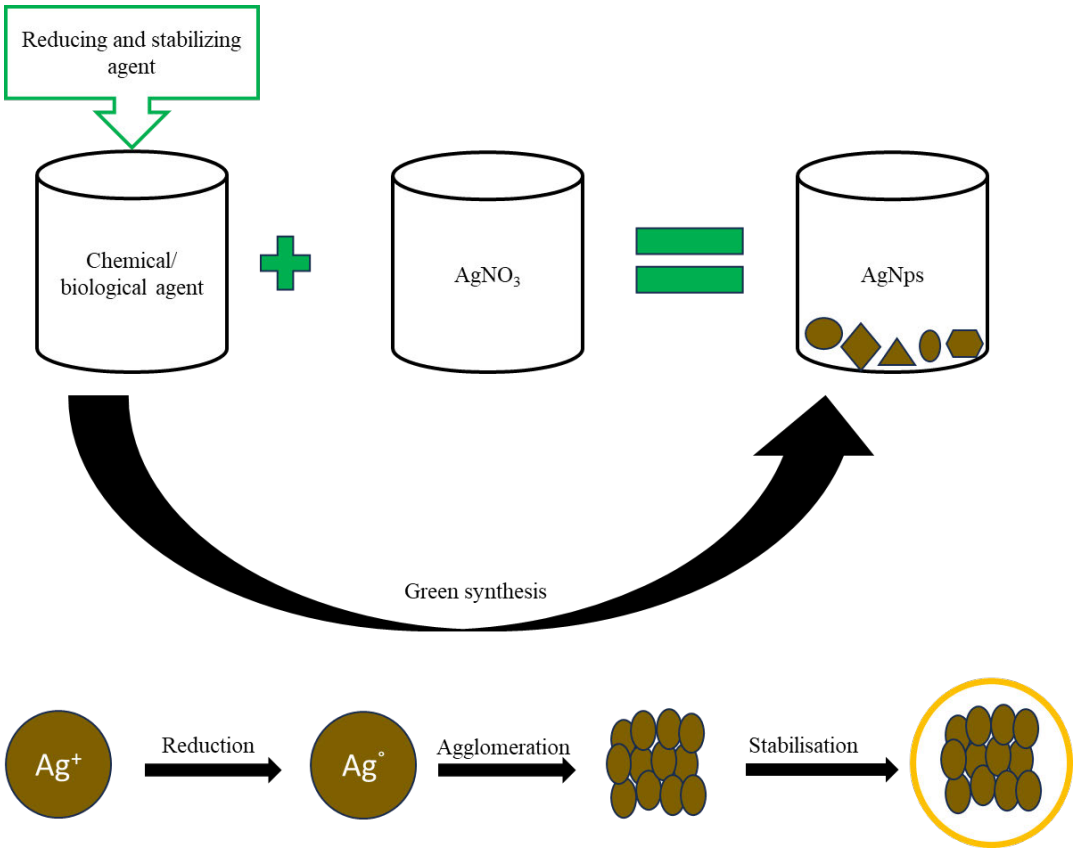

Figure 2.3: Mechanism for the synthesis of silver nanoparticles

2.1.4.4.1.1 Starch as capping and reducing agent in the synthesis of AgNPs

Nontoxic chemicals and renewable materials are selected because they have the advantage of reducing environmental risk. Starch is a highly beneficial raw material that may be used to synthesize a multitude of functional polymers since it is a naturally occurring biopolymer that is abundant and renewable (Madani et al., 2022, Zaman et al., 2022). Accordingly, starch is a biopolymer that is an inexpensive, effective as a surfactant agent and ecologically friendly, its usage as a green capping and stabilizing agent in aqueous solutions has lately grown in importance in the synthesis processes of nanomaterials (Taha et al., 2022). Starch was chosen because it is environmentally safe, biocompatible, and has hydroxyl groups in its template that prevent nanoparticles from aggregating (Yuan et al., 2021). Due to the presence of biological chemicals acting as capping agents on their surfaces, NPs synthesised using this method have no negative effects on the environment and show good biocompatibility with living systems (Batool et al., 2019).

2.1.4.4.1.2 Plants as capping and reducing agent in the synthesis of AgNPs

The synthesis of plant-based nanoparticles involves minimal or no toxic chemicals and biologically safe solvents. Therefore, it is regarded as a green method of producing nanoparticles (Patil, 2020). Consequently, green synthesis of nanoparticles is an environmentally benign method that can open the door for researchers all around the world to investigate the potential of various plants to generate nanoparticles. Plants can be thought of as nano factories that produce metallic nanoparticles in a safe and advantageous manner, with the potential for large-scale production (Wani et al., 2021). In addition to being environmentally benign, plants also produce materials at a faster rate than other biological models. Given its accessibility, green manufacturing of AgNPs via biological extract is a beneficial and advantageous method of producing metallic nanoparticles. Hence, the utilization of plant extracts is currently regarded as being more desirable for the synthesis of metallic NPs due to its simplicity, low cost, one-pot method, and high reaction rate. Notwithstanding, plant extracts have demonstrated significant potential for the synthesis of silver nanoparticles (AgNPs). Accordingly, the synthesis of AgNPs has made considerable use of extracts from either the complete plant or its parts, such as roots, leaves, fruits, bark, flowers, and seeds (Alshameri and Owais, 2022). The metal ions are reduced and aggregated into nanoparticles by both primary (Carbohydrates (simple sugars and polysaccharides), proteins, and lipids) and secondary (alkaloids, glycosides, terpenes, tannins, flavonoids, acetogenins, etc.,) metabolites

found in extracts. Most often, coenzymes, secondary metabolites, and biomolecules found in plant extracts function as reducing and stabilizing agents in the green synthesis of metal nanoparticles (Jagwani and Krishna, 2021). Except in a few cases where external stabilizing chemicals have been applied, plant extracts serve as both a reductant and a stabilizer. AgNPs have been produced using a variety of plants, including medicinal plants, ordinary spices, some exotic weeds, plants that produce essential oils and alkaloids, etc (Wani et al., 2021). Moreover, these plants are utilized to modify the surface of silver nanoparticles, enhancing their capacity as photocatalysts and removal effectiveness. Environmentally friendly nanoparticles made from plant extracts are preferred over chemically made ones used in water treatment. This is because they are less expensive, non-toxic, and not linked to secondary environmental pollution from unpleasant chemicals. This is due to their lower cost, lack of toxicity, and lack of connection to unfavourable chemical-induced secondary environmental pollution. The summary of several studies on the synthesis of nanoparticles using plants as reducing and/ capping agent are depicted in **Table 2.10**. Consequently, plant synthesised nanoparticles shown to have an excellent removal of pharmaceutical industry compounds.

Table 2.10: Reports of plant extract silver nanoparticles

Matrix	Class	Compounds	Nanoparticles	Recoveries	LOQ (µg L^{-1})	References
Wastewater samples	NSAID	ibuprofen	Gold@Silver@Silver chloride (Au@Ag@AgCl) core–double shells nanoparticles (NPs) using *Momordica charantia* leaves extract.	98	0.01 -1	(Devi and Ahmaruzzaman, 2017)
Wastewater samples	Anti-tumor drug	mitoxantrone	Fe NPs loaded on rGO and green tea extract	76.8-99.9	0.1-0.4	(Weng et al., 2018)
Wastewater samples	Anti-epileptic drug	Carbamazepine	Fe/Cu was successfully prepared by green synthesis by Ficus Benjamina leaves	95	0.4	(Abdel-Aziz et al., 2019)
Wastewater samples	Antibiotic and analgesics	Ciprofloxacin, cephalexin, and metronidazole	Fe_3O_4@CuO nanoparticles using Euphorbia polygonifolia extract	89-96	10	(Pakzad et al., 2020)
Wastewater samples	Anti-tumour drug	Mitoxantrone	graphene oxide @ iron nanoparticles (rGO@Fe NPs) were successfully prepared using green tea extract	76.88-99.9	10	(Wu et al., 2020)

Pond, river, tap and wastewater samples	Antibiotic	Sulfisoxazole	Sutherlandia frutescence (S. frutescens), leaf extract was used during the synthesis of Cadmium Sulphide (CdS) nanostructures	91	10	(Munyai et al., 2021)
Wastewater samples	NSAIDs	ibuprofen, naproxen, diclofenac, and ketoprofen	nZVI synthesized from green tea extracts and incorporated into a cationic resin (R-nFe)	27-99	5	(Barka et al., 2023)

2.1.4.4.1.3 Macadamia nut shells as potential capping and reducing agents in the synthesis of nanoparticles.

Researchers working to create affordable and effective materials for the adsorption of pollutants have paid close attention to biomaterials made from agricultural waste. Particularly, nuts are one of the most abundant natural resources that are consumed extensively as highly valued nourishment. However, their by-products, such as leaves, shells, and fruit that is left on the ground, are considered useless as they inedible (Cap et al., 2022). Agricultural wastes, such macadamia nut shells (MNS), are largely cross-linked polymeric chains containing chemically active functional groups, like lignin, cellulose, and hemicellulose (Maleki et al., 2023). This allows them to adsorb various contaminants from water via ion exchange and surface complexation mechanisms (Nekhavhambe et al., 2022). Additionally, they have a highly developed microporous structure and a large surface area, both of which boost their sorption capacity. Approximately 59,050 tons of macadamia nuts in their shell were produced in South Africa as of 2019, the production is anticipated to rise over the following ten years, given the current production and the cultivation of new macadamia trees (Sibulali, 2020). The accumulation of Macadamia shells rises steadily along with the growing rate of the plants that produce macadamia nuts. Waste Macadamia nutshells does not seem to have much of a use other than to heat fields and compact roads. The primary methods for dealing with MNS are to discard and burn them, both of which have resulted in significant resource waste and environmental degradation (Morifi, 2021). As such, making MNS a more valuable resource is an important and pressing issue. The beneficial compounds found in MNS can help create cost-effective and environmentally friendly solutions. Polyphenols are compounds found in the various portions of these nutshells, and they can be used as reducing agents to produce nano-systems (Orooji et al., 2022). The increasing global environmental and economic crises have led to a surge in the development of the usage of biodegradable and ecologically friendly polymers to remove pharmaceuticals from wastewater. Due to the valuable molecules found in nutshells, it would be desirable to create an adsorbent of nanoparticles to extract pharmaceuticals from wastewater. These portions can also be employed as stabilizing and reducing agents for nanoparticles (Aswathi et al., 2022). It was discovered that macadamia nutshells had lignocellulosic properties that make them perfect for adsorption investigations (Morifi et al., 2022). Intriguingly, Macadamia nutshell extracts have become popular in recent years for use in the production of fragrance, hair, and skincare products (Shi et al., 2022). Thus,

application of macadamia nutshell as a reducing and a capping agent can represent a new eco-friendly method for the synthesis of silver nanoparticles.

2.1.4.4.1.4 Moringa oleifera as capping and reducing agent in the synthesis of nanoparticles.

The drumstick tree, or Moringa oleifera, is a species of tree native to north-western India (Raina and Kaushik, 2020). It is a type of economic tree that is typically found in tropical and some subtropical regions. It is also considered as a significant crop in a number of other nations, including the Philippines, Sudan, Ethiopia, and South Africa (Sokunbi et al., 2019). All the plant's parts are deemed valuable and are said to offer a variety of traditional and health benefits, including as treatment and management of asthma, diabetes, obesity, hypertension, and other conditions (Islam et al., 2021). Moringa is a rich source of several phytochemicals, which include phenols, flavonoids, vitamins, minerals, quercetin and kaempferol, thus providing a wonderful synthesis agent for the necessary nanoparticles (Hassan et al., 2021). More bioactive chemicals are present in the leaves, which enhances their therapeutic efficacy. The production of nanoparticles using moringa oleifera and other plants is leading to "truly green chemistry," which is more ecologically friendly and cost-effective than chemical and physical approaches and is easily scaled up for large scale syntheses. Moringa has been used in many studies for the synthesis of nanoparticles (Abel et al., 2021, Mohammed et al., 2022).

2.1.4.4.1.5 Platanus acerifolia (London plane)

The "king of street trees," Platanus acerifolia, is a tree that is commonly planted in metropolitan areas around the world. The tree Platanus acerifolia, is also known as the London Plane (Sanusi and Livesley, 2020). The Platanaceae family includes the plane tree, which is well-known for its majesty and longevity. Every autumn and winter, the Platanus acerifolia sheds its leaves, creating a lot of waste (Akpomie and Conradie, 2022). Currently, groundwater eutrophication and atmospheric pollution are two of the biggest environmental issues caused by the disposal and burning of discarded deciduous leaves. Therefore, it's crucial to find a use for this waste. Notably, platanus acerifolia is inexpensive, easily accessible, and utilizable. Applications for its powdered leaves include the synthesis of nanoparticles and the removal of heavy metals from industrial wastes (Kumar et al., 2022). Therefore, using leaf litter for synthesis of nanoparticles provides advantages for waste reduction and environmental preservation. Platanus acerifolia-derived proteins, carbohydrates, polymers, flavonoids, alkaloids, and a

number of antioxidants have demonstrated their value as capping and stabilizing agents during the production of nanomaterials. It initiates the reduction reaction of Ag^{+} ions by accepting electrons and forms Ag° nanoparticles. Platanus acerifolia is currently being used in the pharmacy industry for the flavonoid-metal chelation mechanism (Wu et al., 2022), Unfortunately, platanus acerifolia leaves have not been used very often in the synthesis of nanoparticles.

2.1.5 Adsorption studies

Adsorption is the most effective way to remove different types of pollutants from wastewater, and it is now being used worldwide (Maksoud et al., 2020). This led to the advancement of adsorption science and technology, which in turn prompted a number of innovative investigations on the technique's potential applications in the treatment of wastewater and water. Globally, people's quality of life has improved as a result of the high-impact findings and patents generated by these investigations. (Unuabonah et al., 2019). Particularly, adsorption is a phenomenon that happens at the surface and is specifically defined as the adherence of contaminants to the surface of an adsorbent by physical, chemical, and electrical attraction. (Rathi and Kumar, 2021). Consequently, the reversible process of adsorption allows atoms, ions, or molecules to build up on the surface of an adsorbent. It is an elementary exothermic reaction based on surfaces (Büyüktiryaki et al., 2020). Moreover, the material that accumulates on the surface of an adsorbent is referred to as an adsorbate. Thus, the adsorption process is produced by the interaction of the active centres of the adsorbent and adsorbate (Zhang et al., 2019). The adsorption process is impacted by the type of the adsorbent and adsorbate, pH, temperature, contact time, pollutant concentration, adsorbent particle size, the presence of other wastes, and the experimental circumstances (Sajid et al., 2022). Adsorption should be studied from a thermodynamic, isotherm and kinetic perspective to learn more about its functioning and mechanism (Mangla et al., 2022). Further investigation will be essential to completely understand the equilibrium adsorption capacity of adsorbents and the adsorption mechanism for pharmaceuticals.

Adsorption is classified into two groups based on the type of interaction that occurs between the adsorbed molecule and the adsorbent surface: chemical (chemisorption) and physical (physisorption) adsorption (Büyüktiryaki et al., 2020). Consequently, in physical adsorption the link between the adsorbent and adsorbate is created by dipole-dipole interaction and van

der Waals forces. Thus, it can be monolayer or multilayer in nature (Oba et al., 2021). Notwithstanding, it normally happens quickly, is exothermic, reversible, and does not need activation energy. As temperatures rise, physical adsorption decreases (Barquilha and Braga, 2021). In contrast, chemisorption occurs when the adsorbent and the adsorbate interact chemically and transfer electrons, respectively (Al-Ghouti and Da'ana, 2020). Adsorbate attaches itself to the solid surface by forming a chemical bond. This interaction is far more powerful than physical adsorption. The amount of enthalpy change is one criterion for separating chemical from physical adsorption. Compared to physisorption, the enthalpy of chemisorption is significantly larger (Alaqarbeh, 2021). Chemical adsorption is known as an endothermic reaction because of the very strong interactions that result in chemical bonds (Gil, 2023).

2.1.5.1 Modelling of adsorption

Several objectives are served by modelling adsorption processes. The primary processes used in the adsorption process are greatly influenced by the nature of the adsorbent and the properties of the contaminant to be eliminated (Rathi and Kumar, 2021). A model can offer a mechanistic understanding of the experimental data, allowing the experimental observation to be grounded in theoretical framework (Khalil et al., 2020). To predict the mechanics of different adsorption systems, modelling experimental data from adsorption processes is a crucial tool (Ayawei et al., 2017, Abbasi et al., 2022). The Mathematical modelling of the adsorption phenomena involves equilibrium isotherm models, adsorption kinetics models and thermodynamics (N'diaye and Kankou, 2020). Model parameters can be used to compare adsorbent capabilities for a particular target pollutant.

2.1.5.1.1 Adsorption isotherms

Adsorption isotherms are essential tools for understanding how sorbates and sorbents interact, particularly the quantity of analyte adsorbed, and the amount left unadsorbed once equilibrium is attained (Azizian and Eris, 2021). They also describe the relationship of equilibrium between the amount of the adsorbed material and the pressure or concentration in the bulk fluid phase at a constant temperature (Ayawei et al., 2017). To fit adsorption experiment data Freundlich, Langmuir, Henry and Temkin isotherms are frequently employed (Al-Ghouti and Da'ana, 2020, Kalam et al., 2021). Nonetheless, the Langmuir and Freundlich two-parameter models are the most used equations because of their popularity, and the relevant information that they provide

(Al-Ghouti and Da'ana, 2020). When pharmaceuticals are absorbed onto various adsorbents, these models suggest that homogenous monolayer or heterogeneous multilayer adsorption will predominate. A significant number of studies used the approach of linear regression modelling for these isotherms. The frequently reported parameters are Qmax which is the maximal adsorption capacity (mg/g), K_L, the equilibrium constant for Langmuir adsorption and the R_L factor which determines the desired kind of adsorption for the adsorption process in Langmuir isotherm. In the Freundlich model, K_F the Freundlich constant, and "n" the adsorption strength constant and 1/n the heterogeneity factor. The data obtained from the parameters of these isotherms is used to assess the correlation coefficient and the standard errors for each parameter to find the best fit. Isotherms parameters in **Table 2.11** shows adsorption of pharmaceuticals onto MIPs under certain experimental temperature, pH, agitation speed, contact time, initial concentration of adsorbate solution, and concentration of adsorbent conditions. It was observed in **Table 2.11** that the linearized Freundlich model for nevirapine (Khulu et al., 2021), carbamazepine (Hu et al., 2023) and naproxen (Husin et al., 2021) was favoured with higher R^2 values of 0.9071, 0.9950 and 0.9964 compared to 0.8765, 0.9614 and 0.8409 for the Langmuir model. This assumes heterogeneity of the binding surface energies of the MIP resulting in multiple interactions between nevirapine and the MIP. Given the obtained correlation coefficients, the Langmuir isotherm was well-fitted by diclofenac (Nkosi et al., 2022), sulfamethoxazole (Qiu et al., 2020), ciprofloxacin (Bazi et al., 2021), and tetracycline (Khatibi et al., 2021). Consequently, the strong agreement and good fit for the Langmuir isotherm was perhaps evidence of the dominant nature for the adsorption of these compounds, which may frequently lead to monolayer adsorption on the surface of the adsorbents.

Table 2.11: Adsorption isotherms data corresponding to adsorption of pharmaceuticals by Molecularly Imprinted Polymers (MIPs)

Pharmaceutical	**Class**	**Freundlich**			**Langmuir**				**References**
		K_F	**n or 1/n**	**R^2**	**Q_{max} (mg g^{-1})**	**R_L**	**K_L**	**R^2**	
Tetracycline	Antibiotic	35.85	1.981	0.953	416.5	0.847	0.0018	0.994	(Khatibi et al., 2021)
Sulfamethoxazole		26	0.575 ± 0.003	0.965	77 ± 3	-	0.498 ± 0.003	0.998	(Qiu et al., 2020)
Ciprofloxacin		17.71	0.043	0.941	112.3	0.0017	0.171	0.999	(Bazi et al., 2021)
Diclofenac	NSAIDs	-	-	0.9918	5.643	-	1.160	0.9999	(S'busiso et al., 2022)
Naproxen		4.0486	1.133	0.9964	90.91	0.0474	0.3453	0.8409	(Husin et al., 2021)
Nevirapine	ARV	2.8	1.042	0.9071	188	-	3.19×10^{-3}	0.8765	(Khulu et al., 2021)
Carbamazepine	antiepileptic	8.60	2.78	0.9950	40.42	-	0.10	0.9614	(Hu et al., 2023)

2.1.5.1.2 Adsorption kinetics

A basic theory for assessing the adsorption process is called adsorption kinetics (Vareda, 2023). Adsorption kinetics, which governs the rate at which adsorption occurs, is the most important factor to consider when developing an adsorption system (Al-Ghouti and Da'ana, 2020). The dynamics of batch adsorption experiments are explained by kinetic equations. These investigations aid in clarifying the process' physicochemical features, such as the rate-limiting step and the adsorption rate. The pseudo-first-order (Lagergren) and pseudo-second-order models are by far the most employed equations for describing adsorption dynamics (González-López et al., 2022). The R^2, the pseudo-first-order rate constant (k_1), the pseudo-second-order adsorption rate constant (k_2), and the amount of adsorbate adsorbed at equilibrium (q_e) are the most frequently reported parameters for adsorption kinetics. Notably, the adsorption kinetic parameters of various pharmaceuticals using MIPs as an adsorbent are presented in **Table 2.12**. The reported R^2 values for the pseudo-first order was 0.5748, 0.952, 0.3252, 0.9423, 0.104, 0.978 and 0.7819 while for the pseudo-second order, the R^2 values was 0.9968, 0.9999, 0.9990, 0.9960, 0.9999,0.979 and 0.9999 for nevirapine (Khulu et al., 2021), ciprofloxacin (Bazi et al., 2021), diclofenac (Nkosi et al., 2022), ibuprofen (Nkosi et al., 2022), naproxen (Husin et al., 2021), sulfamethoxazole (Qiu et al., 2020) and carbamazepine (Hu et al., 2023), respectively. A poor correlation coefficient was found for first-order compared to the pseudo-second-order model, showing that the first-order kinetic model is less suitable since it did not obey the straight line. Hence, these results showed that the adsorption process followed the pseudo-second-order kinetic modelling, indicating that the interaction between the MIP and these pharmaceuticals was through chemisorption. Moreover, the results of the adsorption capacity show that the predicted adsorption capacity (qe_{cal}) from the pseudo-second-order models is closer to the experimental adsorption capacity (qe_{exp}) than the pseudo-first-order kinetics, so the main mechanism of ciprofloxacin, sulfamethoxazole, diclofenac, naproxen, nevirapine and carbamazepine adsorption process by MIP is chemical adsorption (Qiu et al., 2020., Nkosi et al., 2022).

Table 2.12: Kinetics parameters corresponding to adsorption of pharmaceuticals by Molecularly Imprinted Polymers (MIPs)

Pharmaceutical	**Class**	**Psuedo-first-order**				**Psuedo-second-order**			**References**
		qe_{exp} (mg g^{-1})	**qe_{cal} (mg g^{-1})**	**K_1 (min^{-1})**	**R^2**	**Q_{cal} (mg g^{-1})**	**K_2 (g mg^{-1} min^{-1})**	**R^2**	
Sulfamethoxazole	Antibiotic	12.3 ± 0.2	11.9 ± 0.3	0.471 ± 0.004	0.978	13.8 ± 0.7	0.001 ± 0.004	0.979	(Qiu et al., 2020)
Ciprofloxacin		112.3	14.46	0.046	0.952	123.4	0.007	0.9999	(Bazi et al., 2021)
Diclofenac	NSAIDs	1.247	1.411	-	0.3252	-	11.8	0.9990	(S'busiso et al., 2022)
Ibuprofen		1.248	1.350	-	0.9423	-	12.1	0.9960	(S'busiso et al., 2022)
Naproxen		3.064	0.1852	0.0119	0.104	2.994	0.2816	0.9999	(Husin et al., 2021)
Nevirapine	ARV	299.1 ± 7.6	27.9	5.98×10^{-3}	0.5748	147.1	2.83×10^{-3}	0.9968	(Khulu et al., 2021)
Carbamazepine	Antiepileptic	8.87	1.54	0.029	0.7819	8.86	0.14	0.9999	(Hu et al., 2023)

2.1.5.1.3 Thermodynamics studies

Predicting the mechanisms of adsorption requires the use of thermodynamic studies. Three thermodynamic parameters are evaluated for adsorption thermodynamics, and their values are determined. Thermodynamic metrics like standard change in enthalpy ΔH°, standard change in entropy changes $\Delta S°$, and standard change in Gibbs free energy $\Delta G°$ are used to evaluate the spontaneous nature or feasibility, exothermic or endothermic nature, and the system entropy changes. They are crucial thermodynamic variables for the study of adsorption mechanisms since they can attest to the process's feasibility, spontaneity, and heat exchange (Gorban et al., 2021). The literature thermodynamic parameters obtained under experimental conditions of pharmaceuticals initial concentration, agitation speed, pH, contact time, and temperature are shown in **Table 2.13**. The positive signs of $\Delta H°$ and $\Delta S°$ indicated that the adsorption process of tetracycline (Khatibi et al., 2021), carbamazepine (Hu et al., 2023) and diclofenac (Liu et al., 2022) obeyed an endothermic nature and there was an irregular increase of randomness on their interaction with the adsorbent. This might be brought on by the water molecule's increased translational entropy as well as the decrease in the absorption of pharmaceuticals. Moreover, the negative values of $\Delta S°$ was brought on by the decreasing randomness at the solid-solution interface during the adsorption phase, and the negative value of $\Delta H°$ indicates that the adsorption process was exothermic for ciprofloxacin (Bazi et al., 2021) and naproxen (Husin et al., 2021) adsorption. In addition, the reported value of $\Delta G°$ was negative, indicating that the adsorption of ciprofloxacin (Bazi et al., 2021) and naproxen (Husin et al., 2021) was spontaneous, thermodynamically possible, and chemically regulated at low temperature.

Table 2.13: Thermodynamics parameters corresponding to adsorption of pharmaceuticals by molecularly imprinted polymers (MIPs)

Pharmaceutical	**Class**	**Temperature (K)**	**ΔG° (kJ mol^{-1})**	**ΔH° (KJ mol^{-1})**	**ΔS° (kJ mol^{-1} K^{-1})**	**References**
Tetracycline	Antibiotic	293	-14.37	41.75	0.195	(Khatibi et al., 2021)
Ciprofloxacin		293	-7.47	-9.27	-3.3 x 10^{-3}	(Bazi et al., 2021)
Carbamazepine	Antiepileptic	298	-5.02	41.54	0.15	(Hu et al., 2023)
Naproxen	NSAIDs	298	-2965.31	-23.61	-0.06625	(Husin et al., 2021)
Diclofenac		298	-25.56	0.0337	0.0014	(Liu et al., 2022)

2.1.6 Conclusion

The review covered the effect of pharmaceuticals on human health and the environment. Compared to the rest of the globe, South Africa has much less research on environmental assessment and the removal of pharmaceuticals from WWTPs, but the studies that have been conducted have been extremely useful in understanding the country's current condition. The findings of the current study add to previously published information about the presence of pharmaceuticals in African WWTPs. These findings highlight the significance of more research to evaluate a larger variety of pharmaceuticals in order to properly understand the extent of environmental pollution. Notably, there is an urgent need to develop easier, cost effective, quicker, selective and sensitive methods for the analysis and removal of these compounds due to the severity of the health issues linked to environmental toxins. Consequently, this review emphasized the variety of methods used to prepare MIPs as selective extraction media for specific compounds from complicated samples. Moreover, it demonstrates how the use of MIPs offers a straightforward means for developing reliable, adaptable, and highly selective SPE procedures with better analytical features. According to the information given in this review, MIPs offer a promising material for identifying and removing the presence of various contaminants in wastewater. Nanotechnology has taken a transcendent interest for wastewater treatment, due to its small size, large surface area, large porosity, and high chemical reaction of the nanomaterials. They have better properties, whether used for catalytic or adsorption. Accordingly, silver nanoparticles have a variety of uses because of their distinctive characteristics. Their synthesis will be significantly impacted by plant-mediated synthesis in the ensuing decades. Plant extracts are a cheap, readily scaled-up, and environmentally safe method of producing metallic nanoparticles. Proteins, carbohydrates, alkaloids, tannins, phenolics, oils, and saponins are just a few of the numerous chemical substances found in plant extracts. These substances also have medical significance and can function as reducing and capping agents for the synthesis of AgNPs. A synthesis using plant extracts can produce nanoparticles with a regulated size and form. Although some of the plants may not have been utilized to remove pharmaceuticals from wastewater, their application for synthesis of nanoparticles highlights the need of incorporating MIPs on these materials. Moreover, the review demonstrated the extreme selectivity of the adsorption process. Consequently, the Langmuir and Freundlich adsorption isotherm models are typically employed to assess the adsorption capacity of various adsorbents, as this review article clearly indicates. Future

research on the prevalence and fate of developing pharmaceutical contaminants in environmental waters will be greatly aided by the insights gained from this study.

2.1.7 References

ABAFE, O. A., SPÄTH, J., FICK, J., JANSSON, S., BUCKLEY, C., STARK, A., PIETRUSCHKA, B. & MARTINCIGH, B. S. 2018. LC-MS/MS determination of antiretroviral drugs in influents and effluents from wastewater treatment plants in KwaZulu-Natal, South Africa. *Chemosphere,* 200**,** 660-670.

ABBASI, E., MOGHADDAM, M. R. A. & KOWSARI, E. 2022. A systematic and critical review on development of machine learning based-ensemble models for prediction of adsorption process efficiency. *Journal of Cleaner Production***,** 134588.

ABBASI, S. & HAERI, S. A. 2021. Biodegradable materials and their applications in sample preparation techniques–A review. *Microchemical Journal,* 171**,** 106831.

ABDALLAH, M. A.-E., NGUYEN, K.-H., EBELE, A. J., ATIA, N. N., ALI, H. R. H. & HARRAD, S. 2019. A single run, rapid polarity switching method for determination of 30 pharmaceuticals and personal care products in waste water using Q-Exactive Orbitrap high resolution accurate mass spectrometry. *Journal of Chromatography A,* 1588**,** 68-76.

ABEL, S., TESFAYE, J. L., NAGAPRASAD, N., SHANMUGAM, R., DWARAMPUDI, L. P. & KRISHNARAJ, R. 2021. Synthesis and characterization of zinc oxide nanoparticles using moringa leaf extract. *Journal of Nanomaterials,* 2021**,** 1-6.

ADEOLA, A. O. & FORBES, P. B. 2022. Antiretroviral drugs in African surface waters: prevalence, analysis, and potential remediation. *Environmental Toxicology and Chemistry,* 41**,** 247-262.

AHMED, S. F., MOFIJUR, M., RAFA, N., CHOWDHURY, A. T., CHOWDHURY, S., NAHRIN, M., ISLAM, A. S. & ONG, H. C. 2022. Green approaches in synthesising nanomaterials for environmental nanobioremediation: Technological advancements, applications, benefits and challenges. *Environmental Research,* 204**,** 111967.

AJIBOLA, A., ADEBIYI, A., NWAEKE, D., AJIBOLA, F. & ADEWUYI, G. 2021. Analysis, occurrence and ecological risk assessment of diclofenac and ibuprofen residues in wastewater from three wastewater treatment plants in south-western Nigeria. *Journal of Applied Sciences and Environmental Management,* 25**,** 330-340.

AKGÖNÜLLÜ, S., KıLıÇ, S., ESEN, C. & DENIZLI, A. 2023. Molecularly imprinted polymer-based sensors for protein detection. *Polymers,* 15**,** 629.

AKPOMIE, K. G. & CONRADIE, J. 2022. Sequestration of thiazolyl blue tetrazolium bromide and bromophenol blue onto biochar derived from American sycamore leaves. *International Journal of Environmental Analytical Chemistry***,** 1-18.

AL-GHOUTI, M. A. & DA'ANA, D. A. 2020. Guidelines for the use and interpretation of adsorption isotherm models: A review. *Journal of hazardous materials,* 393**,** 122383.

AL-KHATTAF, F. S. 2021. Gold and silver nanoparticles: Green synthesis, microbes, mechanism, factors, plant disease management and environmental risks. *Saudi Journal of Biological Sciences,* 28**,** 3624-3631.

ALAQARBEH, M. 2021. Adsorption phenomena: Definition, mechanisms, and adsorption types: Short review. *RHAZES: Green and Applied Chemistry,* 13**,** 43-51.

ALI, M., HOQUE, M., SAFDAR HOSSAIN, S. & BISWAS, M. 2020. Nanoadsorbents for wastewater treatment: next generation biotechnological solution. *International Journal of Environmental Science and Technology,* 17**,** 4095-4132.

ALI, N. F. M., SAJID, M., ABD HALIM, W. I. T., MOHAMED, A. H., ZAIN, N. N. M., KAMARUZAMAN, S., HANAPI, N. S. M., IBRAHIM, W. N. W. & YAHAYA, N. 2022. Recent advances in solid phase extraction methods for the determination of bisphenol A and its analogues in environmental matrices: an updated review. *Microchemical Journal***,** 108158.

ALMEIDA, C. M. 2021. Overview of Sample Preparation and Chromatographic Methods to Analysis Pharmaceutical Active Compounds in Waters Matrices. *Separations,* 8**,** 16.

ALSHAMERI, A. W. & OWAIS, M. 2022. Antibacterial and cytotoxic potency of the plant-mediated synthesis of metallic nanoparticles Ag NPs and ZnO NPs: A Review. *OpenNano***,** 100077.

ALZUBAIDI, A. K., AL-KAABI, W. J., ALI, A. A., ALBUKHATY, S., AL-KARAGOLY, H., SULAIMAN, G. M., ASIRI, M. & KHANE, Y. 2023. Green synthesis and characterization of silver nanoparticles using flaxseed extract and evaluation of their antibacterial and antioxidant activities. *Applied Sciences,* 13**,** 2182.

AMBAYE, T., VACCARI, M., VAN HULLEBUSCH, E. D., AMRANE, A. & RTIMI, S. 2021. Mechanisms and adsorption capacities of biochar for the removal of organic and inorganic pollutants from industrial wastewater. *International Journal of Environmental Science and Technology***,** 1-22.

ANAND, U., ADELODUN, B., CABREROS, C., KUMAR, P., SURESH, S., DEY, A., BALLESTEROS JR, F. & BONTEMPI, E. 2022. Occurrence, transformation, bioaccumulation, risk and analysis of pharmaceutical and personal care products from wastewater: a review. *Environmental Chemistry Letters,* 20**,** 3883-3904.

ARABI, M., OSTOVAN, A., BAGHERI, A. R., GUO, X., WANG, L., LI, J., WANG, X., LI, B. & CHEN, L. 2020. Strategies of molecular imprinting-based solid-phase extraction prior to chromatographic analysis. *TrAC Trends in Analytical Chemistry,* 128**,** 115923.

ARIF, R. & UDDIN, R. 2021. A review on recent developments in the biosynthesis of silver nanoparticles and its biomedical applications. *Medical Devices & Sensors,* 4**,** e10158.

ASWATHI, V., MEERA, S., MARIA, C. A. & NIDHIN, M. 2022. Green synthesis of nanoparticles from biodegradable waste extracts and their applications: a critical review. *Nanotechnology for Environmental Engineering***,** 1-21.

AYANKOJO, A. G., REUT, J., NGUYEN, V. B. C., BOROZNJAK, R. & SYRITSKI, V. 2022. Advances in Detection of Antibiotic Pollutants in Aqueous Media Using Molecular Imprinting Technique—A Review. *Biosensors,* 12**,** 441.

AYAWEI, N., EBELEGI, A. N. & WANKASI, D. 2017. Modelling and interpretation of adsorption isotherms. *Journal of chemistry,* 2017.

AZIZIAN, S. & ERIS, S. 2021. Adsorption isotherms and kinetics. *Interface science and technology.* Elsevier.

BADAWY, M. E., EL-NOUBY, M. A., KIMANI, P. K., LIM, L. W. & RABEA, E. I. 2022. A review of the modern principles and applications of solid-phase extraction techniques in chromatographic analysis. *Analytical Sciences,* 38**,** 1457-1487.

BAHRANI, S., ASLANI, R., HASHEMI, S. A., MOUSAVI, S. M. & GHAEDI, M. 2021. Introduction to molecularly imprinted polymer. *Interface Science and Technology.* Elsevier.

BAIG, N., KAMMAKAKAM, I. & FALATH, W. 2021. Nanomaterials: A review of synthesis methods, properties, recent progress, and challenges. *Materials Advances,* 2**,** 1821-1871.

BARQUILHA, C. E. & BRAGA, M. C. 2021. Adsorption of organic and inorganic pollutants onto biochars: Challenges, operating conditions, and mechanisms. *Bioresource Technology Reports,* 15**,** 100728.

BATOOL, S., HUSSAIN, Z., NIAZI, M. B. K., LIAQAT, U. & AFZAL, M. 2019. Biogenic synthesis of silver nanoparticles and evaluation of physical and antimicrobial properties of Ag/PVA/starch nanocomposites hydrogel membranes for wound dressing application. *Journal of Drug Delivery Science and Technology,* 52**,** 403-414.

BATUCAN, N. S. P., TREMBLAY, L. A., NORTHCOTT, G. L. & MATTHAEI, C. D. 2022. Medicating the environment? A critical review on the risks of carbamazepine, diclofenac and ibuprofen to aquatic organisms. *Environmental Advances,* 7**,** 100164.

BAZI, M., BALARAK, D., KHATIBI, A. D., SIDDIQUI, S. H. & MOSTAFAPOUR, F. K. 2021. Investigation of Isotherm, Kinetics and Thermodynamics of Ciprofloxacin Adsorption by Molecularly Imprinted Polymer from Aqueous Solutions. *International Journal of Pharmaceutical Investigation,* 11.

BHATT, P., BHANDARI, G. & BILAL, M. 2022. Occurrence, toxicity impacts and mitigation of emerging micropollutants in the aquatic environments: Recent tendencies and perspectives. *Journal of Environmental chemical engineering***,** 107598.

BILAL, M., IHSANULLAH, I., YOUNAS, M. & SHAH, M. U. H. 2021. Recent advances in applications of low-cost adsorbents for the removal of heavy metals from water: A critical review. *Separation and Purification Technology,* 278**,** 119510.

BISOGNIN, R. P., WOLFF, D. B., CARISSIMI, E., PRESTES, O. D. & ZANELLA, R. 2021. Occurrence and fate of pharmaceuticals in effluent and sludge from a wastewater treatment plant in Brazil. *Environmental Technology,* 42**,** 2292-2303.

BISWAS, S., FATEMA, J., DEBNATH, T. & RASHID, T. U. 2021. Chitosan–clay composites for wastewater treatment: a state-of-the-art review. *ACS ES&T Water,* 1**,** 1055-1085.

BOSMAN, P., COMBÈS, A., LAMBERT, M., LAVISON-BOMPARD, G. & PICHON, V. 2021. Development and Application of Molecularly Imprinted Polymers for the Selective Extraction of Chlordecone from Bovine Serum. *Separations,* 8**,** 237.

BOUKADIDA, M., JAOUED-GRAYAA, N., ANENE, A., CHEVALIER, Y. & HBAIEB, S. 2023. Effect of cross-linking agents on the adsorption of histamine on molecularly imprinted polyacrylamide. *Polymer***,** 125724.

BOUVAREL, T. 2020. *Molecularly imprinted polymers for the miniaturized analysis of drug and neurotransmitter traces in biological samples.* Sorbonne Université.

BÜYÜKTIRYAKI, S., KEÇILI, R. & HUSSAIN, C. M. 2020. Functionalized nanomaterials in dispersive solid phase extraction: advances & prospects. *TrAC Trends in Analytical Chemistry,* 127**,** 115893.

CAO, Y., NAKHJIRI, A. T. & GHADIRI, M. 2021. Numerical investigation of ibuprofen removal from pharmaceutical wastewater using adsorption process. *Scientific reports,* 11**,** 24478.

CAP, S., BOTS, P. & SCHERER, L. 2022. Environmental, nutritional and social assessment of nuts. *Sustainability Science***,** 1-17.

CAPRIOTTI, A. L., CAVALIERE, C., LA BARBERA, G., MONTONE, C. M., PIOVESANA, S. & LAGANÀ, A. 2019. Recent applications of magnetic solid-phase extraction for sample preparation. *Chromatographia,* 82**,** 1251-1274.

CASTILLO-HENRÍQUEZ, L., ALFARO-AGUILAR, K., UGALDE-ÁLVAREZ, J., VEGA-FERNÁNDEZ, L., MONTES DE OCA-VÁSQUEZ, G. & VEGA-BAUDRIT, J. R. 2020. Green synthesis of gold and silver nanoparticles from plant extracts and their possible applications as antimicrobial agents in the agricultural area. *Nanomaterials,* 10**,** 1763.

CHADHA, U., BHARDWAJ, P., AGARWAL, R., RAWAT, P., AGARWAL, R., GUPTA, I., PANJWANI, M., SINGH, S., AHUJA, C. & SELVARAJ, S. K. 2022. Recent progress and growth in biosensors technology: A critical review. *Journal of Industrial and Engineering Chemistry*.

CHAUHAN, S., SHAFI, T., DUBEY, B. K. & CHOWDHURY, S. 2023. Biochar-mediated removal of pharmaceutical compounds from aqueous matrices via adsorption. *Waste Disposal & Sustainable Energy,* 5**,** 37-62.

CHAVES, M. J. S., KULZER, J., PUJOL DE LIMA, P. D. R., BARBOSA, S. C. & PRIMEL, E. G. 2022. Updated knowledge, partitioning and ecological risk of pharmaceuticals and personal care products in global aquatic environments. *Environ Sci Process Impacts,* 24**,** 1982-2008.

CHEN, H., GUO, J., WANG, Y., DONG, W., ZHAO, Y. & SUN, L. 2022. Bio-Inspired Imprinting Materials for Biomedical Applications. *Advanced Science,* 9**,** 2202038.

CHEN, X., WU, X., LUAN, T., JIANG, R. & OUYANG, G. 2021. Sample preparation and instrumental methods for illicit drugs in environmental and biological samples: A review. *Journal of Chromatography A,* 1640**,** 461961.

CHOKSHI, A., SIFRI, Z., CENNIMO, D. & HORNG, H. 2019. Global contributors to antibiotic resistance. *Journal of global infectious diseases,* 11**,** 36.

CONTIN, M., DOBRECKY, C. & MANUELA, S. 2022. New Trends in Sample Preparation for Pharmaceutical and Biological Analysis by Chromatographic Methods. *Recent Advances in Analytical Techniques: Volume 5,* 5**,** 32-92.

CUI, Y., DING, L. & DING, J. 2022. Recent advances of magnetic molecularly imprinted materials: From materials design to complex sample pretreatment. *TrAC Trends in Analytical Chemistry***,** 116514.

DAI, M., ZHANG, Y., WU, Y., SUN, R., ZONG, W. & KONG, Q. 2021. Mechanism involved in the treatment of sulfamethoxazole in wastewater using a constructed wetland microbial fuel cell system. *Journal of Environmental Chemical Engineering,* 9**,** 106193.

DU, Y., YAN, X., CHEN, Y., WU, Y., QIU, Q., LI, Y. & WU, D. 2022. Magnetic polyimide nanosheet microspheres for trace analysis of estrogens in aqueous samples by magnetic solid-phase extraction-gas chromatography–mass spectrometry. *Journal of Chromatography A,* 1675**,** 463184.

DUAN, Y.-P., DAI, C.-M. & ZHANG, Y.-L. 2013. Selective trace enrichment of acidic pharmaceuticals in real water and sediment samples based on solid-phase extraction using multi-templates molecularly imprinted polymers. *Analytica chimica acta,* 758**,** 93-100.

DUGHERI, S., MARRUBINI, G., MUCCI, N., CAPPELLI, G., BONARI, A., POMPILIO, I., TREVISANI, L. & ARCANGELI, G. 2021. A review of micro-solid-phase extraction techniques and devices applied in sample pretreatment coupled with chromatographic analysis. *Acta Chromatographica,* 33**,** 99-111.

EL BOUZIDI, K., DATIR, R. P., KWAGHE, V., ROY, S., FRAMPTON, D., BREUER, J., OGBANUFE, O., MURTALA-IBRAHIM, F., CHARURAT, M. & DAKUM, P. 2022. Deep sequencing of HIV-1 reveals extensive subtype variation and drug resistance after failure of first-line antiretroviral regimens in Nigeria. *Journal of Antimicrobial Chemotherapy,* 77**,** 474-482.

ELUGOKE, S. E., ADEKUNLE, A. S., FAYEMI, O. E., AKPAN, E. D., MAMBA, B. B., SHERIF, E. S. M. & EBENSO, E. E. 2021. Molecularly imprinted polymers (MIPs) based electrochemical sensors for the determination of catecholamine neurotransmitters–Review. *Electrochemical Science Advances,* 1**,** e2000026.

EZEUKO, A. S., OJEMAYE, M. O., OKOH, O. O. & OKOH, A. I. 2021. Potentials of metallic nanoparticles for the removal of antibiotic resistant bacteria and antibiotic resistance genes from wastewater: A critical review. *Journal of Water Process Engineering,* 41**,** 102041.

FALEYE, A., ADEGOKE, A., RAMLUCKAN, K., FICK, J., BUX, F. & STENSTRÖM, T. 2019. Concentration and reduction of antibiotic residues in selected wastewater treatment plants and receiving waterbodies in Durban, South Africa. *Science of The Total Environment,* 678**,** 10-20.

FANG, L., JIA, M., ZHAO, H., KANG, L., SHI, L., ZHOU, L. & KONG, W. 2021. Molecularly imprinted polymer-based optical sensors for pesticides in foods: Recent advances and future trends. *Trends in Food Science & Technology,* 116**,** 387-404.

FAROOQ, S., WU, H., NIE, J., AHMAD, S., MUHAMMAD, I., ZEESHAN, M., KHAN, R. & ASIM, M. 2022. Application, advancement and green aspects of magnetic molecularly imprinted polymers in pesticide residue detection. *Science of The Total Environment,* 804**,** 150293.

FERNANDES, J. P., ALMEIDA, C. M. R., SALGADO, M. A., CARVALHO, M. F. & MUCHA, A. P. 2021. Pharmaceutical compounds in aquatic environments—Occurrence, fate and bioremediation prospective. *Toxics,* 9**,** 257.

FERNÁNDEZ-FERNÁNDEZ, V., RAMIL, M., CELA, R. & RODRÍGUEZ, I. 2022. Solid-phase extraction and fractionation of multiclass pollutants from wastewater followed by liquid chromatography tandem-mass spectrometry analysis. *Analytical and Bioanalytical Chemistry,* 414**,** 4149-4165.

FERNÁNDEZ, L. P., BRASCA, R., REPETTI, M. R., ATTADEMO, A. M., PELTZER, P. M., LAJMANOVICH, R. C. & CULZONI, M. J. 2022. Bioaccumulation of abacavir and efavirenz in Rhinella arenarum tadpoles after exposure to environmentally relevant concentrations. *Chemosphere,* 301**,** 134631.

FRESCO-CALA, B., BATISTA, A. D. & CÁRDENAS, S. 2020. Molecularly imprinted polymer micro-and nano-particles: A review. *Molecules,* 25**,** 4740.

FU, Y., PESSAGNO, F., MANESIOTIS, P., BORRULL, F., FONTANALS, N. & MARCÉ, R. M. 2022. Preparation and evaluation of molecularly imprinted polymers as selective SPE sorbents for the determination of cathinones in river water. *Microchemical Journal,* 175**,** 107100.

GAHLAWAT, G. & CHOUDHURY, A. R. 2019. A review on the biosynthesis of metal and metal salt nanoparticles by microbes. *RSC advances,* 9**,** 12944-12967.

GHORBANI, M., SEYEDIN, O. & AGHAMOHAMMADHASSAN, M. 2020. Adsorptive removal of lead (II) ion from water and wastewater media using carbon-based nanomaterials as unique sorbents: A review. *Journal of environmental management,* 254**,** 109814.

GIL, A. 2023. Classical and new insights into the methodology for characterizing adsorbents and metal catalysts by chemical adsorption. *Catalysis Today*.

GONZÁLEZ-LÓPEZ, M. E., LAUREANO-ANZALDO, C. M., PÉREZ-FONSECA, A. A., ARELLANO, M. & ROBLEDO-ORTÍZ, J. R. 2022. A critical overview of adsorption models linearization: methodological and statistical inconsistencies. *Separation & Purification Reviews,* 51**,** 358-372.

GONZÁLEZ PEÑA, O. I., LÓPEZ ZAVALA, M. Á. & CABRAL RUELAS, H. 2021. Pharmaceuticals market, consumption trends and disease incidence are not driving the pharmaceutical research on water and wastewater. *International journal of environmental research and public health,* 18**,** 2532.

GORBAN, A., TYUKINA, T., POKIDYSHEVA, L. & SMIRNOVA, E. 2021. Dynamic and thermodynamic models of adaptation. *Physics of Life Reviews,* 37**,** 17-64.

GU, Y., LI, Y., REN, D., SUN, L., ZHUANG, Y., YI, L. & WANG, S. 2022. Recent advances in nanomaterial-assisted electrochemical sensors for food safety analysis. *Food Frontiers,* 3**,** 453-479.

HAGAROVÁ, I. 2020. Magnetic solid phase extraction as a promising technique for fast separation of metallic nanoparticles and their ionic species: a review of recent advances. *Journal of Analytical Methods in Chemistry,* 2020.

HANSEN, F., ØIESTAD, E. L. & PEDERSEN-BJERGAARD, S. 2020. Bioanalysis of pharmaceuticals using liquid-phase microextraction combined with liquid

chromatography–mass spectrometry. *Journal of pharmaceutical and biomedical analysis,* 189**,** 113446.

HASANAH, A. N., SAFITRI, N., ZULFA, A., NELI, N. & RAHAYU, D. 2021. Factors affecting preparation of molecularly imprinted polymer and methods on finding template-monomer interaction as the key of selective properties of the materials. *Molecules,* 26**,** 5612.

HASSAN, M. A., XU, T., TIAN, Y., ZHONG, Y., ALI, F. A. Z., YANG, X. & LU, B. 2021. Health benefits and phenolic compounds of Moringa oleifera leaves: A comprehensive review. *Phytomedicine,* 93**,** 153771.

HAWASH, H. B., MONEER, A. A., GALHOUM, A. A., ELGARAHY, A. M., MOHAMED, W. A., SAMY, M., EL-SEEDI, H. R., GABALLAH, M. S., MUBARAK, M. F. & ATTIA, N. F. 2023. Occurrence and spatial distribution of pharmaceuticals and personal care products (PPCPs) in the aquatic environment, their characteristics, and adopted legislations. *Journal of Water Process Engineering,* 52**,** 103490.

HERRERA-CHACÓN, A., CETÓ, X. & DEL VALLE, M. 2021. Molecularly imprinted polymers-towards electrochemical sensors and electronic tongues. *Analytical and bioanalytical chemistry,* 413**,** 6117-6140.

HLENGWA, N. & MAHLAMBI, P. 2020. SPE-LC-PDA method development and application for the analysis of selected pharmaceuticals in river and wastewater samples from South Africa. *Water SA,* 46**,** 514-522.

HORN, S., VOGT, T., GERBER, E., VOGT, B., BOUWMAN, H. & PIETERS, R. 2022. HIV-antiretrovirals in river water from Gauteng, South Africa: Mixed messages of wastewater inflows as source. *Science of The Total Environment,* 806**,** 150346.

HU, C., LI, J., KE, J., LIANG, J., LIU, Q., WANG, Q. & HUANG, W. 2023. The preparation and removal performance of carbamazepine/oxcarbazepine double template magnetic molecularly imprinted polymers. *Separation and Purification Technology,* 306**,** 122556.

HU, C., YANG, Z., YAN, F. & SUN, B. 2019. Extraction of the toluene exposure biomarkers hippuric acid and methylhippuric acid using a magnetic molecularly imprinted polymer, and their quantitation by LC-MS/MS. *Microchimica Acta,* 186**,** 1-9.

HU, T., CHEN, R., WANG, Q., HE, C. & LIU, S. 2021. Recent advances and applications of molecularly imprinted polymers in solid-phase extraction for real sample analysis. *Journal of Separation Science,* 44**,** 274-309.

HUSIN, N. A., MUHAMAD, M., YAHAYA, N., MISKAM, M., KAMAL, N. N. S. N. M., ASMAN, S., RAOOV, M. & ZAIN, N. N. M. 2021. Application of a new choline-imidazole based deep eutectic solvents in hybrid magnetic molecularly imprinted polymer for efficient and selective removal of naproxen from aqueous samples. *Materials Chemistry and Physics,* 261**,** 124228.

ISLAM, Z., ISLAM, S., HOSSEN, F., MAHTAB-UL-ISLAM, K., HASAN, M. & KARIM, R. 2021. Moringa oleifera is a prominent source of nutrients with potential health benefits. *International Journal of Food Science,* 2021.

JAGWANI, D. & KRISHNA, P. H. 2021. Nature's nano-assets: Green synthesis, characterization techniques and applications–a graphical review. *Materials Today: Proceedings,* 46**,** 2307-2317.

JAKUBUS, A., GODLEWSKA, K., GROMELSKI, M., JAGIELLO, K., PUZYN, T., STEPNOWSKI, P. & PASZKIEWICZ, M. 2019. The possibility to use multi-walled carbon nanotubes as a sorbent for dispersive solid phase extraction of selected pharmaceuticals and their metabolites: effect of extraction condition. *Microchemical Journal,* 146**,** 1113-1125.

JAMIESON, O., MECOZZI, F., CRAPNELL, R. D., BATTELL, W., HUDSON, A., NOVAKOVIC, K., SACHDEVA, A., CANFAROTTA, F., HERDES, C. & BANKS, C. E. 2021. Approaches to the rational design of molecularly imprinted polymers developed for the selective extraction or detection of antibiotics in environmental and food samples. *physica status solidi (a),* 218**,** 2100021.

JAYASINGHE, G. T. M., DOMÍNGUEZ-GONZÁLEZ, R., BERMEJO-BARRERA, P. & MOREDA-PIÑEIRO, A. 2020. Miniaturized vortex assisted-dispersive molecularly imprinted polymer micro-solid phase extraction and HPLC-MS/MS for assessing trace aflatoxins in cultured fish. *Analytical Methods,* 12**,** 4351-4362.

JIMÉNEZ-SKRZYPEK, G., GONZÁLEZ-CURBELO, M., GONZÁLEZ-SÁLAMO, J., ORTEGA-ZAMORA, C. & HERNÁNDEZ-BORGES, J. 2021. Application of Functionalized Magnetic Nanoparticles for Organic Analyte Extraction. *Analytical Applications of Functionalized Magnetic Nanoparticles.* Royal Society of Chemistry.

JUBEH, B., BREIJYEH, Z. & KARAMAN, R. 2020. Resistance of gram-positive bacteria to current antibacterial agents and overcoming approaches. *Molecules,* 25**,** 2888.

K'OREJE, K. O., KANDIE, F. J., VERGEYNST, L., ABIRA, M. A., VAN LANGENHOVE, H., OKOTH, M. & DEMEESTERE, K. 2018. Occurrence, fate and removal of pharmaceuticals, personal care products and pesticides in wastewater stabilization ponds and receiving rivers in the Nzoia Basin, Kenya. *Science of the Total Environment,* 637**,** 336-348.

KAHILU, G. M., BADA, S. & MULOPO, J. 2022. Coal Discards and Sewage Sludge Derived-Hydrochar for HIV Antiretroviral Pollutant Removal from Wastewater and Spent Adsorption Residue Evaluation for Sustainable Carbon Management. *Sustainability,* 14**,** 15113.

KALAM, S., ABU-KHAMSIN, S. A., KAMAL, M. S. & PATIL, S. 2021. Surfactant adsorption isotherms: A review. *ACS omega,* 6**,** 32342-32348.

KANU, A. B. 2021. Recent developments in sample preparation techniques combined with high-performance liquid chromatography: A critical review. *Journal of Chromatography A,* 1654**,** 462444.

KAYA, S. I., CETINKAYA, A. & OZKAN, S. A. 2022a. Molecularly imprinted polymers as highly selective sorbents in sample preparation techniques and their applications in environmental water analysis. *Trends in Environmental Analytical Chemistry***,** e00193.

KAYA, S. I., GUMUS, E., CETINKAYA, A., ZOR, E. & OZKAN, S. A. 2022b. Trends in on-site removal, treatment, and sensitive assay of common pharmaceuticals in surface waters. *TrAC Trends in Analytical Chemistry***,** 116556.

KHALIL, A. M., MEMON, F. A., TABISH, T. A., SALMON, D., ZHANG, S. & BUTLER, D. 2020. Nanostructured porous graphene for efficient removal of emerging contaminants (pharmaceuticals) from water. *Chemical Engineering Journal,* 398**,** 125440.

KHAN, A., AZIZ, H., KHAN, N., HASAN, M., AHMED, S., FAROOQI, I., DHINGRA, A., VAMBOL, V., CHANGANI, F. & YOUSEFI, M. 2021. Impact, disease outbreak and the eco-hazards associated with pharmaceutical residues: a critical review. *International Journal of Environmental Science and Technology***,** 1-12.

KHAN, S. A., JAIN, M., PANDEY, A., PANT, K. K., ZIORA, Z. M., BLASKOVICH, M. A., SHETTI, N. P. & AMINABHAVI, T. M. 2022a. Leveraging the potential of silver nanoparticles-based materials towards sustainable water treatment. *Journal of Environmental Management,* 319**,** 115675.

KHAN, Y., SADIA, H., ALI SHAH, S. Z., KHAN, M. N., SHAH, A. A., ULLAH, N., ULLAH, M. F., BIBI, H., BAFAKEEH, O. T. & KHEDHER, N. B. 2022b.

Classification, synthetic, and characterization approaches to nanoparticles, and their applications in various fields of nanotechnology: a review. *Catalysts,* 12**,** 1386.
KHASAWNEH, O. F. S. & PALANIANDY, P. 2021. Occurrence and removal of pharmaceuticals in wastewater treatment plants. *Process Safety and Environmental Protection,* 150**,** 532-556.
KHATIBI, A. D., MAHVI, A. H., MENGELIZADEH, N. & BALARAK, D. 2021. Adsorption–desorption of tetracycline onto molecularly imprinted polymer: Isotherm, kinetics, and thermodynamics studies. *Desal. Water Treat,* 230**,** 240-251.
KHULU, S., NCUBE, S., KGAME, T., MAVHUNGA, E. & CHIMUKA, L. 2021. Synthesis, characterization and application of a molecularly imprinted polymer as an adsorbent for solid-phase extraction of selected pharmaceuticals from water samples. *Polymer Bulletin***,** 1-21.
KOŁECKA, K., GAJEWSKA, M. & CABAN, M. 2022. From the pills to environment–Prediction and tracking of non-steroidal anti-inflammatory drug concentrations in wastewater. *Science of The Total Environment,* 825**,** 153611.
KULKARNI, A. & MILLER, S. E. 2022. Analysis of pharmaceuticals in the environment. *Contemporary Chemical Approaches for Green and Sustainable Drugs.* Elsevier.
KUMAR, V., DWIVEDI, S. & OH, S. 2022. A review on microbial-integrated techniques as promising cleaner option for removal of chromium, cadmium and lead from industrial wastewater. *Journal of Water Process Engineering,* 47**,** 102727.
LI, Z., WANG, J., CHEN, X., HU, S., GONG, T. & XIAN, Q. 2019. A novel molecularly imprinted polymer-solid phase extraction method coupled with high performance liquid chromatography tandem mass spectrometry for the determination of nitrosamines in water and beverage samples. *Food chemistry,* 292**,** 267-274.
LIU, Y., LI, W., GAO, Y., WANG, J., CHENG, G., CHEN, J., LI, X. & ZHU, G. 2022. Highly efficient and rapid removal of non-steroidal anti-inflammatory drugs from environmental samples based on an eco-friendly ZIF-67-molecularly imprinted composite. *Chemical Engineering Journal,* 443**,** 136396.
LOWDON, J. W., DILIËN, H., SINGLA, P., PEETERS, M., CLEIJ, T. J., VAN GRINSVEN, B. & EERSELS, K. 2020. MIPs for commercial application in low-cost sensors and assays–An overview of the current status quo. *Sensors and Actuators B: Chemical,* 325**,** 128973.
LU, W., LIU, J., LI, J., WANG, X., LV, M., CUI, R. & CHEN, L. 2019. Dual-template molecularly imprinted polymers for dispersive solid-phase extraction of fluoroquinolones in water samples coupled with high performance liquid chromatography. *Analyst,* 144**,** 1292-1302.
MADANI, M., HOSNY, S., ALSHANGITI, D. M., NADY, N., ALKHURSANI, S. A., ALKHALDI, H., AL-GAHTANY, S. A., GHOBASHY, M. M. & GABER, G. A. 2022. Green synthesis of nanoparticles for varied applications: Green renewable resources and energy-efficient synthetic routes. *Nanotechnology Reviews,* 11**,** 731-759.
MADIKIZELA, L. M., NOMNGONGO, P. N. & PAKADE, V. E. 2022. Synthesis of molecularly imprinted polymers for extraction of fluoroquinolones in environmental, food and biological samples. *Journal of Pharmaceutical and Biomedical Analysis,* 208**,** 114447.
MAKSOUD, M. A., ELGARAHY, A. M., FARRELL, C., ALA'A, H., ROONEY, D. W. & OSMAN, A. I. 2020. Insight on water remediation application using magnetic nanomaterials and biosorbents. *Coordination Chemistry Reviews,* 403**,** 213096.
MALEKI, B., SINGH, B., EAMAEILI, H., VENKATESH, Y. K., TALESH, S. S. A. & SEETHARAMAN, S. 2023. Transesterification of waste cooking oil to biodiesel by

walnut shell/sawdust as a novel, low-cost and green heterogeneous catalyst: Optimization via RSM and ANN. *Industrial Crops and Products,* 193**,** 116261.
MALIK, M. I., SHAIKH, H., MUSTAFA, G. & BHANGER, M. I. 2019. Recent applications of molecularly imprinted polymers in analytical chemistry. *Separation & Purification Reviews,* 48**,** 179-219.
MANGALGIRI, K. P., IBITOYE, T. & BLANEY, L. 2022. Molar absorption coefficients and acid dissociation constants for fluoroquinolone, sulfonamide, and tetracycline antibiotics of environmental concern. *Science of The Total Environment,* 835**,** 155508.
MANGLA, D., SHARMA, A. & IKRAM, S. 2022. Critical review on adsorptive removal of antibiotics: Present situation, challenges and future perspective. *Journal of Hazardous Materials,* 425**,** 127946.
MANOUSI, N. & ZACHARIADIS, G. A. 2020. Recent advances in the extraction of polycyclic aromatic hydrocarbons from environmental samples. *Molecules,* 25**,** 2182.
MARAGOU, N. C., THOMAIDIS, N. S., THEODORIDIS, G. A., LAMPI, E. N. & KOUPPARIS, M. A. 2020. Determination of bisphenol A in canned food by microwave assisted extraction, molecularly imprinted polymer-solid phase extraction and liquid chromatography-mass spectrometry. *Journal of Chromatography B,* 1137**,** 121938.
MARANATA, G. J., SURYA, N. O. & HASANAH, A. N. 2021. Optimising factors affecting solid phase extraction performances of molecular imprinted polymer as recent sample preparation technique. *Heliyon,* 7**,** e05934.
MARMON, P., OWEN, S. F. & MARGIOTTA-CASALUCI, L. 2021. Pharmacology-informed prediction of the risk posed to fish by mixtures of non-steroidal anti-inflammatory drugs (NSAIDs) in the environment. *Environment international,* 146**,** 106222.
MASSIMA MOUELE, E. S., TIJANI, J. O., BADMUS, K. O., PEREAO, O., BABAJIDE, O., ZHANG, C., SHAO, T., SOSNIN, E., TARASENKO, V. & FATOBA, O. O. 2021. Removal of pharmaceutical residues from water and wastewater using dielectric barrier discharge methods—A review. *International Journal of Environmental Research and Public Health,* 18**,** 1683.
MAZARI, S. A., ALI, E., ABRO, R., KHAN, F. S. A., AHMED, I., AHMED, M., NIZAMUDDIN, S., SIDDIQUI, T. H., HOSSAIN, N. & MUBARAK, N. M. 2021. Nanomaterials: Applications, waste-handling, environmental toxicities, and future challenges–A review. *Journal of Environmental Chemical Engineering,* 9**,** 105028.
MHUKA, V., DUBE, S. & NINDI, M. M. 2020. Occurrence of pharmaceutical and personal care products (PPCPs) in wastewater and receiving waters in South Africa using LC-Orbitrap™ MS. *Emerging Contaminants,* 6**,** 250-258.
MOHAMMED, A. A., MOHAMED, A., EL-NAGGAR, N. E.-A., MAHROUS, H., NASR, G. M., ABDELLA, A., AHMED, R. H., IRMAK, S., ELSAYED, M. S. & SELIM, S. 2022. Antioxidant and antibacterial activities of silver nanoparticles biosynthesized by Moringa Oleifera through response surface methodology. *Journal of Nanomaterials,* 2022**,** 1-15.
MOHIUDDIN, I., BHOGAL, S., GROVER, A., MALIK, A. K. & AULAKH, J. S. 2021. Simultaneous determination of amitriptyline, nortriptyline, and clomipramine in aqueous samples using selective multi-template molecularly imprinted polymers. *Environmental Nanotechnology, Monitoring & Management,* 16**,** 100527.
MOHIUDDIN, I., GROVER, A., AULAKH, J. S., LEE, S.-S., MALIK, A. K. & KIM, K.-H. 2020. Porous molecularly-imprinted polymer for detecting diclofenac in aqueous pharmaceutical compounds. *Chemical Engineering Journal,* 382**,** 123002.
MONDAL, P., NANDAN, A., AJITHKUMAR, S., SIDDIQUI, N. A., RAJA, S., KOLA, A. K. & BALAKRISHNAN, D. 2023. Sustainable application of nanoparticles in

wastewater treatment: Fate, current trend & paradigm shift. *Environmental Research*, 116071.
MORIFI, E., CHIMUKA, L., RICHARDS, H., SENYOLO, L. & PILLAY, K. 2022. Modified macadamia nutshell nanocomposite for selective removal of hexavalent chromium from wastewater. *South African Journal of Chemical Engineering,* 42, 176-187.
MORIFI, E. L. 2021. *Modified Macadamia Nutshells Composite for the Removal of Heavy Metal Pollutants from Wastewater*, University of Johannesburg (South Africa).
MOSLAH, B., HAPESHI, E., JRAD, A., FATTA-KASSINOS, D. & HEDHILI, A. 2018. Pharmaceuticals and illicit drugs in wastewater samples in north-eastern Tunisia. *Environmental Science and Pollution Research,* 25, 18226-18241.
MTHIYANE, Z. L., MAKHUBELA, N., NYONI, H., MADIKIZELA, L. M., MASEKO, B. R. & NCUBE, S. 2023. Determination of antibiotics during treatment of hospital wastewater using automated solid-phase extraction followed by UHPLC-MS: Occurrence, removal and environmental risks. *Environmental Technology*, 1-31.
MTOLO, S. P., MAHLAMBI, P. N. & MADIKIZELA, L. M. 2019. Synthesis and application of a molecularly imprinted polymer in selective solid-phase extraction of efavirenz from water. *Water Science and Technology,* 79, 356-365.
MURDAYA, N., TRIADENDA, A. L., RAHAYU, D. & HASANAH, A. N. 2022. A Review: Using Multiple Templates for Molecular Imprinted Polymer: Is It Good? *Polymers,* 14, 4441.
MUSARURWA, H. & TAVENGWA, N. T. 2022. Stimuli-responsive molecularly imprinted polymers as adsorbents of analytes in complex matrices. *Microchemical Journal*, 107750.
MUSTAPHA, T., MISNI, N., ITHNIN, N. R., DASKUM, A. M. & UNYAH, N. Z. 2022. A review on plants and microorganisms mediated synthesis of silver nanoparticles, role of plants metabolites and applications. *International Journal of Environmental Research and Public Health,* 19, 674.
N'DIAYE, A. D. & KANKOU, M. S. A. 2020. Modeling of adsorption isotherms of pharmaceutical products onto various adsorbents: A Short Review. *J. Mater. Environ. Sci,* 11, 1264-1276.
NAS, B., DOLU, T. & KOYUNCU, S. 2021. Behavior and removal of ciprofloxacin and sulfamethoxazole antibiotics in three different types of full-scale wastewater treatment plants: a comparative study. *Water, Air, & Soil Pollution,* 232, 127.
NEKHAVHAMBE, H. H., MUDZIELWANA, R., GITARI, M. W., AYINDE, W. B. & IZEVBEKHAI, O. U. 2022. Fluoride Bio-Sorption Efficiency and Antimicrobial Potency of Macadamia Nut Shells. *Materials,* 15, 1065.
NGQWALA, N. P. & MUCHESA, P. 2020. Occurrence of pharmaceuticals in aquatic environments: A review and potential impacts in South Africa. *South African Journal of Science,* 116, 1-7.
NGUMBA, E., GACHANJA, A., NYIRENDA, J., MALDONADO, J. & TUHKANEN, T. 2020. Occurrence of antibiotics and antiretroviral drugs in source-separated urine, groundwater, surface water and wastewater in the peri-urban area of Chunga in Lusaka, Zambia. *Water SA,* 46, 278-284.
NGWENYA, N. & MAHLAMBI, P. 2023. Methods optimization and application: Solid phase extraction, ultrasonic extraction and Soxhlet extraction for the determination of antiretroviral drugs in river water, wastewater, sludge, soil and sediment. *Journal of Pharmaceutical and Biomedical Analysis,* 230, 115358.
NOURI, N., KHORRAM, P., DUMAN, O., SIBEL, T. & HASSAN, S. 2020. Overview of nanosorbents used in solid phase extraction techniques for the monitoring of emerging

organic contaminants in water and wastewater samples. *Trends in Environmental Analytical Chemistry,* 25**,** e00081.
NOWAK, P. M., WIETECHA-POSŁUSZNY, R. & PAWLISZYN, J. 2021. White Analytical Chemistry: An approach to reconcile the principles of Green Analytical Chemistry and functionality. *TrAC Trends in Analytical Chemistry,* 138**,** 116223.
NYAGA, M. N., NYAGAH, D. M. & NJAGI, A. 2020. Pharmaceutical waste: Overview, management, and impact of improper disposal.
NYAMUKAMBA, P., MOLOTO, M. J., TAVENGWA, N. & EJIDIKE, I. P. 2019. Evaluating physicochemical parameters, heavy metals, and antibiotics in the influents and final effluents of South African wastewater treatment plants. *Polish Journal of Environmental Studies,* 28**,** 1305-1312.
OBA, S. N., IGHALO, J. O., ANIAGOR, C. O. & IGWEGBE, C. A. 2021. Removal of ibuprofen from aqueous media by adsorption: A comprehensive review. *Science of The Total Environment,* 780**,** 146608.
OLESZKIEWICZ, P., KRYSINSKI, J., RELIGIONI, U. & MERKS, P. Access to medicines via non-pharmacy outlets in European countries—a review of regulations and the influence on the self-medication phenomenon. Healthcare, 2021. MDPI, 123.
OROOJI, Y., HAN, N., NEZAFAT, Z., SHAFIEI, N., SHEN, Z., NASROLLAHZADEH, M., KARIMI-MALEH, H., LUQUE, R., BOKHARI, A. & KLEMEŠ, J. J. 2022. Valorisation of nuts biowaste: prospects in sustainable bio (nano) catalysts and environmental applications. *Journal of Cleaner Production***,** 131220.
ORTÚZAR, M., ESTERHUIZEN, M., OLICÓN-HERNÁNDEZ, D. R., GONZÁLEZ-LÓPEZ, J. & ARANDA, E. 2022. Pharmaceutical pollution in aquatic environments: A concise review of environmental impacts and bioremediation systems. *Frontiers in Microbiology,* 13.
PALENCIA, M., LERMA, T. A., GARCÉS, V., MORA, M. A., MARTÍNEZ, J. M. & PALENCIA, S. L. 2021. *Eco-Friendly Functional Polymers: An Approach from Application-Targeted Green Chemistry*, Elsevier.
PANHWAR, S., KEERIO, H. A., ALI, A., AFTAB, A., CHANG, M. A., KHOKHAR, N. H. & KHOKHAR, H. 2022. Synthesis and Characterization Approaches of Silver Nano particles for Various Novel Applications. *Advances in Materials and Processing Technologies,* 8**,** 4106-4121.
PAPAGIANNAKI, D., BELAY, M. H., GONÇALVES, N. P., ROBOTTI, E., BIANCO-PREVOT, A., BINETTI, R. & CALZA, P. 2022. From monitoring to treatment, how to improve water quality: The pharmaceuticals case. *Chemical Engineering Journal Advances***,** 100245.
PATEL, M., KUMAR, R., KISHOR, K., MLSNA, T., PITTMAN JR, C. U. & MOHAN, D. 2019. Pharmaceuticals of emerging concern in aquatic systems: chemistry, occurrence, effects, and removal methods. *Chemical reviews,* 119**,** 3510-3673.
PATIL, S. P. 2020. Ficus carica assisted green synthesis of metal nanoparticles: A mini review. *Biotechnology Reports,* 28**,** e00569.
PHOON, B. L., ONG, C. C., SAHEED, M. S. M., SHOW, P.-L., CHANG, J.-S., LING, T. C., LAM, S. S. & JUAN, J. C. 2020. Conventional and emerging technologies for removal of antibiotics from wastewater. *Journal of hazardous materials,* 400**,** 122961.
PŁOTKA-WASYLKA, J., JATKOWSKA, N., PASZKIEWICZ, M., CABAN, M., FARES, M. Y., DOGAN, A., GARRIGUES, S., MANOUSI, N., KALOGIOURI, N. & NOWAK, P. M. 2023. Miniaturized Solid Phase Extraction techniques for different kind of pollutants analysis: State of the art and future perspectives–PART 1. *TrAC Trends in Analytical Chemistry***,** 117034.

POLIANCIUC, S. I., GURZĂU, A. E., KISS, B., ŞTEFAN, M. G. & LOGHIN, F. 2020. Antibiotics in the environment: causes and consequences. *Medicine and pharmacy reports,* 93**,** 231.

PRATAMA, K. F., MANIK, M. E. R., RAHAYU, D. & HASANAH, A. N. 2020. Effect of the molecularly imprinted polymer component ratio on analytical performance. *Chemical and Pharmaceutical Bulletin,* 68**,** 1013-1024.

QIU, L., JARIA, G., GIL, M. V., FENG, J., DAI, Y., ESTEVES, V. I., OTERO, M. & CALISTO, V. 2020. Core− shell molecularly imprinted polymers on magnetic yeast for the removal of sulfamethoxazole from water. *Polymers,* 12**,** 1385.

QUESADA, H. B., BAPTISTA, A. T. A., CUSIOLI, L. F., SEIBERT, D., DE OLIVEIRA BEZERRA, C. & BERGAMASCO, R. 2019. Surface water pollution by pharmaceuticals and an alternative of removal by low-cost adsorbents: A review. *Chemosphere,* 222**,** 766-780.

RAHMAN, S., BOZAL-PALABIYIK, B., UNAL, D. N., ERKMEN, C., SIDDIQ, M., SHAH, A. & USLU, B. 2022. Molecularly imprinted polymers (MIPs) combined with nanomaterials as electrochemical sensing applications for environmental pollutants. *Trends in Environmental Analytical Chemistry***,** e00176.

RAINA, A. P. & KAUSHIK, S. 2020. Nutritional and phytochemical composition of Moringa oleifera seeds: A multipurpose potential species in India. *Medicinal Plants-International Journal of Phytomedicines and Related Industries,* 12**,** 633-639.

RAJPAL, S., SINGH, S., MISHRA, P. & BHAKTA, S. 2023. Role of monomer compositions for molecularly imprinted polymers (MIPs). *Molecularly Imprinted Polymers (MIPs).* Elsevier.

RAMIN, N. A., RAMACHANDRAN, M. R., SALEH, N. M., MAT ALI, Z. M. & ASMAN, S. 2023. Magnetic Nanoparticles Molecularly Imprinted Polymers: A Review. *Current Nanoscience,* 19**,** 372-400.

RASHED, M. N. 2013. Adsorption technique for the removal of organic pollutants from water and wastewater. *Organic pollutants-monitoring, risk and treatment,* 7**,** 167-194.

RASTOGI, A., TIWARI, M. K. & GHANGREKAR, M. M. 2021. A review on environmental occurrence, toxicity and microbial degradation of Non-Steroidal Anti-Inflammatory Drugs (NSAIDs). *Journal of Environmental Management,* 300**,** 113694.

RATHI, B. S. & KUMAR, P. S. 2021. Application of adsorption process for effective removal of emerging contaminants from water and wastewater. *Environmental Pollution,* 280**,** 116995.

RATHI, B. S., KUMAR, P. S. & VO, D.-V. N. 2021. Critical review on hazardous pollutants in water environment: Occurrence, monitoring, fate, removal technologies and risk assessment. *Science of The Total Environment,* 797**,** 149134.

RAVEENDRAN, P., FU, J. & WALLEN, S. L. 2003. Completely "green" synthesis and stabilization of metal nanoparticles. *Journal of the American Chemical Society,* 125**,** 13940-13941.

REMYA, R., JULIUS, A., SUMAN, T., ARANGANATHAN, L., DHAS, T. S., MOHANAVEL, V., KARTHICK, A. & MUHIBBULLAH, M. 2022. Biofabrication of silver nanoparticles and current research of its environmental applications. *Journal of Nanomaterials,* 2022.

ROY, A., SHARMA, A., YADAV, S., JULE, L. T. & KRISHNARAJ, R. 2021. Nanomaterials for remediation of environmental pollutants. *Bioinorganic Chemistry and Applications,* 2021.

S'BUSISO, M. N., MAHLAMBI, P. N. & CHIMUKA, L. 2022. Synthesis, characterisation and optimisation of bulk molecularly imprinted polymers from nonsteroidal anti-inflammatory drugs. *South African Journal of Chemistry,* 76**,** 56–64-56–64.

ŠAFAŘíKOVÁ, M. & ŠAFAŘíK, I. 1999. Magnetic solid-phase extraction. *Journal of Magnetism and Magnetic Materials,* 194**,** 108-112.

SAHOO, T. R. & PRELOT, B. 2020. Adsorption processes for the removal of contaminants from wastewater: the perspective role of nanomaterials and nanotechnology. *Nanomaterials for the detection and removal of wastewater pollutants.* Elsevier.

SAJID, M., BARI, S., REHMAN, M. S. U., ASHFAQ, M., GUOLIANG, Y. & MUSTAFA, G. 2022. Adsorption characteristics of paracetamol removal onto activated carbon prepared from Cannabis sativum Hemp. *Alexandria Engineering Journal,* 61**,** 7203-7212.

SAJID, M., NAZAL, M. K. & IHSANULLAH, I. 2021. Novel materials for dispersive (micro) solid-phase extraction of polycyclic aromatic hydrocarbons in environmental water samples: A review. *Analytica Chimica Acta,* 1141**,** 246-262.

SAJINI, T. & MATHEW, B. 2021. A brief overview of molecularly imprinted polymers: Highlighting computational design, nano and photo-responsive imprinting. *Talanta Open,* 4**,** 100072.

SANUSI, R. & LIVESLEY, S. J. 2020. London Plane trees (Platanus x acerifolia) before, during and after a heatwave: Losing leaves means less cooling benefit. *Urban forestry & urban greening,* 54**,** 126746.

SATHYA, K., NAGARAJAN, K., CARLIN GEOR MALAR, G., RAJALAKSHMI, S. & RAJA LAKSHMI, P. 2022. A comprehensive review on comparison among effluent treatment methods and modern methods of treatment of industrial wastewater effluent from different sources. *Applied Water Science,* 12**,** 70.

SELLERGREN, B. 1994. Direct drug determination by selective sample enrichment on an imprinted polymer. *Analytical chemistry,* 66**,** 1578-1582.

SENGAR, A. & VIJAYANANDAN, A. 2022. Human health and ecological risk assessment of 98 pharmaceuticals and personal care products (PPCPs) detected in Indian surface and wastewaters. *Science of the Total Environment,* 807**,** 150677.

SERWECIŃSKA, L. 2020. Antimicrobials and antibiotic-resistant bacteria: a risk to the environment and to public health. *Water,* 12**,** 3313.

SHAH, S. S., SHAIKH, M. N., KHAN, M. Y., ALFASANE, M. A., RAHMAN, M. M. & AZIZ, M. A. 2021. Present status and future prospects of jute in nanotechnology: A review. *The Chemical Record,* 21**,** 1631-1665.

SHAKOOR, M. B., UL HASAN, I. M., AHMAD, S. R., FARID, M., MAJID, M., BIBI, I., JILANI, A., KOKAB, T. & NIAZI, N. K. 2022. Developments in Membrane Technologies and Ion-Exchange Methods for Arsenic Removal from Aquatic Ecosystems. *Arsenic in Plants: Uptake, Consequences and Remediation Techniques***,** 315-329.

SHETTY, K., BHANDARI, A. & YADAV, K. S. 2022. Nanoparticles incorporated in nanofibers using electrospinning: A novel nano-in-nano delivery system. *Journal of Controlled Release,* 350**,** 421-434.

SHI, R., TAO, L., TU, X., ZHANG, C., XIONG, Z., RAMI HOROWITZ, A., ASHER, J. B., HE, J. & HU, F. 2022. Metabolite Profiling and Transcriptome Analyses Provide Insight Into Phenolic and Flavonoid Biosynthesis in the Nutshell of Macadamia Ternifolia. *Frontiers in Genetics,* 12**,** 2886.

SIBULALI, A. 2020. Market Intelligence Report: Macadamia Nuts Industry. *South Africa, Western Cape Department of Agriculture*.

SIDHU, A. K., VERMA, N. & KAUSHAL, P. 2022. Role of biogenic capping agents in the synthesis of metallic nanoparticles and evaluation of their therapeutic potential. *Frontiers in Nanotechnology,* 3**,** 105.

SOKUNBI, O., AJANI, O., LAWANSON, A. & AMAO, E. 2019. Antibiotic potential of Moringa leaf (Moringa oleifera Lam.) crude extract in bull semen extender. *European Journal of Medicinal Plants,* 9**,** 1-8.

SONG, Z., LI, J., LU, W., LI, B., YANG, G., BI, Y., ARABI, M., WANG, X., MA, J. & CHEN, L. 2022. Molecularly imprinted polymers based materials and their applications in chromatographic and electrophoretic separations. *TrAC Trends in Analytical Chemistry,* 146**,** 116504.

SPÄTH, J., ARUMUGAM, P., LINDBERG, R. H., ABAFE, O. A., JANSSON, S., FICK, J. & BUCKLEY, C. A. 2021. Biochar for the removal of detected micropollutants in South African domestic wastewater: a case study from a demonstration-scale decentralised wastewater treatment system in eThekwini. *Water SA,* 47**,** 396–416-396–416.

SULLIVAN, M. V., ALLABUSH, F., BUNKA, D., TOLLEY, A., MENDES, P. M., TUCKER, J. H. & TURNER, N. W. 2021. Hybrid aptamer-molecularly imprinted polymer (AptaMIP) nanoparticles selective for the antibiotic moxifloxacin. *Polymer Chemistry,* 12**,** 4394-4405.

SULLIVAN, M. V., HENDERSON, A., HAND, R. A. & TURNER, N. W. 2022. A molecularly imprinted polymer nanoparticle-based surface plasmon resonance sensor platform for antibiotic detection in river water and milk. *Analytical and Bioanalytical Chemistry,* 414**,** 3687-3696.

SUN, D., SONG, Z., ZHANG, Y., WANG, Y., LV, M., LIU, H., WANG, L., LU, W., LI, J. & CHEN, L. 2021. Recent advances in molecular-imprinting-based solid-phase extraction of antibiotics residues coupled with chromatographic analysis. *Frontiers in Environmental Chemistry,* 2**,** 703961.

SUSEELA, M. N. L., VISWANADH, M. K., MEHATA, A. K., PRIYA, V., SETIA, V. A., MALIK, A. K., GOKUL, P., SELVIN, J. & MUTHU, M. S. 2023. Advances in solid-phase extraction techniques: role of nanosorbents for the enrichment of antibiotics for analytical quantification. *Journal of Chromatography A***,** 463937.

SUZAEI, F. M., DARYANAVARD, S. M., ABDEL-REHIM, A., BASSYOUNI, F. & ABDEL-REHIM, M. 2023. Recent molecularly imprinted polymers applications in bioanalysis. *Chemical Papers,* 77**,** 619-655.

SYED YAACOB, S. F. F., SUWAIBATU, M., RAJA JAMIL, R. Z., MOHAMED ZAIN, N. N., RAOOV, M. & MOHD SUAH, F. B. 2023. Review of molecular imprinting polymer: Basic characteristics and removal of phenolic contaminants based on the functionalized cyclodextrin monomer. *Journal of Chemical Technology & Biotechnology,* 98**,** 312-330.

SZÉKELY, A. & KLUSSMANN, M. 2019. Molecular Radical Chain Initiators for Ambient-to Low-Temperature Applications. *Chemistry–An Asian Journal,* 14**,** 105-115.

TAHA, I. M., ZAGHLOOL, A., NASR, A., NAGIB, A., EL AZAB, I. H., MERSAL, G. A., IBRAHIM, M. M. & FAHMY, A. 2022. Impact of Starch Coating Embedded with Silver Nanoparticles on Strawberry Storage Time. *Polymers,* 14**,** 1439.

TORTELLA, G., RUBILAR, O., DURÁN, N., DIEZ, M., MARTÍNEZ, M., PARADA, J. & SEABRA, A. 2020. Silver nanoparticles: Toxicity in model organisms as an overview of its hazard for human health and the environment. *Journal of hazardous materials,* 390**,** 121974.

TSALBOURIS, A., KALOGIOURI, N. P., KABIR, A., FURTON, K. G. & SAMANIDOU, V. F. 2021. Bisphenol A migration to alcoholic and non-alcoholic beverages–An improved molecular imprinted solid phase extraction method prior to detection with HPLC-DAD. *Microchemical Journal,* 162**,** 105846.

TURIEL, E. & MARTÍN-ESTEBAN, A. 2019. Molecularly imprinted polymers-based microextraction techniques. *TrAC Trends in Analytical Chemistry,* 118**,** 574-586.

UNUABONAH, E. I., OMOROGIE, M. O. & OLADOJA, N. A. 2019. Modeling in adsorption: fundamentals and applications. *Composite nanoadsorbents.* Elsevier.

VAREDA, J. P. 2023. On validity, physical meaning, mechanism insights and regression of adsorption kinetic models. *Journal of Molecular Liquids***,** 121416.

VILLARREAL-LUCIO, D. S., VARGAS-BERRONES, K. X., DÍAZ DE LEÓN-MARTÍNEZ, L. & FLORES-RAMÍEZ, R. 2022. Molecularly imprinted polymers for environmental adsorption applications. *Environmental Science and Pollution Research***,** 1-20.

VINAYAGAM, V., MURUGAN, S., KUMARESAN, R., NARAYANAN, M., SILLANPÄÄ, M., DAI VIET, N. V., KUSHWAHA, O. S., JENIS, P., POTDAR, P. & GADIYA, S. 2022. Sustainable adsorbents for the removal of pharmaceuticals from wastewater: A review. *Chemosphere***,** 134597.

WALENG, N. J. & NOMNGONGO, P. N. 2022. Occurrence of pharmaceuticals in the environmental waters: African and Asian perspectives. *Environmental Chemistry and Ecotoxicology,* 4**,** 50-66.

WAN, Q., LIU, H., DENG, Z., BU, J., LI, T., YANG, Y. & ZHONG, S. 2021. A critical review of molecularly imprinted solid phase extraction technology. *Journal of Polymer Research,* 28**,** 1-16.

WANG, J., HAN, Q., WANG, K., LI, S., LUO, W., LIANG, Q., ZHONG, J. & DING, M. 2022. Recent advances in development of functional magnetic adsorbents for selective separation of proteins/peptides. *Talanta***,** 123919.

WANI, I. A., AHMAD, T. & KHOSLA, A. 2021. Recent advances in anticancer and antimicrobial activity of silver nanoparticles synthesized using phytochemicals and organic polymers. *Nanotechnology,* 32**,** 462001.

WEN, Y. 2020. Recent advances in solid-phase extraction techniques with nanomaterials. *Handbook of Nanomaterials in Analytical Chemistry***,** 57-73.

WU, X., TANG, Y., OSMAN, E. E., WAN, J., JIANG, W., YANG, G., XIONG, J., ZHU, Q. & HU, J.-F. 2022. Bioassay-guided isolation of new flavonoid glycosides from platanus× acerifolia leaves and their staphylococcus aureus inhibitory effects. *Molecules,* 27**,** 5357.

XU, J., MIAO, H., WANG, J. & PAN, G. 2020. Molecularly imprinted synthetic antibodies: from chemical design to biomedical applications. *Small,* 16**,** 1906644.

YADAV, N., GARG, V. K., CHHILLAR, A. K. & RANA, J. S. 2021. Detection and remediation of pollutants to maintain ecosustainability employing nanotechnology: A review. *Chemosphere,* 280**,** 130792.

YANG, Y. & SHEN, X. 2022. Preparation and application of molecularly imprinted polymers for flavonoids: Review and perspective. *Molecules,* 27**,** 7355.

YIN, S.-J., ZHAO, J. & YANG, F.-Q. 2021. Recent applications of magnetic solid phase extraction in sample preparation for phytochemical analysis. *Journal of Pharmaceutical and Biomedical Analysis,* 192**,** 113675.

YOON, B. K., JEON, W.-Y., SUT, T. N., CHO, N.-J. & JACKMAN, J. A. 2020. Stopping membrane-enveloped viruses with nanotechnology strategies: Toward antiviral drug development and pandemic preparedness. *ACS nano,* 15**,** 125-148.

YU, M., WANG, L., HU, L., LI, Y., LUO, D. & MEI, S. 2019. Recent applications of magnetic composites as extraction adsorbents for determination of environmental pollutants. *TrAC Trends in Analytical Chemistry,* 119**,** 115611.

YUAN, T., ZENG, J., WANG, B., CHENG, Z., GAO, W., XU, J. & CHEN, K. 2021. Silver nanoparticles immobilized on cellulose nanofibrils for starch-based nanocomposites

with high antibacterial, biocompatible, and mechanical properties. *Cellulose,* 28**,** 855-869.

ZAMAN, A., ALI, M. S., ORASUGH, J. T., BANERJEE, P. & CHATTOPADHYAY, D. 2022. Biopolymer-based nanocomposites for removal of hazardous dyes from water bodies. *Innovations in environmental biotechnology.* Springer.

ZARE, E. N., FALLAH, Z., LE, V. T., DOAN, V.-D., MUDHOO, A., JOO, S.-W., VASSEGHIAN, Y., TAJBAKHSH, M., MORADI, O. & SILLANPÄÄ, M. 2022. Remediation of pharmaceuticals from contaminated water by molecularly imprinted polymers: a review. *Environmental Chemistry Letters***,** 1-36.

ZHANG, H. 2020. Molecularly imprinted nanoparticles for biomedical applications. *Advanced Materials,* 32**,** 1806328.

ZHANG, S., ANGE, K. U., ALI, N., YANG, Y., KHAN, A., ALI, F., SAJID, M., TIAN, C. T. & BILAL, M. 2022. Analytical perspective and environmental remediation potentials of magnetic composite nanosorbents—A review. *Chemosphere***,** 135312.

ZHANG, Y., ZHU, C., LIU, F., YUAN, Y., WU, H. & LI, A. 2019. Effects of ionic strength on removal of toxic pollutants from aqueous media with multifarious adsorbents: A review. *Science of the Total Environment,* 646**,** 265-279.

ZHOU, X.-Y., LI, C.-X., ZHANG, J.-B., TANG, J.-T., YANG, X., ALBARMAQI, R. A., LI, Y.-Y. & KUANG, Y.-Q. 2022. Association of human leukocyte antigen alleles and hypersensitivity of Efavirenz/Nevirapine in HIV-infected Chinese patients. *AIDS Research and Human Retroviruses,* 38**,** 884-889.

ZHU, G., CHENG, G., WANG, P., LI, W., WANG, Y. & FAN, J. 2019. Water compatible imprinted polymer prepared in water for selective solid phase extraction and determination of ciprofloxacin in real samples. *Talanta,* 200**,** 307-315.

ZHU, M., LI, X., GE, L., ZI, Y., QI, M., LI, Y., LI, D. & MU, C. 2020. Green synthesis of κ-carrageenan@ Ag submicron-particles with high aqueous stability, robust antibacterial activity and low cytotoxicity. *Materials Science and Engineering: C,* 106**,** 110185.

ZOU, D., LI, P., YANG, C., HAN, D. & YAN, H. 2022. Rapid determination of perfluorinated compounds in pork samples using a molecularly imprinted phenolic resin adsorbent in dispersive solid phase extraction-liquid chromatography tandem mass spectrometry. *Analytica Chimica Acta,* 1226**,** 340271.

Chapter 3

Removal of multiple classes of pharmaceuticals from wastewater using multi-template molecularly imprinted polymer (MIP) as an adsorbent: kinetic, isotherm and thermodynamic studies

Abstract

Numerous pharmaceutical drug classes have been found in diverse environmental compartments (e.g., biota, water, and sediments), and further research is being carried out to fully comprehend their fate in the aquatic environment. The goal of this study was to synthesize and characterize a multi-template molecularly imprinted polymer (MIP) using sulfamethoxazole (SMX), nevirapine (Nvp), and ibuprofen (Ibu) drugs as target templates. Characteristics of the polymers by SEM revealed that the synthesized MIP had a rougher surface than the non-imprinted polymer (NIP) which signals its high adsorption capacity. According to the FTIR spectrum, functional groups of OH, C=C, and C=O that develop from the template during synthesis are involved in the formation of the MIP. The high temperature 280-450 °C and 270-500 °C at which NIP and MIP degradation occurred in the TGA findings showed that the polymer is temperature stable. Notably, the optimum removal results were obtained when a temperature of 40 °C, pH 7, mass dosage of 40 mg and contact time of 10 minutes were used for adsorption studies. Under these conditions, the pharmaceutical drug removal percentage of 75-99% was achieved. The calculated maximum monolayer adsorption capacities were, 3.89, 4.97, and 3.40 mg g^{-1} for SMX, Nvp, and Ibu respectively. Statistical analysis revealed that adsorbent dosage, concentration, and pH have statistical significance with $p<0.05$, whereas temperature and time did not show any statistical significance. It was discovered that the adsorption process adhered to the pseudo-second order kinetic model, according to the kinetic studies, whereas the thermodynamic data demonstrated the endothermic and spontaneous nature of the adsorption process. The synthesized MIP showed to be highly selective towards the target analytes compared to the competitor. Moreover, for MIP regeneration, 40 mg of MIP that had previously adsorbed SMX, Nvp, and Ibu was washed for 10 min in a 9:1, v/v acetonitrile/acetic acid solution before being utilized again to adsorb SMX, Nvp, and Ibu in the next cycle. The procedure was repeated up to 5 cycles. Accordingly, the MIP particles were preserved with adsorption efficiency of >90 %. This therefore indicated that MIP can be efficiently reused.

Keywords: adsorption, pharmaceuticals, wastewater, molecularly imprinted polymer

3.1 Introduction

Pharmaceutical compounds are used to cure, prevent and diagnose a variety of diseases and thus prolong human and animal health. However, their intensive usage results in their presence in the environment and thus provides a risk to the environment, especially in aquatic habitats, which can have ecotoxicological impacts (Meléndez-Marmolejo et al., 2022). The majority of pharmaceutical compounds found in aqueous matrices are derived from human intake, which causes both the original and metabolized pharmaceuticals to be excreted. Also, the improper disposal of unused medications, which is typically done by flushing them down the sink or toilet or throwing them in trash that is going to be dumped in landfills (Sanusi et al., 2023). Pharmaceuticals are highly polar and water-soluble thus, they manage to evade wastewater treatment process (Waleng and Nomngongo, 2022). Due to their ability to bypass wastewater treatment facilities, pharmaceuticals are often found in the water supply (Zare et al., 2022). Other pharmaceuticals only partially break down, and some of their metabolites may even be deconjugated back into their biologically active forms. As a result, they may be found in higher concentrations in wastewater effluents compared to the corresponding influent water.

Pharmaceutical residues can have ecotoxic effects, influence hormones, and lead to drug resistance, despite the fact that they exist in the aquatic ecosystem in extremely modest concentrations (ng - µg L^{-1}). (Ravikumar et al., 2022). Effluents from wastewater treatment plants (WWTPs) typically include relatively high quantities of pharmaceuticals because current wastewater treatment technologies are usually ineffective at removing them (Samal et al., 2022). This indicates that more efficient treatment techniques are needed to reduce the potential impacts of these contaminants. Therefore, there is a pressing necessity to develop efficient and affordable methods that can be utilized to remove pharmaceuticals from water sources. It is crucial to provide a long-term solution based on social, techno-economical, and environmental conditions in a sustainable way to meet current demands without harming the environment. For example, by using affordable sustainable adsorbents and avoiding the direct disposal of pharmaceuticals in water supplies. Consequently, adsorption is considered an innovative method for the efficient removal of pharmaceutical compounds in water bodies (Birniwa et al., 2023). Notably, several adsorbents have demonstrated their efficacy for the removal of

pharmaceuticals; however, they are not selective, and in any event they are unable to remove pollutants in trace levels despite their outstanding adsorption characteristics (Vinayagam et al., 2022). Hence, finding new and dependable adsorbent to remove pharmaceuticals from the environment is required due to the widespread usage of pharmaceuticals worldwide. Particularly, molecularly imprinted polymers (MIPs) were developed in response to the environmental samples complexity, and they are currently being utilized for improving analytical techniques selectivity. (Azizi and Bottaro, 2020). Regarding the organic chemical's adsorption from aqueous solutions, MIP-based adsorbents are better than alternatives like activated carbon because they are reusable (Okutucu, 2020). Moreso, MIP aspect of reuse goes very well with the concept of green chemistry. MIPs are adsorbents that have been carefully developed to exhibit enhanced specificity for a particular structure or for a very close comparable structure, and they are frequently employed in a variety of applications (Kaya et al., 2022). The simplicity of preparation and the capability for designing "tailor-made" binding sites that may be created by simply altering the synthesis procedure for the appropriate target molecule used as a template during the polymerization process are the key benefits of MIPs (Arabi et al., 2021). The development of several MIP applications for pharmaceutical adsorption and removal has been facilitated by the advantages of MIPs, including their low cost of operation, high selectivity, reusability, stability at pH and temperature extremes, and ease of preparation (Liu and Poma, 2021).

Notably, most investigations in environmental monitoring focuses on synthesizing MIPs that specifically target one pharmaceutical or a group of pharmaceuticals within the same class. Pharmaceuticals are composed of mixtures of many pharmaceutical classes, some of which share similar physicochemical properties, rather than existing in isolation in the environment. (Godoy et al., 2019). The requirement for approaches that make it possible to analyse many compounds as opposed to those that only analyse one analyte at a time is emphasized by principle no. 8 of the 12 principles of green analytical chemistry (López-Lorente et al., 2022). This principle highlights the necessity of techniques that allow for evaluation of several compounds as opposed to those that examine one analyte at a time. The limitation of MIPs to only identify a single target with an ion or template molecule prevents the practical implementation for the simultaneous recognition, enrichment, and removal of several targets (Wang et al., 2023). By simultaneously using multiple targets serving as template molecules, the multi-template MIPs may generate varieties of recognition sites on a single polymeric material. Determining a single MIP that can be utilized to target three distinct types of

pharmaceuticals from environmental water sources was the goal of the current work as a result. The model compounds included an antibiotic (sulfamethoxazole), antiretroviral (nevirapine), and non-steroidal anti-inflammatory drug (ibuprofen). To the best of our knowledge, no molecularly imprinted polymer has been described for the simultaneous removal of sulfamethoxazole, nevirapine and ibuprofen in an aqueous environment, including a thorough analysis of adsorption kinetics and isotherms. **Table 3.1** shows the physicochemical properties and molecular structure of the model pharmaceuticals compounds.

Table 3.1: Physicochemical properties of the three selected pharmaceuticals

Pharmaceutical	**Class**	**Chemical structure**	**Molecular weight (g/mol)**	**pKa**	**Log K_{ow}**	**Water solubility (mg/mL)**
Nevirapine	ARVDs	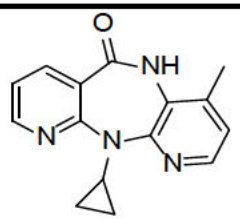	266.294	2.8	3.89	0.1
Sulfamethoxazole	Antibiotics	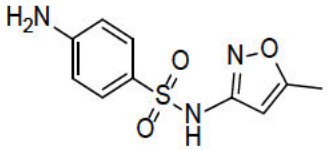	253.28	5.6	0.89	0.61
Ibuprofen		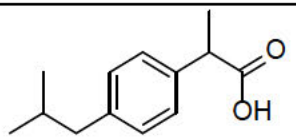	206.29	4.85	3.97	0.021
Diclofenac	NSAIDs	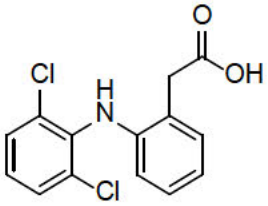	296.148	4.15	4.02	0.1

3.2 Methodology

3.2.1 Chemicals and Reagents

Nevirapine, ibuprofen, sulfamethoxazole, diclofenac, 2-vinylpyridine, 1,1-azobis-(cyclohexane carbonitrile) (98 %), EGDMA (98 %), acetonitrile (≥99.9 %), glacial acetic acid (100%) and toluene (99.7 %), were all purchased from Sigma-Aldrich (Johannesburg, South Africa).

3.2.2 Synthesis of multi-template MIP

In this study, the use of a multi-template molecularly imprinted polymer (MIP) as a selective adsorbent to remove sulfamethoxazole, nevirapine, and ibuprofen from wastewater was reported. The synthesis of MIPs was adopted with slight modifications from a method used by Madikizela and co-workers (Madikizela and Chimuka, 2016a). The MIP bulk polymerization was carried out in two steps. In the initial step, the process of synthesis involved dissolving 20 mg of 1,1′-azobis-(cyclohexane carbonitrile) in 50 mL of toluene, after which 1.51 mL of ethylene glycol dimethacrylate (EGDMA) was added. After a 10-minute nitrogen purge, the reaction flask was sealed. The reaction was then allowed to occur for 16 hours at 60 °C in an oil bath while being constantly stirred. In the second step, 25 mg of each pharmaceutical (ibuprofen, nevirapine and sulfamethoxazole) was dissolved in 25mL of acetonitrile. Thereafter, 1 mL of 2-vinylpyridine, 3.85 mL ethylene glycol dimethacrylate (EGDMA), 60 mg 1,1′-azobis-(cyclohexane carbonitrile) and 25 mL of toluene was added. The resulting mixture was transferred into the first reaction flask and deoxygenated by purging with nitrogen for 15 minutes and sealed. The reaction was conducted for 24 hours at 80 °C in an oil bath. The resultant polymer was dried in an oven at 100 °C. After that, the polymer was ground, sieved, and particles between 25 and 50 µm were gathered. The elution of the templates from the resulting polymer was performed through the application of Soxhlet extraction procedure by washing the polymer repeatedly with a mixture of acetonitrile: acetic acid (9:1 v/v) until the templates were not detected by the LC-MS system. Thereafter, the polymer was washed with 100% acetonitrile to wash off acetic acid. The NIP was prepared following the same procedure but with the absence of the template in the polymerization mixture.

3.2.3 Instrumentation

The FMH SHKO 20 rotary orbital shaker (DLD Scientific, Durban, South Africa) was used to shake samples for optimisation. The analysis of the selected pharmaceuticals was performed using a LC Shimadzu 2020 series (Shimadzu, Tokyo, Japan). The separation of the target analytes was performed using a Shim-Pack GIST C18-HP (150 × 4.6 mm i.d, 3,5 µm particle size) column (Shimadzu, Tokyo, Japan). The column temperature was kept at 40 ºC. The mobile phase was pumped isocratically at a flow rate of 0.4 mL min^{-1} with a composition of 0.1 % formic acid in water and acetonitrile (10:90). The injection volume was 10 µL in ambient column temperature. The UV/VIS detector was set at 210 nm for all template measurements. 100 mg/L stock solution of targeted pharmaceuticals was prepared by dissolving 10 mg of each template (sulfamethoxazole, Ibuprofen and nevirapine) in acetonitrile. From the stock solution, a concentration range of standards ranging from 0.1-2 mg/L was prepared. These standard solutions were analysed with the LC-MS system and used for the construction of the calibration curve. The compounds were successfully quantified using the LC-MS with detection limits of 0.25, 0.14 and 0.18 mg L^{-1} and quantification limits of 0.75, 0.42 and 0.53 mg L^{-1} for SMX, NVP, and Ibu, respectively. According to **Figure 3.1**, the LC-MS chromatograms indicate the peaks of the three compounds with their respective retention times of 4.2, 4.9, and 5.9 minutes for SMX, Nvp, and Ibu at a wavelength of 210 nm.

.

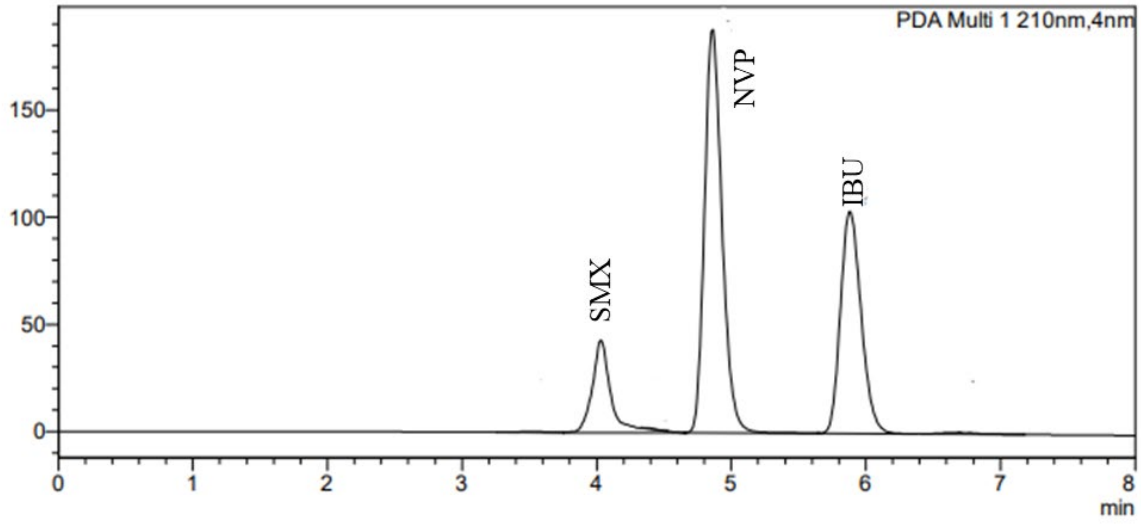

Figure 3.1: LC-MS chromatogram of sulfamethoxazole (SMX), nevirapine (NVP) and ibuprofen (IBU) at a PDA wavelength of 210 nm.

3.2.4 Characterisation of polymers

To ensure the potential for the compounds to be selectively adsorbed and extracted as well as the stability of the polymer, the produced polymers were evaluated using a variety of techniques. Thermogravimetric analysis was conducted using an Anton Paar TGA instrument (Mettler Toledo, Columbus, USA) to evaluate the polymer's thermal stability. Fourier transform infrared (FTIR) spectroscopy (PerkinElmer Inc., United States) was utilized for identification of functional groups in the MIP . A JOEL model JSM 6700F scanning electron microscope instrument (Tokyo, Japan) was used to assess the morphology of the synthesised polymers. X-ray diffraction (XRD) patterns were obtained with a Rigaku MiniFlex 600 (Rigaku Tokyo, Japan) instrument.

3.2.5 Sampling

Samples of wastewater were collected from the Darvill WWTPs in Pietermaritzburg, KwaZulu-Natal Province, South Africa. This WWTPs receive sewerage from both domestic and industrial wastes. The samples were collected from October to December 2022. The samples were collected in dark brown bottles, stored in a cooler box and were then transported to the laboratory where they were stored in the refrigerator (4°C) for further analysis.

3.3 Optimisation of adsorption studies

All the parameters were fixed for the tested range in order to determine the factors that will influence adsorption, such as adsorbent mass dosage, temperature, initial concentration, contact time, and pH on the adsorption process. For the purpose of determining the impact of these parameters on the adsorption process of the three pharmaceuticals in aqueous solutions, initial concentrations of pharmaceuticals (0.2-2 mg L^{-1}), various pH (3-10), temperature range (25-70 °C), contact time (10-60 minutes), and adsorbent dose (10-50 mg) were investigated. The adsorption experiment was performed in wastewater samples that had already been spiked with the mixture of the selected pharmaceuticals to make a final concentration of 1 mg L^{-1}. The solutions were then filtered, and LC-MS-2020 was used to analyse the concentration of the selected pharmaceuticals in the supernatant. The quantity of SMX, Nvp and Ibu which had undergone adsorption onto the MIP at equipoised conditions, was estimated using equation 3.1 and the effective removal percentage of the pharmaceuticals was obtained by employing equation 3.2.

$$qe = \frac{(C_i - C_e)V}{m} \quad \text{(Eq 3.1)}$$

$$Removal\ \% = \frac{(C_i - C_e)}{C_i}\ X\ 100 \quad \text{(Eq 3.2)}$$

Wherein the quantity of the pharmaceuticals present initially is denoted by C_i of the reaction and C_e is the pharmaceuticals concentration during equilibrium condition correspondingly; mass in mg of adsorbent is represented as m and the working volume (mL) of the solution is depicted as V.

3.4 Selectivity study

MIP selectivity for three pharmaceuticals was conducted at room temperature in batch rebinding experiments using optimum conditions, which were 10 mg of the polymer mixed with a water sample (pH 7.0) that was previously spiked to make a final concentration of 1 mg L^{-1} mixture of ibuprofen, nevirapine, sulfamethoxazole and diclofenac (as a competitor) and agitated for 10 minutes. The partition coefficient and selectivity coefficient were used to assess the imprinted polymers selectivity toward the three chosen pharmaceuticals and the competitor. Equation (3.3) was used to determine the impact of imprinting on selectivity.

$$K_d = \frac{(C_i - C_e)V}{m} \quad \text{(eq 3.3)}$$

$$k = \frac{K_d(Template)}{K_d(Competitor)} \quad \text{(eq 3.4)}$$

$$k' = \frac{K_d(MIP)}{K_d(NIP)} \quad \text{(eq 3.5)}$$

Where K_d (mg g^{-1}) is the partition coefficient, C_i is the initial solution concentration, C_e is the final solution concentration, V (mL) is the volume of the solution, and m (mg) is the mass of the polymer. Furthermore, the selectivity coefficient for the binding of SMX, Nvp and Ibu in the existence of a competitor was calculated using equation (3.4), where *k* is the selectivity coefficient (Nkosi et al., 2022). Additionally, using the relative selectivity coefficient (*k*') in accordance with equation 3.5, the selectivity of the MIP with regard to the NIP was determined.

3.5 Reusability

After adsorption of SMX, Nvp and Ibu, the MIP was regenerated through washing with a mixture of acetonitrile/acetic acid (9:1, v/v), which removed the drugs from the binding sites. Following that, 10 mL of pure acetonitrile was used to regenerate the MIP particles in order to desorb any undesirable compounds. Thereafter, the regenerated MIP was applied in the

adsorption of SMX, Nvp and Ibu from aqueous solutions for the next cycle. This procedure was performed five times, with each adsorption cycle lasting 10 minutes.

3.6 Results and discussion

3.6.1 Characterisation

3.6.1.1 Scanning Electron Microscope (SEM)

Scanning electron microscope (SEM) was used for careful consideration of MIP and NIP morphology and smoothness. The morphologies of unwashed and washed MIP and NIP samples are shown in **Figure 3.2**. The results in **Figure 3.2** (a) and (b) indicate that the uneven forms of the polymer particles are a frequent characteristic of synthetic materials generated by bulk polymerization techniques, which can be attributed to the milling and sieving processes. (Babaeipour and Jabbari, 2023). Larger particle sizes and extremely rough surfaces on the MIP can be attributed to formation of selective cavities within the polymer matrix and are signs that the MIP had been properly prepared. This suggest that MIP can adsorb analytes of interest much better than NIP because of the roughness of its particles, which can result in a higher surface area than NIP. MIPs are generally found to have higher specific surface areas because of their increased porosity and visible imprinting cavities (Ndunda, 2020). The smaller particles were removed during the washing process compared to unwashed MIP (**Fig. 3.2 a and c**) (Sadia et al., 2023).

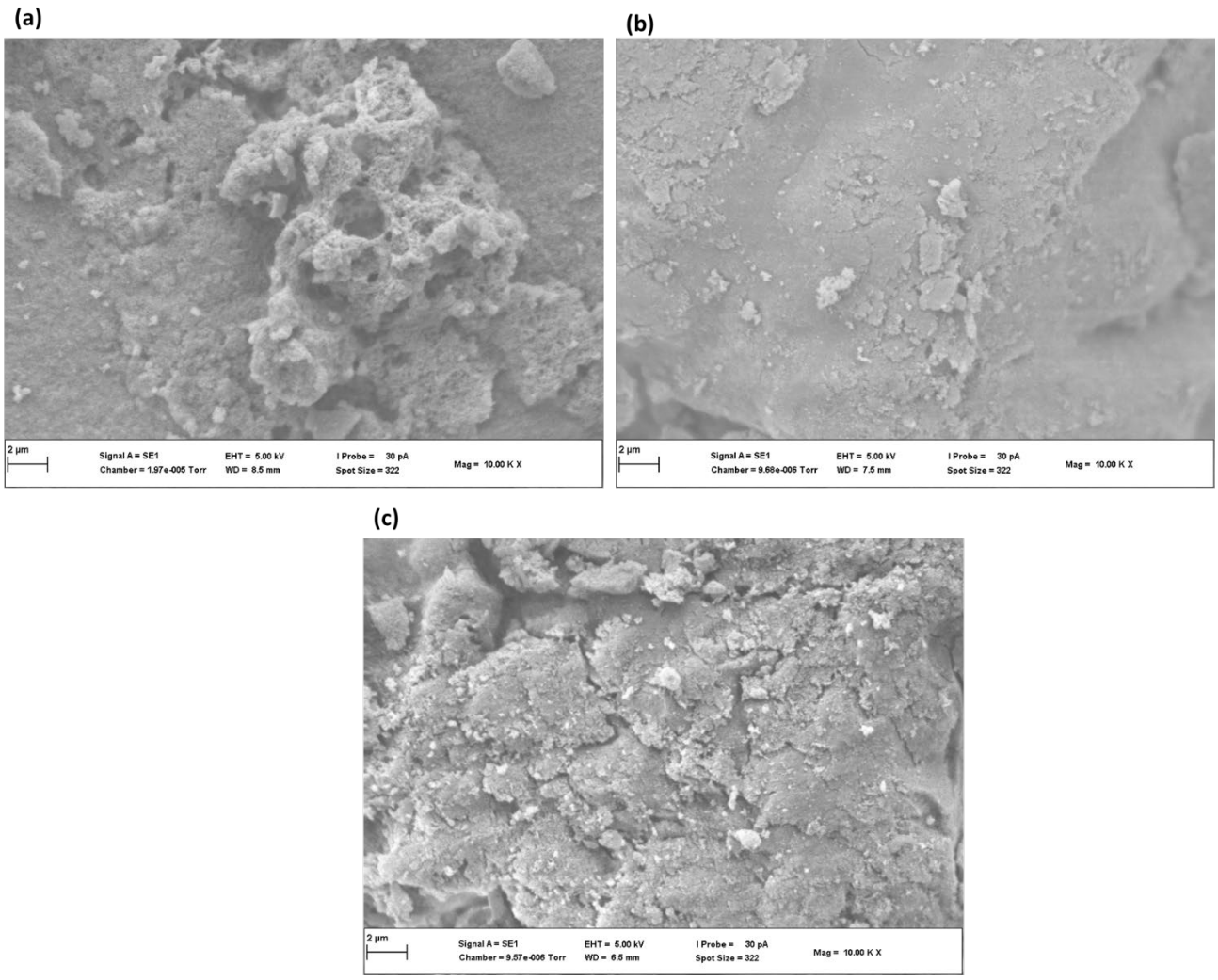

Figure 3.2: SEM images of (a) washed MIP, (b) NIP and (c) unwashed MIP.

3.6.1.2 Fourier transform infrared (FTIR) spectroscopy

The polymers functional groups were identified via FT-IR characterization. The NIP and washed MIP results in **Figure 3.3** demonstrate that the bands' positions and shapes are the same, showing that they were made from the same monomer and crosslinker and were synthesized in a similar manner. Each functional group on the NIP showed intense peaks compared to the washed MIP. The free exposed functional monomers, which were randomly distributed and did not engage in any self-assembly, were most likely the cause of the intense peaks observed (Ndunda, 2020). The -C-O, C=O, and C=C bonds indicative of the ester and alkene functional groups within ethylene glycol dimethacrylate (EGDMA) and the -C-O, -CH3, and C=C bonds significant of the carboxylic acid and alkene functional groups within 2-vinyl pyridine (2-VP) were the observed FT-IR peaks for the NIP and washed MIP structures, respectively. The -CH_2 stretching peak was likewise seen at 2953 cm^{-1} due to the methylene

group in 2-VP and EGDMA. The carbonyl group C=O stretching peak was seen in both MIP and NIP at 1700 cm^{-1}, which might have originated from the template and cross-linking molecules. Weak arrangement bands from 1600 cm^{-1} to 1200 cm^{-1} and sharp bands at 1100 cm^{-1} specifically on MIPs spectra demonstrate the presence of an aromatic ring of the target compounds (-C=O, C-O and -C-N). The interface between templates and monomer offered changeable peaks in the spectrums, which exhibited a broad -OH stretching vibration peak at 3600 cm^{-1} for unwashed MIPs, this peak is not observed on the unwashed MIP, thus signifying successful templates removal from the washed MIP. Furthermore, the unwashed MIP exhibited a discernible resolvement of the unified/distinct peak at about 1639 cm^{-1} after washing treatments, indicating the existence of carbonyl groups derived from the crosslinking and template molecules. Conversely, the washed MIP and NIP traces at approximately 1600-1640 cm^{-1} indicate that this peak has decreased due to the absence of a template. FTIR analysis confirmed the existence of the hydrogen bonding interactions and validity of the mechanism that takes place during the synthesis of the polymers (Meléndez-Marmolejo et al., 2022). In terms of the imprinting effect, MIPs have template-specific binding sites in contrast to NIPs because of the interaction between the template and the functional monomer to produce a pre-polymerization complex. On the other hand, MIPs form background binding sites and are therefore good controls in providing information on binding resulting from low affinity background binding sites. In addition, NIPs are prone to functional monomer aggregation, which reduces the population of functional groups that are available to form background binding sites. As a result, NIPs that experience functional monomer aggregation are deemed to be poor control polymers since they have reduced background binding sites and may give rise to very low binding capacities compared to MIPs giving an impression of imprinting while in the real sense no imprinting effect occurs (Ndunda, 2020). Thus, the imprinting effect, functional monomer aggregation, or variation in surface area/surface morphology could be responsible for the reported discrepancies in MIPs and NIPs performance, according to Roland and coworkers (Roland et al., 2023).

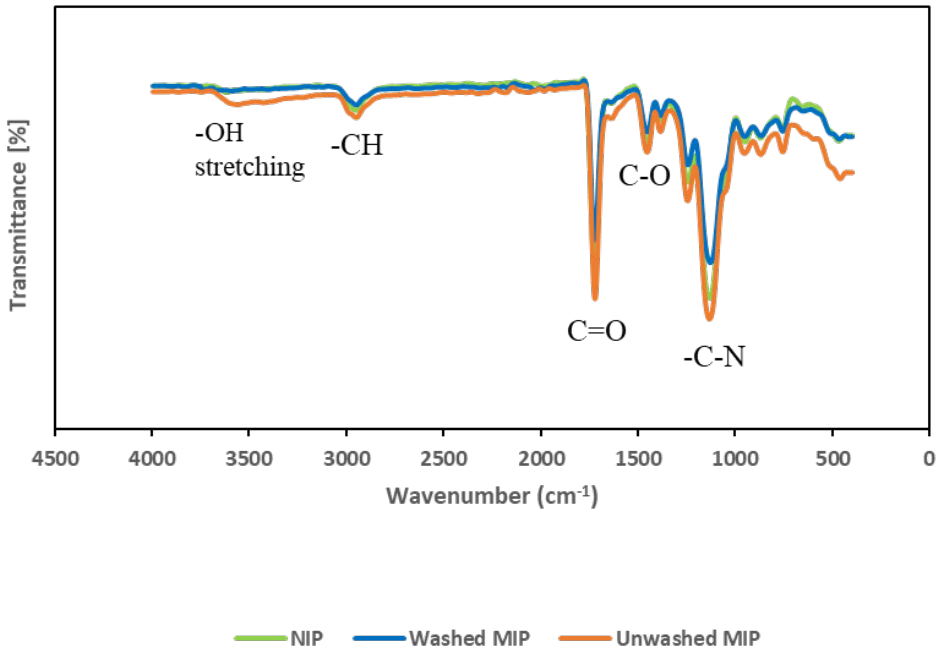

Figure 3.3: FT-IR spectra of unwashed MIP, washed MIP and NIP

3.6.1.3 Thermogravimetric analysis (TGA) and Differential scanning calorimetry (DSC)

The TGA was performed to investigate thermal stability for both MIP and NIP at a temperature range of 25 °C to 700 °C. **Figure 3.4** demonstrates the weight loss percentages (TGA curves) and derivatives TGA curves of washed and unwashed MIP as well as NIP sample. The polymers exhibited no weight loss and showed stability from 100- 265 °C. However, above this temperature, the washed MIP began to degrade more quickly than unwashed MIP and NIP. This might be as a result of the recognition of active sites in the cavities of the washed MIP sample, which were very sensitive to higher temperatures, in contrast to the unwashed MIP sample, where the presence of hydrogen bonds led to increased thermal stability for those given sites. Additionally, because there was no template, there were no active sites in the NIP sample (Tegegne et al., 2021). The polymers degraded rapidly with rapid weight loss from 270 °C to 500 °C, 280-450 °C and 290-450 °C for washed MIP, NIP and unwashed MIP, respectively, due to breakdown of the main carbon skeleton of the polymer. Similar results were reported by Feroz and co-workers for their MIP and NIP (Feroz et al., 2020). Eventually, the washed MIP polymer was broken down completely at 600 °C with <1% residual mass. Unwashed MIP and NIP decomposed at a temperature around 510 °C. This was due to thermal decomposition of the crosslinker (EGDMA) from the polymer structure. Moreover, the differences on thermal decomposition might have been caused by structural changes that might have happened during the template removal procedure (Nkosi et al., 2022). Additionally, by contrasting the thermal

curves of the NIP and unwashed MIP samples, they showed that the network structure of washed MIP contributed to the unwashed MIP slightly higher stability than the NIP sample. Differential scanning calorimetry (DSC) is one of the thermal decomposition analyses which has many applications in chemistry such as detecting changes in enthalpy and the specific heat capacity. DSC thermograms of washed MIP, unwashed MIP and NIP showed an exothermic peak at 351, 371 and 476 °C, respectively which is associated with the thermal decomposition of the polymers. The DSC results reported by Madikizela and coworkers on their multi template MIP was 360 °C (Madikizela et al., 2017).

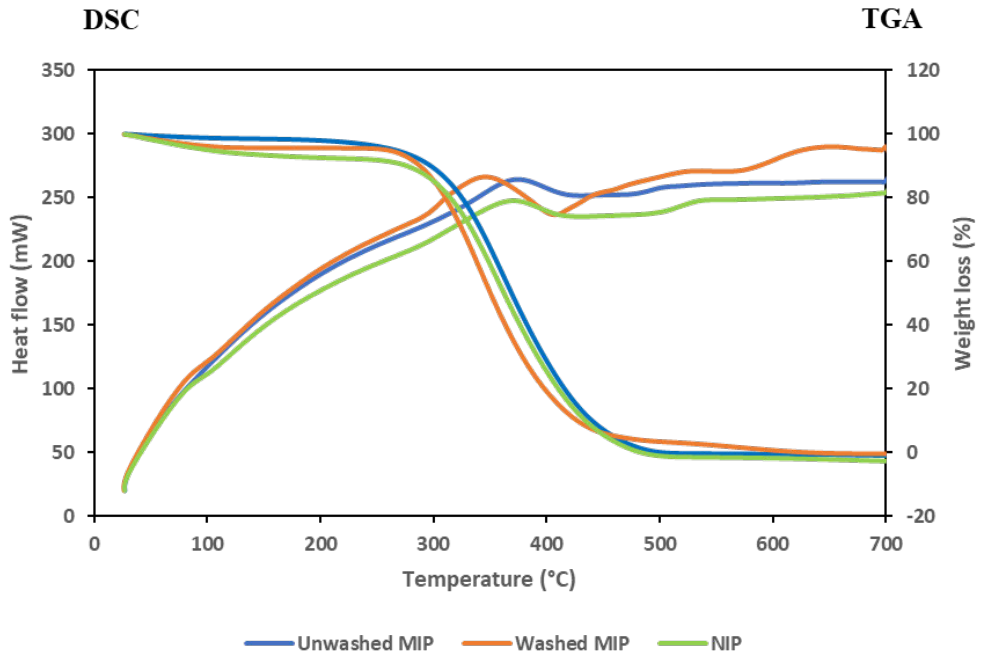

Figure 3.4: TGA and DSC analysis of unwashed MIP, washed MIP and NIP

3.6.1.4 X-ray diffraction (XRD)

The synthesized polymers XRD patterns are shown in **Figure 3.5**. Additionally, the XRD pattern demonstrated that the polymers were similar, with broad peaks at 2 theta values of 17.15, 17.55, and 17.44° for unwashed MIP, washed MIP, and NIP, respectively. This is explained by their similar chemical compositions and also mimics the polymers amorphous nature. Another small peak appeared at 39.44, 40.09, and 39.57° for unwashed MIP, washed MIP, and NIP, which indicates that the interlayer spacing increases. Since the washed MIP surface has more precise binding sites than the unwashed MIP and NIP surface does, it has a higher degree of order (Anirudhan et al., 2021).

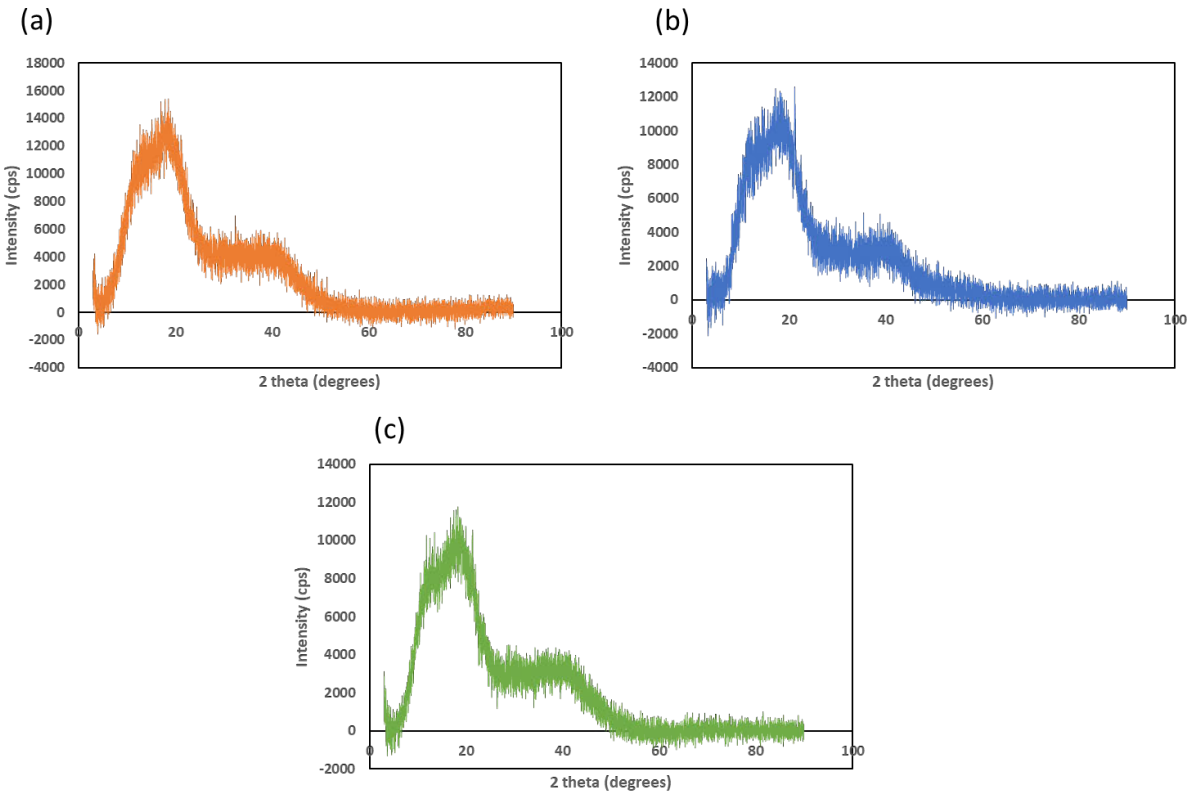

Figure 3.5: X-ray diffraction of (a) unwashed MIP, (b) washed MIP and (c) NIP.

3.6.2 Optimization of parameters

3.6.2.1 Effect of pH

To achieve the highest possible adsorption effectiveness of target compounds, the influence of the pH must be taken into consideration. The chemistry of the adsorbate and the surface binding sites of the adsorbent are both impacted by the pH of the solution, which in turn impacts how pharmaceutical compounds are extracted (Tegegne et al., 2021). Sample pH showed a significant impact on all pharmaceuticals examined for adsorption efficiency. Results portrayed in **Figure 3.6 A** clearly show that the sample pH plays a vital role in the adsorption of the three pharmaceuticals by the synthesized polymer. There was an apparent increase in % removal efficiency from pH 2 to pH 7. According to this, the primary factors for sorption were the hydrophobic contact and hydrogen bond between the acidic compounds and the specific binding sites. The highest removal percentage was observed at pH 7 (> 95%) indicating that the adsorbent showed good adsorption competence in the neutral medium. However, as the pH of the solution increased from 9 to 10, the removal efficiency of the pharmaceuticals decreased. This might be related to the functional groups on the adsorbent and the pKa of the selected pharmaceuticals (**Table 3.1**). The selected pharmaceuticals have a negative charge when pH is

more than 7, and 2-vinylpyridine monomer, which is used to make MIP has a pKa of 4.98, which also has a negative charge. As a result, the binding affinity between the selected pharmaceuticals and MIP was overcome by electrostatic repulsive interactions, and hydrophobic interactions which took over as the primary driving force during the adsorption process. This outcome is in line with a study that found that as the pH value of the solution increased, the amount of pharmaceutical compounds that adsorb onto MIP polymers decreased (Amaly et al., 2021). Notably, a slight decline in adsorption at basic pH was due to the negative ion predominance in compounds and on the MIP surface, which could result in electrostatic repulsion accumulation because hydroxyl (OH^-) groups were formed around the modified adsorbent and would result in low percentage removal (Mbhele et al., 2018). Furthermore, a similar electrostatic interaction could occur due to the presence of oxygen atom in the three pharmaceutical compounds. The pH of 7 gave the highest removal percentage range of 93-98% for all tested compounds, therefore was considered the best pH for the interaction of templates and MIP sites.

3.6.2.2 Effect of mass dosage

An increase in removal efficiency for the selected pharmaceutical compounds was observed when the adsorbent mass was varied from 10 to 50 mg (**Figure 3.6 B**). An increase in MIP dosage causes an increase in active sites for pharmaceutical compounds to bind which means more of these compounds are adsorbed on the MIP surfaces. The extraction efficiency for all the investigated compounds varied from 92-95% when 40 mg of the MIP was used. The close proximity of the extraction efficiency range may be attributable to the use of multiple templates, which shows that all target compounds had approximately equal chances of being adsorbed. There was no major variation in the removal efficiency of the three compounds when the adsorbent mass exceeded 40 mg. This means that during the increase in adsorbent mass, more binding sites in the polymer become available and the removal efficiency is enhanced until the equilibrium is reached at a mass of 40 mg (Qwane et al., 2020). Therefore, 40 mg was chosen as an optimum mass of adsorbent for the simultaneous adsorption of SMX, Nvp and Ibu.

3.6.2.3 Effect of contact time

The impact of contact time was discovered to be a crucial factor in ensuring maximal adsorption efficiency. An extraction efficiency greater than 90 % was achieved within 10 min

of contact between the adsorbents and the three compounds (**Figure 3.6 C**). For MIP, the extraction efficiency attained increased gradually from 95 % in the contact time of 10 minutes to 100 % in 60 minutes. The results demonstrated that there was faster adsorption and that the majority of the adsorbate-adsorbent interaction occurred during the first 10 minutes. The MIP has a large number of available empty adsorption sites, which helps to speed up the initial uptake of the templates as they are adsorbed onto the MIP's adsorption sites (Khatibi et al., 2021). This means the surface of the MIP reached its saturation point within 10 minutes. The maximum pharmaceutical adsorption onto the MIP was reported to be possible in as low as 2 minutes of contact time, in contrast to prior research. Notably, the removal percentage at 10 minutes ranged from 95-99%, hence it was chosen as the optimum time because prolonging the shaking time did not considerably increase the % removal.

3.6.2.4 Effect of temperature

It can be seen from **Figure 3.6 D** that by increasing the temperature from 20 °C to 70 °C, the removal efficiency also increased. This could be as a result of the increase in kinetic effect, thus leading to increased mobility of the adsorbates molecule as temperature increased. As the temperature rises, the adsorbent surface's bond breakdown results in pore enlargement, increasing the removal efficiency and might increase interaction between MIP and the templates. Analytes tend to have reduced kinetic energy at low temperatures, making it more difficult for them to gain access to the active site of the adsorbent. Accordingly, as the temperature increased, the kinetic energy of the analytes increased, allowing the maximum amount of adsorbate molecules to reach the adsorbent surface. From the results, the maximum adsorption for the three compounds occurred at a temperature of 40 °C. The results reported by Khatibi and co-workers also show that MIP adsorbed at higher temperatures (Khatibi et al., 2021). The high adsorption recorded indicates the process is endothermic.

3.6.2.5 Effect on concentration

To comprehend how varying concentrations affect the adsorbent capacity, the initial concentration of the target analyte's effect on the polymer's removal efficiency was investigated. The removal efficiency increased as a function of initial concentration (**Figure 3.6 E)**; this was observed until the adsorbent reached equilibrium at 1 mg L^{-1} . After 1 mg L^{-1} (1-2 mg L^{-1}) the removal efficiency stabilized as a result of reaching equilibrium, hence increasing the adsorbent concentration further would no longer be able to increase the %

removal. This may mean that at higher concentrations, the MIP was becoming saturated. Therefore, 1 mg L^{-1} was the optimum concentration for the removal of the selected pharmaceuticals using MIP. This study was conducted to investigate the effect of the three selected pharmaceuticals' concentrations on their adsorption onto the MIP. This is crucial since it makes it possible to determine the MIP's maximum adsorption capacity. Notably, the three compounds harmony towards the MIP was evidently in the following order: Ibu< SMX < Nvp. This affinity may be explained by the molecular structure of the drugs (**Table 3.1**), SMX and Nvp have two benzene rings, which are more hydrophobic, while Ibu only has one. As a result, these three pharmaceuticals interact with MIP through hydrogen bonds and -interactions between the aromatic rings (Meléndez-Marmolejo et al., 2022, Husein et al., 2019). The drug's molecular weight and subsequent molecule size are additional factors; the molecule with the higher molecular weight is given preference on the surface of the MIPs. The molecular weights are 266.3, 253.3 and 206.3 g/mol for Nvp, SMX and Ibu, correspondingly organized in the subsequent descending order: Ibu < SMX< NVP.

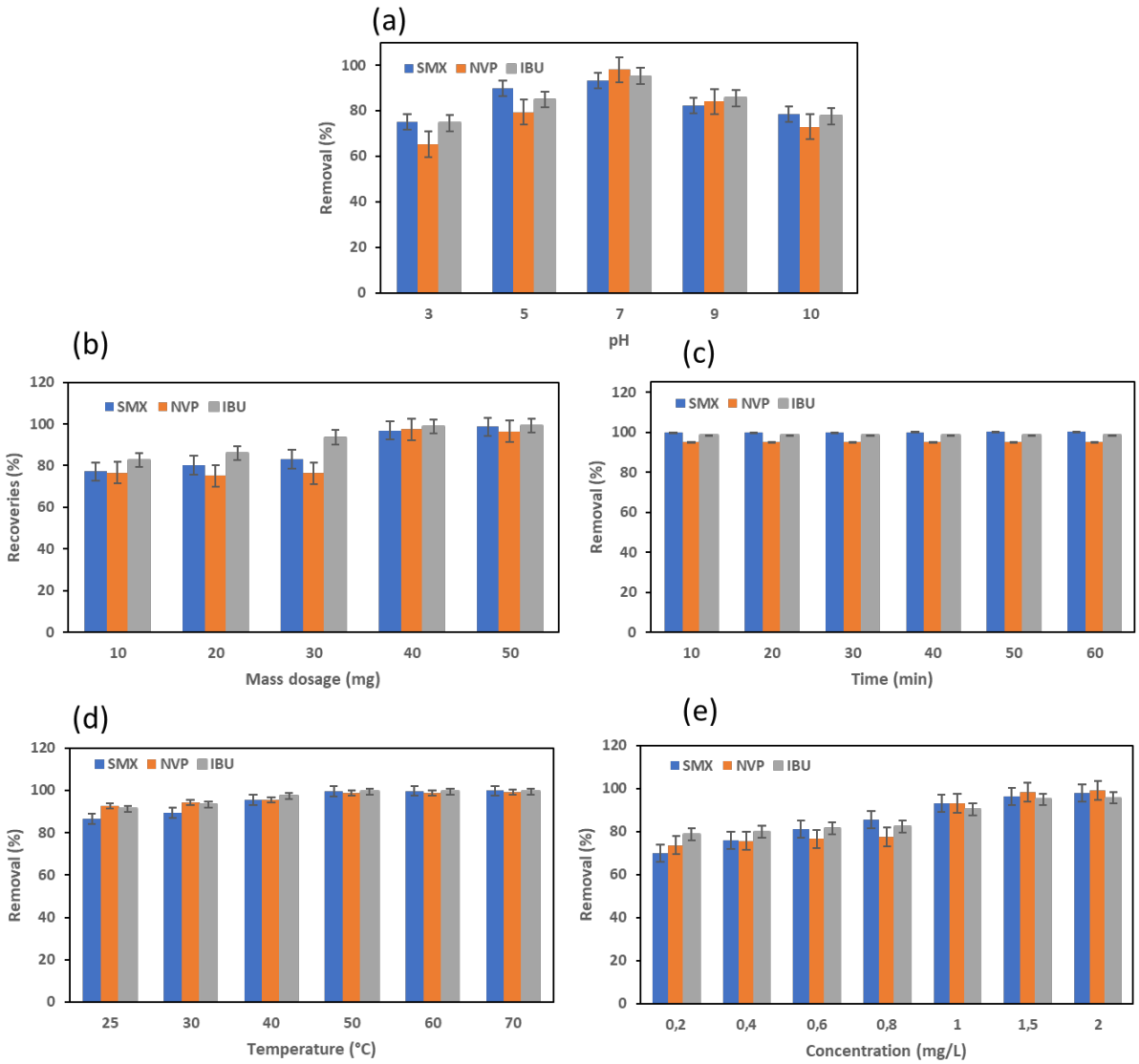

Figure 3.6: Effect of (a)pH, (b)mass dosage, (c)contact time, (d)temperature and (d)concentration on the removal of SMX, Nvp and Ibu.

3.6.3 Statistical analysis

Statistical parameters like Fischer's exact test (F value), probability of error (p value), and sum of squares (SS) values for each parameter can be examined in the model using ANOVA. Moreover, ANOVA was conducted in order to evaluate the significance of the differences. Statistical significance was evaluated at p, 0.05 level. Generally, a high F value indicates significance for a model, and a p value of less than 0.05 (a 5% chance deviation) ensures this. As shown in **Table 3.2**, ANOVA results show that the model has an F value of 5.48 with a p value of < 0.05 indicating that the model is significant. The results further revealed that effects of initial concentration, adsorbent dosage, and pH were statistically significant at a confidence

level of 95% with $p < 0.05$ and F value larger than F critical. However, the individual effect of contact time and temperature showed no statistical significant with a $p>0.05$ and a smaller F value, which means that it can be neglected during the removal process (Abdel–Gawad and Abd El–Aziz, 2019). This confirms the result shown in the main and interaction effect graphs in **Figure 3.6**.

Table 3.2: ANOVA of the model and process parameters

Parameters	**Sum of square**	**Df**	**Mean square**	**F value**	**F crit**	**P value**
ANOVA	20895	4	3483	5.48	2.51	$1.09x10^{-3}$
Mass	975	4	244	45.61	3.84	$1.5x10^{-5}$
Concentration	1673	6	279	30.79	3.00	$1.29\ x10^{-6}$
pH	992	4	248	18.99	3.84	$3.81\ x10^{-3}$
Contact time	$3.85\ x10^{-3}$	5	$7.69x10^{-5}$	$8.79\ x10^{-2}$	3.33	0.99
Temperature	0.3094	5	0.0619	2.997	3.33	0.066
Residual	6148	4	636			
Error	0.21	6	4.34			
Total	27043	25				

ANOVA was used to develop a mathematical model for optimal process prediction, taking into account each parametric level's contribution to the response. The sum of squares (SS) value for each parameter was used to aid in understanding how each process variable affects the desired response. This was computed into respective percentage as illustrated in equation 3.6 (Show et al., 2020).

$$\%\ Contribution = \frac{SS_p}{SS_m} X\ 100 \qquad \text{(Eq 3.6)}$$

In this case, SS_m stands for the sum of squares of the ANOVA model, whereas SS_p stands for the sum of squares for a particular parameter. As seen in **Table 3.3**, it can be noted that the removal efficiency of the targeted pharmaceuticals using MIP as an adsorbent was influenced by concentration, followed by pH and mass dosage. Contact time and temperature showed a very little influence.

Table 3.3: Contribution factor of each parameter

Parameters	**Contribution factor (%)**
Mass	4.67
Concentration	8.01
pH	4.75
Contact ime	$1.71x10^{-5}$
Temperature	$1.48x10^{-3}$

3.6.4 Adsorption kinetics

To analyse the kinetic adsorption behaviour, the pseudo-first-order model and pseudo-second-order model were used and calculated by the following equations:

Pseudo-first-order model:

$$q_t = q_e\ (1\text{-}e^{k_1 t}) \qquad \text{(Eq 3.7)}$$

Pseudo-second-order model:

$$q_t = \frac{qe^2 k_2 t}{1+k_2 q_e t} \qquad \text{(Eq 3.8)}$$

where q_t (mg g^{-1}) and q_e (mg g^{-1}) represent the adsorption capacity of the three compounds on MIP at time t (min) and at equilibrium, respectively; k_1 (min^{-1}) and k_2 (g mg^{-1} min^{-1}) are the adsorption rate constants of pseudo-first-order and pseudo-second-order model, respectively (da Silva et al., 2019).

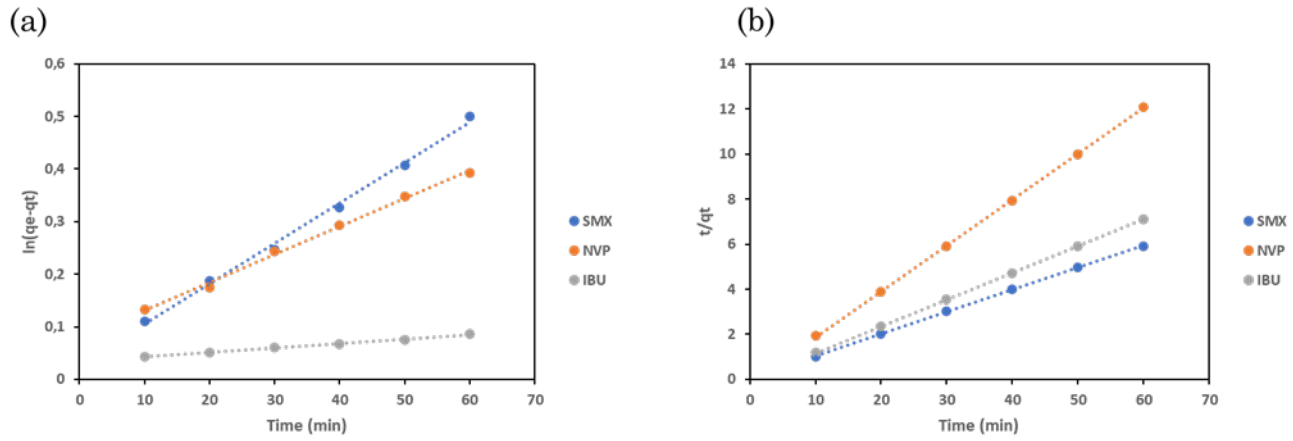

Figure 3.7: Plots of (a) pseudo-first-order and (b) pseudo-second-order for the three selected pharmaceuticals

The kinetic profile of SMX, Nvp and Ibu adsorption onto MIP surface at different time intervals is depicted in **Figure 3.7 A** and **B**. The kinetic data result shown in **Table 3.4**, based on the regression value (R^2) for polymers, less linearity is seen in the pseudo-first order model regression coefficient R^2, which was found to be 0. 0.996 to 0.9982 while for a pseudo-second-order they were 0.9998 to 0.9999. Notably, the R^2 of the pseudo-second order model most accurately described the MIP adsorption process of all the studied pharmaceuticals, suggesting that chemical interactions may be related to the adsorption process. The implication of this finding is that the adsorption of three class of pharmaceuticals by MIP is likely to be kinetically controlled as a pseudo-second-order reaction and adsorption depends on both the adsorbent and adsorbate concentrations (Bullen et al., 2021). Moreover, the maximum adsorption capacity of SMX, Nvp and Ibu analysed with the pseudo-second-order model was very close to the experimental value. The pseudo-second-order kinetic model proved to be most suitable for explaining the adsorption process of three compounds on polymers, suggesting that the most significant step in the adsorption process was chemical adsorption. Accordingly, the pseudo-second-order overall rate constant (K_2) suggests that Ibu had a faster rate of adsorption, which was faster than the rate of chemisorption governing the adsorption of NVP and SMX. This might be as a result of Ibu smaller molecular weight relative to other compounds, which causes it to be adsorbed more quickly (Ramírez et al., 2021).

Table 3.4: Kinetic models data for the MIP

Analyte	**Pseudo-first- order**				**Pseudo-second order**			
	q_e (mg g^{-1}) Exp	**q_e (mg g^{-1}) Cal**	**K_1** (x 10^{-4})	**R^2**	**q_e (mg g^{-1}) Exp**	**qe (mg g^{-1}) Cal**	**K_2**	**R^2**
Sulfamethoxazole	10.75	0.9719	1.283	0.996	10.75	10.20	0.1819	0.9999
Nevirapine	5.84	0.6375	8.83	0.9968	5.84	4.92	0.266	0.9998
Ibuprofen	9.55	1.035	1.33	0.9982	9.55	8.45	1.178	0.9999

3.6.5 Adsorption Isotherms

Adsorption isotherms are used to determine the mechanism of adsorption, which describes how ions or molecules of the adsorbate interact with adsorbent surface sites. Langmuir model and Freundlich model were used to fit the adsorption process. The models were calculated by the following equations and the calculation results are shown in **Table 3.5**:

Langmuir model:

$$q_e = \frac{q_m K_L C_e}{1 + K_L C_e} \qquad \text{(Eq 3.9)}$$

Freundlich model:

$$q_e = K_F C_e^{\,1/n} \qquad \text{(Eq 3.10)}$$

where q_e (mg g^{-1}) and q_m (mg g^{-1}) represent the equilibrium adsorption capacity and maximum adsorption capacity of the three compounds, respectively; C_e represents concentration of the pharmaceuticals at adsorption equilibrium; K_L (L mg^{-1}) and K_F ((mg g^{-1}) (L mg^{-1})$^{1/n}$) represent the Langmuir model constant and Freundlich model constant, respectively; 1/n represents the adsorption strength constant (Rajahmundry et al., 2021).

The values of the Freundlich (K_F, n, and R^2) and Langmuir (K_L, R_l and R^2) parameters presented in **Table 3.5** indicates the favourable adsorption of Ibu, Nvp, and SMX adsorbed onto the MIP surface. According to the Freundlich model, the heterogeneity of the adsorption surface is expressed in terms of adsorption intensity n; a smaller 1/n value indicates a more heterogeneous surface and an n value between 1 and 10 indicates a favourable process. The 1/n values were found to be 0.286 to 0.407 indicating a favourable process. Additionally, the n-values were greater than 1 and higher K_F value suggesting that adsorption is advantageous and that it is a physical process. This indicated that the adsorption system of MIP and the three pharmaceuticals was favourable for the Freundlich model. The nature of adsorption in Langmuir model is explained by the separation factor (R_L) by exhibiting the relationship between adsorbate and adsorbent. The isotherm model for adsorption can be favourable ($0 < R_L < 1$), unfavourable ($R_L > 1$), linear ($R_L = 1$) and irreversible ($R_L = 0$), that is reliant on the equilibrium parameter R_L. Under this investigation, the R_L values were found to be 0.1275 to 0.5309 indicating the favourability of the adsorption and that it happened on heterogeneous surfaces. As can be seen from **Table 3.5**, the data fit both the Freundlich and Langmuir

isotherms. The experimental data may be effectively described by both adsorption models based on the R^2 values. The obtained results from the isotherm data fitting confirmed that both Langmuir and Freundlich isotherms can efficiently describe the adsorption data with R^2 values larger than 0.99. Nonetheless, the slightly higher correlation coefficients indicated that the Langmuir isotherm provided a better fit, which confirms monolayer adsorption, in which every pharmaceutical molecule was adsorbed on different localized adsorption sites without any adsorbate transmigrating in the plane of the surfaces, resulting in uniform energies of monolayer adsorption onto the adsorbent surface. Tegegne and co-workers also reported on a similar case where both models best fitted the adsorption of pharmaceuticals using MIP (Tegegne et al., 2021). Moreover, the maximum adsorption capacity obtained was in the range of 3.40-4.97 mg g^{-1}. On the basis of the comparison of qe values calculated, there was an insignificant disparity between qe values from the Langmuir model and the experimental values. These findings confirmed that the proposed adsorption system favour the Langmuir isotherm. The Langmuir adsorption confirms adsorption as a chemical occurrence, which assumes that all the vacant adsorption active sites are related, the adsorbed species cannot interact, and a monolayer is formed throughout the adsorption process. The literature results on the adsorption of pharmaceuticals by MIP was also reported to favour the Langmuir isotherms (Meléndez-Marmolejo et al., 2022).

Table 3.5: Adsorption isotherm data for the MIP

Isotherm	**Parameters**	**MIP templates**		
		Sulfamethoxazole	**Nevirapine**	**Ibuprofen**
Freundlich	K_f (L mg^{-1})	0.276	0.4457	0.9976
	N	3.45	3.5	2.46
	1/n	0.290	0.286	0.407
	R^2	0.9953	0.9928	0.9824
Langmuir	Q_{max} (mg g^{-1})	3.89	4.97	3.40
	K_L (L mg^{-1})	0.8846	0.1408	0.2884
	R_L	0.1275	0.454	0.5309
	R^2	0.9937	0.9973	0.9992

3.6.6 Thermodynamics

Thermodynamic parameters were calculated by the following equations:

$$\Delta G° = -RT\ lnK_L \qquad \text{(Eq 3.11)}$$

$$lnK_L = \frac{\Delta S°}{R} - \frac{\Delta H°}{RT} \qquad \text{(Eq 3.12)}$$

where ΔG° (kJ mol^{-1}), ΔH° (kJ mol^{-1}) and ΔS° (kJ mol^{-1}) represent standard free energy change, enthalpy change and entropy change, respectively; T (K) represents reaction temperature; R (8.314 J mol^{-1} K^{-1}) represents universal gas constant; K_L the equilibrium constant for adsorption, can be calculated from the relationship between the equilibrium concentration (Ce) and the amount adsorbed at equilibrium (qe) at different temperatures. Equation (3.12) is known as the Van´t Hof equation and ΔH° and ΔS° can be determined from the slope and the intercept of the graph of ln K_L as a function of 1/T (Lima et al., 2019). The three thermodynamic parameters, Gibbs free energy change (ΔG°), enthalpy change (ΔH°), and entropy change (ΔS°), were utilized to determine the adsorption mechanism of SMX, Nvp, and Ibu by the polymers. **Table 3.6** shows the values of ΔH°, ΔG° and ΔS° calculated from the slope and intercept of the plot of lnK_L and 1/T in **Figure 3.8**. As the temperature increased, the negative value of ΔG° and its magnitude increased suggesting that the adsorption process was spontaneous and thermodynamically favourable. This is because at higher temperature, ions are easily desolvated and therefore their adsorption becomes more favourable (Adebayo et al., 2019).

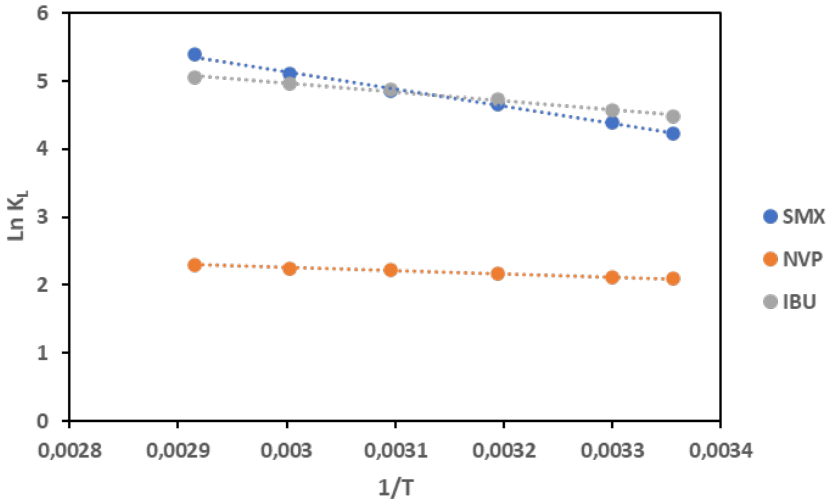

Figure 3.8: Plot of lnK_L and 1/T for the adsorption of SMX, Nvp and Ibu by MIP.

The adsorption process reactions obeyed an endothermic character and an irregular increase of randomness in the interaction of the three chemicals with MIP, as evidenced by the positive signs of ΔH° and ΔS°. This explains the increase in % removal percentage as the temperature solution rises, **Figure 3.6 D**. Notably, the type of adsorption can be explained in terms of the magnitude of Δ H°. The heat evolved during physisorption generally lies in the range of 2.1-20.9 kJ mol^{-1}, while the heat of chemisorption falls into a range of 80-200 kJ mol^{-1}. Hence, the adsorption of the three compounds onto MIP may be attributed to a physical adsorption process. The process of physisorption is caused by a broad range of weak Van der Waals forces, electrostatic and hydrogen interaction between adsorbent (MIP) and adsorbates (SMX, Nvp and Ibu) (Hasanah et al., 2021, Saleh, 2022).

Table 3.6: Thermodynamics parameters for the MIP and NIP adsorbents

Compounds	**ΔG° (kJ mol^{-1})**						**ΔH° (kJ mol^{-1})**	**ΔS° (J mol^{-1} K^{-1})**	**R^2**
	298 K	**303 K**	**313 K**	**323 K**	**333 K**	**343 K**			
Sulfamethoxazole	-10.48	-11.07	-12.16	-13.03	-14.14	-15.37	21.13	106.1	0.9948
Nevirapine	-5.18	-5.34	-5.64	-5.95	-6.22	-6.56	3.85	30.31	0.9962
Ibuprofen	-11.13	-11.50	-12.34	-13.09	-13.77	-14.42	10.93	74.16	0.9897

3.6.7 Selectivity

The competitor diclofenac was selected as it may be able to compete for binding sites on the MIP cavities imprinted with the three compounds due to it physicochemical similarities to SMX, Nvp and Ibu (**Table 3.1**). The result in **Figure 3.9** shows the removal efficiency for SMX, NVP and Ibu in the presence of the competitor was greater than 80%. It appears that MIP was more effective in removing SMX, Nvp, and Ibu than it was at removing diclofenac, this therefore suggests that MIP was more selective. Although MIP can interact similarly with the other compounds, it binds SMX, Nvp and Ibu strongly due to molecular recognition. The removal efficiency of diclofenac was below 60%. This was linked to the lack of molecular

recognition, which is significantly influenced by the functional groups, molecular structure, and size of the imprinting molecule. This might have hindered diclofenac from binding strongly to the MIP.

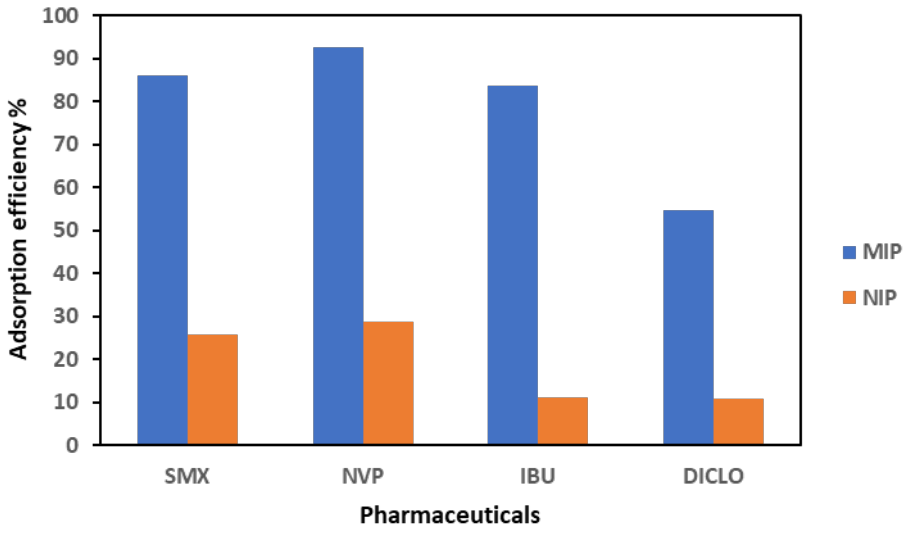

Figure 3.9: Removal efficiency selectivity of SMX, NVP, Ibu and Diclo from the MIP.

The results in **Table 3.7** summarises the K_d and *k* values of the pharmaceuticals. The compounds exhibited greater binding capabilities on MIP as compared to NIP. The selectivity of MIP and NIP towards selected pharmaceuticals in the presence of diclofenac revealed that MIP has a greater selectivity towards the target compounds than NIP in aqueous sample. This further indicates that MIP has higher molecular recognition of selected pharmaceuticals with respect to NIP. This was displayed by MIP high adsorption efficiencies compared to NIP as seen in **Figure 3.9**. The selectivity factor (*k*) obtained for MIP is greater than 1 in all cases, which indicates the molecular memory of the MIP for the selected pharmaceuticals, it interactions, and size (Espinoza-Torres et al., 2023). This further indicates the high selectivity of MIP towards the target pharmaceuticals. Accordingly, the selectivity factor values for the of MIP were in the following order: Ibu>SMX>Nvp. This may indicate the capability of the compounds to selectively bind to the imprinted polymer to form hydrogen bond with the imprinted polymer's surface functional groups particularly in the monomer (2-vinyl pyridine) serving as a component of the polymer. Accordingly, the compounds imprinting cavities are made based on the interaction of the template's functionality and the shape, size, and amount of hydrogen bonding (Ndunda, 2020). Furthermore, the relative selectivity (*k'*) indicated the magnitude of selectivity of the MIP in relation to the NIP, where values were greater than one, which implies that the MIP was more selective to the selected pharmaceuticals.

Table 3.7: Selectivity of MIP towards the pharmaceuticals

Pharmaceuticals	**K_d MIP (mg g^{-1})**	**K_d NIP (mg g^{-1})**	***k* (MIP)**	***k* (NIP)**	***k'***
Sulfamethoxazole	0.86	0.25	1.56	0.71	3.44
Nevirapine	0.84	0.26	1.52	0.74	3.23
Ibuprofen	0.93	0.33	1.69	0.71	2.82
Diclofenac	0.55	0.35	-	-	1.57

3.6.8 Reusability

The reusability results in **Figure 3.10** demonstrate that MIP particles maintained their quality even after the fifth cycle reuse with it adsorption efficiency being >90 %. The findings revealed that despite repeated cyclic oscillations and other external stresses, the spatial structure of MIPs was not affected (Amaly et al., 2021). The imprinted layer continued to exhibit strong activity and good reusability. Moreover, the outcome of regeneration tests over multiple adsorption and desorption cycles demonstrates the well-known benefit of MIPs over the majority of traditional adsorbents, which are typically used once and discarded. This is significant since it reduces costs and excessive material use.

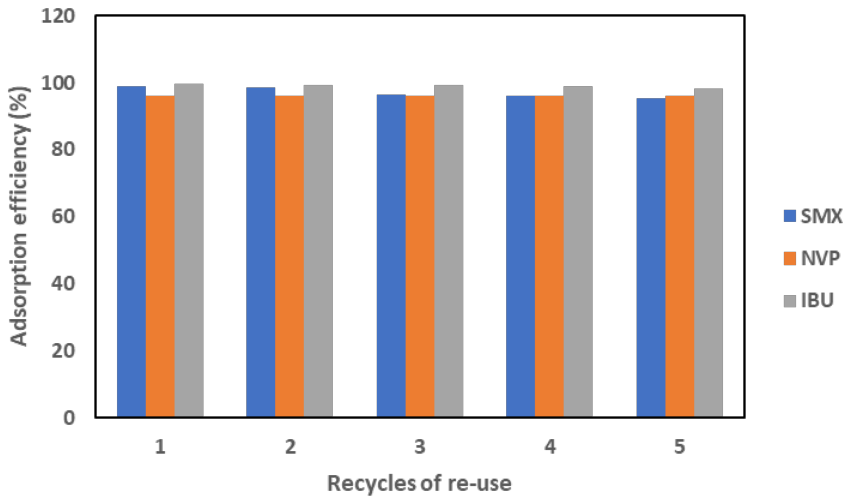

Figure 3.10: Reusability cycles of the MIP.

3.6.9 Comparison with other research studies

Comparison with reported MIP-based adsorbent approaches was undertaken to further establish the merits of the studied method for the analysis of target pharmaceutical compounds. Notably, no studies have been published in the literature regarding the simultaneous adsorption

and removal of ibuprofen, nevirapine, and sulfamethoxazole using MIP in an aqueous environment. The results in **Table 3.8** displays findings from a few current investigations on the adsorption capacity and removal efficiency of the target pharmaceuticals considered for this study using MIP in aqueous solution. These values and the study that was reported were compared. Accordingly, the values acquired in this study were found to be lower than the majority of the studies reported. Notably, most studies mainly focus on synthesizing MIPs that target a single pharmaceutical or a group of pharmaceuticals belonging to the same class. Nonetheless, this study focused on MIP synthesis that targeted multiple classes of pharmaceuticals. Thus, the competitive adsorption of the pharmaceuticals onto the MIP surface might have resulted in less adsorption of these analytes leading to lower adsorption capacity. Given that the goal of the study was to use MIP cross-selectivity with three model compounds from various pharmaceutical classes, the findings are generally favourable.

Table 3.8: Comparison between the current study and published MIP studies.

Pharmaceutical compounds	**Adsorption capacity (mg g^{-1})**	**Removal efficiency (%)**	**Reference**
Sulfamethoxazole	38.04	-	(Xie et al., 2022)
	24	-	(Qiu et al., 2020)
	284.66	91-106	(Cheng et al., 2022)
Nevirapine	-	46-69	(Khulu et al., 2021)
	206	43-69	(Khulu et al., 2022)
Ibuprofen	35	14.5	(Stachowiak et al., 2023)
	3.6	57-69	(Madikizela and Chimuka, 2016b)
Sulfamethoxazole	3.89	70-98	This work
Nevirapine	4.97	74-99	
Ibuprofen	3.40	79-96	

-: not reported

3.7 Conclusion

This research sought to synthesise and characterize a molecularly imprinted polymer for the simultaneous adsorption and extraction of sulfamethoxazole, nevirapine and ibuprofen in an aqueous solution, as well as conduct extensive studies on the isotherm, kinetics, and thermodynamics of adsorption. The FTIR, TGA, and SEM analyses were used to describe the structure, morphology, and content of the multi template MIP. The outcomes demonstrated the effective synthesis of the multi-template MIP. Using MIP as the adsorbent, a batch adsorption experiment was carried out to identify the variables influencing the adsorption efficacy. Using ANOVA statistical analysis, it was discovered that the dosage, concentration, and pH of the adsorbent had statistical significance with $p<0.05$, whereas temperature and time showed no statistical significance. Furthermore, concentration had the greatest impact on the targeted pharmaceuticals' removal efficiency when using MIP as an adsorbent, followed by pH and mass dosage as indicated by their percentage contribution. Contact time and temperature had the least impact. Although both the Freundlich and Langmuir adsorption isotherms were able to fit the experimental data, the latter provided a better explanation of equilibrium behaviour. Consequently, the Langmuir model in the adsorption isotherm provided the best fit to the experimental data showing the monolayer nature of the binding sites in the adsorbent and the pseudo-second-order kinetic model showing chemisorption occurs during adsorption. Additionally, endothermic and entropy increases occurred spontaneously during the adsorption process. The research has successfully synthesized molecularly imprinted polymers with good extraction efficiencies and strong selectivity toward the selected types of pharmaceuticals. When looking for materials to solve environmental issues, the reuse process is essential; for this reason, it is important to research and ensure the material's effectiveness in various adsorption cycles. MIPs showed to have a stable structure and a high recycling value, so they may satisfy the demands of water treatment for adsorbent materials.

3.8 References

ABDEL–GAWAD, S. A. & ABD EL–AZIZ, H. M. 2019. Removal of pharmaceuticals from aqueous medium using entrapped activated carbon in alginate. *Air, Soil and Water Research,* 12**,** 1178622119848761.

ADEBAYO, G., JAMIU, W., OKORO, H., OKEOLA, F., ADESINA, A. & FEYISETAN, O. 2019. Kinetics, thermodynamics and isothermal modelling of liquid phase adsorption of methylene blue onto moringa pod husk activated carbon. *South African Journal of Chemistry,* 72**,** 263-237.

AMALY, N., ISTAMBOULIE, G., EL-MOGHAZY, A. Y. & NOGUER, T. 2021. Reusable molecularly imprinted polymeric nanospheres for diclofenac removal from water samples. *Journal of Chemical Research,* 45**,** 102-110.

ANIRUDHAN, T., MANI, A. & ATHIRA, V. 2021. Molecularly imprinted electrochemical sensing platform for 2-Aminoadipic acid, a diabetes biomarker. *Reactive and Functional Polymers,* 168**,** 105056.

ARABI, M., OSTOVAN, A., LI, J., WANG, X., ZHANG, Z., CHOO, J. & CHEN, L. 2021. Molecular imprinting: green perspectives and strategies. *Advanced Materials,* 33**,** 2100543.

AZIZI, A. & BOTTARO, C. S. 2020. A critical review of molecularly imprinted polymers for the analysis of organic pollutants in environmental water samples. *Journal of Chromatography A,* 1614**,** 460603.

BABAEIPOUR, V. & JABBARI, F. 2023. Pre-polymerization process simulation, synthesis and investigation the properties of dipicolinic acid molecularly imprinted polymers. *Polymer Bulletin***,** 1-18.

BIRNIWA, A. H., ALI, U., KUTTY, S. R. M., JAGABA, A. H. & NOOR, A. 2023. Innovative and eco-friendly technologies for the upgradation of pharmaceutical wastewater treatment processes. *The Treatment of Pharmaceutical Wastewater.* Elsevier.

BULLEN, J. C., SALEESONGSOM, S., GALLAGHER, K. & WEISS, D. J. 2021. A revised pseudo-second-order kinetic model for adsorption, sensitive to changes in adsorbate and adsorbent concentrations. *Langmuir,* 37**,** 3189-3201.

CHENG, G., LI, X., LI, X., CHEN, J., LIU, Y., ZHAO, G. & ZHU, G. 2022. Surface imprinted polymer on a metal-organic framework for rapid and highly selective adsorption of sulfamethoxazole in environmental samples. *Journal of Hazardous Materials,* 423**,** 127087.

DA SILVA, R. C. S., SANTOS, M. N., PIRES, B. C., DINALI, L. A. F., SUQUILA, F. A. C., TARLEY, C. R. T. & BORGES, K. B. 2019. Assessment of surfactants on performance of molecularly imprinted polymer toward adsorption of pharmaceutical. *Journal of Environmental Chemical Engineering,* 7**,** 103037.

ESPINOZA-TORRES, S., LÓPEZ, R., SOTOMAYOR, M. D., TUESTA, J. C., PICASSO, G. & KHAN, S. 2023. Synthesis, Characterization, and Evaluation of a Novel Molecularly Imprinted Polymer (MIP) for Selective Quantification of Curcumin in Real Food Sample by UV-Vis Spectrophotometry. *Polymers,* 15**,** 3332.

FEROZ, M., LOPES, I. C., UR REHMAN, H., ATA, S. & VADGAMA, P. 2020. A novel molecular imprinted polymer layer electrode for enhanced sensitivity electrochemical determination of the antidepressant fluoxetine. *Journal of Electroanalytical Chemistry,* 878**,** 114693.

GODOY, A. A., DE OLIVEIRA, Á. C., SILVA, J. G. M., DE JESUS AZEVEDO, C. C., DOMINGUES, I., NOGUEIRA, A. J. A. & KUMMROW, F. 2019. Single and mixture toxicity of four pharmaceuticals of environmental concern to aquatic organisms, including a behavioral assessment. *Chemosphere,* 235**,** 373-382.

HASANAH, A. N., SAFITRI, N., ZULFA, A., NELI, N. & RAHAYU, D. 2021. Factors affecting preparation of molecularly imprinted polymer and methods on finding template-monomer interaction as the key of selective properties of the materials. *Molecules,* 26**,** 5612.

HUSEIN, D. Z., HASSANIEN, R. & AL-HAKKANI, M. F. 2019. Green-synthesized copper nano-adsorbent for the removal of pharmaceutical pollutants from real wastewater samples. *Heliyon,* 5.

KAYA, S. I., CETINKAYA, A. & OZKAN, S. A. 2022. Molecularly imprinted polymers as highly selective sorbents in sample preparation techniques and their applications in environmental water analysis. *Trends in Environmental Analytical Chemistry***,** e00193.

KHATIBI, A. D., MAHVI, A. H., MENGELIZADEH, N. & BALARAK, D. 2021. Adsorption–desorption of tetracycline onto molecularly imprinted polymer: Isotherm, kinetics, and thermodynamics studies. *Desal. Water Treat,* 230**,** 240-251.

KHULU, S., NCUBE, S., KGAME, T., MAVHUNGA, E. & CHIMUKA, L. 2021. Synthesis, characterization and application of a molecularly imprinted polymer as an adsorbent for solid-phase extraction of selected pharmaceuticals from water samples. *Polymer Bulletin***,** 1-21.

KHULU, S., NCUBE, S., NUAPIA, Y., MADIKIZELA, L. M., TUTU, H., RICHARDS, H., NDUNGU, K., MAVHUNGA, E. & CHIMUKA, L. 2022. Multivariate optimization of a two-way technique for extraction of pharmaceuticals in surface water using a combination of membrane assisted solvent extraction and a molecularly imprinted polymer. *Chemosphere,* 286**,** 131973.

LIMA, E. C., HOSSEINI-BANDEGHARAEI, A., MORENO-PIRAJÁN, J. C. & ANASTOPOULOS, I. 2019. A critical review of the estimation of the thermodynamic parameters on adsorption equilibria. Wrong use of equilibrium constant in the Van't Hoof equation for calculation of thermodynamic parameters of adsorption. *Journal of molecular liquids,* 273**,** 425-434.

LIU, R. & POMA, A. 2021. Advances in molecularly imprinted polymers as drug delivery systems. *Molecules,* 26**,** 3589.

LÓPEZ-LORENTE, Á. I., PENA-PEREIRA, F., PEDERSEN-BJERGAARD, S., ZUIN, V. G., OZKAN, S. A. & PSILLAKIS, E. 2022. The ten principles of green sample preparation. *TrAC Trends in Analytical Chemistry,* 148**,** 116530.

MADIKIZELA, L. M. & CHIMUKA, L. 2016a. Determination of ibuprofen, naproxen and diclofenac in aqueous samples using a multi-template molecularly imprinted polymer as selective adsorbent for solid-phase extraction. *Journal of pharmaceutical and biomedical analysis,* 128**,** 210-215.

MADIKIZELA, L. M. & CHIMUKA, L. 2016b. Synthesis, adsorption and selectivity studies of a polymer imprinted with naproxen, ibuprofen and diclofenac. *Journal of Environmental Chemical Engineering,* 4**,** 4029-4037.

MADIKIZELA, L. M., MDLULI, P. S. & CHIMUKA, L. 2017. An initial assessment of naproxen, ibuprofen and diclofenac in Ladysmith water resources in South Africa using molecularly imprinted solid-phase extraction followed by high performance liquid chromatography-photodiode array detection. *South African Journal of Chemistry,* 70**,** 145-153.

MBHELE, Z. E., NCUBE, S. & MADIKIZELA, L. M. 2018. Synthesis of a molecularly imprinted polymer and its application in selective extraction of fenoprofen from wastewater. *Environmental Science and Pollution Research,* 25**,** 36724-36735.

MELÉNDEZ-MARMOLEJO, J., DÍAZ DE LEÓN-MARTÍNEZ, L., GALVÁN-ROMERO, V., VILLARREAL-LUCIO, S., OCAMPO-PÉREZ, R., MEDELLÍN-CASTILLO, N. A., PADILLA-ORTEGA, E., RODRÍGUEZ-TORRES, I. & FLORES-RAMÍREZ, R.

2022. Design and application of molecularly imprinted polymers for adsorption and environmental assessment of anti-inflammatory drugs in wastewater samples. *Environmental Science and Pollution Research,* 29**,** 45885-45902.

NDUNDA, E. N. 2020. Molecularly imprinted polymers—A closer look at the control polymer used in determining the imprinting effect: A mini review. *Journal of Molecular Recognition,* 33**,** e2855.

OKUTUCU, B. 2020. Wastewater Treatment Using Imprinted Polymeric Adsorbents. *Waste in Textile and Leather Sectors.* IntechOpen London, UK.

QIU, L., JARIA, G., GIL, M. V., FENG, J., DAI, Y., ESTEVES, V. I., OTERO, M. & CALISTO, V. 2020. Core− shell molecularly imprinted polymers on magnetic yeast for the removal of sulfamethoxazole from water. *Polymers,* 12**,** 1385.

QWANE, S. N., MDLULI, P. S. & MADIKIZELA, L. M. 2020. Synthesis, characterization and application of a molecularly imprinted polymer in selective adsorption of abacavir from polluted water. *South African Journal of Chemistry,* 73**,** 84-91.

RAJAHMUNDRY, G. K., GARLAPATI, C., KUMAR, P. S., ALWI, R. S. & VO, D.-V. N. 2021. Statistical analysis of adsorption isotherm models and its appropriate selection. *Chemosphere,* 276**,** 130176.

RAMÍREZ, A. A. C., GARCÍA, E. R., MEDINA, R. L., LARIOS, J. L. C., PARRA, R. S. & FRANCO, A. M. M. 2021. Selective Adsorption of Aqueous Diclofenac Sodium, Naproxen Sodium, and Ibuprofen Using a Stable Fe3O4–FeBTC Metal–Organic Framework. *Materials,* 14.

RAVIKUMAR, Y., YUN, J., ZHANG, G., ZABED, H. M. & QI, X. 2022. A review on constructed wetlands-based removal of pharmaceutical contaminants derived from non-point source pollution. *Environmental Technology & Innovation,* 26**,** 102504.

ROLAND, R. M., BHAWANI, S. A. & IBRAHIM, M. N. M. 2023. Synthesis of molecularly imprinted polymer for the removal of cyanazine from aqueous samples. *Chemical and Biological Technologies in Agriculture,* 10**,** 92.

S'BUSISO, M. N., MAHLAMBI, P. N. & CHIMUKA, L. 2022. Synthesis, characterisation and optimisation of bulk molecularly imprinted polymers from nonsteroidal anti-inflammatory drugs. *South African Journal of Chemistry,* 76**,** 56–64-56–64.

SADIA, M., AHMAD, I., UL-SALEHEEN, Z., ZUBAIR, M., ZAHOOR, M., ULLAH, R., BARI, A. & ZEKKER, I. 2023. Synthesis and Characterization of MIPs for Selective Removal of Textile Dye Acid Black-234 from Wastewater Sample. *Molecules,* 28**,** 1555.

SALEH, T. A. 2022. Adsorption technology and surface science. *Interface Science and Technology.* Elsevier.

SAMAL, K., MAHAPATRA, S. & ALI, M. H. 2022. Pharmaceutical wastewater as Emerging Contaminants (EC): Treatment technologies, impact on environment and human health. *Energy Nexus***,** 100076.

SANUSI, I. O., OLUTONA, G. O., WAWATA, I. G. & ONOHUEAN, H. 2023. Occurrence, environmental impact and fate of pharmaceuticals in groundwater and surface water: a critical review. *Environmental Science and Pollution Research***,** 1-20.

SHOW, S., KARMAKAR, B. & HALDER, G. 2020. Sorptive uptake of anti-inflammatory drug ibuprofen by waste biomass–derived biochar: experimental and statistical analysis. *Biomass Conversion and Biorefinery***,** 1-19.

STACHOWIAK, M., CEGŁOWSKI, M. & KURCZEWSKA, J. 2023. Hybrid chitosan/molecularly imprinted polymer hydrogel beads doped with iron for selective ibuprofen adsorption. *International Journal of Biological Macromolecules,* 251**,** 126356.

TEGEGNE, B., CHIMUKA, L., CHANDRAVANSHI, B. S. & ZEWGE, F. 2021. Molecularly imprinted polymer for adsorption of venlafaxine, albendazole, ciprofloxacin and norfloxacin in aqueous environment. *Separation Science and Technology,* 56**,** 2217-2231.

VINAYAGAM, V., MURUGAN, S., KUMARESAN, R., NARAYANAN, M., SILLANPÄÄ, M., DAI VIET, N. V., KUSHWAHA, O. S., JENIS, P., POTDAR, P. & GADIYA, S. 2022. Sustainable adsorbents for the removal of pharmaceuticals from wastewater: A review. *Chemosphere,* 300**,** 134597.

WALENG, N. J. & NOMNGONGO, P. N. 2022. Occurrence of pharmaceuticals in the environmental waters: African and Asian perspectives. *Environmental Chemistry and Ecotoxicology,* 4**,** 50-66.

WANG, S., ZHANG, L., ZENG, J., HU, X., WANG, X., YU, L., WANG, D., CHENG, L., AHMED, R. & ROMANOVSKI, V. 2023. Multi-templates molecularly imprinted polymers for simultaneous recognition of multiple targets: From academy to application. *TrAC Trends in Analytical Chemistry***,** 117173.

XIE, Y., WAN, J., YAN, Z., WANG, Y., XIAO, T., HOU, J. & CHEN, H. 2022. Targeted degradation of sulfamethoxazole in wastewater by molecularly imprinted MOFs in advanced oxidation processes: Degradation pathways and mechanism. *Chemical Engineering Journal,* 429**,** 132237.

ZARE, E. N., FALLAH, Z., LE, V. T., DOAN, V.-D., MUDHOO, A., JOO, S.-W., VASSEGHIAN, Y., TAJBAKHSH, M., MORADI, O. & SILLANPÄÄ, M. 2022. Remediation of pharmaceuticals from contaminated water by molecularly imprinted polymers: a review. *Environmental Chemistry Letters,* 20**,** 2629-2664.

Chapter 4

Efficacy assessment of molecularly imprinted polymer incorporated with starch and macadamia-capped silver nanoparticles for the removal of multi-class pharmaceuticals in wastewater

Abstract

The presence of pharmaceuticals in water bodies has been reported to be mainly due to their incomplete removal by conventional wastewater treatment processes. This results in their release into the aquatic environment with treated effluent where they pose a significant threat to human health and aquatic life. Therefore, it is extremely important to remove these pollutants from the aquatic environment using affordable, yet highly efficient materials. The integration of nanomaterials to molecularly imprinted polymers (MIPs) results in combined attributes from both components to yield highly multifunctional materials with improved adsorption capacity of pharmaceuticals from water. The goal of this study was therefore to incorporate silver nanoparticles (AgNPs) into MIPs using sulfamethoxazole, nevirapine, and ibuprofen drugs as target compounds. The AgNPs were synthesised using starch and macadamia nutshells as reducing and capping agents, respectively. The formation of silver nanoparticles was confirmed by UV-visible spectroscopy peaks at 414 and 416 nm for the starch and macadamia nanoMIPs, respectively. Thermogravimetric analysis showed that the nano particles stability was improved upon their incorporation into the MIPs. The transmission electron microscope revealed the starch and macadamia nanoMIPs are spherical in shape with amorphous MIP network around the AgNPs. The scanning electron microscopy showed a rough surface on the starch and macadamia nanoMIPs anticipating high adsorption capability of the pharmaceuticals onto the adsorbents surface. Fourier transform infrared spectroscopy highlighted C=O, C-N, C-O are the key active functional groups that could be responsible for formation of starch (St) and macadamia (MCD) nanoMIPs. The X-ray diffraction analysis showed crystalline nature with (111), (200), (220), (311) and (222) reflections indicating a face-centred cubic (fcc) structure of AgNps. The optimum removal results for St-nanoMIP were obtained when a temperature of 30 °C, sample pH of 7, initial concentration of 0.6 mg L^{-1}, mass dosage of 50 mg and contact time of 10 minutes was used. The MCD-nanoMIPs optimum conditions were obtained at a temperature of 40 °C, sample pH of 7, concentration of 0.2 mg L^{-1}, mass dosage of 20 mg and a contact time of 10 minutes.

At these conditions, the removal percentage of 90-99% was achieved for the St-nanoMIP and between 92-99.9% for MCD-nanoMIP. The ANOVA analysis also revealed that the chosen parameters have a significant difference on the adsorption capacity of the pharmaceuticals onto the surface of the starch and macadamia nanoMIPs. Their contribution was found to be in the following order, mass dosage>temperature>pH>concentration>contact time for St-nanoMIP, and temperature>mass dosage>concentration>pH>contact time for MCD-nanoMIP. The experimental data for St/MCD-AgNPs was fitted to the Freundlich and Langmuir adsorption isotherms, based on the slightly higher correlation coefficients, the non-linear Langmuir isotherm model produced an improved fit. The non-linear Freundlich model best fitted for the St/MCD-nanoMIPs. Additionally, the adsorption kinetics of St/MCD-nanoMIPs have been demonstrated to be highly accurately described by the linear pseudo-second order model, whereas the thermodynamic data showed that the adsorption process was spontaneous and endothermic for both St/MCD nanoMIPs adsorbents. Notably, the incorporation of nanoparticles into the MIP showed improved qualities and were highly selective and effective in removing the selected pharmaceuticals from wastewater.

Keywords: nanoMIPs, starch, macadamia, pharmaceuticals, adsorption

4.1 Introduction

Pharmaceutical compounds are continually introduced into the environment, primarily through agricultural activities, manufacturing industries, veterinary, hospital effluents and wastewater treatment plants (WWTPs) effluents (Waleng and Nomngongo, 2022). The WWTPs are recognized as the primary contributors to aquatic systems contamination by pharmaceuticals which has raised concerns worldwide. This is due to that pharmaceuticals are widely used especially to improve human health and thus are excreted as urine and faecal waste leading to their large amounts entering the WWTPs. Owing to the restricted capability of the current wastewater treatment technologies, the majority of pharmaceuticals cannot be completely removed from wastewater resulting in their release into water bodies (Pereira et al., 2020). Consequently, the search for low-cost, effective, greener and highly selective removal techniques is necessary. One of the most promising methods in the removal of pharmaceuticals is using adsorption since it can be readily integrated into the present water treatment systems (Morin-Crini et al., 2022). The most prevalent adsorbents used in wastewater treatment include activated carbon, zeolites, clays, chitosan, and others. Even though these adsorbents have excellent adsorption capacities, they are frequently unable to efficiently remove pharmaceuticals especially from complex samples as they are not selective (Nordin et al., 2023). Therefore, enhancing adsorbent's selectivity for pharmaceuticals may give a workable alternative. For instance, molecularly imprinted polymers (MIP), are potent molecular receptors capable of selectively recognizing specific pharmaceuticals during the adsorption process. This results from the MIPs advantageous characteristics, including high affinity, predetermination, high stability, and versatility in molecular recognition (Sadia et al., 2023). Furthermore, they are easy to prepare, are low cost, and can be reused several times. Accordingly, MIPs are synthetic polymers made by copolymerizing a complex made of a cross-linking component, a functional monomer, and a molecular template (Sajini and Mathew, 2021). These polymers have unique pores designed for the target molecule. Typically, the chosen monomer forms a bond with the imprint compounds through H-bonding/van der Waals, electrostatics, covalent bonds, or metal-linker coordination. After the imprinting template has been removed, there may be a specific cavity with particular geometries and functional groups that can complement the template molecule. Nevertheless, there are several problems with traditional molecular imprinting polymers, including low mass transfer efficiency and irregular binding site loading (Refaat et al., 2019).

An approach to overcome these issues has been provided by a change in the focus of MIP research from bulk polymers to nanomaterials, which has caused an advancement in the field

(He et al., 2021). Molecularly imprinted nanoparticles, or nanoMIPs are a major development in imprinting technology since they solve a number of problems with bulk polymerized MIP. These consist of irregular form, incomplete template removal, delayed mass transfers, and uneven recognition site distribution (Fresco-Cala et al., 2020). A hybrid material with potential and novel features emerges when MIP and nanoparticles are combined (Garnier et al., 2021). In the fabrication of nanoMIPs, nanoparticles often serve as the support or core of the imprinted polymer. To increase the material's surface area or provide the sorbent with a new or additional property, the nanoparticles can only be embedded in the polymeric network (Khdary et al., 2023). Additionally, nanoparticles can be used to enhance the MIP's chemical or physical characteristics in order to increase detectability. These distinctive qualities are primarily influenced by the type of nanoparticle as well as their size and shape, allowing for the use of one type or another depending on the particular analytical necessity. Nanoparticles have drawn a lot of interest due to the remarkable electrical, magnetic, thermal, and catalytic properties that are produced because of their reduced particle size (Joudeh and Linke, 2022). As a result, there are now more opportunities for developing novel analytical techniques. Incorporating nanoparticles into the polymer structure is thus a novel method of synthesizing novel MIPs.

Silver-based NPs satisfy several requirements related to wastewater treatment methods (Fiorati et al., 2020, Ashique et al., 2022). This is due to their significant conductance, chemical durability, good catalytic activity, higher extinction coefficients, sharper extinction bands, significant field enhancements, optical, electrical and binding capabilities (Khan et al., 2022, Mo et al., 2022). Silver nanoparticles' size, as well as their structure, shape, and size distribution, have a significant impact on its chemical and physical properties. As a result, it is essential to adjust these properties, which is frequently accomplished by modifying synthesis methods, reducing agents and stabilizers or capping agents (Szczyglewska et al., 2023).

Typically, toxic chemicals and solvents are used in chemical and physical processes to produce nanoparticles (Ying et al., 2022). However, because of their toxicity, these reducing chemicals may have negative effects on the environment, which is why there is a growing interest in using green materials to reduce AgNPs (Nie et al., 2023). In contrast, green synthesis uses natural, nontoxic, and eco-friendly materials for generating nanoparticles. Some environmentally friendly materials can serve as both capping and stabilizing agents at the same time, which saves energy and prevents the use of hazardous and toxic chemicals (Monga et al., 2020).

Consequently, the preparation of nanoparticles inside polymers offers numerous benefits from the standpoint of green synthesis. These include the ability to have a significant number of hydroxyl and carboxyl groups capable of complexing metal Ag ions, which allows for precise

control of the size, shape, and distribution of nanoparticles and improves their biological composition and biodegradability (Madani et al., 2022). When synthesizing nanoparticles, the method is simple, straightforward and does not require specialized equipment. The method begins by mixing an aqueous metal salt silver nitrate ($AgNO_3$) solution with a water-based extract derived from a suitable chemical/plant source. At this step, the chemical/plant extract also serves as capping agents, coating and stabilizing the nanoparticles.

The Ag ions are transformed from their mono- or divalent oxidation states (Ag^+) to zero-valent ones (Ag°) by biochemical reduction of the metal salt solution, which also starts the nucleation of nanoparticles. Smaller nearby particles then form clusters with the former larger thermodynamically stable nanoparticles. Silver nanoparticles may be biologically produced from organic waste, which makes them more affordable, efficient, low-cost, and ecologically benign than other technologies, competing with the waste to wealth objective (Gowda et al., 2022). Accordingly, waste (shells) from macadamia nut contains a variety of valuable materials, including cellulose, lignin, and hemicellulose. As a green reducing agent, macadamia nut shells can help with the production of bionanomaterials and offer a less expensive method (Aswathi et al., 2023). Moreover, when it comes to environmental applications, starch is far more affordable and environmentally friendly, due to its chemical structure, biocompatibility, and biodegradability (Khoo et al., 2023, Nxumalo and Mahlambi, 2023).

Consequently, the goal of the current study was to synthesize AgNPs incorporated with MIPs utilizing a bio-green technique, using starch and macadamia nut shells as a capping agent and a reducing agent to convert Ag^+ to Ag°. As opposed to other dispersants, starch is widely acknowledged to be both more affordable and environmentally friendly. This study further aimed to compare the effectiveness of the starch and macadamia capped silver nanoparticles and incorporate them into molecularly imprinted polymer (nanoMIPs) for the removal of antibiotic (sulfamethoxazole), antiretroviral drug (nevirapine) and non-steroidal anti-inflammatory drug (ibuprofen) from wastewater. The selected pharmaceuticals are amongst the most distributed and highly consumed pharmaceuticals. Nevirapine is used to manage and treat human immunodeficiency virus (HIV), to prevent mother to child transmission of HIV (Abafe et al., 2018). Whereas, ibuprofen is commonly prescribed as an antipyretic, analgesic, and anti-inflammatory to alleviate fever, headache, muscle pain, menstrual discomfort, neurological pain, and post-surgical pain, and it is a widely recognized anti-inflammatory with significant human consumption rates (Jan-Roblero and Cruz-Maya, 2023). Sulfamethoxazole is used to treat diarrhoea, urinary tract infection, and is commonly administered to HIV-positive

individuals as a broad-spectrum prophylactic against bacterial infections and protozoa (Marzaman et al., 2023). The distribution and consumption of these pharmaceuticals therefore leads to their high detection in WWTPs resulting to their continuous discharge into the receiving rivers where they might adversely affect aquatic life. Also, they might end up in drinking water leading to drug resistance by the human body upon prolonged unintentional consumption. Finally, in order to comprehend the nature of the adsorption process of the selected pharmaceuticals onto the produced nanoMIPs, research on the adsorption isotherms, kinetics, and thermodynamics studies were conducted. To the best of the authors knowledge, this work was conducted for the first time...

4.2 Methodology

4.2.1 Chemicals

The following products were purchased from Sigma-Aldrich (Johannesburg, South Africa): nevirapine, ibuprofen, sulfamethoxazole, 2-vinylpyridine, 1,1-azobis-(cyclohexane carbonitrile) (98 %), EGDMA (98 %), acetonitrile (≥99.9% %), and acetone (99.8%), toluene (99.7%). Merck (Johannesburg, South Africa) provided analytical grade sodium hydroxide (NaOH) (99.9%), silver nitrate ($AgNO_3$) (99.8%), and soluble starch (99.9%). Macadamia nut shells were collected from Department of Agriculture in Hilton, Pietermaritzburg.

4.2.2 Standard preparation

The stock solution was prepared by dissolving 10 mg of each compound in acetonitrile to make up a concentration of about 100 mg L^{-1}. The concentration range of 0.2 to 1.5 mg L^{-1} prepared from the stock solution was used for the calibration of the LC-MS instrument.

4.2.3 Instrument

The analysis of the selected pharmaceuticals was performed using LC Shimadzu 2020 series purchased from Shimadzu (Tokyo, Japan). The separation of the target analytes was performed using Shim-Pack GIST C18-HP (150 × 4.6 mm i.d, 3,5 µm particle size) column purchased from Shimadzu (Tokyo, Japan). The column temperature was kept at 40 ºC. The mobile phase was pumped isocratically at a flow rate of 0.4 mL min^{-1} with a composition of 0.1 % formic acid in water and acetonitrile (10:90). The injection volume was 10 µL in ambient column temperature. The UV/vis detector was set at 210 nm for all template measurement. This method was adopted from Hlengwa and co-workers and was modified (Hlengwa and Mahlambi, 2020).

4.2.4 Sampling and sample preparation

Wastewater samples were collected from three wastewater treatment plants located in KwaZulu-Natal Province, South Africa. The plants were Darvill Wastewater Treatment Plant (WWTP) located in Pietermaritzburg, and Amanzimtoti and Northern WWTPs which are located in Durban. These WWTPs receive sewerage from both domestic and industrial wastes. Effluent samples were collected in dark brown bottles and stored in a cooler box. The samples were then transported to the laboratory where they were stored in the refrigerator (4°C) for further analysis. The MRC SMM450 sample mill was used to ground the macadamia nutshells which were then sieved into 250 µm using King test VB 200/300 sieve shaker from DLD Scientific (Durban, South Africa).

4.2.5 Synthesis of silver nanoparticles

A solution of alkali dissolved starch and macadamia was prepared by placing 1 g of each and mixing with 0.25 g of NaOH pellets in 100 mL of ultrapure water in an Erlenmeyer flask. It was discovered that NaOH is crucial for producing particular intermediates in the reduction of Ag^{+} to Ag^{0} as well as for accelerating the reduction and nucleation rates by boosting the oxidation of starch and macadamia, which in turn speeds up the creation of AgNPs. The solution was stirred by a magnetic stirrer at 80 °C for about 10 minutes to obtain a clear solution. Thereafter, 20 mL of 0.1 M $AgNO_3$ solution was added dropwise to the reaction mixture of starch and macadamia. The reaction mixtures were held under continuous stirring for 60 minutes. After the addition of $AgNO_3$ solution, the starch reaction medium acquired a clear yellow colour which changed to brown and finally to dark brown colour showing the formation of starch silver nanoparticles (St-AgNPs). The macadamia medium changed from brown to dark brown, an indication of the formation of macadamia silver nanoparticles (MCD-AgNPs). After the reaction was complete, the colloidal solution was allowed to cool down slowly for 30 minutes to 25 °C. Then the reaction media were precipitated using acetone. The powdered precipitates were collected by centrifugation at 4500 rpm for 15 minutes, washed twice with acetone and water to remove the unreacted materials and impurities. The collected AgNPs were then oven-dried at 80 °C for 15 minutes (Okaiyeto et al., 2021).

4.2.6 Synthesis of molecularly imprinted polymer silver nanoparticles (nanoMIPs)

With a few minor adjustments, the synthesis of MIPs was implemented from the method employed by Madikizela and colleagues (Madikizela and Chimuka, 2016). Two steps were taken in the MIP bulk polymerization process. In the first step, 20 mg of 1,1′-azobis-(cyclohexane carbonitrile) were dissolved in 50 mL of toluene, and then 1.51 mL of ethylene glycol dimethacrylate (EGDMA) was added. After sealing the reaction flask, nitrogen was purged for ten minutes. After that, the reaction was left to occur for 16 hours at 60 °C in an oil bath while being constantly stirred. In the second step, 25 mL of acetonitrile was used to dissolve 25 mg of each pharmaceutical (ibuprofen, nevirapine, and sulfamethoxazole). Thereafter, 1 mL of 2-vinylpyridine, 3.85 mL ethylene glycol dimethacrylate (EGDMA), 60 mg 1,1′-azobis-(cyclohexane carbonitrile), 100 mg of the synthesised St/MCD-AgNPs and 25 mL of toluene were added. After being added into the first reaction flask, the mixture was sealed and nitrogen-purged for 15 minutes to remove any remaining oxygen. The reaction was allowed to proceed for 24 hours at 80 °C in an oil bath. The resulting polymer was oven dried overnight at 100 °C. Following milling and sieving of the polymer, particles between 25 and 50 µm were collected. Soxhlet extraction was used to elute the templates from the resultant polymer by repeatedly washing it with a 9:1 v/v mixture of acetonitrile and acetic acid until the LC-MS system was unable to detect the templates. The polymer was then washed with 100% acetonitrile to wash off acetic acid. The same procedure in the absence of the template in the polymerization mixture was followed for the preparation of non-imprinted polymer (NIP).

4.2.7 Characterisation of nanomaterials

A Perkin Elmer Lambda 25 UV-Vis spectrophotometer was used for all-optical studies at 200-800 nm wavelength range at room temperature. A Fourier transform infrared (Perkin Elmer) spectrometer (400 FTIR) equipped with a universal ATR sampling accessory was used to assess the functional groups present in the nanoMIPs. The structure of the nanoparticles was studied using a JEOL JEM-2100 transmission electron microscope (TEM) operating at 200 kV. Zeiss Ultra Plus Field Emission Gun Scanning electron microscopy (FEG-SEM) instrument (Tokyo, Japan) was used to assess surface morphology of the synthesised polymers. To evaluate the thermal stability of the polymer, thermogravimetric (TGA) analysis was conducted using Anton Paar instrument (Mettler Toledo, Columbus, USA). X-ray diffraction (XRD) patterns were obtained from Rigaku MiniFlex 600 (Rigaku Tokyo, Japan). Raman spectra were recorded on a Via Renishaw Raman spectrometer in (Renishaw, England).

4.3 Adsorption studies

A batch technique was used to study the adsorption of the selected pharmaceuticals, allowing for the convenient examination of the parameters that affect the adsorption process. Parameters such as concentration of (0.2-1.5 mg L^{-1}), agitation time (10-60 minutes), sample pH (2-10), AgNPs mass dose (10-50 mg), and temperature (25-70 °C) were optimized by changing one parameter at a time while keeping the others constant. The samples were put into 100 mL conical flasks and agitated on a shaker at 150 rpm. The supernatant was then analysed using a LC-MS. Additionally, batch adsorption tests were conducted to assess kinetic data and thermodynamic parameters. To determine the most appropriate rate equation, kinetic data were tested based on pseudo-first and pseudo-second-order rate equations. Equations (4.1) and (4.2) were used to calculate the adsorption capacity (mg g^{-1}) and adsorption efficiency (%) or removal (%) for all experimental conditions that affected the adsorption (Husein et al., 2019).

$$q_e = \frac{(C_0 - C_e)V}{W} \qquad \text{Eq 4.1}$$

$$Removal\ (\%) = \frac{(C_0 - C_e)}{C_0} X\ 100 \qquad \text{Eq 4.2}$$

Where V is the volume of the solution in litres (L) and W is the mass of the nanoMIPs in milligrams, C_o represents the initial concentration (mg L^{-1}) before the adsorption and C_e the final concentration (mg L^{-1}) of the target compound remaining in solution after adsorption.

4.4 Data analysis

The F-test, and ANOVA statistical analyses of the adsorption experiments were conducted to obtain statistical information about the efficiency of the St/MCD-nanoMIPs material for sulfamethoxazole, nevirapine and ibuprofen removal. Understanding how each process variable affects the intended response is also made easier for the process by looking at the sum of square value for each parameter. The percentage contribution was calculated by equation (4.3) (Show et al., 2020).

$$\%\ Contribution = \frac{SS_p}{SS_m} X\ 100 \qquad \text{Eq 4.3}$$

In this case, SS_m stands for the sum of squares of the model, and SS_p stands for the sum of squares for a chosen parameter.

4.5 Adsorption isotherms

Using Langmuir and Freundlich equations, the adsorption isotherms were studied for a range of initial pharmaceuticals concentrations.

Langmuir isotherm: The Langmuir isotherm model assumes that adsorption is a homogeneous process in which adsorbate is adsorbed in the form of a monolayer onto adsorbent, with adsorption taking place at a fixed number of adsorption sites, with no lateral interaction or transmigration of the adsorbate molecule in the plane of the adsorbent (Kalam et al., 2021). The linear and non-linear Langmuir model in equation (4.4) and (4.5) is given by:

$$q_e = \frac{Q_{max} K_L C_e}{1 + K_L C_e} \quad \text{Eq 4.4}$$

$$\frac{1}{q_e} = \frac{1}{K_L C_e} + \frac{R_L}{K_L} \quad \text{Eq 4.5}$$

where, Q_{max} = the maximum monolayer adsorption capacity of the adsorbent (mg g^{-1}), q_e = equilibrium adsorption capacity of the adsorbent (mg g^{-1}), K_L = the Langmuir constant (L mg^{-1}) and Ce = equilibrium concentration of template (mg L^{-1}). The separation factor or equilibrium parameter, indicated as R_L, is an important parameter connected to the Langmuir model and is used to determine whether surfactant adsorption is favourable or unfavourable.

$$R_L = \frac{1}{1 + K_L C_O} \quad \text{Eq 4.6}$$

Where K_L and C_o are the Langmuir constant and highest initial concentration of pharmaceuticals, respectively.

Freundlich isotherm: This empirical model is applicable to multilayer adsorption on heterogeneous surfaces. It is presumptively assumed that the adsorption heat distribution and affinities for the heterogeneous surface are not uniform (Kalam et al., 2021). The linear and non-linear Freundlich isotherm are defined in equation (4.7) and (4.8), respectively (Gabr et al., 2023).

$$ln q_e = ln K_F + \frac{1}{n} ln C_e \quad \text{Eq 4.7}$$

$$q_e = K_F C_e^{\,1/n} \quad \text{Eq 4.8}$$

where C_e, q_e represent, the concentration of template and the amount of template adsorbed at equilibrium respectively. The Freundlich isotherm model's constants are the adsorption capacity (K_F) and adsorption intensity (1/n). Additionally, the exponent (1/n) indicates the capacity and favourability of the adsorbent/adsorbate system (Shikuku and Jemutai-Kimosop, 2020).

4.6 Adsorption kinetics

Two kinetic models, pseudo-first order and pseudo-second order models, were used to determine the adsorption rate. The two kinetic models are represented by equations (4.9-4.12), respectively (Parashar et al., 2022).

$$ln(q_e - q_t) = lnq_e - k_1 t$$ (linear pseudo-first order) Eq 4.9

$$\frac{1}{q_t} = \frac{1}{k_2 q_e^2} + \frac{t}{q_t}$$ (linear pseudo-second order) Eq 4.10

$$q_t = q_e(1 + e^{K_1 t})$$ (non-linear pseudo-first order) Eq 4.11

$$q_t = \frac{qe^2 k_2 t}{1 + k_2 q_e t}$$ (non-linear pseudo-second order) Eq 4.12

where q_t (mg g^{-1}) and q_e (mg g^{-1}) represent the adsorption capacity of the three compounds on Ag-nanoMIPs at time t (min) and at equilibrium, respectively; k_1 (min^{-1}) and k_2 (g mg^{-1} min^{-1}) are the adsorption rate constants of pseudo-first-order and pseudo-second-order model, respectively.

Error analysis

The root mean square error (RMSE) was used to evaluate the linear and non-linear adsorption kinetics. The following is the expression for the RMSE equation:(Okpara et al., 2021)

$$RMSE = \sqrt{\frac{1}{n-1}\sum_{i=1}^{n}(q_{exp} - q_{calc})^2}$$ Eq 4.13

Where n is the number of measurements, q_{calc} is the adsorption capacity determined from the kinetic equation model, and q_{exp} is the adsorption capacity from the experiment.

4.7 Adsorption thermodynamics

The adsorption energetics was investigated in the range 298-343 K. The thermodynamic functions, enthalpy change (ΔH°), Gibb's free energy (ΔG°), and entropy (ΔS°) were determined using Equations (4.14) and (4.15):

$$\Delta G° = -RT\ lnK_L$$ Eq 4.14

$$lnK_L = \frac{\Delta S°}{R} - \frac{\Delta H°}{RT}$$ Eq 4.15

where ΔG° is the change in the Gibbs free energy (kJ mol^{-1}); ΔH° is the change in enthalpy (kJ mol^{-1}), and ΔS° is the change in entropy (J mol^{-1}. K), R = gas constant (8.314 J mol^{-1} K), T = thermodynamic temperature (K) and K_L is the thermodynamic equilibrium constant (Lima et al., 2019).

4.8 Selectivity of the nanoMIPs

Fenoprofen, which functions as a competitor for the binding sites of St/MCD-nanoMIPs, was used to test the selectivity of the nanoMIPs. The selective adsorption performance of St/MCD-nanoMIPs were prepared in batch rebinding experiments using optimum conditions, which

were deionised water (pH 7.0) that was previously spiked to make a final concentration of 1 mg L^{-1} each for both St-nanoMIP and MCD-nanoMIP with mixture of sulfamethoxazole, nevirapine, ibuprofen, and fenoprofen (as a competitor). The spiked solution (10 mL) was poured into a flask containing 50 mg of the St-nanoMIPs and 20 mg for the MCD-nanoMIP and stirred at ambient temperature for 10 minutes. The distribution coefficients (K_d), and selectivity coefficients (k) of the selected templates and the competitor can be obtained according to the following equations:

$$K_d = \frac{C_o - C_e}{W} V \qquad \text{Eq 4.16}$$

Where K_d (mg g^{-1}) denotes the distribution coefficient, C_o is the initial solution concentration, C_e is the final solution concentration, V (mL) is the solution volume, and W (mg) is the polymer weight.

$$k = \frac{K_d Target\ pharmaceutical}{K_d Competitor} \qquad \text{Eq 4.17}$$

Where k is the selectivity coefficient for the distribution coefficient of the selected templates binding in the presence of a competitor (Espinoza-Torres et al., 2023).

4.9 Regeneration of the nanoMIPs

To assess the reusability of the synthesized materials, 50 mg of St-nanoMIP and 20 mg of MCD-nanoMIP that had been previously adsorbed by sulfamethoxazole, nevirapine and ibuprofen were rinsed for 10 min in a 9:1, v/v acetonitrile/acetic acid solution. Thereafter, the St/MCD nanoMIPs were regenerated by 10 mL of pure acetonitrile to desorb unwanted compounds before being used again to adsorb sulfamethoxazole, nevirapine and ibuprofen in the following cycle. Five sequential adsorption cycles, lasting ten minutes each, were carried out in this manner for both St-nanoMIP and MCD-nanoMIP (Mankar et al., 2020).

4.10 Results and discussion

4.10.1 Characterisation

4.10 1.1 UV-Visible analysis

The UV-vis spectra in **Figure 4.1** (A) and (C) showed the appearance of intense absorption peaks at 425 and 427 nm for St-AgNPs and MCD-AgNPs, typically associated with AgNPs and is related to surface plasmon resonance excitation processes (Iqbal et al., 2020). The incorporation of AgNPs into the MIPs (St-nanoMIPs) and (MCD-nanoMIPs) resulted in a narrower absorption peak with a slight shift to lower wavelength at 414 and 416 nm,

respectively **(Figure 4.1** (B) and (D)). This shift indicated that the nanoMIP particles had reduced particle size with narrow size distribution and increased stability (Pu and Xu, 2022).

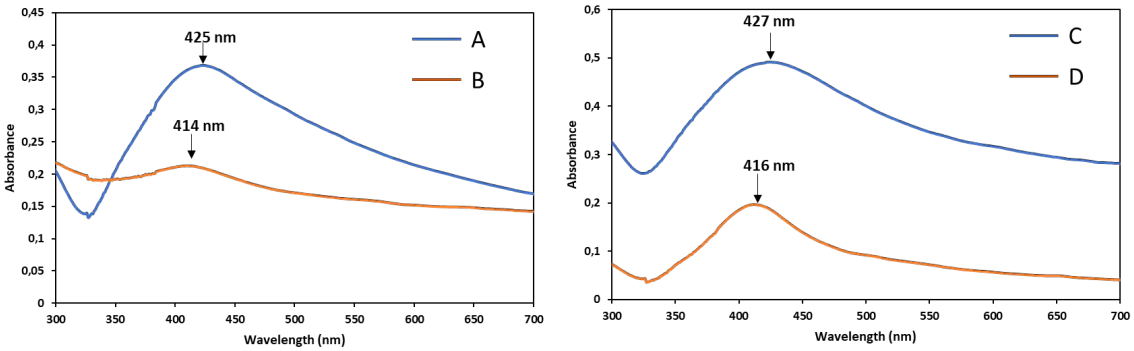

Figure 4.1: UV-Vis spectra of (a) St-AgNPs, (b) St-nanoMIPs (c) MCD-AgNPs and (d) MCD-nanoMIPs

4.10.1.2 Scanning electron microscopy analysis

The scanning electron microscopy micrographs showed that the St-AgNPs (**Figure 4.2 (a)**) has large and small spherical particles, with some regions showing aggregated nanoparticles forming clusters and bunches. The MCD-AgNPs (**Figure 4.2 (b)**) showed a heterogeneous distribution with various spherical particle sizes and some nanoparticles aggregated as clusters. Given AgNPs high surface energy, the observation of larger nanoparticles may be explained by their propensity to agglomerate (Adhikari et al., 2022). The starch-nanoMIPs in **Figure 4.2 (c)** showed to have a rough, and irregular surface with nanoparticles which covered the surface, affirming the incorporation of AgNPs onto the surface of MIP. The MCD-AgNPs (**Figure 4.2 (b)**) showed a heterogeneous distribution with various particle sizes. The starch-nanoMIPs in **Figure 4.2 (c)** showed to have a rough, and irregular surface with microparticles, while the macadamia-nanoMIPs in **Figure 4.2 (d)** had a wrinkled, and rough surface which was due to their imprinted cavities. The rough surface may act as an active site for the uptake of the selected drugs because it is expected to increase the overall surface area (Arabi et al., 2020). Thus, high adsorption capability is anticipated for the nanoMIPs, as evidenced by their larger surface area in comparison to the corresponding silver nanoparticles.

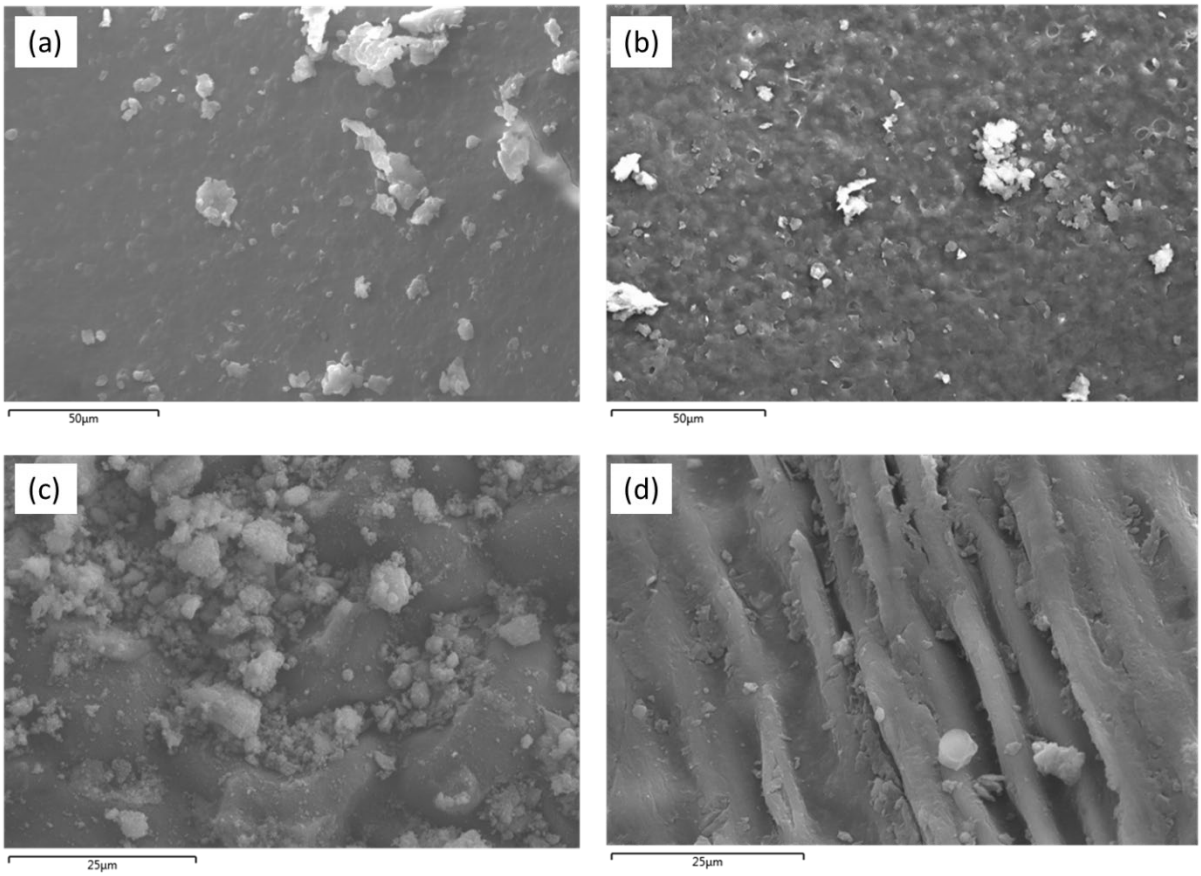

Figure 4.2: SEM images of (a) St-AgNPs and (b) MCD-AgNPs, (c) St-nanoMIPs and (d) MCD-nanoMIPs

4.10.1.3 Transmission electron microscopy analysis

The TEM images in **Figure 4.3 (a)** and **(b)** for both St-AgNPs and MCD-AgNPs confirmed that the nanoparticles are polydisperse, with near-spherical and irregular shape, and are made up of individual crystals. This demonstrates that the silver nanoparticles capped with starch and macadamia are crystalline, and some typical polyhedral nanoparticles (multiple twined nanocrystals) can be observed. St-AgNPs had an average particles diameter of 22.5 nm and MCD-AgNPs had an average diameter of 12 nm. As a result, during the processes of nucleation and growth, starch and macadamia served as both stabilizing and reducing agents. Similar spherical shaped AgNPs with average diameter of 20.08 nm were synthesized by employing glucose as a reducing and a capping agent (Pattnaik et al., 2023). The TEM images of the St and MCD-nanoMIPs showed porous network of the imprinted polymer with nearly spherical shaped AgNPs with an average diameter of 35 nm and 25 nm, respectively, which were dispersed in the polymer network **(Figure 4.3 (c)** and **(d))**. The functional monomers and template molecules molecular interactions causes the polymer chains to assemble in close

proximity, creating a denser network (Yucel et al., 2022). Moreover, few spherical shaped and small AgNPs agglomerates are embedded within the polymeric network, which could explain why the individual particles within each agglomeration are larger than average (Sullivan et al., 2020). Thus, nanoMIPs possess high affinity and specificity toward their targets (Canfarotta et al., 2018).

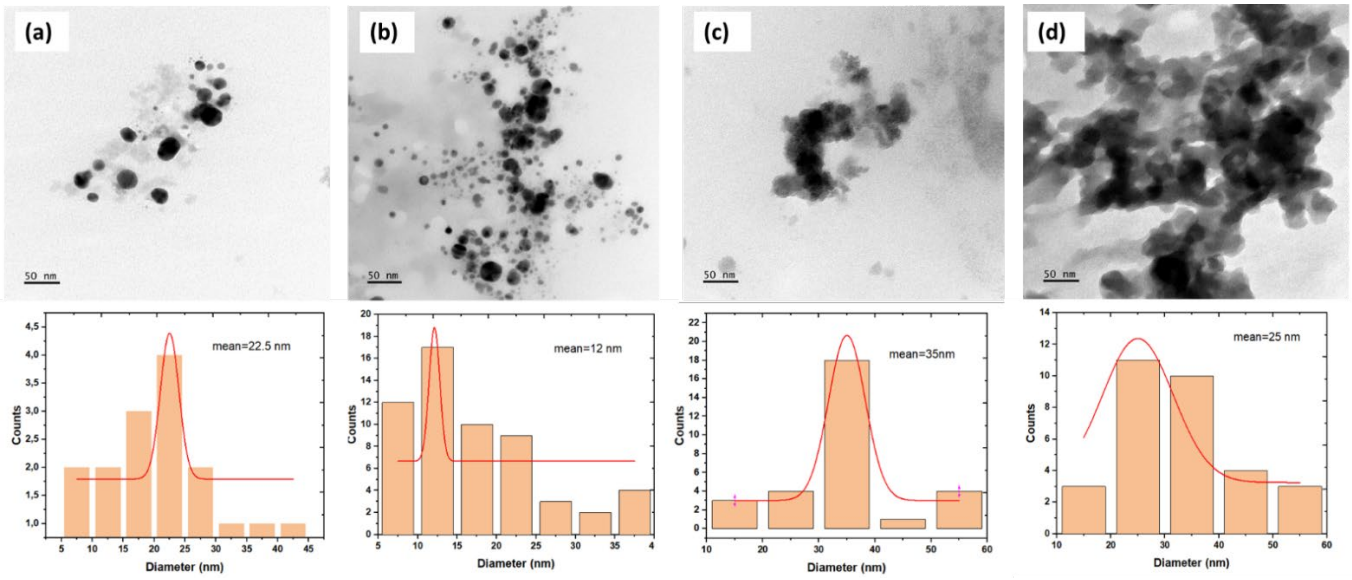

Figure 4.3: TEM images and diameter histograms of (a) St-AgNPs and (b) MCD-AgNPs, (c) St-nanoMIP and (d) MCD-nanoMIP.

4.10.1.4 Thermogravimetric analysis (TGA)

The thermogravimetry study of the synthesized NPs and nanoMIPs revealed their thermal stability, oxidative stability, moisture content, and volatile content. The first observed weight loss for the St and MCD AgNPs (**Figure 4.4 (a)** and **(b)**) was at 100 °C and 142 °C, respectively which was attributed to the loss of entrapped water molecules from the starch and macadamia polymer matrix. On the second stage of decomposition, the starch and MCD degrades at a temperature of roughly 248 °C and 169-425 °C, leaving the AgNPs behind. Additionally. There is a constant third weight loss up to 377 °C for the St-AgNPs, and for the MCD-AgNPs this weight loss was observed at a temperature of 470 °C, which may be caused by the decomposition of polymeric chains. Beyond this temperature only the carbonaceous residues of 25.02% and 7.1% was left for St-nanoMIP and MCD-nanoMIP, respectively (Bhutiya et al., 2020). The MCD-AgNPs decomposed with a weight loss of 93% at 570 °C. Particularly, the St/MCD-nanoMIPs in **Figure 4.4 (c)** and **(d)** also exhibited three decomposition stages: At 180 and 164 °C, the starch and macadamia nanoMIPs had a first mass loss of approximately 2%. This was probably because of the evaporation of the adsorbed acetonitrile used in the

template removal step (Korde et al., 2019). Further, the second thermal decomposition in starch and MCD-nanoMIPs was observed at 300 and 277 °C which was marked as the temperature where the polymers backbone collapses. This was due to decomposition of the monomer and the cross-linker used in the synthesis of St/MCD-nanoMIPs. It was further observed that at 468 and 467 °C, there was 100% thermal decomposition of the starch and macadamia nanoMIPs, respectively. The DSC graph exhibited a sharp endothermic peak between 161.53 and 178.96 °C for MCD-AgNPs and St-AgNPs, respectively, which is primarily due to the crystallization of AgNPs. The DSC shallow exothermic peak for the starch and macadamia nanoMIPs were observed at 369 and 350 °C, respectively, which is associated with the thermal decomposition of the polymers and the crystallization of the AgNPs (Wei et al., 2019). It is remarkable that the weight loss after the total decomposition (700 °C) for the St/MCD-AgNPs was ~90% whereas for the St/MCD-nanoMIPs it was almost ≈100%. Notably, the St/MCD-nanoMIPs showed high thermal stability compared to the St/MCD-AgNPs, thus demonstrating the St/MCD-nanoMIPs ability to endure rigorous operational conditions. However, the St-nanoMIP were more stable than MCD-nanoMIP.

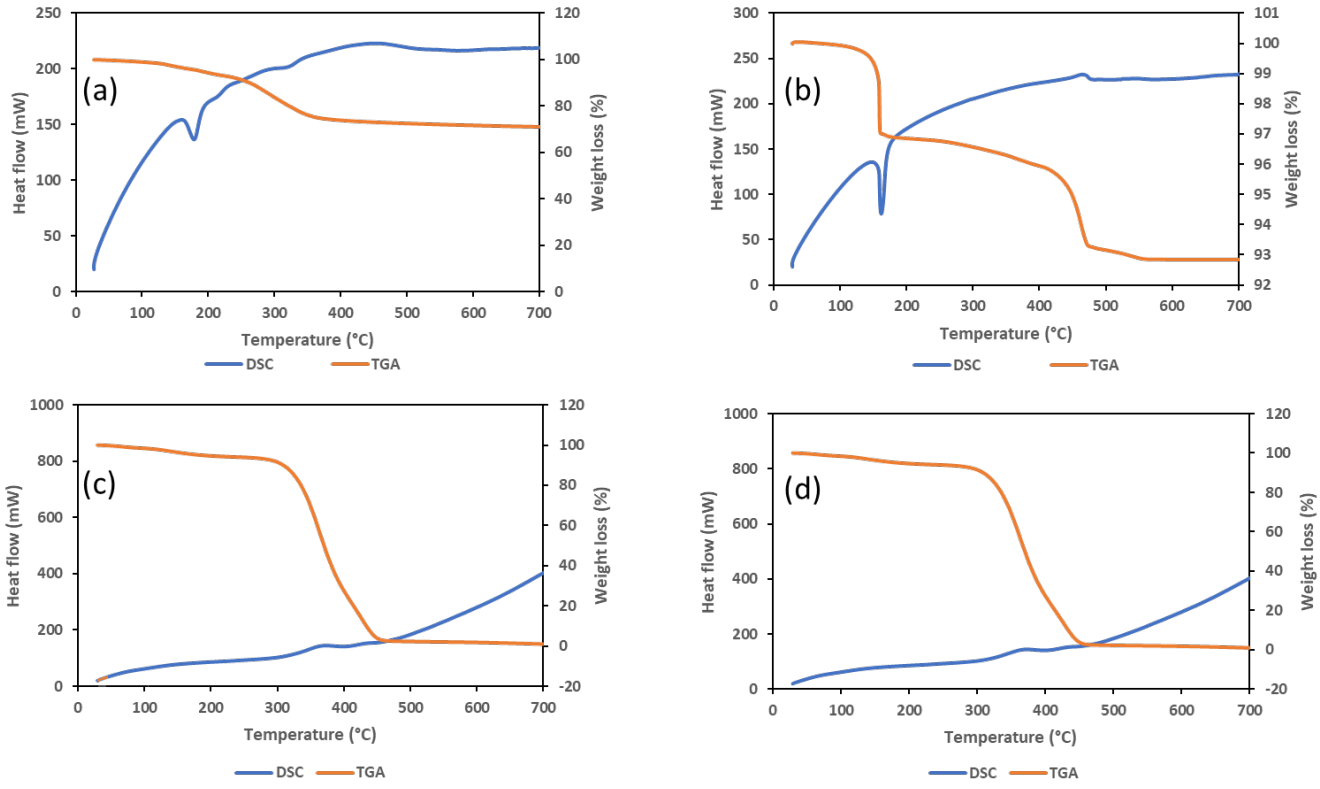

Figure 4.4: TGA and DSC thermographs of (a) St-AgNPs, (b) MCD-AgNPs, (c) St-nanoMIPs and (d) MCD-nanoMIPs

4.10.1.5 X-ray diffraction (XRD)

The St-AgNPs XRD diffraction patterns showed five sharp reflection peaks (**Figure 4.5 (a)**) at 2 theta values of 38.14°, 44.37°, 64.48, 77.44°, and 81.64° which matched to (111), (200), (220), (311) and (222) planes indicating the face-centered cubic phase crystalline structure of metallic silver. Similar reflections were observed for the MCD-AgNPs patterns (**Figure 4.5 (b)**) with distinct diffraction peaks of 2 theta values indicating the metallic silver at 39.10°, 44.47°, 64.61°, 77.71° and 81.70°, respectively. AgNPs have shown to be in strong agreement with the JCPDS No. 04-0783 stated standard values. The discovery of a few unassigned peaks on MCD-AgNPs suggests a silver oxide and/or the bio-organic phase crystallize on the surface of silver nanoparticles as a result of silver's partial oxidation (Adhikari et al., 2022). In comparison to the (111) peak, the (200), (220), and (311) peaks were less intense indicating that the nano assemblies were primarily made of (111) lattice planes. Similar observations of the face centered cubic crystal structure of AgNPs have previously been reported in published research findings employing starch as a reducing and capping agent for the synthesis of AgNPs (Ponsanti et al., 2020). Additionally, the produced AgNPs had high intensity peaks indicating a high degree of crystallinity. The broad diffraction peaks, on the other hand, show that the crystallite size is extremely small. The XRD patterns for the St/MCD nanoMIPs (**Figure. 4.5 (c)** and **(d)**) showed that the silver peaks remain in face-centered cubic phase crystal planes, with additional wide peaks at 19.51 and 19.10° ascribed to the formation of an amorphous phase from the MIP. This suggests that silver remains unchanged with the addition of polymer and maintains its original crystal structure. It also validates the presence of crystalline AgNPs in the MIP particles.

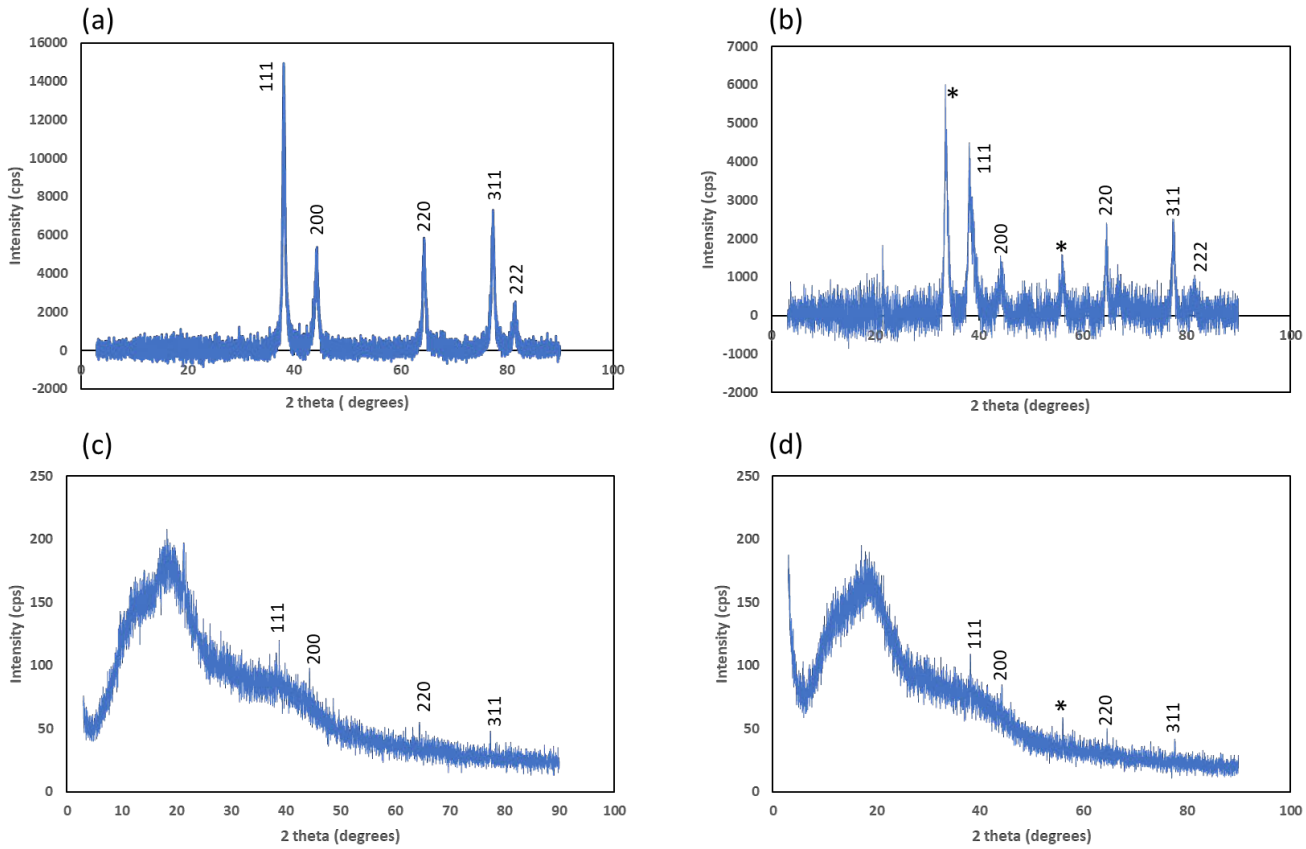

Figure 4.5: XRD patterns of (a) St-AgNPs and (b) MCD-AgNPs, (c) St-nanoMIP and (d) MCD-nanoMIP.

4.10.1.6 Fourier-transform infrared spectroscopy analysis

The O–H stretching of starch and macadamia capped silver nanoparticles was related to the spectra's strong broad band at 3250 cm^{-1} and 3304 cm^{-1} which was linked to the production of inter and intramolecular hydrogen bonds (**Figure 4.6**). At 2917 and 2900 cm^{-1} the starch and macadamia silver nanoparticles showed a C–H band of asymmetric stretching which was attributed to water adsorbed in their amorphous portion. The bands for C–O and C–OH were observed at 1425 and 1233 cm^{-1} for the St-AgNPs, respectively and at 1450 and 1020 cm^{-1} for the MCD-AgNPs. These peaks are assigned to the stretching and vibration of the phenols, ketones, ethers, and esters in the surface of the St and MCD AgNPs adsorbents (Radzikowska-Büchner et al., 2023, Erol et al., 2022). The observed FT-IR peaks in **Figure 4.6** at 1425, 1718, 1238 and 1125 cm^{-1} for MIP structures are characteristic of C=C, C=O, C–O and C–N bonds representative of the ester and alkene functional groups within ethylene glycol dimethacrylate (EGDMA) and the nitrogen in the monomer. These peaks shift in the intensity of some band after impregnation the MIP with AgNPs, indicating that AgNPs were successfully loaded onto

the nanoMIPs (e.g., the C-O band shifted from 1425 to 1450 cm^{-1}). The interaction of MIP with AgNPs was not only seen at the peak shift, but also seen from the intensity of each peak. Accordingly, the wide transmittance bands observed at wavelength regions of 3646 and 3699 cm^{-1} for the starch and macadamia nanoMIPs is linked to vibration and stretching of hydroxyl (OH^-) groups and chemisorbed water. The aliphatic C-H groups, stretching in CH, CH_2, and CH_3 groups, may be attributed to the peaks that appear at approximately 2957.84 cm^{-1} and 2943.42 cm^{-1}, for the St-nanoMIP and MCD-nanoMIP, respectively. The bands at 1718 cm^{-1} and 1724 cm^{-1} for the starch and macadamia nanoMIPs is linked to the carboxylic group (C=O). At 1125 cm^{-1} and 1135 cm^{-1} a C-N stretch frequency of pyridine nitrogen of monomer which forms a hydrogen bonding between a pyridine molecule and pharmaceuticals, was observed for the starch and macadamia nanoMIPs, respectively (Mankar et al., 2020). Accordingly, this peak did not appear in the spectra of St/MCD-AgNPs since it was not incorporated with MIP monomer. Overall, the FTIR spectra demonstrated that the 2-VP polymer matrices with EGDMA crosslinking units had formed successfully. The absorption band at 546 cm^{-1} and 554 cm^{-1} is assigned to the Ag stretching vibration for the starch and macadamia nanoMIPs (Wan Mat Khalir et al., 2020). These peaks were not found in the MIPs that were not incorporated with Ag nanoparticles. The vibration peaks observed in this work appeared identical to those in the MIPs spectra produced by Nkosi and co-workers, utilizing the same monomer and crosslinker, 2-VP and EGDMA (Nkosi et al., 2022).

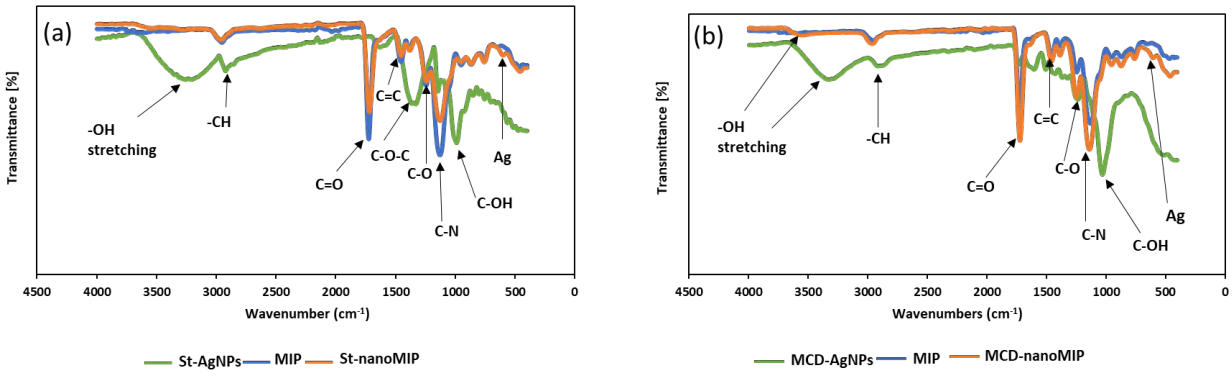

Figure 4.6: FTIR spectrum of (a) St-AgNPs, MIP, St-nanoMIP and (b) MCD-AgNPs, MIP, MCD-nanoMIP.

4.10.1.7 Raman Spectroscopy

The Raman spectra of St-AgNPs (**Figure 4.7 (a)**) consists of a vibrational mode at 1039 cm^{-1} assigned to aromatic stretching vibrations. The bands at 1301 cm^{-1} and 1774 cm^{-1} for the St-AgNPs and at 1051 cm^{-1}, 1340 cm^{-1} and 1582 cm^{-1} for the MCD-AgNPs (**Figure 4.7 (b)**) corresponds to the C=O stretching vibrations of the carboxylate group, respectively. The band at 2089 cm^{-1} is recognized as a characteristic C–H vibration peak. The bands at 156 cm^{-1}, 269 cm^{-1}, 555 cm^{-1} for the St-AgNPs and at 143 cm^{-1} and 709 cm^{-1} for the MCD-AgNPs are due to AgNPs stretching. The bands at 816 cm^{-1} and 907 cm^{-1} are associated with ring deformation and C–H in plane bending vibrations, respectively. Similar Raman spectra was also observed by Joshi and co-workers on their synthesis of silver nanoparticles (Joshi et al., 2018). Accordingly, the fluorescence background was too high to determine the Raman for St and MCD nanoMIPs (**Figure. 4.7 (c)** and **(d)**). This suggest that the embedded silver nanoparticles around the recognition cavities of MIP surely enhance the Raman signals, making it difficult to identify these adsorbents correctly in the Raman spectrometer (Liu et al., 2011).

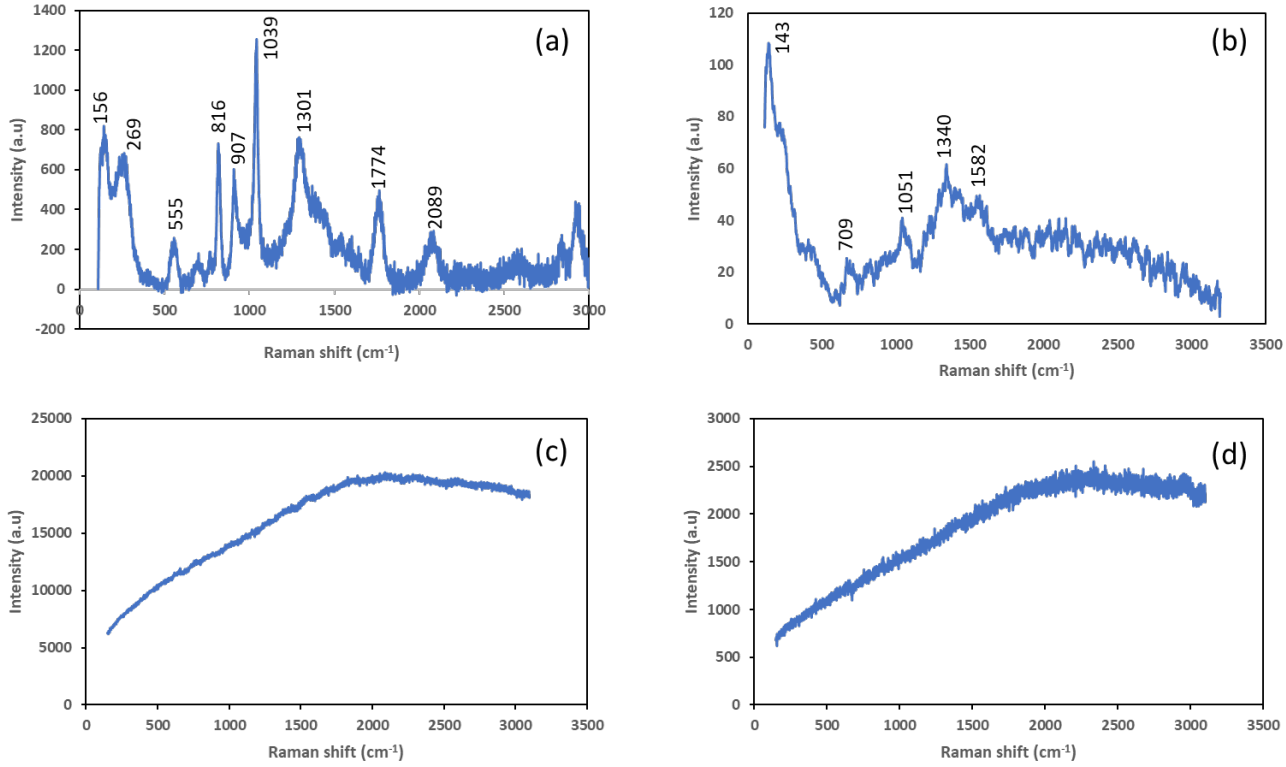

Figure 4.7: Raman spectra of (a)St-AgNPs, (b) MCD-AgNPs, (c) St-nanoMIP and (d) MCD-nanoMIP.

4.10.2 Adsorption studies

4.10.2.1 Effect of sample pH on the adsorption of pharmaceuticals

The effect of sample pH was investigated between a pH of 3 to 10. The results showed that the pH slightly influences the removal efficiency of the pharmaceuticals from aqueous medium and this may be attributed to the slight change in the adsorbate-adsorbent electrostatic interaction. The highest removal percentages of 97-99 % for the St-nanoMIP (**Figure 4.8 (a)**) and 98.9-99.9% for the MCD-nanoMIP (**Figure 4.8 (b)**) on selected pharmaceuticals were achieved at a pH 7 (97-99%). High adsorption at pH 7 can be explained due to the formation of hydrogen binding between carboxylic acid and amine groups in the pharmaceutical compounds with the surface functional groups of the St/MCD-nanoMIPs (Geravi and Ghaemy, 2024). The targeted pharmaceutical compounds functional groups may function as H-acceptors during the H-bonding formation, interacting with the oxygen (O) containing groups such as -OH, C=O and C-O on the surface of the St/MCD-nanoMIPs (Hubetska et al., 2020). Due to the abundance of H^+ ions in solution at acidic pH levels, H^+ ions will compete with pharmaceutical ions to bind the negative charge on the surface of the St/MCD-nanoMIPs. Therefore, the positively charged target pharmaceuticals bind to the negatively charged St/MCD-nanoMIPs surface through electrostatic attraction force. Furthermore, this caused a decrease in the negative charge on the St/MCD-nanoMIPs surface because it increases the concentration of hydrogen (H^+) ions, which improves the adsorption of the positively charged pharmaceuticals cations. For this reason, the St/MCD-nanoMIPs exhibited an increase on the removal efficiencies at lower pH values (Ali et al., 2020). While the slightly low % removal at higher pH values could be caused by the possibility of electrostatic repulsion between the pharmaceutical and the surface of St/MCD-nanoMIPs. Notably, the concentration of hydroxyl (OH^-) ions increases with pH, and the St/MCD-nanoMIPs adsorbents surface gains a negative charge. As a result, the amount of binding and the adsorption capacity of the adsorbents for the target pharmaceuticals decreased because of repulsion between the OH^- ions and the pharmaceuticals' negatively charged ions. The effect of electrostatic repulsion on the pharmaceuticals adsorption shows that their adsorption onto St-AgNPs is controlled by electrostatic or van der Waal's attraction (Adeola et al., 2021). The highest removal percentages (95-99%) of selected pharmaceuticals achieved at a pH value of 7, indicates that the St/MCD nanoMIPs have good adsorption capability in a neutral medium. This was due to the decreasing electrostatic repulsion between the protonated amine or carboxylate groups on target molecules and the positive charge on St/MCD-nanoMIPs surfaces at pH 7 (Hamad and El-Sesy, 2023).

Therefore, π-π interactions, such as the cation π of the protonated amino/carboxylate group of the target pharmaceuticals and π electrons of the adsorbent (St/MCD-nanoMIPs surfaces), as well as H-bonding between pharmaceuticals and the oxygen groups on the adsorbent, are proposed as the main possible mechanisms for the interaction of the target pharmaceuticals on the St/MCD-nanoMIPs surfaces at pH 7.

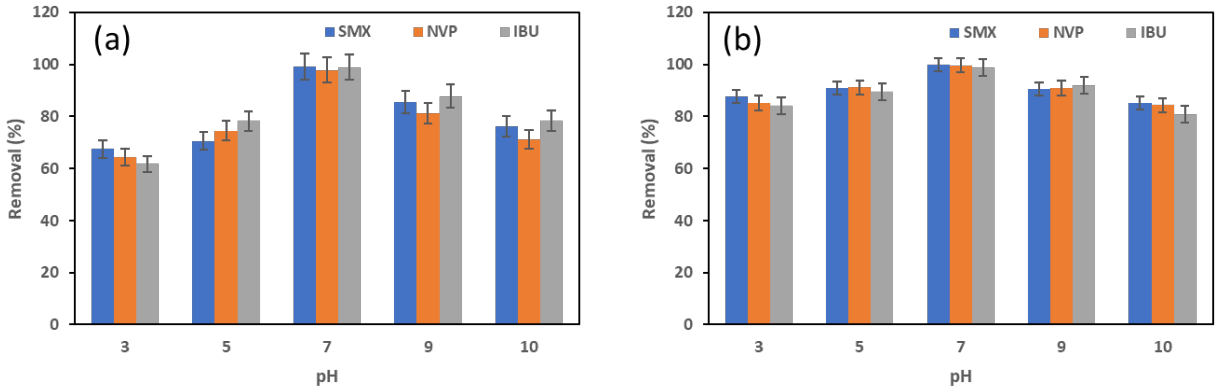

Figure 4.8: Effect of pH on the removal of the selected pharmaceuticals by (a) St-nanoMIP and (b) MCD-nanoMIP.

4.10.2.2 Effect of concentration on the adsorption of pharmaceuticals

The influence of initial concentration was assessed between 0.2 to 1.5 mg L^{-1}. Based on the acquired results, it was noticed that as the concentration increased there was a significant decrease in the percentage removal of the pharmaceuticals. The maximum removal **(**97-99%) for the MCD-nanoMIP (**Figure 4.9 (b))** was observed at a concentration of 0.2 mg L^{-1}. The removal efficiency for the St-nanoMIP increased as a function of initial concentration (**Figure 4.9 (a))**; which was observed until 0.6 mg L^{-1} where the adsorbent reached equilibrium. This indicates that the rate of adsorption was higher and quicker due to a high amount of available active sites to accommodate the presented adsorbate. At high adsorbate concentrations, the active sites on the St/MCD-nanoMIP surface became saturated and thus hindered the adsorption of adsorbates present in the solution. Consequently, the high pharmaceuticals removal at 0.2 mg L^{-1} and 0.6 mg L^{-1} for the St-nanoMIP and MCD-nanoMIP is probably because of the suggested strong affinity between the positively charged pharmaceutical molecules and the negatively charged St/MCD-nanoMIP surface, particularly when the system works at a low initial mass value (Hamad and El-Sesy, 2023).

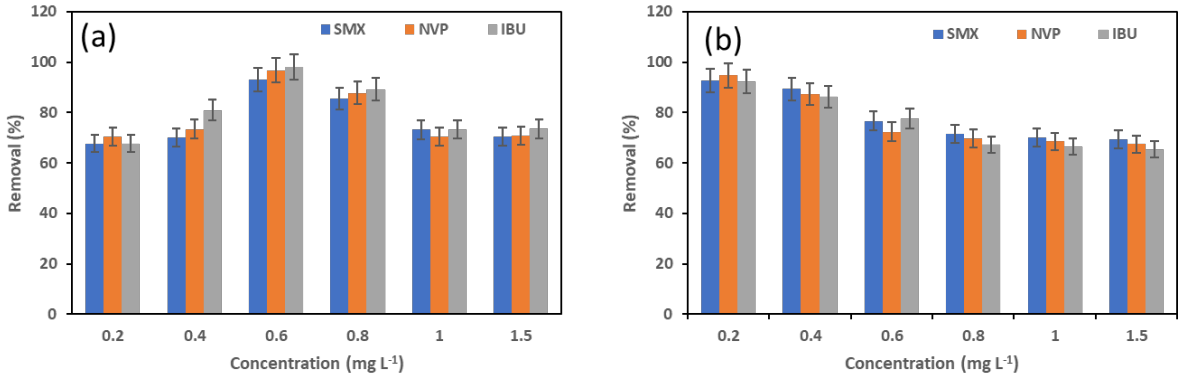

Figure 4.9: Effect of concentration on the removal of the selected pharmaceuticals by (a) St-nanoMIP and (b) MCD-nanoMIP.

4.10.2.3 Effect of adsorbent mass on the adsorption of pharmaceuticals

The effect of adsorbent mass on the adsorption capacity was evaluated between 10 – 50 mg adsorbent. The removal efficiency of sulfamethoxazole, nevirapine and ibuprofen increased with increasing mass of MCD-nanoMIP adsorbent up to 20 mg **(Figure 4.10 (b))**. The reason for the increase could be that the quantity of active sites accessible for the adsorption process increases in tandem with an increase in the mass dosage of the adsorbent. However, further increase in mass could not raise the %removal of the pharmaceuticals. This could be due to the reduction of active sites for pharmaceuticals adsorption resulting from aggregation of the particles of MCD-nanoMIP (Trinh et al., 2020). Accordingly, removal efficiency for the targeted pharmaceutical increased with the increase in mass dosage from 10 to 50 mg for the St-nanoMIP in **Figure 4.10 (a)**. The increase in St-nanoMIP dose leads to the increase the active sites for pharmaceutical compounds to bind which means more of these compounds are adsorbed on the surface. The extraction efficiency for all the investigated compounds varied from 92-98% when 50 mg of the St-nanoMIP was used.

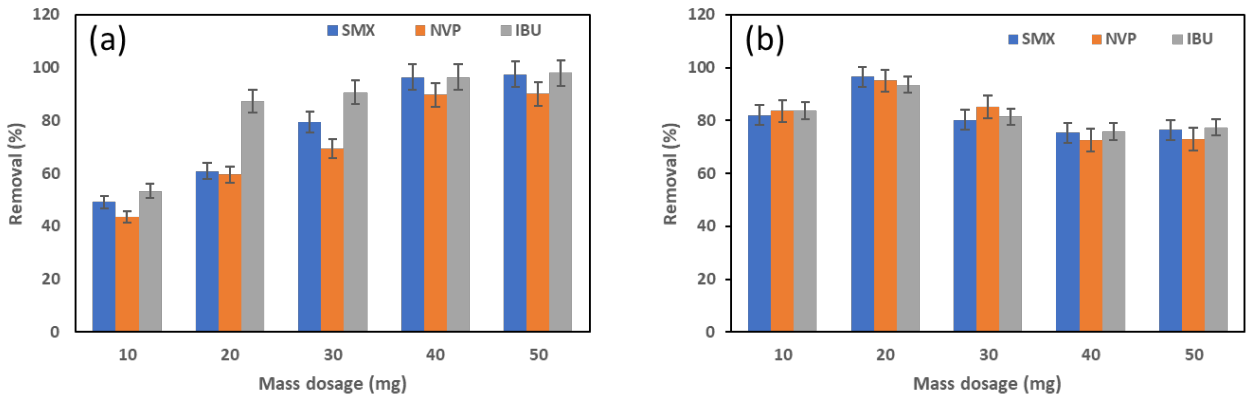

Figure 4.10: Effect of adsorbent mass on the removal of the selected pharmaceuticals by (a) St-nanoMIP and (b) MCD-nanoMIP.

4.10.2.4 Effect of contact time on the adsorption of pharmaceuticals

The impact of contact time was examined between 10-50 minutes. The contact time between the adsorbent and the adsorbate is an essential design parameter that affects how efficiently the adsorption processes work. The removal efficiency increased at 10 minutes with maximum removal % ranging from 94-96% and 96-99.9% for the St-nanoMIP (**Figure 4.11 (a)**) and MCD-nanoMIP (**Figure 4.11 (b)**). Due to the abundance of vacant recognition binding sites, the adsorption happened quickly. Thereafter, there was a slight reduction in the % removal. Competition for the same sites as more pharmaceutical molecules from the sample interact with the adsorbent particles may be the cause of this decrease in adsorption. When the adsorbent particles' capacity is surpassed, molecules with stronger interactions with the adsorbent surface functional groups tend to replace those with weaker adsorptive properties. Also, this may be due to adsorption-desorption of the pharmaceutical compounds after 10 minutes resulting in the observed decrease. Accordingly, the adsorption rate increases early in the process because of the adsorbent's empty pore structure, and it gradually declines over time. As the number of molecules adsorbed on the surface increases over time, the pore ratio in the adsorbent structure decreases (Fakioğlu and Kalpaklı, 2022). Therefore, making it difficult for the pharmaceuticals to occupy the surface-active sites due to the repulsive forces between the pharmaceutical molecules and the bulk phases on the St/MCD-nanoMIPs. Notably, the adsorbent reaches saturation with a decrease in solvent accessible surface area, and the reduced inner surface area results in a decrease in adsorption efficiency with increase reaction time. According to the results, adsorption proceeded more quickly, with the majority of the adsorbate-adsorbent interaction occurring in the first 10 minutes. The adsorption uptake was because there are more

unoccupied active adsorption sites on the St/MCD nanoMIPs surface (Al-Senani and Al-Kadhi, 2020).

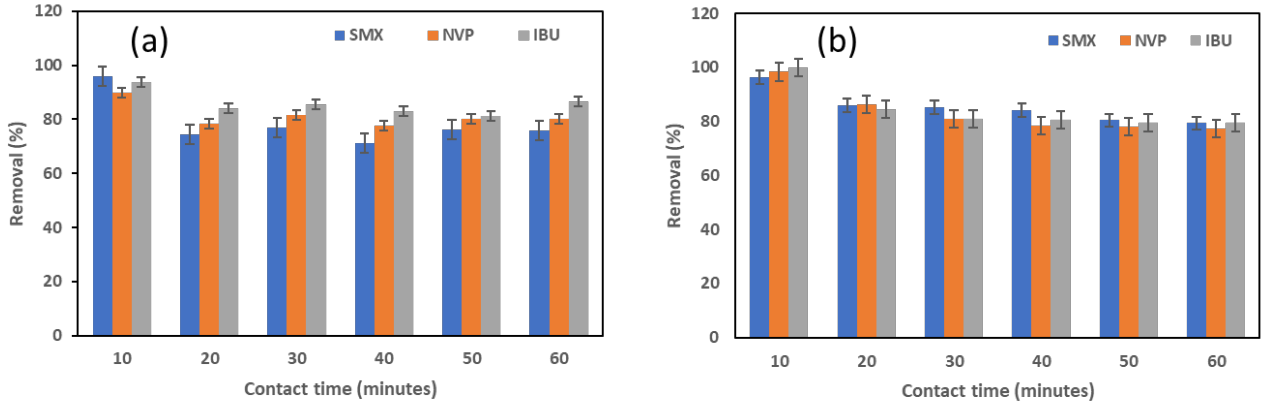

Figure 4.11: Effect of contact time on the removal of the selected pharmaceuticals by (a) St-nanoMIP and (b) MCD-nanoMIP.

4.10.2.5 Effect of temperature on the adsorption of pharmaceuticals

The influence of temperature was assessed between 25 to 70 °C. From the results obtained in **Figure 4.12 (a)**, it was noted that the % removal increased with increasing temperature up to 30 °C and then slightly decreased for the St-nanoMIP. Whereas the maximum adsorption for the pharmaceuticals occurred at a temperature of 40 °C for the MCD-nanoMIP (**Figure 4.12 (b)**). The temperature increase has been reported to cause an increase in total pore volume and porosity of the-nanoMIPs. Furthermore, at higher temperature the highest amount of pharmaceutical molecules reached the nanoMIPs surface as a result of the pharmaceuticals increasing kinetic energy with rising temperature leading to increased adsorption rates. Nonetheless, a slight decline in removal percentage was noted upon an additional rise in temperature after 30 °C. This was caused by the weakening of bonds between the adsorbate and the adsorbent moieties at temperatures (Bhattacharya et al., 2020). The increase in temperature is thought to be a sign that the adsorption process is endothermic. The reduced adsorption efficiency at lower temperature could be due to the tendency of the analytes to have reduced kinetic energy at low temperatures, hence obstructing analytes ability to access the adsorbent active site.

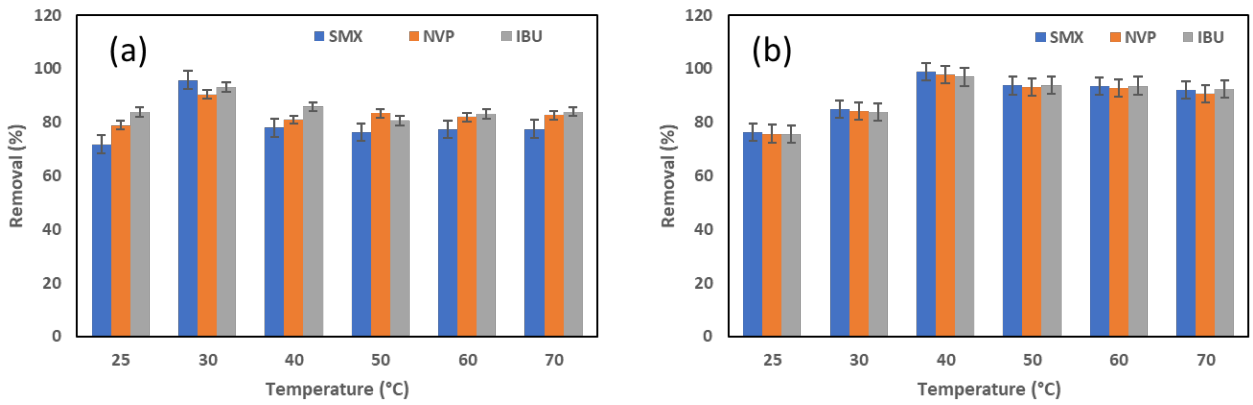

Figure 4.12: Effect of temperature on the removal of the selected pharmaceuticals by (a) St-nanoMIP and (b) MCD-nanoMIP.

4.10.3 Statistical analysis

Using the Fisher's F test and an analysis of variance (ANOVA), the impact of the variables pH, contact time, mass dose, concentration, and temperature on the pharmaceutical's removal process was investigated. The more significant terms of the model are indicated by larger F values and smaller p-values (Davarani et al., 2017). The ANOVA results in **Table S4.2**, show that the model has an F value of 98.2 and 75.32 for the St-nanoMIP and MCD-nanoMIP respectively, which are higher than the F critical value to prove significance. Accordingly, the variables were statistically significant at a 95% confidence level and had a P value < 0.05 for both St-nanoMIP and MCD-nanoMIP. Hence, the effects of concentration, contact time, mass dosage, temperature and pH were shown to significantly affect the removal efficiency of pharmaceuticals from water. This validates the outcome displayed in the main and interaction effect plots (**Figure 4.8** to **Figure 4.12**). The error of the estimate is 2.41 for St-nanoMIP and 3.39 for the MCD-nanoMIP, which means that the percentage of error of the studied parameters is very low. Further validation of the individual parameter's significance is achieved by estimating the percentage contribution factor of each process parameter. The results in **Table S4.3** shows that the mass dosage and temperature are major contributors with contribution factor of 81.05 and 43.74 % for the St-nanoMIP and 70.20 and 84.49% for the MCD-nanoMIP, respectively. Additionally, it was discovered that for St-nanoMIP, their contribution was in the following order: mass dosage>temperature>pH>concentration>contact time, and for MCD-nanoMIP it was temperature>mass dosage>concentration>pH>contact time.

4.10.4 Adsorption kinetics

The pseudo-first order and pseudo-second order models were adopted for the kinetic models of sulfamethoxazole, nevirapine and ibuprofen adsorption by St/MCD-AgNPs and St/MCD-nanoMIPs. The linear and non-linear kinetic plots are depicted in **Figure S4.1** and **S4.2**. The slope and the intercept of each linear and non-linear plots were used to calculate the adsorption rate constants (k_1 and k_2) and the amount of adsorption in equilibrium (qe). The values of the calculated kinetic parameters and regression coefficients are shown in **Table 4.1 and Table 4.2**. The obtained R^2 value for the pseudo-first order kinetic models depict relatively lower values for both the linear and non-linear models, hence indicting poor fitting of these models. In comparison, the R^2 values for both the linear and non-linear pseudo-second order kinetic models demonstrated excellent conformity than the linear and non-linear pseudo-first order kinetic models. However, a stronger fit with the linear model compared to the non-linear model was observed, which explains why the linear pseudo-second order model has received the most reporting (Hidayat et al., 2021). This was further confirmed by their low RMSE values which indicates a higher fit of the model. In comparison to the non-linear model, the pseudo-first order and pseudo-second order linear models offer a considerable benefit by directly calculating the equilibrium absorption capacity (qe) based on the adsorption path over time. In particular, the calculated qe values on the linear pseudo second order model were found to be very close to the obtained experimental values for both adsorbents as indicated in **Table 4.1**. However, for both the linear and non-linear pseudo-first order model, the calculated qe values differed significantly from the experimental data; as a result, high error functions (RMSE) were obtained. Accordingly, the linear regression was observed to be the most appropriate method for defining the kinetics of sulfamethoxazole, nevirapine and ibuprofen adsorption into St/MCD-nanoMIPs in the pseudo-second order model. Notably, pseudo-second-order kinetics indicate the existence of strong interactions or a high affinity between adsorbate and adsorbent. This also indicates the involvement of chemisorption in the rate-determining step in the adsorption mechanism (Hu et al., 2022), hence, the binding of the pharmaceuticals onto the adsorbent surface through strong ionic or hydrogen/covalent bonds. Accordingly, the pseudo-second order constant rates (k_2) varied when comparing the linear and nonlinear models. However, the values of k_2 for all the pharmaceuticals in St-nanoMIP and MCD-nanoMIP were high compared to St/MCD-AgNPs. This is influenced by the adsorbent and adsorbate's binding strength and mass transfer speed (Nyirenda et al., 2022). Overall, the rate of adsorption for the tested pharmaceuticals has proved to be a fast process for the St/MCD-nanoMIPs. However, the behaviour of each compound was different, presumably due to their physicochemical

properties. According to the pseudo-second-order rate constant, the fastest adsorbing compound is nevirapine followed by ibuprofen, and sulfamethoxazole. This can be explained by the molecular weight and $\log K_{ow}$ of the pharmaceuticals (Ilyas et al., 2020). Pharmaceuticals with high molecular weight takes priority on the surface of the adsorbent and those with high $\log K_{ow}$ values are more hydrophobic, hence better, or faster adsorption performance is expected from them. The molecular weights for nevirapine, sulfamethoxazole and ibuprofen are 266.30 mg L^{-1}, 254.28 mg L^{-1} and 206.29 mg L^{-1}. While the $\log K_{ow}$ values are 3.89, 0.89 and 3.97 for nevirapine, sulfamethoxazole and ibuprofen, respectively. As a result, nevirapine exhibits faster rate of adsorption than ibuprofen and sulfamethoxazole because of its higher molecular weight and $\log K_{ow}$.

Table 4.1: Linear kinetics data for the adsorption of the selected pharmaceuticals onto St/MCD-AgNPs and St/MCD-nanoMIP

Adsorbent	**Pharmaceuticals**	**q_e (mg g^{-1}) Exp**	**Pseudo-first order**				**Pseudo second order**			
			q_e (mg g^{-1}) Cal	**k_1**	**R^2**	**RMSE**	**qe (mg g^{-1}) Cal**	**k_2**	**R^2**	**RMSE**
St-AgNPs	Sulfamethoxazole	10.74	5.62	2.5×10^{-4}	0.976	1.81	10.2	0.1254	0.9998	0.22
	Nevirapine	5.84	1.53	5×10^{-5}	0.926	1.64	5.31	0.2268	0.9997	0.22
	Ibuprofen	9.55	1.57	7.83×10^{-5}	0.9916	2.45	8.29	0.1268	0.9997	0.51
St-nanoMIP	Sulfamethoxazole	39.68	33.22	7.33×10^{-5}	0.9949	2.82	39.88	2.09	0.9999	1.14
	Nevirapine	30.02	25.86	1.07×10^{-4}	0.9848	1.87	28.87	2.36	0.9991	0.47
	Ibuprofen	29.50	21.81	9.83×10^{-5}	0.9862	2.80	26.29	2.08	0.9999	1.31
MCD-AgNPs	Sulfamethoxazole	16.6	6.46	1×10^{-5}	0.9989	4.14	9.87	0.2891	0.9999	2.75
	Nevirapine	7.95	2.648	2.33×10^{-5}	0.9974	2.16	5.25	0.6825	0.9999	1.10
	Ibuprofen	10.6	2.33	7.5×10^{-5}	0.9945	3.38	8.87	0.1163	0.9998	0.71
MCD-nanoMIP	Sulfamethoxazole	33.31	27.31	1.43×10^{-3}	0.9530	3.23	31.32	0.521	0.9988	0.81
	Nevirapine	22.52	17.16	2.09×10^{-3}	0.9842	1.71	21.80	0.959	0.9990	0.29
	Ibuprofen	32.10	10.61	5.32×10^{-3}	0.9702	2.42	31.42	0.511	0.9967	0.28

Table 4.2: Non-linear kinetics data for the adsorption of the selected pharmaceuticals onto St/MCD-AgNPs and St/MCD-nanoMIP

Adsorbent	**Pharmaceuticals**	**q_e (mg g^{-1}) Exp**	**Pseudo-first order**				**Pseudo-second order**			
			q_e (mg g^{-1}) Cal	**k_1**	**R^2**	**RMSE**	**qe (mg g^{-1}) Cal**	**k_2**	**R^2**	**RMSE**
St-AgNPs	Sulfamethoxazole	10.74	5.13	1.1×10^{-4}	0.9563	2.00	8.89	0.0454	0.9856	0.76
	Nevirapine	5.84	1.01	2.8×10^{-4}	0.9136	1.85	4.75	0.0268	0.9569	0.44
	Ibuprofen	9.55	1.97	3.97×10^{-4}	0.9382	2.29	9.02	0.0268	0.9566	0.22
St-nanoMIP	Sulfamethoxazole	39.68	30.01	1.25×10^{-5}	0.9621	4.13	37.38	1.12	0.9789	0.94
	Nevirapine	30.02	21.55	1.07×10^{-3}	0.9033	3.63	25.74	1.62	0.9703	1.75
	Ibuprofen	29.50	15.22	3.75×10^{-4}	0.9201	5.49	22.35	1.25	0.9625	2.92
MCD-AgNPs	Sulfamethoxazole	16.6	5.35	2.2×10^{-3}	0.9081	4.59	14.96	0.1992	0.9654	0.67
	Nevirapine	7.95	3.84	5.03×10^{-4}	0.8881	1.68	7.44	0.3325	0.9785	0.21
	Ibuprofen	10.6	1.95	5.9×10^{-5}	0.9241	3.53	9.87	0.2163	0.9396	0.30
MCD-nanoMIP	Sulfamethoxazole	33.31	18.21	2.13×10^{-3}	0.9545	6.94	22.02	5.5×10^{-3}	0.9575	4.61
	Nevirapine	22.52	10.64	2.95×10^{-3}	0.8891	4.38	15.49	0.0257	0.9705	2.87
	Ibuprofen	32.10	8.46	8.28×10^{-3}	0.9034	3.30	24.42	0.1283	0.9535	3.14

4.10.5 Adsorption isotherms

The linear and non-linear Langmuir and Freundlich equilibrium constants and other parameters of the isotherm models are shown in **Table 4.3 and Table 4.4**. The results showed that the adsorption is favourable as the Langmuir dimensionless equilibrium constant (R_L) is larger than zero and less than one (1). However, the non-linear Langmuir model showed that these values were substantially smaller in magnitude as compared to the linear model. The value of the heterogeneity factor 1/n was also less than 1 and greater than zero, therefore demonstrating evidence that the Freundlich isotherm is favourable. It was observed that these isothermal parameters varied slightly for the non-linear Freundlich model. Hence, the adsorption data fitted well with both linear and non-linear Langmuir and Freundlich isotherms. Similar finding were also reported by Rosli and co-workers (Rosli et al., 2021). Further, the R^2 values show that both adsorption models can properly explain the experimental data. The linear and non-linear Langmuir isotherm model shows a slightly better fit compared to the linear and non-linear Freundlich model. The linear Langmuir isotherm model R^2 value, however, was less than that of the non-linear Langmuir isotherm model. This demonstrates that the non-linear Langmuir isotherm model provided the best fit for the experimental data on the adsorption of ibuprofen, nevirapine, and sulfamethoxazole on St/MCD-AgNPs. Therefore, adsorption isotherm fitting confirms that the adsorption took place as monolayer without lateral/further interaction between the pharmaceuticals in the homogeneous surface of both the adsorbent (St-AgNPs and MCD-AgNPs). Chakraborty and co-workers also reported that the non-linear Langmuir isotherms is a more suitable method in their study of the adsorption of ibuprofen onto Cocos nucifera shell biochar (Chakraborty et al., 2019). Additionally, the non-linear model for the St/MCD-nanoMIPs gave higher R^2 values in contrast to the linear model. However, when the non-linear Langmuir and Freundlich isotherms are compared, the R^2 value for the non-linear Freundlich isotherm have high correlation of determination compared to that of the non-linear Langmuir model. Thus, the best correlation for sulfamethoxazole, nevirapine and ibuprofen was observed in the non-linear Freundlich model. This proves that the St/MCD-nanoMIPs possesses heterogeneously distributed active sites formed during nanoparticles molecular imprinting.

Notably, the adsorption capacities (Q_{max}) of the non-linear model were higher than those of the linear model. These results demonstrate that, in comparison to the linear regression, the non-linear regression was more effective in accounting for the adsorption parameters. Therefore, in

order to acquire adsorption isotherms, it is therefore advisable to predominantly use the non-linear regression. Accordingly, the highest adsorption capacity (Q_{max}) for the studied pharmaceuticals was in the order of nevirapine>sulfamethoxazole>ibuprofen with values of 37.41 mg g^{-1}, 30.59 mg g^{-1}, and 29.89 mg g^{-1} for the St-nanoMIP, while the MCD-nanoMIP values were 18.12 mg g^{-1}, 14.91 mg g^{-1} and 11.88 mg g^{-1}, respectively. The molecular structures of the pharmaceutical may be responsible for this affinity (**Table S4.1**), where nevirapine contains two aromatic rings, i.e., more hydrophobicity, while ibuprofen and sulfamethoxazole contain only one aromatic ring hence their interaction with AgNPs is via π-π interaction (Husein et al., 2019). When compared to St/MCD-nanoMIPs, the St/MCD-AgNPs did not exhibit a greater affinity for the targeted pharmaceuticals. Particularly, the Q_{max} values obtained for the St/MCD-nanoMIPs were higher compared to St-AgNPs and MCD-AgNPs. Also, large pores may facilitate solvent penetration and enable easy diffusion of the pharmaceutical compounds onto the adsorbent surface (Yu et al., 2022). This could therefore explain why St/MCD-nanoMIPs show a higher rate of pharmaceuticals adsorption compared to St/MCD-AgNPs as adsorption capacity is affected by the material's pore structure, specifically its pore volume/diameter (Liu et al., 2021).

Table 4.3: Linear isotherms data for the adsorption of the selected pharmaceuticals onto St/MCD-AgNPs and St/MCD-nanoMIPs

Isotherm	Parameters	Sulfamethoxazole				Nevirapine				Ibuprofen			
		St-AgNPs	St-nanoMIP	MCD-AgNPs	MCD-nanoMIP	St-AgNPs	St-nanoMIP	MCD-AgNPs	MCD-nanoMIP	St-AgNPs	St-nanoMIP	MCD-AgNPs	MCD-nanoMIP
Freundlich	K_F (L mg^{-1})	2.15	3.42	2.63	3.35	2.30	3.57	5.05	4.48	1.68	4.63	0.92	4.81
	1/n	0.5922	0.62	0.67	0.40	0.57	0.51	0.98	0.38	0.89	0.51	0.71	0.37
	R^2	0.7726	0.9999	0.9899	0.9923	0.8441	0.9955	0.9945	0.9807	0.8247	0.9993	0.9919	0.9951
Langmuir	Q_{max}	10.94	26.39	11.95	8.20	31.55	32.68	15.87	8.72	4.99	24.95	4.122	8.62
	K_L (L mg^{-1})	3.04	0.874	10.25	0.36	0.1981	0.889	0.3460	0.38	2.4529	0.893	0.9559	0.19
	R_L	0.032	0.144	0.097	0.55	0.3354	0.125	0.2242	0.61	0.039	0.120	0.0947	0.31
	R^2	0.9981	0.9958	0.9949	0.562	0.9951	0.9960	0.9985	0.5792	0.9949	0.9847	0.9951	0.3743

Table 4.4: Non-linear isotherms data for the adsorption of the selected pharmaceuticals onto St/MCD-AgNPs and St/MCD-nanoMIPs

Isotherm	**Parameters**	**Sulfamethoxazole**				**Nevirapine**				**Ibuprofen**			
		St-AgNPs	St-nanoMIP	MCD-AgNPs	MCD-nanoMIP	St-AgNPs	St-nanoMIP	MCD-AgNPs	MCD-nanoMIP	St-AgNPs	St-nanoMIP	MCD-AgNPs	MCD-nanoMIP
Freundlich	K_F(L mg^{-1})	1.07	1.92	1.13	1.36	1.01	1.77	1.71	1.48	0.98	1.69	0.66	1.56
	1/n	0.55	0.60	0.61	0.38	0.55	0.49	0.93	0.40	0.89	0.50	0.70	0.33
	R^2	0.8355	0.9995	0.9850	0.9993	0.8823	0.9965	0.9955	0.9805	0.7627	0.9991	0.9825	0.9965
Langmuir	Q_{max}	10.63	30.59	13.49	11.88	35.33	37.41	20.73	18.12	7.32	29.89	10.43	14.91
	K_L (L mg^{-1})	0.18	0.14	1.43	0.22	0.089	0.55	0.23	0.25	1.33	0.48	0.76	0.095
	R_L	0.022	0.095	0.077	0.36	0.13	0.098	0.16	0.43	0.022	0.089	0.078	0.11
	R^2	0.9991	0.9982	0.9993	0.8621	0.9977	0.9998	0.9985	0.8578	0.9955	0.9923	0.9962	0.6365

4.10.6 Thermodynamics

The values of ΔG°, ΔH° and ΔS° in **Table 4.5**, were calculated from the slope and intercept of the plot of $\ln K_L$ and 1/T in **Figure S4.3**. The adsorption process was thermodynamically favoured and spontaneous, as evidenced by the increasing negative value of ΔG° and its magnitude with rising temperature (298-343 K). This may be the consequence of the adsorbent's pores expanding at a higher temperature, creating bigger pores that allow for a greater diffusion of the pharmaceutical molecules within the adsorbent. Moreover, the adsorption of the selected pharmaceuticals onto St/MCD-AgNPs and St-nanoMIPs was endothermic in nature which was illustrated by the positive values of ΔH° with a value lower than 40 kJ/mol. On the other hand, the negative ΔH° confirms that the adsorption process for the MCD-nanoMIP is of an exothermic nature. These results indicate that the adsorption of sulfamethoxazole, nevirapine and ibuprofen onto St/MCD-AgNPs and St-nanoMIPs is a purely physical process, while it is a chemical process for MCD-nanoMIP (Parashar et al., 2022). The physisorption process was due to the long range weak Van der Waals forces between pharmaceuticals interaction with St/MCD-AgNPs and St-nanoMIPs (Adeola et al., 2021), while chemisorption was due to the ionic or covalent interaction of the pharmaceuticals with MCD-nanoMIP (Alaqarbeh, 2021, Al-Ghouti and Da'ana, 2020). Further, the positive ΔS° values confirmed an irregular increase on the degree of disorderliness/randomness in the pharmaceuticals-nanoparticles/nanoMIPs interaction, thus indicating strong affinity of the pharmaceuticals with the adsorbents. This indicates that the adsorbed solvent molecules, which are displaced by the pharmaceutical species, gain more translational entropy than is lost by the adsorbate ions/molecules, thus allowing for the prevalence of randomness in the system.

Table 4.5: Thermodynamics data for the adsorption of the selected pharmaceuticals onto St/MCD-AgNPs and St/MCD-nanoMIPs

Compounds	**ΔG° (kJ mol^{-1})**						**ΔH° (kJ mol^{-1})**	**ΔS° (J mol^{-1} K^{-1})**	**R^2**
	298 K	**303 K**	**313 K**	**323 K**	**333 K**	**343 K**			
St-AgNPs									
Sulfamethoxazole	-11.13	-11.46	-12.67	-13.90	-15.75	-17.75	32.42	144.9	0.9601
Nevirapine	-5.33	-5.49	-5.71	-6.17	-6.40	-6.63	3.58	29.89	0.9208
Ibuprofen	-9.24	-9.57	-10.17	-10.54	-11.45	-12.30	10.25	65.21	0.9368
St-nanoMIPs									
Sulfamethoxazole	-8,99	-8.73	-9.80	-10.39	-10.97	-11.46	7.51	55.38	0.9979
Nevirapine	-9.88	-9.61	-10.98	-11.69	-12.42	-13.05	10.98	70.14	0.9975
Ibuprofen	-9.90	-9.77	-11.30	-12.02	-12.89	-13.60	13.62	79.47	0.9870
MCD-AgNPs									
Sulfamethoxazole	-11.03	-11.98	-13.05	-13.95	-16.50	-18.32	35.44	155.5	0.9484
Nevirapine	-5.13	-5.42	-5.70	-6.02	-6.30	-6.58	3.58	31.34	0.9507
Ibuprofen	-9.92	-10.12	-10.54	-10.92	-11.33	-11.68	10.81	39.41	0.9676
MCD-nanoMIPs									
Sulfamethoxazole	-9,02	-8,85	-8,34	-7,65	-7,20	-5,52	-30,29	7,64	0,9622
Nevirapine	-8,53	-8,45	-8,75	-8,75	-8,90	-8,82	-5,87	8,88	0,9327
Ibuprofen	-10,12	-9,91	-9,93	-9,73	-9,52	-9,93	-12,19	7,31	0,9433

4.10.7 Selectivity of St/MCD-nanoMIPs

The similar physicochemical properties and size of fenoprofen as the target compounds shows that it has a potential to compete for binding sites on the St/MCD-nanoMIPs cavities imprinted with sulfamethoxazole, nevirapine and ibuprofen. However, the results in **Figure 4.13 (a)** and **(b)** shows that the adsorption efficiency for fenoprofen was 26% for the St-nanoMIP and 30% for the MCD-nanoMIP. This was ascribed to a deficiency in molecular recognition, which is heavily impacted by the imprinting molecule's size, structure, and functional groups. Furthermore, this indicates the specificity and high selectivity of the St/MCD-nanoMIPs. The St/MCD-nanoMIPs selectivity can be explained by taking into account the target pharmaceuticals rigid molecular structure and their precise positions, which are most anticipated to be responsible for the binding site interaction (Chiarello et al., 2021). Notably, the adsorption efficiency of fenoprofen was lower than that of sulfamethoxazole, nevirapine, and ibuprofen, although they all have comparable structures. This suggests that conformation memory is mostly dependent on the memory of the specific functional group. Therefore, in addition to the molecule's size, the distribution of the functional groups themselves was crucial for St/MCD-nanoMIPs molecular recognition. Notably, fenoprofen cannot bring about specific binding in the same way as sulfamethoxazole, nevirapine and ibuprofen because either its size cannot match the cavities, or its functional group positions do not correspond to the functional groups in the cavities of the St/MCD-nanoMIPs. Hence it was easily washed out, leaving sulfamethoxazole, nevirapine and ibuprofen that were specifically bound within the imprinted cavities.

The adsorption efficiency of sulfamethoxazole, nevirapine were between 80-98 % for St-nanoMIP and 71-87 % for the MCD-nanoMIP. The high adsorption efficiencies were due to molecular recognition of the pharmaceuticals on the surface of St/MCD-nanoMIPs. Given its superior surface properties, the St-nanoMIP outperformed the MCD-nanoMIP in terms of adsorption efficiency. The selectivity of each compound on St/MCD-nanoMIPs is summarised by the K_d and k values in **Table 4.6**. The K_d values on the selectivity of St/MCD-nanoMIP were in the following order: nevirapine>sulfamethoxazole>ibuprofen. This could imply that the compounds imprinting cavities were formed as a result of the interaction between the pharmaceuticals functionality and its size, shape, and quantity of hydrogen bonding (Yu et al., 2022). The results obtained show that specific selectivity factor (k) is larger than 1, indicating that the interactions, size and molecular memory of the nanoMIPs for sulfamethoxazole,

nevirapine and ibuprofen demonstrate high selectivity even in the presence of a competitor (Espinoza-Torres et al., 2023).

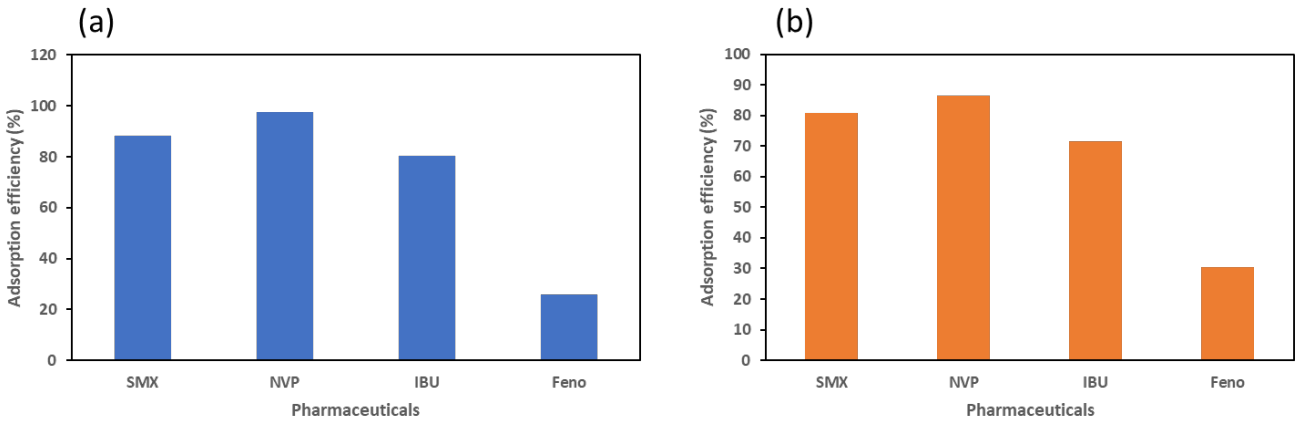

Figure 4.13: Adsorption efficiency of the selected pharmaceuticals in the presence of competitor fenoprofen on (a) St-nanoMIP and (b) MCD-nanoMIP.

Table 4.6: Selectivity of St/MCD-nanoMIPs towards the selected pharmaceuticals

Pharmaceuticals	**St-nanoMIP**		**MCD-nanoMIP**	
	K_d (mg g^{-1})	***k***	**K_d (mg g^{-1})**	***k***
Sulfamethoxazole	0.58	2.76	0.40	1.33
Nevirapine	0.71	3.38	0.47	1.57
Ibuprofen	0.48	2.29	0.37	1.23
Fenoprofen	0.21	-	0.30	-

4.10.8 Regeneration of St/MCD-nanoMIPs

The results in **Figure 4.14 (a)** and **(b)** shows that the St-nanoMIP and MCD-nanoMIP particles remain highly stable even after the 5th cycle with their adsorption efficiency being greater than 90%. This suggests that the St/MCD-nanoMIPs are effectively reusable as they preserve the adsorption capacity. However, a slow loss of particles throughout the washing phases could be the cause of the observed minor decline in MCD-nanoMIPs adsorption performances. Compared to other existing adsorbent materials that require considerable effort to be regenerated, the proven reusability and simple regeneration of St/MCD-nanoMIPs over multiple adsorption/desorption cycles is a crucial factor for a large-scale application. Notably,

the regeneration studies' findings indicate that the St/MCD-nanoMIPs can be reused with little loss of their selectiveness and specificity. This reduces costs as well as the use of virgin resources, which makes them not only economically viable but also significant as alternatives in the water treatment industry.

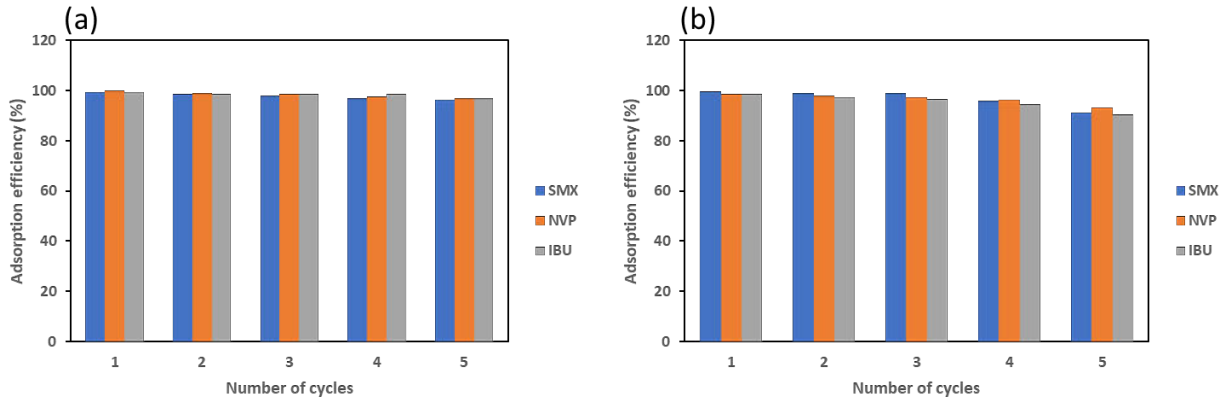

Figure 4.14: Regeneration cycles of (a) St-nanoMIP and (b) MCD-nanoMIP cycle reuse.

4.10.9 Application in wastewater

The applicability of St-nanoMIP and MCD-nanoMIP in wastewater samples was conducted by carrying out adsorptive removal of sulfamethoxazole, nevirapine and ibuprofen from influents and effluents from three different wastewater treatment plants (WWTPs) in KwaZulu-Natal (Darvill, Northern and Amanzimtoti). The samples were first filtered to eliminate particulates and then analysed under the optimum conditions obtained for both St and MCD-nanoMIPs. Notably, the application of St-nanoMIP and MCD-nanoMIP in wastewater was done at the obtained optimum adsorption conditions. The St-nanoMIP concentration was 0.2 mg L^{-1}, pH 7, contact time of 10 minutes, adsorbent mass of 50 mg and temperature of 30 °C. Whereas for the MCD-nanoMIP the conditions were 0.6 mg L^{-1}, 10 minutes, pH 7, adsorbent mass of 20 mg and temperature of 40 °C. As seen in **Table 4.7**, the adsorption capacities for St-nanoMIP range from 52.8-82.8 mg g^{-1} and 51.2-82.9 mg g^{-1} for the influent and effluent, respectively. The MCD-nanoMIP had adsorption capacities ranging from 50.1-64.1 mg g^{-1} for the influent and 45.8 mg g^{-1} and 62 mg g^{-1} for the effluent, respectively for the three WWTPs. It can be noted that, both St-nanoMIP and MCD-nanoMIP exhibited great potential as excellent adsorbents with high adsorption ability for the removal of sulfamethoxazole, nevirapine and ibuprofen. Among the investigated pharmaceuticals, nevirapine exhibited high adsorption capacities in Darvill and Amanzimtoti WWTPs for both St-nanoMIP and MCD-nanoMIP. Nevirapine is widely used to treat HIV and prevent mother-to-child transmission, which could

be the reason for its high environmental detection frequency. (Cerveny et al., 2021). On the other hand, nevirapine was adsorbed more effectively by St/MCD-nanoMIPs in the three WWTPs because it is more aromatic (two benzene rings) and non-polar (log K_{ow} = 3.89), while ibuprofen was the second most adsorbed compound since it has one aromatic ring and is also non-polar (log K_{ow} = 4.85).

Consequently, the size and the hydrophobicity nature of nevirapine and ibuprofen makes them most adsorbable. Sulfamethoxazole was the less adsorbed compound by St/MCD-nanoMIP since it is most hydrophilic compound with Log K_{ow} of 0.89. Nielsen and Bandosz reported a similar trend, noting that compounds with a higher Log K_{ow} adsorb more on organic matter than those with a lower Log K_{ow} (Nielsen and Bandosz, 2016). These findings additionally validate that the strong adsorption interaction of the selected aromatic pharmaceuticals with St/MCD-nanoMIPs, most likely through π–π aromatic ring interaction, H-bonding, or hydrophobic interactions (Agustin et al., 2022, Rosli et al., 2021). Additionally, there were differences in the amounts of pharmaceuticals removed by St/MCD-nanoMIPs from WWTPs, which were primarily related to the characteristics of the influents and how the plants are operated (Khasawneh and Palaniandy, 2021).

Nevirapine had the highest removal efficiency in all WWTPs (82-96%), while ibuprofen had 69.8-76.8% and sulfamethoxazole had 50-72% on their removal by St-nanoMIP. Accordingly, MCD-nanoMIP had the highest removal efficiency for sulfamethoxazole (40-68%), while nevirapine had 54-63% and ibuprofen had 40-50%. Notably, high removal efficiencies were obtained for St-nanoMIP compared to MCD-nanoMIP. These results further indicate that the efficacy varies greatly depending on the adsorbent features. Since WWTPs must treat water containing a combination of pharmaceuticals at the same time, it is important to design an adsorbent with a high efficacy and large surface area for pharmaceuticals to adsorb. Overall, the selected pharmaceuticals were also found in effluent wastewater with adsorption capacities and removal efficiency that were comparable to those of the influents, suggesting that the treatment processes used in WWTPs did not effectively remove the compounds under investigation. This therefore is an indication that there is a need for an efficient method to be applied in WWTPs for the purpose of removing pharmaceuticals.

Table 4.7: Adsorption capacities of selected pharmaceuticals in WWTPs

WWTP	Sampling point	St-nanoMIP						MCD-nanoMIP					
		Sulfamethoxazole		Nevirapine		Ibuprofen		Sulfamethoxazole		Nevirapine		Ibuprofen	
		Qe (mg g^{-1})	RE%	Qe (mg g^{-1})	RE%	Qe (mg g^{-1})	RE%	Qe (mg g^{-1})	RE%	Qe (mg g^{-1})	RE%	Qe (mg g^{-1})	RE%
Darvill	Influent	67.6	70	82.9	96	76.8	80	64.1	68	61.4	60	51.6	50
	Effluent	55.0	63	82.8	95	74.4	79	45.8	40	62.0	63	51.6	50
Northern	Influent	68.7	72	77.9	85	72.8	77	61.0	60	55.7	54	48.9	45
	Effluent	53.8	52	77.3	82	69.8	73	50.9	47	60.3	59	45.9	40
Amanzimtoti	Influent	52.8	51	80.6	91	72.1	77	60.6	59	60.9	60	50.4	47
	Effluent	51.2	50	79.6	88	71.1	75	58.7	55	58.2	54	47.2	42

Qe = adsorption capacity

RE= removal efficiency

4.11 Conclusion

This study revealed that nanoMIPs can be utilized as an efficient adsorbent to remove the selected multi classes of pharmaceuticals from aqueous media. Incorporating nanoparticles to MIPs produces a new substance with improved features, such as increased thermal stability and adsorption capabilities. It was found that the error function (RMSE) values of the linear model were smaller than those of the non-linear model. Hence, the kinetics studies showed that the pseudo-second order linear model best describe the adsorption process and fast adsorption of compounds was observed for St/MCD-nanoMIPs. This was due to the abundance of imprinted cavities, providing nanoMIPs with a high specific surface area and a significant number of binding sites thus enabling a quick pharmaceutical diffusion process into the material.

Both linear and nonlinear models were effective for finding the ideal isotherm and its parameters. Nonetheless, when compared to a linear isotherm, the non-linear isotherm model performed better. The results revealed that the non-linear Freundlich isotherm is a more appropriate model for describing the adsorption of sulfamethoxazole, nevirapine and ibuprofen onto the St/MCD-nanoMIPs. This subsequently demonstrated that the predominant adsorption process for the St/MCD-nanoMIPs is physicochemical adsorption on the heterogeneous surface. However, the Langmuir isotherms demonstrated that monolayer adsorption occurred on the St/MCD-AgNPs, thus indicating that each pharmaceutical molecule was adsorbed on a unique localized adsorption site. Moreover, it also confirmed that there was no adsorbate transmigration in the plane of the surfaces, leading to homogeneous monolayer adsorption onto the adsorbent surface. Meanwhile, the adsorption thermodynamics described the adsorption process as spontaneous, endothermic, and physical in nature. Nonetheless, St/MCD-AgNPs demonstrated lesser adsorption capabilities than St/MCD-nanoMIPs, confirming the significance of St/MCD-nanoMIPs in the observation of enhanced adsorption. The St-nanoMIP showed a fast adsorption rate and high adsorption capacities when compared to MCD-nanoMIPs. Thus, St -nanoMIPs have larger surface area which further favours enhancement in adsorption capacity.

Apart from the ability to adsorb target pharmaceuticals with maximum selectivity and efficiency, another interesting feature of St/MCD-nanoMIPs is regeneration. Regeneration studies conducted over multiple adsorption and desorption cycles demonstrated that the St/MCD-nanoMIPs can be reused more than five times, an indication that the St/MCD-nanoMIPs could be used repeatedly without losing their adsorption efficiency. Therefore, the

use of St/MCD-nanoMIPs as adsorbents to remove pharmaceuticals from wastewater could lower the running costs of the water treatment plants.

The significance/statistical analysis of the findings was assessed using an analysis of variance and the F test, which demonstrated that the effects of contact time, concentration, temperature, adsorbent dosage, and pH were statistically significant. It was confirmed that the high adsorbing capacity of the St/MCD-nanoMIPs compared to the corresponding nanoparticles was due to its high surface area, high selectivity, H-bonding and π–π interaction with the benzene ring of the pharmaceuticals. The St/MCD-nanoMIPs proved to have higher adsorption capacity and good efficiency for the removal of sulfamethoxazole, nevirapine and ibuprofen in wastewater samples. The process was found to be cost-effective, environmentally friendly, versatile, highly selective, reusable, stable and easily applicable paving the way for the possible application of these nanoMIP materials in environmental pollution monitoring, especially of pharmaceuticals as they are not removed by the traditional wastewater treatment techniques.

4.12 References

ABAFE, O. A., SPÄTH, J., FICK, J., JANSSON, S., BUCKLEY, C., STARK, A., PIETRUSCHKA, B. & MARTINCIGH, B. S. 2018. LC-MS/MS determination of antiretroviral drugs in influents and effluents from wastewater treatment plants in KwaZulu-Natal, South Africa. *Chemosphere,* 200**,** 660-670.

ADEOLA, A. O., DE LANGE, J. & FORBES, P. B. 2021. Adsorption of antiretroviral drugs, efavirenz and nevirapine from aqueous solution by graphene wool: Kinetic, equilibrium, thermodynamic and computational studies. *Applied Surface Science Advances,* 6**,** 100157.

ADHIKARI, A., LAMICHHANE, L., ADHIKARI, A., GYAWALI, G., ACHARYA, D., BARAL, E. R. & CHHETRI, K. 2022. Green Synthesis of Silver Nanoparticles Using Artemisia vulgaris Extract and Its Application toward Catalytic and Metal-Sensing Activity. *Inorganics,* 10**,** 113.

AGUSTIN, M. B., MIKKONEN, K. S., KEMELL, M., LAHTINEN, P. & LEHTONEN, M. 2022. Systematic investigation of the adsorption potential of lignin-and cellulose-based nanomaterials towards pharmaceuticals. *Environmental Science: Nano,* 9**,** 2006-2019.

AL-GHOUTI, M. A. & DA'ANA, D. A. 2020. Guidelines for the use and interpretation of adsorption isotherm models: A review. *Journal of hazardous materials,* 393**,** 122383.

AL-SENANI, G. M. & AL-KADHI, N. 2020. The synthesis and effect of silver nanoparticles on the adsorption of Cu2+ from aqueous solutions. *Applied Sciences,* 10**,** 4840.

ALAQARBEH, M. 2021. Adsorption phenomena: definition, mechanisms, and adsorption types: short review. *RHAZES: Green and Applied Chemistry,* 13**,** 43-51.

ALI, F., ALI, N., BIBI, I., SAID, A., NAWAZ, S., ALI, Z., SALMAN, S. M., IQBAL, H. M. & BILAL, M. 2020. Adsorption isotherm, kinetics and thermodynamic of acid blue and basic blue dyes onto activated charcoal. *Case Studies in Chemical and Environmental Engineering,* 2**,** 100040.

ARABI, M., OSTOVAN, A., BAGHERI, A. R., GUO, X., WANG, L., LI, J., WANG, X., LI, B. & CHEN, L. 2020. Strategies of molecular imprinting-based solid-phase extraction prior to chromatographic analysis. *TrAC Trends in Analytical Chemistry,* 128**,** 115923.

ASHIQUE, S., UPADHYAY, A., HUSSAIN, A., BAG, S., CHATERJEE, D., RIHAN, M., MISHRA, N., BHATT, S., PURI, V. & SHARMA, A. 2022. Green biogenic silver nanoparticles, therapeutic uses, recent advances, risk assessment, challenges, and future perspectives. *Journal of Drug Delivery Science and Technology***,** 103876.

ASWATHI, V., MEERA, S., MARIA, C. A. & NIDHIN, M. 2023. Green synthesis of nanoparticles from biodegradable waste extracts and their applications: a critical review. *Nanotechnology for Environmental Engineering,* 8**,** 377-397.

BHATTACHARYA, S., BANERJEE, P., DAS, P., BHOWAL, A., MAJUMDER, S. K. & GHOSH, P. 2020. Removal of aqueous carbamazepine using graphene oxide nanoplatelets: process modelling and optimization. *Sustainable Environment Research,* 30**,** 1-12.

BHUTIYA, P. L., MISRA, N., RASHEED, M. A. & HASAN, S. Z. 2020. Silver nanoparticles deposited algal nanofibrous cellulose sheet for antibacterial activity. *BioNanoScience,* 10**,** 23-33.

CANFAROTTA, F., CZULAK, J., BETLEM, K., SACHDEVA, A., EERSELS, K., VAN GRINSVEN, B., CLEIJ, T. & PEETERS, M. 2018. A novel thermal detection method based on molecularly imprinted nanoparticles as recognition elements. *Nanoscale,* 10**,** 2081-2089.

CERVENY, L., MURTHI, P. & STAUD, F. 2021. HIV in pregnancy: Mother-to-child transmission, pharmacotherapy, and toxicity. *Biochimica et Biophysica Acta (BBA)-Molecular Basis of Disease,* 1867**,** 166206.

CHAKRABORTY, P., SHOW, S., RAHMAN, W. U. & HALDER, G. 2019. Linearity and non-linearity analysis of isotherms and kinetics for ibuprofen remotion using superheated steam and acid modified biochar. *Process Safety and Environmental Protection,* 126**,** 193-204.

CHIARELLO, M., ANFOSSI, L., CAVALERA, S., DI NARDO, F., SERRA, T. & BAGGIANI, C. 2021. NanoMIP-based solid phase extraction of fluoroquinolones from human urine: a proof-of-concept study. *Separations,* 8**,** 226.

DAVARANI, S. S. H., TAHERI, A. R. & RAHMATIAN, N. 2017. Highly selective solid phase extraction and preconcentration of Azathioprine with nano-sized imprinted polymer based on multivariate optimization and its trace determination in biological and pharmaceutical samples. *Materials Science and Engineering: C,* 71**,** 572-583.

EROL, I., CIGERCI, I. H., ÖZKARA, A., AKYıL, D. & AKSU, M. 2022. Synthesis of Moringa oleifera coated silver-containing nanocomposites of a new methacrylate polymer having pendant fluoroarylketone by hydrothermal technique and investigation of thermal, optical, dielectric and biological properties. *Journal of Biomaterials Science, Polymer Edition,* 33**,** 1231-1255.

ESPINOZA-TORRES, S., LÓPEZ, R., SOTOMAYOR, M. D., TUESTA, J. C., PICASSO, G. & KHAN, S. 2023. Synthesis, Characterization, and Evaluation of a Novel Molecularly Imprinted Polymer (MIP) for Selective Quantification of Curcumin in Real Food Sample by UV-Vis Spectrophotometry. *Polymers,* 15**,** 3332.

FAKIOĞLU, M. & KALPAKLı, Y. 2022. Mechanism and behavior of caffeine sorption: affecting factors. *RSC advances,* 12**,** 26504-26513.

FIORATI, A., BELLINGERI, A., PUNTA, C., CORSI, I. & VENDITTI, I. 2020. Silver nanoparticles for water pollution monitoring and treatments: ecosafety challenge and cellulose-based hybrids solution. *Polymers,* 12**,** 1635.

FRESCO-CALA, B., BATISTA, A. D. & CÁRDENAS, S. 2020. Molecularly imprinted polymer micro-and nano-particles: A review. *Molecules,* 25**,** 4740.

GABR, S. S., MUBARAK, M. F., KESHAWY, M., EL SAYED, I. E. T. & ABDEL MOGHNY, T. 2023. Linear and nonlinear regression analysis of phenol and P-nitrophenol adsorption on a hybrid nanocarbon of ACTF: kinetics, isotherm, and thermodynamic modeling. *Applied Water Science,* 13**,** 230.

GARNIER, M., SABBAH, M., MÉNAGER, C. & GRIFFETE, N. 2021. Hybrid molecularly imprinted polymers: the future of nanomedicine? *Nanomaterials,* 11**,** 3091.

GERAVI, H. A. & GHAEMY, M. 2024. Preparation of molecularly imprinted polymer nanoparticles for selective adsorption of caffeine using dual-functionalized Ag2S quantum dots. *Colloids and Surfaces A: Physicochemical and Engineering Aspects,* 680**,** 132735.

GOWDA, B. J., AHMED, M. G., CHINNAM, S., PAUL, K., ASHRAFUZZAMAN, M., CHAVALI, M., GAHTORI, R., PANDIT, S., KESARI, K. K. & GUPTA, P. K. 2022. Current trends in bio-waste mediated metal/metal oxide nanoparticles for drug delivery. *Journal of Drug Delivery Science and Technology,* 71**,** 103305.

HAMAD, M. T. M. H. & EL-SESY, M. E. 2023. Adsorptive removal of levofloxacin and antibiotic resistance genes from hospital wastewater by nano-zero-valent iron and nano-copper using kinetic studies and response surface methodology. *Bioresources and Bioprocessing,* 10**,** 1.

HE, S., ZHANG, L., BAI, S., YANG, H., CUI, Z., ZHANG, X. & LI, Y. 2021. Advances of molecularly imprinted polymers (MIP) and the application in drug delivery. *European Polymer Journal,* 143**,** 110179.

HIDAYAT, A. R. P., SULISTIONO, D. O., MURWANI, I. K., ENDRAWATI, B. F., FANSURI, H., ZULFA, L. L. & EDIATI, R. 2021. Linear and nonlinear isotherm, kinetic and thermodynamic behavior of methyl orange adsorption using modulated Al2O3@ UiO-66 via acetic acid. *Journal of Environmental Chemical Engineering,* 9**,** 106675.

HLENGWA, N. & MAHLAMBI, P. 2020. SPE-LC-PDA method development and application for the analysis of selected pharmaceuticals in river and wastewater samples from South Africa. *Water SA,* 46**,** 514-522.

HU, Y., ZHANG, C., JIAN, Z., CHEN, D., MA, Y. & YANG, W. 2022. Surface-imprinted polymer microsphere based on self-stabilized precipitation polymerization for selective removal of norfloxacin. *Applied Surface Science,* 574**,** 151706.

HUBETSKA, T., KOBYLINSKA, N. & GARCÍA, J. R. 2020. Efficient adsorption of pharmaceutical drugs from aqueous solution using a mesoporous activated carbon. *Adsorption,* 26**,** 251-266.

HUSEIN, D. Z., HASSANIEN, R. & AL-HAKKANI, M. F. 2019. Green-synthesized copper nano-adsorbent for the removal of pharmaceutical pollutants from real wastewater samples. *Heliyon,* 5.

ILYAS, H., MASIH, I. & VAN HULLEBUSCH, E. D. 2020. Pharmaceuticals' removal by constructed wetlands: a critical evaluation and meta-analysis on performance, risk reduction, and role of physicochemical properties on removal mechanisms. *Journal of Water and Health,* 18**,** 253-291.

IQBAL, M., ZAFAR, H., MAHMOOD, A., NIAZI, M. B. K. & ASLAM, M. W. 2020. Starch-capped silver nanoparticles impregnated into propylamine-substituted PVA films with improved antibacterial and mechanical properties for wound-bandage applications. *Polymers,* 12**,** 2112.

JAN-ROBLERO, J. & CRUZ-MAYA, J. A. 2023. Ibuprofen: Toxicology and Biodegradation of an Emerging Contaminant. *Molecules,* 28**,** 2097.

JOSHI, N., JAIN, N., PATHAK, A., SINGH, J., PRASAD, R. & UPADHYAYA, C. P. 2018. Biosynthesis of silver nanoparticles using Carissa carandas berries and its potential antibacterial activities. *Journal of Sol-Gel Science and Technology,* 86**,** 682-689.

JOUDEH, N. & LINKE, D. 2022. Nanoparticle classification, physicochemical properties, characterization, and applications: a comprehensive review for biologists. *Journal of Nanobiotechnology,* 20**,** 262.

KALAM, S., ABU-KHAMSIN, S. A., KAMAL, M. S. & PATIL, S. 2021. Surfactant adsorption isotherms: A review. *ACS omega,* 6**,** 32342-32348.

KHAN, S. A., JAIN, M., PANDEY, A., PANT, K. K., ZIORA, Z. M., BLASKOVICH, M. A., SHETTI, N. P. & AMINABHAVI, T. M. 2022. Leveraging the potential of silver nanoparticles-based materials towards sustainable water treatment. *Journal of Environmental Management,* 319**,** 115675.

KHASAWNEH, O. F. S. & PALANIANDY, P. 2021. Occurrence and removal of pharmaceuticals in wastewater treatment plants. *Process Safety and Environmental Protection,* 150**,** 532-556.

KHDARY, N. H., ALMUARQAB, B. T. & EL ENANY, G. 2023. Nanoparticle-Embedded Polymers and Their Applications: A Review. *Membranes,* 13**,** 537.

KHOO, P. S., ILYAS, R., UDA, M., HASSAN, S. A., NORDIN, A., NORFARHANA, A., AB HAMID, N., RANI, M., ABRAL, H. & NORRRAHIM, M. 2023. Starch-Based

Polymer Materials as Advanced Adsorbents for Sustainable Water Treatment: Current Status, Challenges, and Future Perspectives. *Polymers,* 15**,** 3114.

KORDE, B. A., MANKAR, J. S., PHULE, S. & KRUPADAM, R. J. 2019. Nanoporous imprinted polymers (nanoMIPs) for controlled release of cancer drug. *Materials science and engineering: C,* 99**,** 222-230.

LIMA, E. C., HOSSEINI-BANDEGHARAEI, A., MORENO-PIRAJÁN, J. C. & ANASTOPOULOS, I. 2019. A critical review of the estimation of the thermodynamic parameters on adsorption equilibria. Wrong use of equilibrium constant in the Van't Hoof equation for calculation of thermodynamic parameters of adsorption. *Journal of molecular liquids,* 273**,** 425-434.

LIU, P., LIU, R., GUAN, G., JIANG, C., WANG, S. & ZHANG, Z. 2011. Surface-enhanced Raman scattering sensor for theophylline determination by molecular imprinting on silver nanoparticles. *Analyst,* 136**,** 4152-4158.

LIU, W., ZHANG, Y., WANG, S., BAI, L., DENG, Y. & TAO, J. 2021. Effect of pore size distribution and amination on adsorption capacities of polymeric adsorbents. *Molecules,* 26**,** 5267.

MADANI, M., HOSNY, S., ALSHANGITI, D. M., NADY, N., ALKHURSANI, S. A., ALKHALDI, H., AL-GAHTANY, S. A., GHOBASHY, M. M. & GABER, G. A. 2022. Green synthesis of nanoparticles for varied applications: Green renewable resources and energy-efficient synthetic routes. *Nanotechnology Reviews,* 11**,** 731-759.

MADIKIZELA, L. M. & CHIMUKA, L. 2016. Determination of ibuprofen, naproxen and diclofenac in aqueous samples using a multi-template molecularly imprinted polymer as selective adsorbent for solid-phase extraction. *Journal of pharmaceutical and biomedical analysis,* 128**,** 210-215.

MANKAR, J. S., SHARMA, M. D. & KRUPADAM, R. J. 2020. Molecularly imprinted nanoparticles (nanoMIPs): an efficient new adsorbent for removal of arsenic from water. *Journal of Materials Science,* 55**,** 6810-6825.

MARZAMAN, A. N. F., ROSKA, T. P., SARTINI, S., UTAMI, R. N., SULISTIAWATI, S., ENGGI, C. K., MANGGAU, M. A., RAHMAN, L., SHASTRI, V. P. & PERMANA, A. D. 2023. Recent Advances in Pharmaceutical Approaches of Antimicrobial Agents for Selective Delivery in Various Administration Routes. *Antibiotics,* 12**,** 822.

MO, F., ZHOU, Q. & HE, Y. 2022. Nano–Ag: Environmental applications and perspectives. *Science of The Total Environment,* 829**,** 154644.

MONGA, Y., KUMAR, P., SHARMA, R. K., FILIP, J., VARMA, R. S., ZBOŘIL, R. & GAWANDE, M. B. 2020. Sustainable synthesis of nanoscale zerovalent iron particles for environmental remediation. *ChemSusChem,* 13**,** 3288-3305.

MORIN-CRINI, N., LICHTFOUSE, E., FOURMENTIN, M., RIBEIRO, A. R. L., NOUTSOPOULOS, C., MAPELLI, F., FENYVESI, É., VIEIRA, M. G. A., PICOS-CORRALES, L. A. & MORENO-PIRAJÁN, J. C. 2022. Removal of emerging contaminants from wastewater using advanced treatments. A review. *Environmental Chemistry Letters,* 20**,** 1333-1375.

NIE, P., ZHAO, Y. & XU, H. 2023. Synthesis, applications, toxicity and toxicity mechanisms of silver nanoparticles: A review. *Ecotoxicology and Environmental Safety,* 253**,** 114636.

NIELSEN, L. & BANDOSZ, T. J. 2016. Analysis of the competitive adsorption of pharmaceuticals on waste derived materials. *Chemical Engineering Journal,* 287**,** 139-147.

NORDIN, A. H., NORFARHANA, A. S., NOOR, S. F. M., PAIMAN, S. H., NORDIN, M. L., HUSNA, S. M. N., ILYAS, R. A., NGADI, N., BAKAR, A. A. & AHMAD, Z. 2023. Recent Advances in Using Adsorbent Derived from Agricultural Waste for Antibiotics

and Non-Steroidal Anti-Inflammatory Wastewater Treatment: A Review. *Separations,* 10**,** 300.

NXUMALO, N. L. & MAHLAMBI, P. N. 2023. Molecularly Imprinted Polymer-Based Adsorbents for the Selective Removal of Pharmaceuticals from Wastewater: Adsorption Kinetics, Isotherms, and Thermodynamics Studies. *Industrial & Engineering Chemistry Research*.

NYIRENDA, J., KALABA, G. & MUNYATI, O. 2022. Synthesis and characterization of an activated carbon-supported silver-silica nanocomposite for adsorption of heavy metal ions from water. *Results in Engineering,* 15**,** 100553.

OKAIYETO, K., HOPPE, H. & OKOH, A. I. 2021. Plant-based synthesis of silver nanoparticles using aqueous leaf extract of Salvia officinalis: characterization and its antiplasmodial activity. *Journal of Cluster Science,* 32**,** 101-109.

OKPARA, O. G., OGBEIDE, O. M., IKE, O. C., MENECHUKWU, K. C. & EJIKE, E. C. 2021. Optimum isotherm by linear and nonlinear regression methods for lead (II) ions adsorption from aqueous solutions using synthesized coconut shell–activated carbon (SCSAC). *Toxin Reviews,* 40**,** 901-914.

PARASHAR, A., SIKARWAR, S. & JAIN, R. 2022. Removal of pharmaceuticals from wastewater using magnetic iron oxide nanoparticles (IOPs). *International Journal of Environmental Analytical Chemistry,* 102**,** 117-133.

PATTNAIK, C., MISHRA, R., SAHU, A. K., SAHOO, L. N., SAHOO, N. K., TRIPATHY, S. K. & SAHOO, S. 2023. Green synthesis of glucose-capped stable silver nanoparticles: a cost-effective sensor for the selective detection of Hg 2+ ions in aqueous solutions. *Sensors & Diagnostics,* 2**,** 647-656.

PEREIRA, A., SILVA, L., LARANJEIRO, C., LINO, C. & PENA, A. 2020. Selected pharmaceuticals in different aquatic compartments: Part I—Source, fate and occurrence. *Molecules,* 25**,** 1026.

PONSANTI, K., TANGNORAWICH, B., NGERNYUANG, N. & PECHYEN, C. 2020. A flower shape-green synthesis and characterization of silver nanoparticles (AgNPs) with different starch as a reducing agent. *Journal of materials Research and Technology,* 9**,** 11003-11012.

PU, H. & XU, L. 2022. Molecularly imprinted nanoparticles synthesized by electrochemically mediated atom transfer radical precipitation polymerization. *Macromolecular Chemistry and Physics,* 223**,** 2100478.

RADZIKOWSKA-BÜCHNER, E., FLIEGER, W., PASIECZNA-PATKOWSKA, S., FRANUS, W., PANEK, R., KORONA-GŁOWNIAK, I., SUŚNIAK, K., RAJTAR, B., ŚWIĄTEK, Ł. & ŻUK, N. 2023. Antimicrobial and Apoptotic Efficacy of Plant-Mediated Silver Nanoparticles. *Molecules,* 28**,** 5519.

REFAAT, D., AGGOUR, M. G., FARGHALI, A. A., MAHAJAN, R., WIKLANDER, J. G., NICHOLLS, I. A. & PILETSKY, S. A. 2019. Strategies for molecular imprinting and the evolution of MIP nanoparticles as plastic antibodies—Synthesis and applications. *International journal of molecular sciences,* 20**,** 6304.

ROSLI, F. A., AHMAD, H., JUMBRI, K., ABDULLAH, A. H., KAMARUZAMAN, S. & FATHIHAH ABDULLAH, N. A. 2021. Efficient removal of pharmaceuticals from water using graphene nanoplatelets as adsorbent. *Royal Society open science,* 8**,** 201076.

S'BUSISO, M. N., MAHLAMBI, P. N. & CHIMUKA, L. 2022. Synthesis, characterisation and optimisation of bulk molecularly imprinted polymers from nonsteroidal anti-inflammatory drugs. *South African Journal of Chemistry,* 76**,** 56–64-56–64.

SADIA, M., AHMAD, I., UL-SALEHEEN, Z., ZUBAIR, M., ZAHOOR, M., ULLAH, R., BARI, A. & ZEKKER, I. 2023. Synthesis and Characterization of MIPs for Selective

Removal of Textile Dye Acid Black-234 from Wastewater Sample. *Molecules,* 28**,** 1555.

SAJINI, T. & MATHEW, B. 2021. A brief overview of molecularly imprinted polymers: Highlighting computational design, nano and photo-responsive imprinting. *Talanta Open,* 4**,** 100072.

SHIKUKU, V. O. & JEMUTAI-KIMOSOP, S. 2020. Efficient removal of sulfamethoxazole onto sugarcane bagasse-derived biochar: Two and three-parameter isotherms, kinetics and thermodynamics. *South African Journal of Chemistry,* 73**,** 111–119-111–119.

SHOW, S., KARMAKAR, B. & HALDER, G. 2020. Sorptive uptake of anti-inflammatory drug ibuprofen by waste biomass–derived biochar: experimental and statistical analysis. *Biomass Conversion and Biorefinery***,** 1-19.

SULLIVAN, M. V., STOCKBURN, W. J., HAWES, P. C., MERCER, T. & REDDY, S. M. 2020. Green synthesis as a simple and rapid route to protein modified magnetic nanoparticles for use in the development of a fluorometric molecularly imprinted polymer-based assay for detection of myoglobin. *Nanotechnology,* 32**,** 095502.

SZCZYGLEWSKA, P., FELICZAK-GUZIK, A. & NOWAK, I. 2023. Nanotechnology–General Aspects: A Chemical Reduction Approach to the Synthesis of Nanoparticles. *Molecules,* 28**,** 4932.

TRINH, V., NGUYEN, T., VAN, H., HOANG, L., NGUYEN, T., HA, L., VU, X., PHAM, T., NGUYEN, T. & QUANG, N. 2020. Phosphate adsorption by silver nanoparticles-loaded activated carbon derived from tea residue. Sci Rep 10: 1–13.

WALENG, N. J. & NOMNGONGO, P. N. 2022. Occurrence of pharmaceuticals in the environmental waters: African and Asian perspectives. *Environmental Chemistry and Ecotoxicology,* 4**,** 50-66.

WAN MAT KHALIR, W. K. A., SHAMELI, K., JAZAYERI, S. D., OTHMAN, N. A., CHE JUSOH, N. W. & HASSAN, N. M. 2020. Biosynthesized silver nanoparticles by aqueous stem extract of Entada spiralis and screening of their biomedical activity. *Frontiers in chemistry,* 8**,** 620.

WEI, Z.-H., ZHANG, R.-R., MU, L.-N., HUANG, Y.-P. & LIU, Z.-S. 2019. Fabrication of core-shell sol-gel hybrid molecularly imprinted polymer based on metal–organic framework. *European Polymer Journal,* 121**,** 109301.

YING, S., GUAN, Z., OFOEGBU, P. C., CLUBB, P., RICO, C., HE, F. & HONG, J. 2022. Green synthesis of nanoparticles: Current developments and limitations. *Environmental Technology & Innovation,* 26**,** 102336.

YU, M., LI, H., XIE, J., XU, Y. & LU, X. 2022. A descriptive and comparative analysis on the adsorption of PPCPs by molecularly imprinted polymers. *Talanta,* 236**,** 122875.

YUCEL, N., GULEN, H. & CAKIR HATIR, P. 2022. Molecularly imprinted polymer nanoparticles for the recognition of ellagic acid. *Journal of Applied Polymer Science,* 139**,** e52952.

Chapter 5

Efficacy assessment of molecularly imprinted polymer incorporated with platanus acerifolia and moringa oleifera capped silver nanoparticles for the removal of multi-class pharmaceuticals in wastewater

Abstract

Pharmaceuticals are one of the most prevalent contaminants discovered in water systems. The ineffectiveness of traditional wastewater treatment procedures to completely remove them results in their release into the rivers with the effluent water. Thus, there is a pressing need to remove pharmaceuticals effectively using different methods. Utilizing affordable technologies while maintaining standards for health and safety is one of the main problems in the wastewater treatment industry. In this study, a cost effective and highly selective molecularly imprinted polymer (MIP) was combined with silver nanoparticles (AgNPs) capped with platanus acerifolia (PL) and moringa oleifera (MO) for selective removal of sulfamethoxazole, nevirapine and ibuprofen in wastewater. Moreover, the study focused on adsorption parameters, including temperature, pH, adsorbent dosage, adsorbate concentration, and contact time. The transmission electron microscopy results revealed that the MO/PL-AgNPs and MO/PL-nanoMIPs are nanosized and spherical in shape. The XRD confirmed a face centered cubic crystalline of silver nanoparticles onto the MO/PL-AgNPs and MO/PL-nanoMIPs. The adsorption experimental data for both nano-adsorbents (MO/PL-AgNPs and MO/PL-nanoMIPs) fitted with the linear Langmuir model which indicates that the binding occurred on the homogeneous surface. Furthermore, the MO/PL-nanoMIPs adsorption capacities for the target pharmaceuticals were higher compared to MO/PL-AgNPs indicating that the nanoMIPs have larger surface areas which further enhances the adsorption capacity. The linear pseudo-second order kinetic model best fitted on MO/PL-nanoMIPs which implied adsorption through chemisorption, while the thermodynamic results revealed that the adsorption process was spontaneous and endothermic. The MO/PL-nanoMIPs confirmed the high efficiency for the removal of target pharmaceuticals in wastewater. The method was successfully applied to remove the presence of these pharmaceuticals in wastewater samples. The removal efficiency of >61% in influent water samples and >45% in effluent water samples were observed. The lower removal efficiency may be attributed to the presence of other material present in both water samples, thus further studies reporting on the impact of physicochemical parameters in water are recommended.

5.1 Introduction

Water pollution from pharmaceuticals is a constant concern to both human health and the environment (Samal et al., 2022). The development of analytical techniques has made it possible to find pharmaceuticals in several environmental matrices, including drinking water, sediments, waste effluents, surface water, and subsurface water (Sahani et al., 2022). The prevalence of pharmaceuticals in aquatic ecosystems demonstrates the ineffectiveness of traditional wastewater treatment procedures, necessitating the urgent need for pharmaceuticals to be removed as effectively as possible via alternative techniques (Birniwa et al., 2023). Utilizing affordable technologies while maintaining standards for health and safety is one of the main problems in the wastewater treatment industry. Particularly, MIPs offers excellent mechanical and chemical stability, low cost, long shelf life, strong anti-interference ability, and high selectivity in the removal of pharmaceuticals from wastewater. They adsorb quickly and with great selectivity on target analytes (Gkika et al., 2024). Accordingly, MIP is a polymer that is surrounded by target analytes, and the resulting polymer matrix is printed with precise cavities that have a three-dimensional structure that complements the analytes' size, shape, and binding sides. Nonetheless, the majority of MIP examples documented in the literature are predicated on the synthesis of bulk polymers (such as monoliths), which are typically associated with poor surface area and, hence, low binding capacity (Kuhn et al., 2020). A novel approach to this problem is the use of MIP nanoparticles, or nanoMIPs, which provide increased surface area, fast binding kinetics, stability, exceptional selectivity, and sensitivity (Zhang et al., 2023). Notably, molecular imprinting-based nanoparticles are nanoparticles combined with molecular imprinting technology to produce custom binding sites for the identification of certain environmental contaminants. The inventive combination of the underlying components in nanoparticles results in a unique design platform with great synthetic versatility, enhancing the overall adsorption performances, such as high adsorption capacity, short equilibrium time, good selectivity, and convenient usability. Therefore, the potential of nanoMIP adsorbents to remove environmental contaminants is of significant scientific and technological interest due to their small size effect, combination flexibility/versatility, specificity and improved performance (Wang et al., 2023). Further, silver nanoparticles (AgNPs) are versatile, simple-to-prepare, low-cost materials and have a large surface area and high surface energy, which promotes surface reactivity and adsorption in the adsorptive site (Azeez et al., 2020). Chemically synthesized nanoparticles use chemicals as a reducing and capping agents, converting Ag ions to AgNPs. However, these methods are not very biocompatible, and they have harmful effects (Ratan et al., 2020). Accordingly, growing

interest has been shown recently in the use of green chemistry to synthesize AgNPs in order to minimize the use and production of harmful compounds. An alternative that has recently surfaced is the synthesis of nanoparticles using plants biomass due to their abundant availability and phytochemical profile as reducing and stabilizing agents (Soni et al., 2021). AgNPs mediated by plants biomass are non-hazardous, economical, environmentally benign, and easily synthesised. They act as natural agents for capping, stabilizing, and reducing (Jain et al., 2021). Notably, some plants are used as capping and reducing agents at the same time to reduce energy consumption (Ying et al., 2022). Plants utilized in the synthesis process are abundant in polyphenols and bioactive chemicals that support the stabilization and reduction process and have a significant impact on the characteristics of the final nanoparticles (Wahab et al., 2021). Platanus acerifolia and moringa oleifera leaf extract are abundantly rich in polyphenols and in diverse groups of phytochemicals which can be used in the synthesis of nanoparticles (Shende et al., 2018, Shalaby et al., 2022). In contrast, both moringa oleifera and platanus acerifolia are inexpensive, widely/readily available materials that can be used in the synthesis of silver nanoparticles and can enhance the adsorption capabilities for the removal of ibuprofen, nevirapine, and sulfamethoxazole. The substantial global consumption of sulfamethoxazole, nevirapine, and ibuprofen, along with their known physicochemical and toxicological features, have sparked significant scientific interest in these pharmaceutical compounds. These pharmaceuticals become a concern to human health when they are present in aquatic environments because of their toxicity and ability to cause bacterial resistance, yet their consumption rate is increasing (Waleng and Nomngongo, 2022, Ngqwala and Muchesa, 2020). Hence, the main objective of this study was to prepare a silver nanoparticles molecularly imprinted polymer for selective and sustainable removal of sulfamethoxazole, nevirapine and ibuprofen in wastewater. In this study, the nanoMIPs were then synthesized by imprinting the MIP with PL and MO silver nanoparticles. Following synthesis, the materials were characterized chemically and physically to examine their morphology, structure, and other characteristics. To assess the removal capability towards the target pharmaceuticals, studies were conducted on the adsorption kinetics, isotherms, thermodynamics, regeneration performance, and selective adsorption ability of nanoMIP materials.

5.2 Materials and methods

5.2.1 Chemicals

All chemicals, solvents and media used in this study were of analytical grade and purchased from Sigma Aldrich, (Johannesburg, South Africa). Analytical grade sodium hydroxide

(NaOH) (99.9%), silver nitrate ($AgNO_3$) (99.8%), and soluble starch (99.9%). were supplied by Merck (Pty) Ltd (Johannesburg, South Africa). The Platanus acerifolia leaves were collected from the University of KwaZulu-Natal in Pietermaritzburg campus (South Africa). Moringa oleifera leaves powder was supplied by the Department of Agriculture and Rural Development located in Hilton, KwaZulu Natal.

5.2.2 Sample Preparation

100 mg/L stock solution of targeted pharmaceuticals was prepared by dissolving 10 mg of each template (sulfamethoxazole, Ibuprofen and nevirapine) in 100 mL of acetonitrile. From the stock solution a concentration range of standards ranging from 0.1-2 mg/L were prepared by appropriate dilutions of the stock solution. These standard solutions were analysed with the LC-MS system and used for the construction of the calibration curve. The Platanus acerifolia leaves were washed with tap water and left to dry overnight at room temperature. The MRC SMM450 sample mill was used to grind the Platanus acerifolia which were then sieved into 250 µm a using King test VB 200/300 sieve shaker from DLD Scientific (Durban, South Africa). The fine powder was soaked in ultrapure water and agitated for 3 hours with continuous stirring, thereafter, left to dry in the oven overnight at a temperature 105 ˚C.

5.2.3 Instrumentation and chromatographic conditions

The analytical method reported by Hlengwa and Mahlambi was used in the analysis of the selected pollutant in this study (Hlengwa and Mahlambi, 2020). Briefly, a Shimadzu LC 2020 series (Tokyo, Japan) coupled with a UV/Vis detector set at 210 nm was used to analyse the pharmaceuticals. The compounds were separated on a Shim-Pack GIST C18-HP (150 × 4.6 mm i.d., 3,5 µm particle size) column (Tokyo, Japan) with a column temperature of 40 ˚C. The mobile phase comprised of 0.1% formic acid in water: ACN (10:90) at a constant flow of 0.4 mL/min. The injection volume of 10 µL was used for the analysis.

5.2.4 Environmental sample collection

The wastewater samples were obtained from three treatment plants in the South African province of KwaZulu-Natal. The Northern and Amanzimtoti wastewater treatment plants (WWTPs) are situated in Durban, while the Darvill WWTP is situated in Pietermaritzburg. These WWTPs receive sewerage from both domestic and industrial wastes. Effluent samples were collected in 2.5 L dark brown bottles and stored in a ice box. The samples were then

transported to the laboratory where they were stored in the refrigerator (4°C) for further analysis.

5.2.5 Synthesis of moringa oleifera and platanus acerifolia AgNPs

Platanus acerifolia and Moringa oleifera leaves powder was dissolved in an alkali solution (1 g of each was added), along with 0.25 g of NaOH platelets, in 100 mL of ultrapure water in an Erlenmeyer flask. This was done to increase the oxidation of Platanus acerifolia and Moringa oleifera, which in turn accelerated the nucleation and reduction rates by promoting AgNPs formation. After that, the mixture was agitated for 10 minutes at 80 °C using a magnetic stirrer while adding dropwise 20 mL of 0.1 M $AgNO_3$ solution. The mixtures were then held under continuous stirring for 1 hour. The Moringa oleifera reaction medium acquired a yellow colour then changed to dark brown colour showing the formation of silver nanoparticles (MO-AgNPs). Whereas the Platanus acerifolia medium change from brown to black, showing the formation of silver nanoparticles (PL-AgNPs). The colloidal solutions were allowed to gradually cool to 25 °C in 30 minutes following the completion of their reactions. After the reaction, the MO/PL-AgNPs were collected by centrifugation at 4500 rpm for 15 minutes to remove the larger-sized particles and then washed twice with acetone and water to remove the unreacted materials and impurities. Following collection, the MO/PL-AgNPs were oven-dried for 15 minutes at 80 °C (Okaiyeto et al., 2021).

5.2.6 Synthesis of MIP nanoparticles

The synthesis of multi-template molecularly imprinted polymer (MIP) as selective adsorbent for the removal of nevirapine, ibuprofen and sulfamethoxazole from wastewater was adopted with minor adjustments from a method used by Madikizela and co-workers (Madikizela and Chimuka, 2016). The MIP bulk polymerization was performed in two steps. The synthesis began with the dissolution of 20 mg of 1,1′-azobis-(cyclohexane carbonitrile) in 50 mL of toluene, to which 1.51 mL of ethylene glycol dimethacrylate (EGDMA) was added. Following that the reaction flask was then purged with nitrogen for 10 minutes and sealed. After that, the reaction was allowed to occur for 16 hours at 60 °C while being constantly stirred in an oil bath. The second step involved dissolving 25 mg of each pharmaceutical (ibuprofen, nevirapine, and sulfamethoxazole) in 25 mL of acetonitrile. Then, 25 mL of toluene, 60 mg of 1,1′-azobis-(cyclohexane carbonitrile), 100 mg of the synthesized MO/PA-AgNPs, 1 mL of 2-vinylpyridine, and 3.85 mL of ethylene glycol dimethacrylate (EGDMA) were added. The

final mixture was then put into the first reaction flask, sealed, and nitrogen-purged for 15 minutes to remove any remaining oxygen. After that, the reaction continued for 24 hours at 80 °C in an oil bath. The resultant polymer was oven dried at 100 °C. After that, the polymer was milled, sieved and particles with sizes between 25 to 50 μm were collected. The Soxhlet extraction method was used to elute the templates from the resultant polymer by repeatedly washing it with a 9:1 v/v mixture of acetonitrile and acetic acid until the templates were not detected on the LC-MS. After that, 100% acetonitrile was used to wash the polymer in order to remove the acetic acid.

5.3 Characterisation

All-optical studies were conducted at room temperature using a Perkin Elmer Lambda 25 UV-Vis spectrophotometer in the 200-800 nm wavelength range. TEM (JEOL JEM1230, Tokyo, Japan) was used to assess the MO/PL-AgNPs and MO/PL-nanoMIPs formulation's morphology and particle size. The morphological and particles size of the AgNPs and nanoMIPs formulation were evaluated using TEM (JEOL JEM1230, Tokyo, Japan The surface morphology of the synthesized MO/PL-AgNPs and MO/PL-nanoMIPs was evaluated using a Zeiss Ultra Plus Field Emission Gun Scanning Electron Microscopy (FEG-SEM) instrument (Tokyo, Japan). Thermogravimetric (TGA) analysis was performed with an Anton Paar analyzer (Mettler Toledo, Columbus, USA) to assess the thermal stability of the synthesized MO/PL-AgNPs and MO/PL-nanoMIPs. The Rigaku MiniFlex 600 (Rigaku Tokyo, Japan) provided the X-ray diffraction (XRD) patterns for the synthesized MO/PL-AgNPs and MO/PL-nanoMIPs. A Raman spectrometer in Via Renishaw (Renishaw, England) was used to record Raman spectra. To assess the functional groups present in the MO/PL-AgNPs and MO/PL-nanoMIPs, the Perkin Elmer spectrum Fourier transform infrared Spectrometer (400 FTIR) equipped with a universal ATR sampling accessory was used.

5.4 Adsorption experiments

A series of adsorption experiments were conducted by preparing solutions of pharmaceutical compounds (i.e., sulfamethoxazole, nevirapine and ibuprofen) in water at different initial concentrations ranging from 0.2 to 1.5 mg/L. To observe pH effect, the adsorption experiments were carried out at the pH range of 2-10, adjusted by adding aliquots of 0.01 M NaOH or HCl. The agitation time was set between 10-60 minutes, the mass dosage of MO/PL-nanoMIPs

ranging from 10-50 mg, and temperature ranging from 25-70 °C. One parameter at a time was changed while the other remained fixed in order to optimize the settings. The percentage removal and adsorption capacity of MO/PL-nanoMIPs, respectively, were determined using the following equations:

$$Removal\ (\%) = \frac{(C_0 - C_e)}{C_0} X\ 100 \qquad 5.1$$

$$q_e = \frac{(C_0 - C_e)V}{W} \qquad 5.2$$

C_o and C_e are the initial and residual concentrations of pharmaceuticals in solution, expressed in mg/L, respectively. V (L) is the volume of the pharmaceutical solution used, and W (mg) is the weight of MO/PL-nanoMIPs used.

5.5 Statistical analysis

The adsorption experiments were statistically analysed using the F-test and ANOVA to determine the efficacy of the MO/PL-nanoMIPs material in the removal of sulfamethoxazole, nevirapine, and ibuprofen Examining each parameter's sum of square value facilitates the process's understanding of how each process variable influences the desired response. Equation 5.3 is used to show the percentage contribution of each variable to the outcome. (Show et al., 2020).

$$\%\ Contribution = \frac{SS_p}{SS_m} X\ 100 \qquad 5.3$$

The sum of squares for the model in this instance is denoted by SS_m, and the sum of squares for a selected parameter is denoted by SS_p.

5.6 Adsorption kinetics

Adsorption is a time-dependent process, so it's important to assess the adsorption process' rate-limiting step in order to remove pharmaceuticals from various wastewaters. The kinetic models of linear pseudo first order, linear pseudo second order, non-linear pseudo first order, and non-linear pseudo second order were determined through the use of the adsorption capacities measured at different contact times. The linear pseudo-first order model is defined by the following equation (Paranjape and Sadgir, 2023):

$$ln(q_e - q_t) = lnq_e - k_1 t \qquad 5.4$$

An x-axis representing time t (min) and a y-axis representing ln (qe - qt) was used to construct a line graph and determine a constant value for pseudo first order adsorption (k_1) and qe calculation (qe_{cal}). This was followed by the plotting of a line graph with time t (min) as the x axis and t/q_t as the y axis using the linear pseudo second order model in equation 5.5 below.

$$\frac{1}{q_t} = \frac{1}{k_2 q_e{}^2} + \frac{t}{q_t} \qquad 5.5$$

The equation of non-linear pseudo first order and non-linear pseudo second order, in equation 5.6 and 5.7 were used to plot a graph using time t (minutes) as the x axis and q_t as the y axis.

$$q_t = q_e(1 + e^{K_1 t}) \qquad 5.6$$

$$q_t = \frac{qe^2 k_2 t}{1 + k_2 q_e t} \qquad 5.7$$

The amounts of pharmaceuticals adsorbed per unit mass of the adsorbent at equilibrium and time t are denoted by qe and qt (mg/g), respectively, and the adsorption rate constants for the pseudo first and pseudo second order kinetic models are k_1 and k_2 (min^{-1}), respectively.

5.7 Adsorption equilibrium

The results from the adsorption at varied concentrations were used to determine the linear Langmuir and Freundlich isotherms and non-linear Langmuir and Freundlich isotherms. The Langmuir isotherm model is predicated on the idea that homogeneous surfaces with monolayers have uniform active sites. Equation 5.8 and 5.9 is an expression for the non-linear and linear Langmuir equation (Paranjape and Sadgir, 2023).

$$\frac{1}{q_e} = \frac{1}{K_L C_e} + \frac{R_L}{K_L} \qquad 5.8$$

$$q_e = \frac{Q_{max} K_L C_e}{1 + K_L C_e} \qquad 5.9$$

where the equilibrium adsorption capacity of the adsorbent (mg/g) is expressed as q_e, the maximum monolayer adsorption capacity is represented by Q_{max} (mg/g), C_e (mg/L) is the concentration at equilibrium concentration and the Langmuir adsorption constant is represented by K_L (L/mg). The equilibrium parameter, also known as the separation factor, or RL presented in equation 5.10, is a crucial component of the Langmuir model that establishes the favourable or unfavourable conditions for surfactant adsorption.

$$R_L = \frac{1}{1+ K_L C_O} \quad 5.10$$

The application of the linear and non-linear Freundlich isotherm, which can be expressed by equations 5.11 and 5.12, is used for multi-layer adsorption on heterogeneous surfaces (Gabr et al., 2023).

$$lnq_e = lnK_F + \frac{1}{n} lnC_e \quad 5.11$$

$$q_e = K_F {C_e}^{1/n} \quad 5.12$$

where C_e and q_e denote for the equilibrium template concentration and amount adsorbed, respectively. The constants of the Freundlich isotherm model are the adsorption intensity (1/n) and the adsorption capacity (K_F). Furthermore, the capacity and favourability of the adsorbent/adsorbate system are indicated by the exponent (1/n).

5.8 Error analysis

The linear and non-linear adsorption kinetics were assessed using the root mean square error (RMSE). The RMSE equation has the following expression:

$$RMSE = \sqrt{\frac{1}{n-1}\sum_{i=1}^{n}\left(q_{exp} - q_{calc}\right)^2} \quad 5.13$$

where q_{calc} is the adsorption capacity derived from the kinetic equation model, n is the number of observations, and q_{exp} is the adsorption capacity derived from the experiment (Ahmadi et al., 2019).

5.9 Thermodynamics

The nature of the adsorption process and its viability were investigated through thermodynamic studies for pharmaceuticals uptake by AgNPs and nanoMIPs at seven different temperatures. Parameters like the enthalpy change (ΔH°), entropy change (ΔS°), and Gibbs free energy change (ΔG°) were utilized to assess the spontaneity of the adsorption process and provide an insight into potential removal mechanisms (Alnajrani and Alsager, 2020).

$$\Delta G° = -RT\ lnq_e/c_e \quad 5.14$$

$$lnq_e/c_e = \frac{\Delta S°}{R} - \frac{\Delta H°}{RT} \quad 5.15$$

The variables in this equation are the free energy change (ΔG°), the enthalpy change (ΔH°), the entropy change (ΔS°), T the absolute temperature (K), and R, the gas constant (8.314 J/mol K),

c_e represents the target pharmaceuticals concentration at equilibrium (mg/L) and q_e is the adsorption capacity at equilibrium (mg/g).

5.10 Selectivity of MO/PL-nanoMIPs

The selectivity of the nanoMIPs was tested using fenoprofen, which competes with the binding sites of MO/PL-nanoMIPs. The optimal conditions for preparing MO/PL-nanoMIPs selective adsorption performance were batch rebinding experiments with deionized water (pH 7.0). The water was spiked to produce a final concentration of 1 mg/L for both MO-nanoMIP and PL-nanoMIP with a mixture of sulfamethoxazole, nevirapine, ibuprofen, while and fenoprofen was used as a competitor. After adding 10 mL of the spiked solution to a flask with 30 mg of MO-nanoMIPs and 20 mg of PL-nanoMIPs, the mixture was shaken for ten minutes at room temperature. The distribution coefficients (K_d), and selectivity coefficients (k) of the targeted pharmaceuticals and the competitor were acquired according to the following equations (Espinoza-Torres et al., 2023):

$$K_d = \frac{C_o - C_e}{W} V \qquad 5.16$$

where the polymer weight is W (mg), the solution volume is V (mL), the initial and final solution concentrations are C_o and C_e, respectively, and the distribution coefficient is denoted by K_d (mg/g).

$$k = \frac{K_d Target\ pharmaceutical}{K_d Competitor} \qquad 5.17$$

Where k is the selectivity coefficient for the distribution coefficient of the targeted pharmaceuticals binding in the presence of a competitor.

5.11 Reusability of nanoMIPs

In order to evaluate the reusability of the synthesized materials 30 mg of MO-nanoMIP and 20 mg of PL-nanoMIP that had previously adsorbed sulfamethoxazole, nevirapine, and ibuprofen were washed for 10 minutes in a 9:1, v/v acetonitrile/acetic acid solution. The MO/PL-nanoMIPs were then regenerated using 10 mL of pure acetonitrile to desorb undesirable compounds. In the subsequent cycle, these MO/PL-nanoMIP adsorbents were then utilized yet again to adsorb sulfamethoxazole, nevirapine, and ibuprofen. Five repeated cycles of

adsorption–regeneration tests were performed to confirm MO/PL-nanoMIP stability and reusability (Mankar et al., 2020). The experimental conditions for the adsorption stage were maintained constant throughout each cycle.

5.12 Results and discussion

5.12.1 Characterisation

5.12.1.1 UV-Visible Spectroscopy

The peak observed in **Figure 5.1 (a)** and **(b)** at 436 nm and 407 nm represents surface plasmon resonance (SPR), which is caused by the excitation of free electrons in the silver metal (Khane et al., 2022). This showed that when exposed to the bioactive components of the plant extract, the silver ion was reduced to elemental silver and eventually to silver nanoparticles, changing the optical properties of the silver nitrate solution. Accordingly, the UV spectra for the MO and PL-nanoMIPs showed a shift and a decrease in wavelength (431 nm and 404 nm). This can be attributed to size reduction and increase in stability of the particles when the AgNPs are incorporated with MIP.

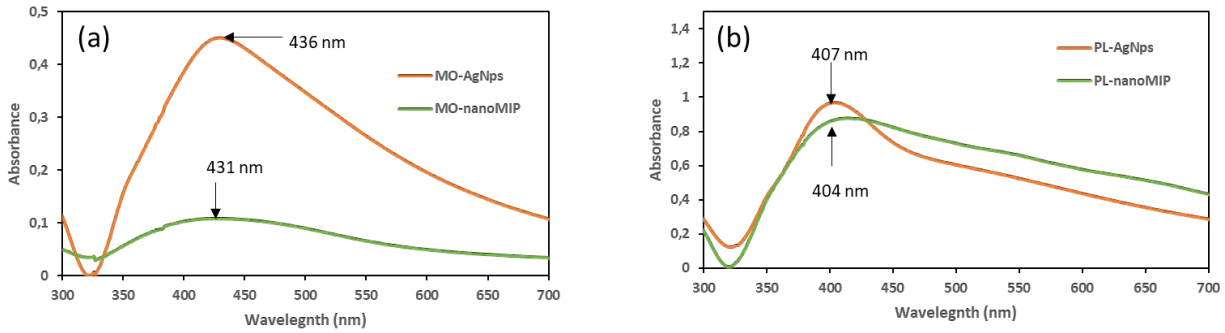

Figure 5.1: UV spectra of (a) MO-AgNPs and MO-nanoMIPs and (b) PL-AgNPs and PL-nanoMIPs

5.12.1.2 Scanning Electron Microscope (SEM)

The SEM images verified the formation of silver nanoparticles. The SEM image of MO-AgNPs in **Figure 5.2 (a)** shows that the nanoparticles are well dispersed having irregular shape with elongated, polyhedral and some spherical shapes of heterogeneous sizes. The PL-AgNPs shows a smooth and wrinkled surface with nanoparticles predominantly spherical and slightly aggregated into larger particles (**Figure 5.2 (b)**). The wrinkled surface of PL-AgNPs is said to be the consequence of interactions between functional groups that include oxygen

(Spilarewicz-Stanek et al., 2016). This aggregation may be due to the presence of secondary metabolites in the PL leaf extracts. Even within the aggregates, the nanoparticles were not in direct contact, indicating that the nanoparticles were stabilized by a capping agent. According to SEM images of MO-nanoMIP and PL-nanoMIP in **Figure 5.2 (c)** and **(d)**, their surfaces were uneven, and their morphology has many pores of varying sizes and shapes, which indicated that there were a lot of active sites available for the adsorption of pharmaceuticals. The presence of cavities in the nanoMIPs structure allowed pharmaceutical compounds to permeate the surface of the adsorbents, which was beneficial to the adsorption process. According to the comparison of the MO/PL-AgNPs and MO/PL-nanoMIPs sizes, the formation of a polymeric network on the MO/PL-nanoMIPs surface was suggested by the increasing particle size (Geravi and Ghaemy, 2024).

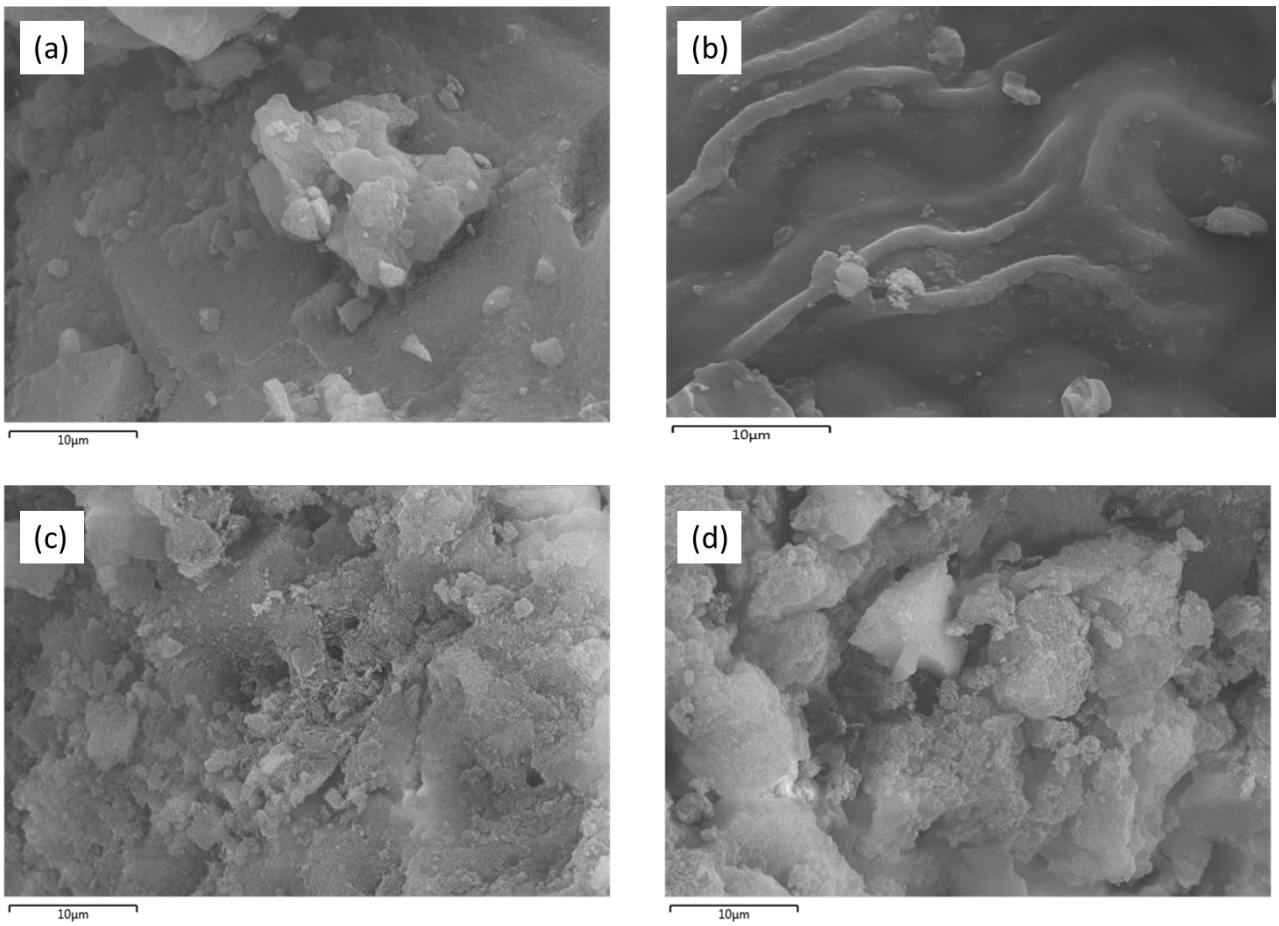

Figure 5.2: SEM images of (a) MO AgNPs, (b) PL-AgNPs, (c) MO-nanoMIP and (d) PL nanoMIP

5.12.1.3 Transmission electron microscopy (TEM)

A high-resolution TEM image (**Figure 5.3 (a) and (b)**) revealed that the MO-AgNPs and PL-AgNPs are uniform and have an irregular shape but are predominantly spherical. The particle size distribution histogram in **Figure 5.3 (e)** and **(f)** shows that the synthesized MO-AgNPs and PL-AgNPs have an average diameter of 22.79 nm and 17.40 nm, respectively. Interestingly, MO-AgNPs were entrapped within a matrix as seen on the TEM image (**Figure 5.3 (a)**). It was determined that this cloud-like structure is made of organic material derived from plant extract that engulfs the synthesized MO-AgNPs (**Figure 5.3 (a)**) and serves as a capping agent (Zulkifli et al., 2020, Nakhaeitazreji et al., 2023). Further, the TEM images shown in **Figure 5.3 (c)** and **(d)**, depicted the porous network nature of both MO and PL-nanoMIPs. Pharmaceuticals can attach to and diffuse toward the recognition sites more easily with such a porous structure's increased surface area (Kuhn et al., 2020). Notably, the silver nanoparticles had a nanosized structure where tiny particles with some spherical aggregate morphology bonded together and embedded in the polymer (MO and PL-nanoMIPs) surface to form nanosized clusters. These nanosized clusters has a mean average of 65.11 nm and 38.48 nm as observed on the MO and PL-nanoMIPs particle size distribution histogram in **Figure 5.3 (g)** and **(h)**. Notably, the agglomeration in some regions of the MO/PL-nanoMIPs was due to narrow distribution nanoparticles being monodispersed in their dispersion (Nasraoui et al., 2022).

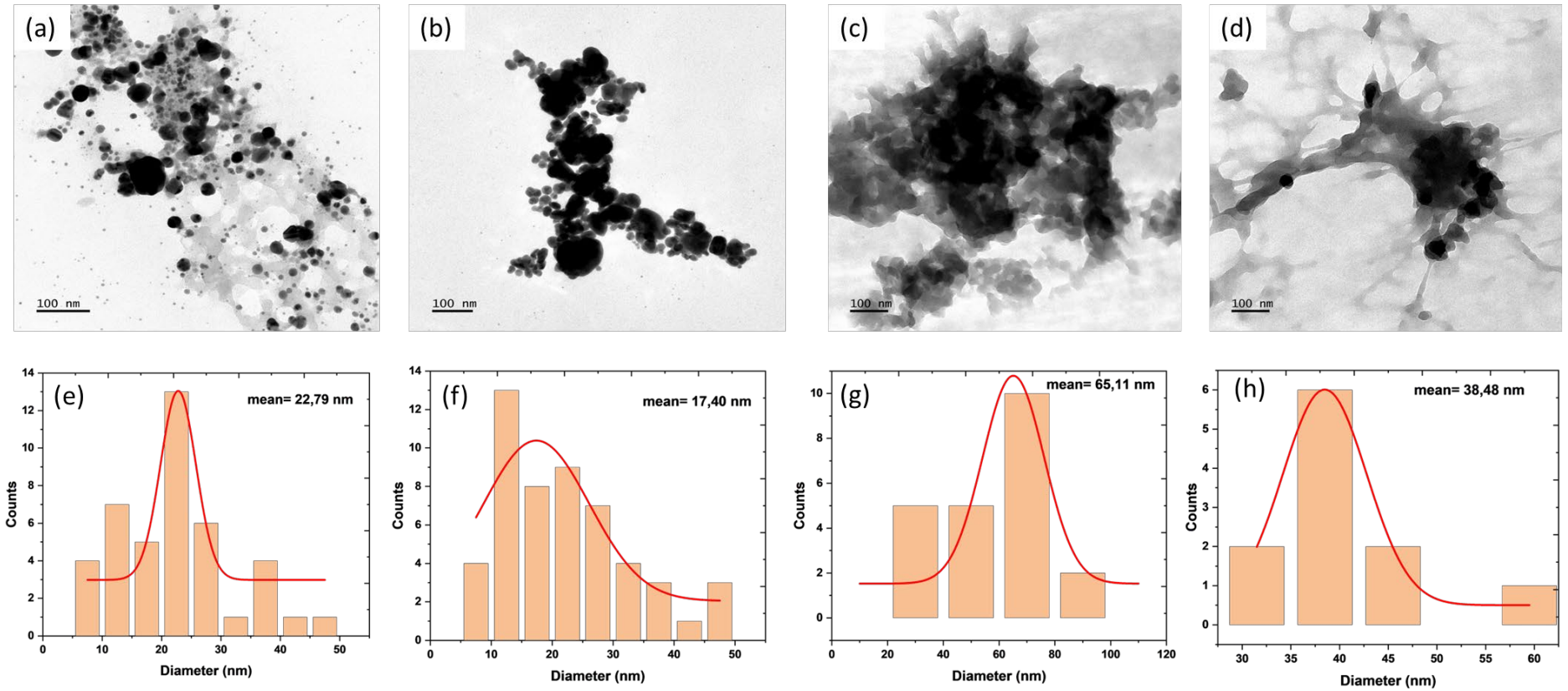

Figure 5.3: TEM images of (a) MO AgNPs, (b) PL-AgNPs, (c) MO-nanoMIP and (d) PL nanoMIPs

5.12.1.4 Fourier transform infrared spectroscopy (FTIR)

The results in **Figure 5.4 (a)** and **(b)** demonstrate the functional groups present in MO/PL-AgNPs and MO/PL-nanoMIPs. The strong and broad peak for MO-AgNPs at 3275 cm^{-1} and PL-AgNPs at 3250.31 cm^{-1} at corresponded to the stretching of OH functional (hydroxyl) groups. These peaks are known to be associated with stretching vibrations of hydroxyl groups in alcohols or phenolic compounds, CH_2 and CH_3 functional groups (Moodley et al., 2018). The peaks at 2906.34-2840.42 cm^{-1} and 2856.90-2840.42 cm^{-1} for MO-AgNPs and PL-AgNPs were due to the asymmetric and symmetric stretching of aliphatic (C-H sp3) groups, respectively (Bindhu et al., 2020). The presence of aromatic rings can be confirmed by the band at 1522.17 cm^{-1} and 1596.32 cm^{-1}, ascribed to C=C double bonds in ring structure for MO-AgNPs and PL-AgNPs (Thach et al., 2021). The peak at the wavenumber value 1293.54 cm^{-1} and 1217.32 cm^{-1} for MO and PL-AgNPs is associated with N-H bending. A broad band at 1101.04 cm^{-1} and 1021.65 cm^{-1} is generally found with oxidised carbons and has been assigned to C-O stretching in acids, alcohols, phenols, ethers and/or esters groups. In the area of 3606 cm^{-1} for the MIP, a broad band is formed which is a characteristic peak of the -OH group accompanied by the appearance of C-H band at 2920.77 cm^{-1}, C=O (carboxylic acid) in the frequency region 1693.38 cm^{-1} and C-N at 1084 cm^{-1} followed with C=C in the 1423.31 cm^{-1} region assumed to be derived from the functional groups of the hydroxyl functional group in alcohols and phenolic compounds, aromatic ring and amine in the 2-VP monomer and the esters and alkenes EGDMA crosslinker, respectively (Zhao et al., 2023, Thach et al., 2021). These peaks appearance confirms that the MIP contained these moieties and that they could interact with the molecules in the template. Notably, the nanoMIPs also contained these peaks with a slight shift in the wavenumbers which indicate the successful synthesis of the combination of AgNPs with MIPs. The presence of hydroxyl groups (OH) in the MO and PL-nanoMIPs, caused by the chemisorbed water, is indicated by the band around 3509.86 cm^{-1} and 3542.82 cm^{-1}, respectively. The peaks at 2947.54 cm^{-1} and 2945.48 cm^{-1} reflects the C-H stretching frequency either symmetric or asymmetric due to the presence of the aliphatic hydrocarbons chains and aromatic rings of alcohol/phenolic compounds in the MO and PL-nanoMIPs (Ravi et al., 2020). The strong stretching vibration absorption of the carboxylic acid group (C=O) in MO and PL-nanoMIPs was observed at 1719.91 cm^{-1} and 1724.03 cm^{-1}. The characteristics absorption peaks for MO-nanoMIP at 1141.12 and 1450 cm^{-1} were due to the C -N and C=C stretching vibration of the amines and pyridine ring on the 2-VP monomer used in the synthesis of MIP and the nanoMIPs (Geravi and

Ghaemy, 2024). While the PL-nanoMIP showed a C-N and C=C bands at 1132.88 cm^{-1} and 1458.32 cm^{-1}, respectively.

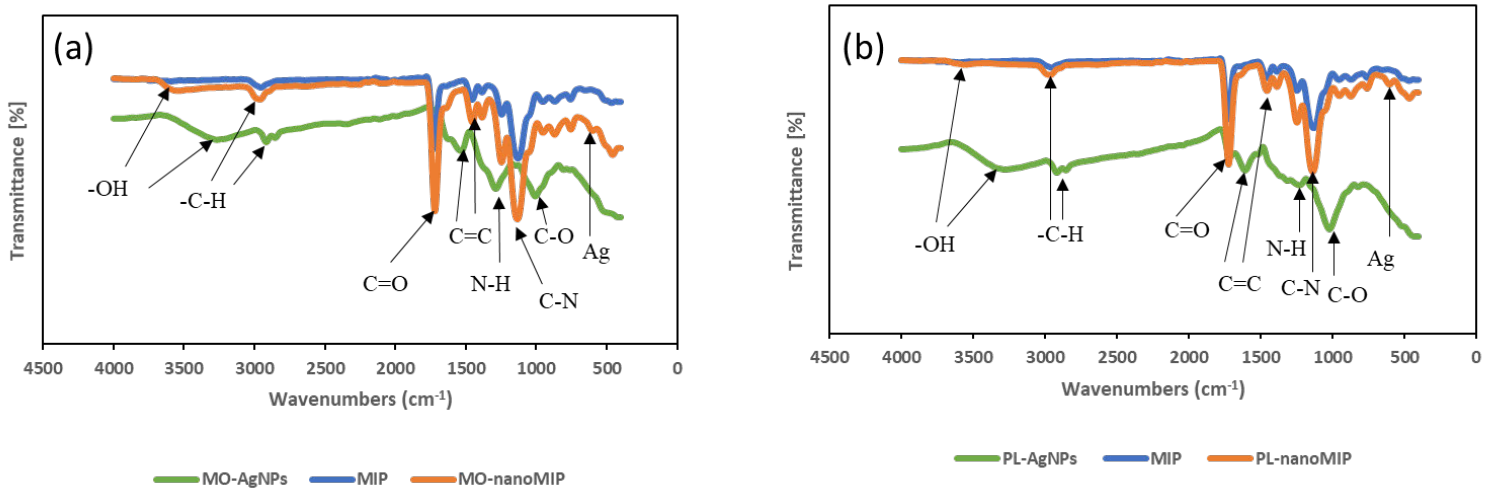

Figure 5.4: FTIR spectrum of (a) MIP, MO-AgNPs, MO-nanoMIP and (b) MIP, PL-AgNPs, PL-nanoMIP

5.12.1.5 Thermogravimetric analysis (TGA) and Differential scanning calorimetry (DSC)

The TGA curve clearly indicates an initial weight loss observed at around 150 °C and 128 °C, due to the loss of bound and unbound water molecules present in the obtained MO and PL-silver nanoparticles (**Figure 5.5 (a) and (b)**). A second weight loss appeared while temperature increases at 174.71-300 °C and 146.73-227.73 °C which accounted a 27% of the total MO and 3.5 % of PL-AgNPs weight. The breakdown of organic compounds like phenolic acid and carbohydrates is the cause of this weight loss (David and Moldovan, 2020). A steady loss of weight appeared until 369.71-700 °C and 254.51-700 °C For MO and PL-AgNPs which accounted for 29%, probably determined by the thermal degradation of resistant aromatic compound and the decomposition of biogenic salt, such as carbonates. Accordingly, the DSC showed a sharp endothermic peak for MO-AgNPs 165.95 °C and 269.75 °C for PL-AgNPs. According to **Figure 5.5 (c)** and **(d)**, thermal analysis of MO and PL-nanoMIPs showed three weight loss steps. The first weight loss of 5% occurred around 170.9 °C and 168.53 °C for the MO and PL-nanoMIPs due to the loss of the adsorbed water and the residue solvent molecules. There was a significant weight loss of about 63% from 205 °C to 500 °C and 198.5 °C to 488 °C for MO and PL-nanoMIPs, which can be attributed to the decomposition of the polymer shell and loss of side groups such as acids and ester groups. The polymer was completely decomposed which was attributed to the decomposition of the polymer shell and loss of side groups such as acids and ester groups at 512 °C and 500 °C for the MO and PL-nanoMIPs, respectively. This further indicates that the AgNPs were successfully embedded on the MIP. The corresponding DSC thermogram showed a prominent exothermic peak at 458.05 °C and 363.29 °C might be due to the loss of pyridine and CO_2 molecules (Thach et al., 2021). These peaks are also attributed to the crystallization of AgNPs.

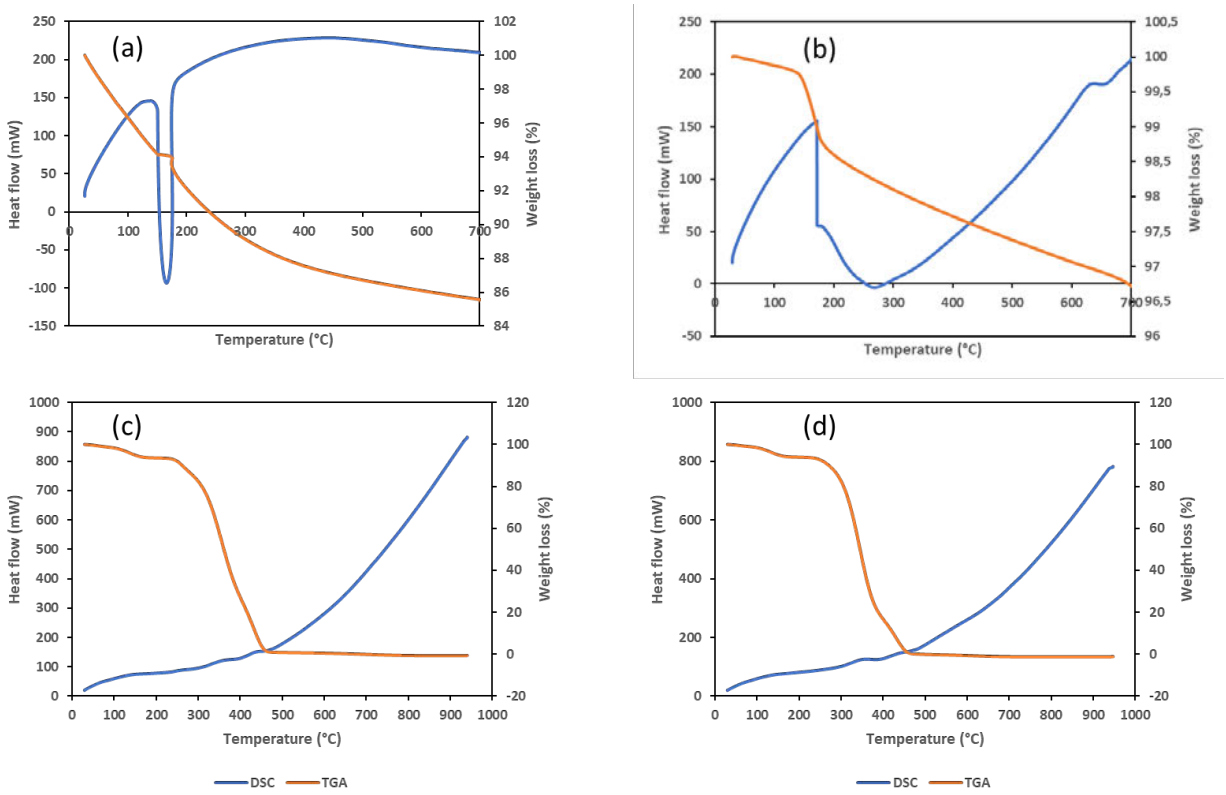

Figure 5.5: TGA of (a) MO AgNPs, (b) PL-AgNPs, (c) MO-nanoMIP and (d) PL nanoMIPs

5.12.1.6 X-ray diffraction (XRD)

X-ray diffraction (XRD) analysis was used to further characterize the MO/PL-AgNPs. As illustrated in **Figure 5.6 (a)** and **(b),** all samples with specific diffraction peaks were highly crystallized materials. Accordingly, five predominant diffraction peaks located at 2θ = 38.06°, 44.26°, 64.34°, 77.30°, and 81.53° for PL-AgNPs and 2θ=38.08°, 44.29, 64.37° , 77.41°, and 81.37° for MO-AgNPs matched the Miller planes of the face centered cubic Ag^0 phase (111), (200), (220), (311), and (222), respectively. Notably, the diffraction peak positions for the MO/PL-nanoMIPs remained unchanged. This indicates that AgNPs still retains in its original crystal structure and does not change with the addition of the polymer and confirmed the successful formation of crystalline MO/PL-AgNPs in the MIP particles. Moreover, an amorphous broad and less intense peak was observed at 2θ = 19.40° and 17.81° for PL and MO nanoMIPs which is indicative of the polymer. Additionally, the intensity of the XRD peaks decreased after incorporation the nanoparticles with MIP because of the effect of the lower crystalline content in nanoMIPs and the amorphous polymeric surface of MIP (**Figure 5.6 (c)** and **(d)**) (Nurhayati and Royani, 2016). Similar observations were reported by Jiang and coworkers on their XRD characterization for

determination on sulfamethazine using molecularly imprinted polymers decorated with silver nanoparticles (Jiang et al., 2023).

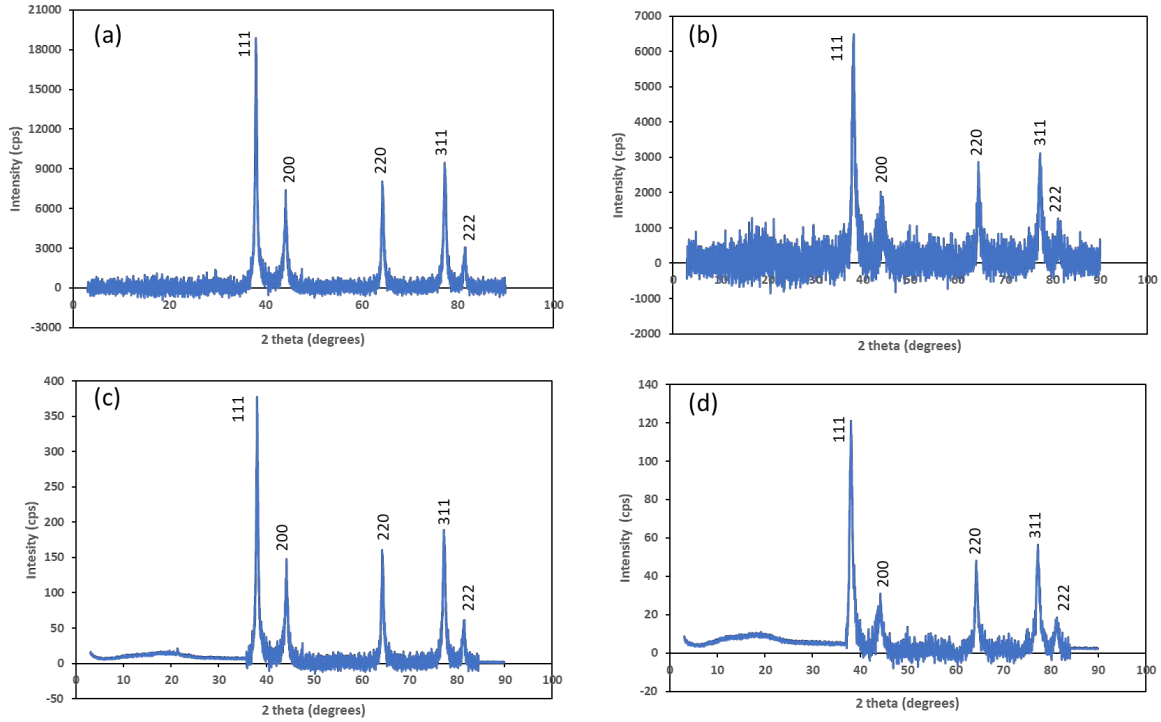

Figure 5.6: X-ray diffraction patterns of (a) PL-AgNPs, (b)MO-AgNPs, (c) PL-nanoMIP and (d) MO-nanoMIP

5.12.1.7 Raman spectra

The Raman bands of MO-AgNPs detected in 1794 and 2033 cm^{-1}, have been assigned to the aromatic C-C stretching, whereas for PL-AgNPs these bands were detected at 1359, and 1597 cm^{-1}. Moreover, the band at 1041 cm^{-1} for PL-AgNPs has been attributed to C-O-C, while band at 820 cm^{-1} for the PL-AgNPs is due to AgNPs stretching. The band at 2304 cm^{-1} is recognized as a characteristic C–H vibration peak. Accordingly, the fluorescence background was too high to determine the Raman for MO and PL-nanoMIPs (**Figure 5.7 (c)** and **(d)**). This suggest that the embedded silver nanoparticles around the recognition cavities of MIP surely enhance the Raman signals, making it difficult to identify these adsorbents correctly in the Raman spectrometer (Liu et al., 2011). However, the broad bands at 1592 cm^{-1} for the PL-nanoMIP can be attributed to the polymeric backbone of crosslinker used in the preparation of MIP interaction with AgNPs.

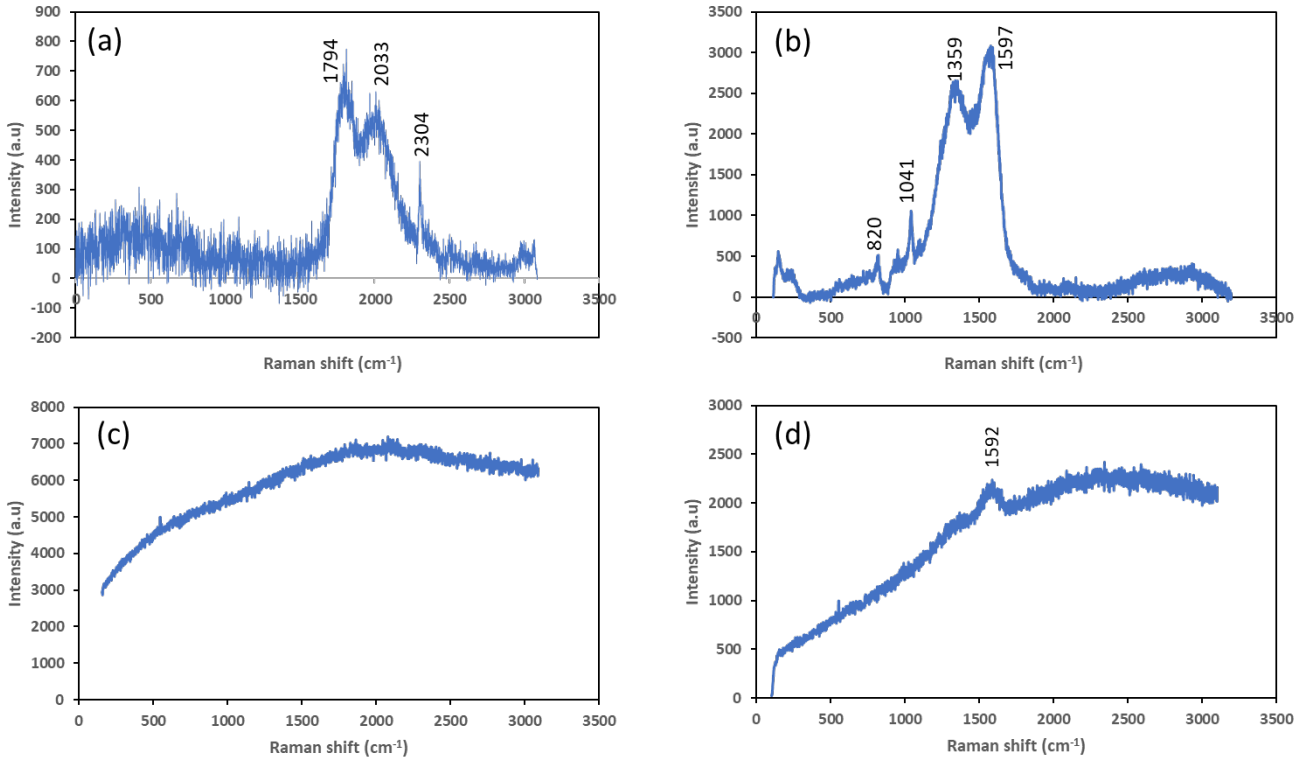

Figure 5.7: Raman spectra of (a) MO-AgNPs, (b) PL-AgNPs. (c) MO-nanoMIP and (d) PL-nanoMIP.

5.12.2 Optimization of parameters

5.12.2.1 pH effect

Effect of pH on the removal of sulfamethoxazole, nevirapine and ibuprofen by MO-nanoMIP and PL-nanoMIP can be seen in **Figure 5.8 (a)** and **(b)**. It was observed from the results that the adsorption of these pharmaceuticals increases with an increase in pH of the solution to a maximum around a pH ~7.0 (99.2-99.5% and 98.32 -99.61% for MO and PL-nanoMIPs), and then decreases as the pH becomes more basic. Maximum removal efficiency at pH 7 can be explained due to the formation of hydrogen bond between carboxylic acid and amine groups in the imprinting structure and the functional groups in pharmaceutical molecules (Geravi and Ghaemy, 2024). Moreover, the pharmaceutical compounds sulfamethoxazole, nevirapine, and ibuprofen existed neutrally when the pH was increase to a range between their pKa. Notably, both MO and PL-nanoMIPs exhibited high % removal efficiencies from pH 3 to 5, due to that the MO/PL-nanoMIPs surface charge acquires more positive charge particles from the acidic pH solution increasing the electrostatic attraction between target pharmaceutical and the MO/PL-nanoMIP adsorbents. Furthermore, at acidic pH, the surface of adsorbents acquires a positive surface

charge due to dissociation of H^+ and protonation from the amine group (Ezeuko et al., 2022). Therefore, it was assumed that these compounds would bind to the MO/PL-nanoMIPs via hydrogen bonding or electrostatic interactions in the positively charged form, and highest removal was noted (Qiu et al., 2022). At pH>7, higher concentrations of basic hydroxyl ions are present, which builds a bridge between the molecules of the MO/PL-nanoMIPs and the pharmaceutical compounds (Ravi et al., 2020). Consequently, the surface of the MO/PL-nanoMIPs adsorbents is closely associated with -OH ions, which may prevent the pharmaceutical ions from reaching the surface of the functional groups due to repulsive forces. As a result, the pharmaceuticals and the OH-free ion compete to occupy the adsorbent's surface, which lowers the pharmaceutical's ability to bind to the adsorbent.

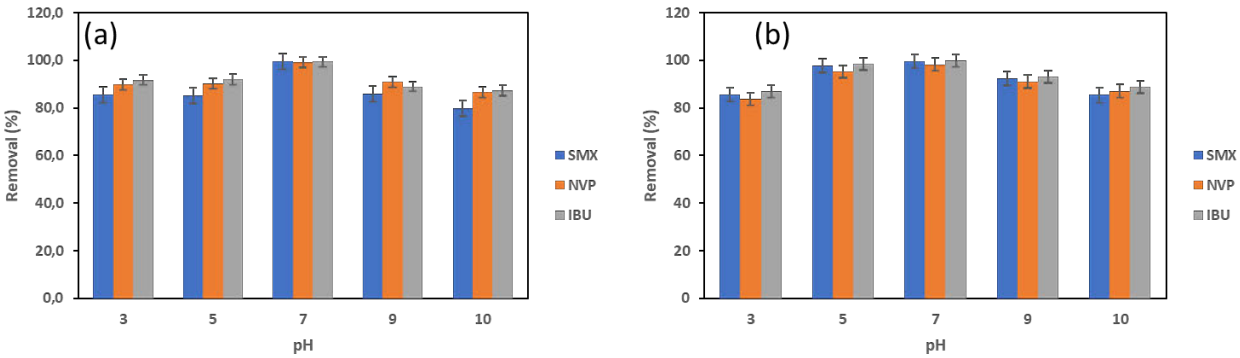

Figure 5.8: effect of pH on (a) MO-nanoMIP and (b) PL-nanoMIP

5.12.2.2 Concentration effect

As revealed in **Figure 5.9 (a)** and **(b)**, the adsorption effectiveness of the MO and PL-nanoMIPs adsorbent decreased as the concentration of target pharmaceuticals was increased. At lower concentrations, the active sites of the MO and PL-nanoMIPs surface are mostly empty, which resulted in high adsorption rates leading to increased pharmaceuticals diffusion to the adsorbent surface. The initial adsorbate concentration increase had less of an impact on the PL-nanoMIP adsorbent compared to the MO-nanoMIP. The PL-nanoMIP pharmaceuticals removal efficiency decreased from 100 to 77.7%, whereas for MO-nanoMIP removal efficiency decreased from 99.3% to 61.8% at concentration of 0.2 to 1.5 mg/L, respectively. It was noted that the increase in concentration resulted removal % decline. One possible reason for this decrease could be the MO/PL-nanoMIP adsorbents restricted number of active sites., which get more saturated as the concentration of the pharmaceuticals increases. Furthermore, once

pharmaceuticals reach saturation, it results in quick exhaustion of the binding sites on the adsorbents surface as the number of pharmaceutical molecules is increased. This leads to an electrostatic repulsion interaction between the pharmaceutical compounds and the adsorbent surface, which reduces the effectiveness of pharmaceutical removal. Notably, higher adsorbate concentrations restrict access to adsorption sites, hence the removal of pharmaceuticals relies on the initial concentration (Bankole et al., 2023).

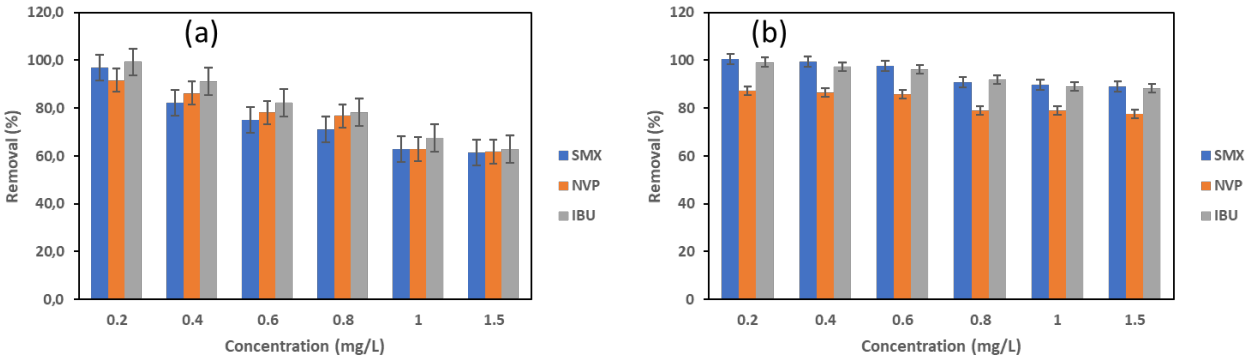

Figure 5.9: Effect of concentration on (a) MO-nanoMIP and (b) PL-nanoMIP

5.12.2.3 Effect of mass dosage

The results in **Figure 5.10** shows an increase in % removal with the increase in mass dosage for MO/PL-nanoMIP. The maximum removal efficiency obtained at the mass dosage of 30 mg was in the range of 100-97.7% for MO-nanoMIP (**Figure 5.10 (a)**) and between 100.1-99.4% for PL-nanoMIP at 20 mg (**Figure 5.10 (b)**). Interestingly, the larger surface area and additional adsorption sites produced by increasing the number of MO/PL-nanoMIP adsorbent particles led to an improvement in removal efficiency. This increase also resulted in an increase in the number of pharmaceuticals bound to the adsorbent weight (Hamad and El-Sesy, 2023). The %removal efficiency for both MO and PL-nanoMIP adsorbents declined as the adsorbent dosage increased, potentially due to the aggregation of adsorbent high mass dosesage that decreased the adsorbent surface area. (Kebede et al., 2020). Moreso, it may also have been caused by that, the MO/PL-nanoMIPs surface has undergone equilibrium, or from insufficient pharmaceutical ions in the solution relative to the available binding sites or from interference between the increased adsorbent dose and binding sites. Furthermore, the results demonstrated that MO/PL-nanoMIPs had more binding sites for the removal of the targeted pharmaceuticals.

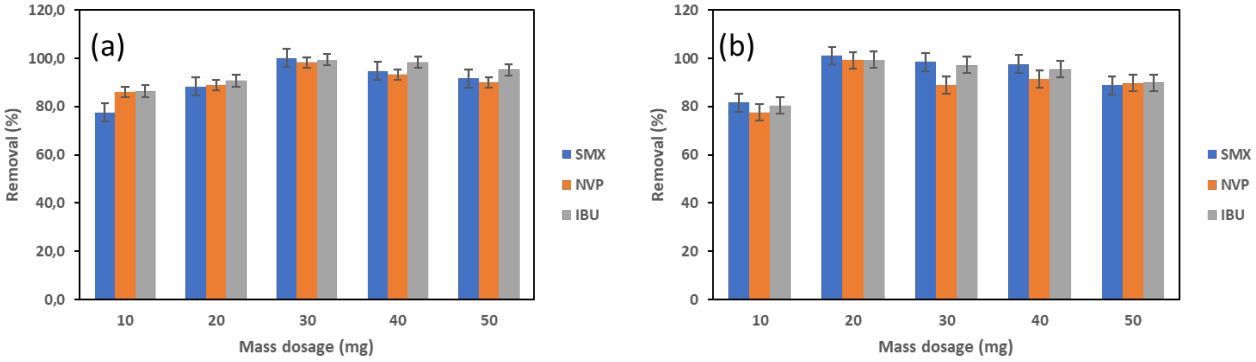

Figure 5.10: Effect of mass dosage on (a) Mo-nanoMIP and (b) PL-nanoMIP

5.12.2.4 Effect of contact time

The targeted pharmaceuticals were removed faster in the initial stages for both <O and PL-nanoMIP adsorbents, as seen in **Figure 5.11 (a)** and **(b)**, with the maximum removal (more than 90%) occurring in just 10 minutes of contact time. Hence the contact time of 10 min was considered as equilibrium time. During the early phases of adsorption, there were a lot of open surface sites. Nevertheless, over time, the repulsive forces between the bulk phases and the solute molecules on the solid caused them to become nearly saturated with selected pharmaceuticals and challenging to occupy. Beyond 10 minutes, pharmaceuticals % removal was observed to decrease slightly by 0.20-0.26%. Majority of the empty regions on the surface of the adsorbents were occupied by pharmaceutical molecules, reducing the amount of accessible active sites and causing the pharmaceutical removal efficiency to decrease.

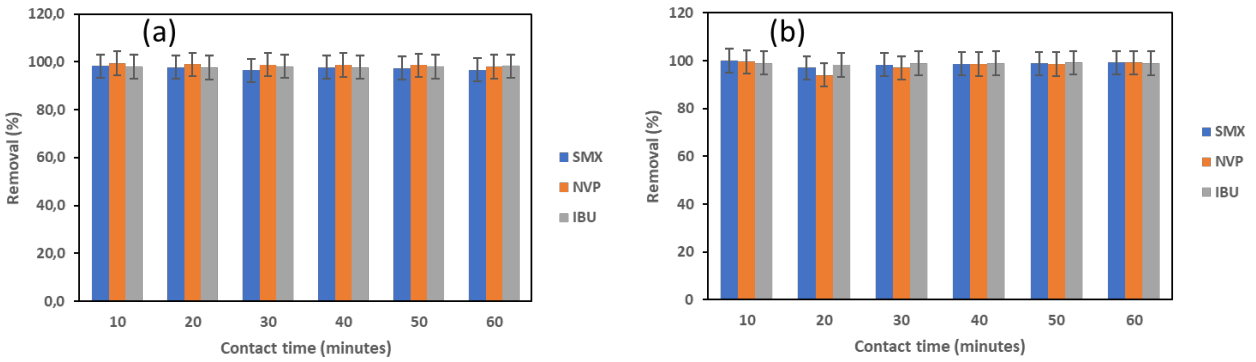

Figure 5.11: Effect of contact time on (a) MO-nanoMIP and (b) PL-nanoMIP

5.12.2.5 Effect of temperature

According to the graph in **Figure 5.12 (a)** and **(b)**, removal efficiency percentages for both MO and PL-nanoMIPs increased as temperature increased. This is because the pore enlarges, and new active sites are developed as a result of bond breakage on the adsorbent surface. For MO-nanoMIP, maximum removal% was found to be 97.1-98.7% at 40 °C and for PL-nanoMIP, the highest removal efficiency was 99.95-100.20 % at 30 °C. Consequently, the optimal removal percentage was observed at 40 °C and 35 °C for MO and PL-nanoMIPs, respectively. Notably, the adsorption process of MO/PL-nanoMIPs is propelled by chemisorption, which is the reason why more removal was seen at high temperature(s). An increase in the rate of adsorption accompanied by a rise in temperature is thought to indicate that the adsorption process is endothermic (Bhattacharya et al., 2020). In contrast, beyond the optimal temperatures of MO and PL-nanoMIPs (40 °C and 30 °C), the targeted pharmaceuticals occupied all active sites, causing adsorption effectiveness to slow down as physical adsorption caused the intermolecular tensions between pharmaceuticals and adsorbents to break down at high temperatures. According to Altaf and colleagues, the increased updraft movement of pharmaceutical molecules at higher temperatures resulted in a decrease in pharmaceutical uptake, thus reduces the active sites and pharmaceuticals (Altaf et al., 2021). Notably, when the attraction between the pharmaceuticals and active sites weakened, there would be very little adsorption at high temperatures. An additional reasoning for the decline in removal efficiency as temperature rises could be that the system's heat energy increases, giving the adsorbate molecules more kinetic energy and making them more mobile (Natarajan et al., 2021). This reduced pharmaceuticals-surface adhesion resulting in a lower interaction with MO/PL-nanoMIP adsorbent's surface functionality, which in turn causes a decrease in removal efficiency.

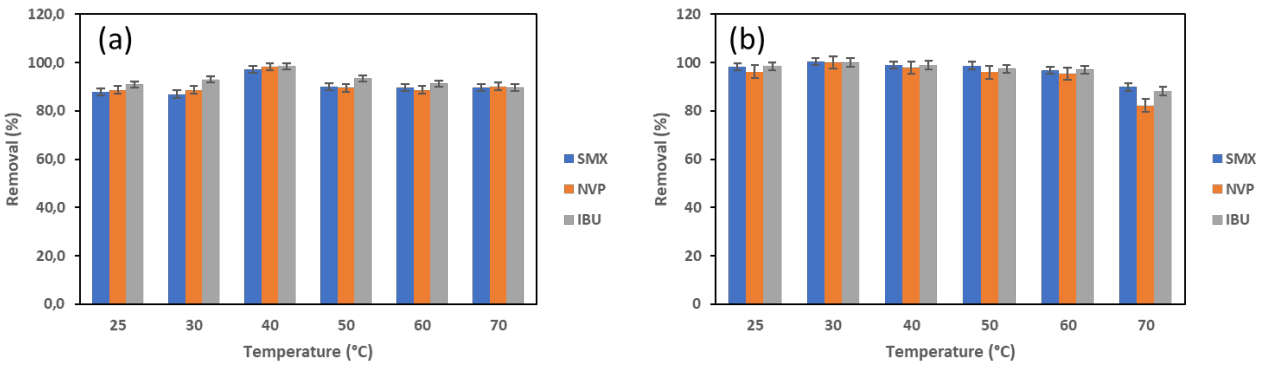

Figure 5.12: Effect of temperature on (a) Mo-nanoMIP and (b) PL-nanoMIP

5.12.3 Statistical analysis

The effects of pH, contact time, mass dose, concentration, and temperature on the pharmaceutical's removal process were examined using the Fisher's F test and an analysis of variance (ANOVA). Notably, Models and variables are deemed important in statistical research when they have high F-values and low P-values (less than 0.05) (Moradi et al., 2023). The ANOVA results in **Table S5.2**, show that the model has an F value of 3.53 and 3.51 for the MO-nanoMIP and PL-nanoMIP respectively, which are higher than the F critical value (2.71) therefore proving the significance of the model. Accordingly, the variables were statistically significant at a 95% confidence level and had a low probability value $P< 0.05$ suggesting that the ANOVA model was highly significant, for both MO-nanoMIP and PL-nanoMIP. Moreso, the p-value for the concentration, contact time, mass dosage, temperature and pH parameters were found to be within the significance limit (less than 0.05), which shows that these parameters significantly affect the removal efficiency of pharmaceuticals. Accordingly, the Fisher's F-test indicated, with 95% confidence, that the regression model explained a large amount of the variation in the dependent variable because $F_{cal} > F_{crit}$ for all the parameters. This provides confirmation for the results shown in the main and interaction effect plots (**Figure 5.8 to Figure 5.12**). Consequently, there was a small percentage of error in the examined parameters, as evidenced by the estimate errors of 2.98 for MO-nanoMIP and 1.76 for PL-nanoMIP. The significance of each individual parameter was further validated by calculating the % contribution factor of each process parameter. As indicated by the data in Table S3, it was observed that for the MO-nanoMIP the concentration had the highest contribution for the removal efficiency of the target pharmaceuticals, followed by mass dose, pH, temperature and lastly contact time with contribution factors being 35.88%, 6.26%, 5.09%, 2.43% and 0.019%, respectively. Particularly, for the Pl-nanoMIP, the mass dosage had the greatest influence (10.11%), followed by concentration (7.70%), pH (6.31%), temperature (4.94%) and contact time (0.25%).

5.12.4 Adsorption kinetics

The results in **Table 5.1** and **Table 5.2** show the determined qe, k_1 and k_2, the related linear regression coefficient R^2, and root mean square error (RSME) values for MO and PL-nanoMIP. These parameters were obtained from the linear and non-linear kinetic plots are depicted in **Figure S5.1** and **S5.2**. Based on the linear and non-linear pseudo-first-order model, it was discovered that the experimental qe values for MO/PL-AgNPs and the

MO/PL-nanoMIPs did not match those calculated. This suggests that the adsorption kinetics of sulfamethoxazole, nevirapine, and ibuprofen on these adsorbents are not adequately represented by either linear of non-linear pseudo-first order model. Furthermore, the results show that for MO/PL-AgNPs and MO/PL-nanoMIPs, the pseudo-second order kinetic parameters, as determined by linear and nonlinear methods, were found to differ slightly. However, the RSME values were lower for the linear pseudo-second order model than non-linear pseudo-second order. This therefore confirms low error function and the good fit of the experimental data with linear pseudo-second order. Further, it was observed that the MO/PL-AgNPs, had a high R^2 values for linear pseudo-second order (>0.999) in contrast to MO/PL-nanoMIPs. Moreover, the calculated values of qe values for the linear pseudo-second order fitted well with the experimental data for MO/PL-AgNPs and MO/PL-nanoMIPs. This suggests that the linear regression method of the pseudo-second order adsorption mechanism provides a more accurate description of the adsorption process. However, the qe values for the MO/PL-nanoMIPs were higher than those of MO/PL-AgNPs, indicating that the nanoMIPs have higher adsorption capacity for the target pharmaceuticals compared to AgNPs alone. According to the best fit to the pseudo-second order model, the rate-limiting stage in the process is chemisorption, which involves the exchange of electrons to generate valence forces between the functional groups of the adsorbents and the targeted pharmaceuticals (Meléndez-Marmolejo et al., 2022). The reaction rate constant k_2 was used to measure how quickly equilibrium was reached. Notably, when it is relatively high, equilibrium is established in a relatively short amount of time (Sekulic et al., 2019). Hence, it can be notable that k_2 values increased in the order of IBP < SMX <NPX. This suggests that the initial availability of active adsorption sites influenced the molecular weight and rate of pharmaceuticals adsorption onto the adsorbent surface. Consequently, ibuprofen, sulfamethoxazole, and nevirapine have molecular weights of 266.30 mg/L, 254.28 mg/L, and 206.29 mg/L, respectively. As a result, ibuprofen, a smaller molecule, had a higher adsorption capacity (Q_{max}) than two larger nevirapine and sulfamethoxazole molecules. This is probably because smaller molecules can more easily and readily bind to all of the accessible sites on the adsorbent, including those that are contained in tiny micropores. Similar results were also reported by Ravi and colleagues for the removal of pharmaceutical pollutants from water using novel porous organic polymers based on phenyl phosphate (Ravi et al., 2020).

Table 5.1: Linear kinetics data for the adsorption of the selected pharmaceuticals onto MO/PL-AgNPs and MO/PL-nanoMIP

Adsorbent	**Pharmaceuticals**	**q_e (mg/g) Exp**	**Pseudo-first order**				**Pseudo-second order**			
			q_e (mg/g) Cal	**k_1**	**R^2**	**RMSE**	**qe (mg/g) Cal**	**k_2**	**R^2**	**RMSE**
MO-AgNPs	Sulfamethoxazole	10.49	7.37	1.67×10^{-5}	0.9975	1.19	10.02	0.2021	0.9997	0.38
	Nevirapine	5.88	3.54	1.67×10^{-5}	0.9980	1.49	4.84	0.1913	0.9999	0.18
	Ibuprofen	9.24	5.95	3.67×10^{-5}	0.9995	1.80	8.50	0.2554	0.9998	0.09
MO-nanoMIP	Sulfamethoxazole	120.33	24.30	1.00×10^{-5}	0.353	4.17	119.4	0.0637	0.9993	0.17
	Nevirapine	66.89	6.25	8.33×10^{-6}	0.1789	2.30	65.78	0.0158	0.9974	0.18
	Ibuprofen	169.22	35.40	1.33×10^{-5}	0.1819	4.23	167.8	0.1644	0.9995	0.11
PL-AgNPs	Sulfamethoxazole	11.0	5.39	1.83×10^{-5}	0.9951	2.85	9.71	0.2889	0.9999	0.05
	Nevirapine	5.48	1.62	4.50×10^{-5}	0.9929	2.40	4.94	0.2470	0.9999	0.13
	Ibuprofen	9.62	3.06	4.83×10^{-5}	0.9967	2.14	8.79	0.3847	0.9999	0.09
PL-nanoMIP	Sulfamethoxazole	136.02	53.11	8.00×10^{-5}	0.7102	4.18	135.8	0.0532	0.9977	0.09
	Nevirapine	80.25	45.11	5.00×10^{-5}	0.1656	6.26	79.44	0.0278	0.9978	0.13
	Ibuprofen	151.33	134.5	1.00×10^{-4}	0.1502	12.39	150.9	0.0918	0.9991	0.56

Table 5.2: Non-linear kinetics data for the adsorption of the selected pharmaceuticals onto MO/PL-AgNPs and MO/PL-nanoMIP

Adsorbent	**Pharmaceuticals**	**q_e (mg/g) Exp**	**Pseudo-first order**				**Pseudo-second order**			
			q_e (mg/g) Cal	**k_1**	**R^2**	**RMSE**	**qe (mg/g) Cal**	**k_2**	**R^2**	**RMSE**
MO-AgNPs	Sulfamethoxazole	10.88	5.44	1.85×10^{-5}	0.9598	1.81	9.63	0.2002	0.9899	0.51
	Nevirapine	5.78	3.89	1.87×10^{-5}	0.9479	1.82	5.06	0.1816	0.9996	0.29
	Ibuprofen	9.59	6.42	1.58×10^{-5}	0.9455	1.47	9.02	0.2505	0.9990	0.23
MO-nanoMIP	Sulfamethoxazole	120.36	20.02	1.20×10^{-5}	0.1853	3.00	117.03	0.0626	0.9967	1.36
	Nevirapine	66.87	2.42	1.33×10^{-6}	0.3599	5.27	66.01	0.0145	0.9989	0.35
	Ibuprofen	169.42	31.82	1.13×10^{-5}	0.4697	6.72	169.02	0.1622	0.9996	0.16
PL-AgNPs	Sulfamethoxazole	11.69	4.22	3.44×10^{-5}	0.9432	2.36	10.11	0.2875	0.9956	0.65
	Nevirapine	5.96	1.22	4.23×10^{-6}	0.8390	2.05	5.46	0.2463	0.9995	0.20
	Ibuprofen	9.89	3.21	2.33×10^{-5}	0.9647	1.59	9.38	0.3812	0.9988	0.21
PL-nanoMIP	Sulfamethoxazole	136.19	40.31	5.77×10^{-5}	0.8962	8.25	135.9	0.0501	0.9986	0.12
	Nevirapine	80.63	39.22	9.80×10^{-5}	0.3745	8.51	79.62	0.0265	0.9997	0.41
	Ibuprofen	151.48	110.8	3.23×10^{-5}	0.8936	12.92	148.3	0.0891	0.9999	1.30

5.12.5 Adsorption isotherms

The Langmuir and Freundlich isotherms (linear and non-linear models) for the adsorption of sulfamethoxazole, nevirapine, and ibuprofen by MO/PL-AgNPs and MO/PL-nanoMIPs are shown in **Table 5.3** and **Table 5.4**. The Langmuir constants (linear and non-linear) separation factor (K_L) and equilibrium constant (R_L) were less than one (1) and higher than zero. This shows how favourable the adsorption was for the MO/PL-AgNPs and MO/PL-nanoMIPs. The results demonstrated the homogeneous nature of the MO/PL-AgNPs and MO/PL-nanoMIPs adsorbents by the monolayer sulfamethoxazole, nevirapine, and ibuprofen adsorption process. The linear and non-linear models for the Freundlich isotherm heterogeneity 1/n values were less than 1 and greater than zero, therefore indicating that both linear and non-linear Freundlich isotherm are favourable. Additionally, a suitable adsorption capacity is indicated by a Freundlich constant (K_F) between 2 and 10 (Kryuchkova et al., 2021). Notably the MO/PL-nanoMIPs K_F values obtained were within the range compared to MP/PL-AgNPs, meaning good adsorption capacity of MO/PL-nanoMIP adsorbents towards the pharmaceuticals studied. From the experimental value, the linear Langmuir isotherm co-relation coefficient R^2 values were found to be closer to 0.999 compared to that of the linear Freundlich model. This specifies that the linear Langmuir model better fitted to adsorption of sulfamethoxazole, nevirapine and ibuprofen onto the MO/PL-AgNPs and MO/PL-nanoMIPs. Therefore, verifying that the adsorption occurred within the monolayer homogeneous site of the adsorbent surface. Which indicates that once the pharmaceutical molecules occupy the adsorptive site, no more adsorption takes place (Ezeuko et al., 2022). The maximum adsorption capacity (Q_{max}), which is commonly used to assess adsorbents' levels of efficiency, was measured using a Langmuir isotherm. Given the large specific surface area and the pore structure of mesoporous material. the Q_{max} values of MO/PL-nanoMIPs were significantly higher than MO/PL-AgNPs. However, The PL-nanoMIP presented a stronger affinity towards the selected pharmaceuticals with Q_{max} value being higher than that of MO-nanoMIPs. Hence, the PL-nanoMIP maximum equilibrium adsorption capacities for ibuprofen, sulfamethoxazole and nevirapine were 94.34, 27.24, and 110.1 mg/g, respectively. The Q_{max} showed direct correlation with molar mass of the adsorbate with ibuprofen exhibiting the highest adsorption capacity followed by sulfamethoxazole and nevirapine exhibiting the lowest adsorption capacities. Because sulfamethoxazole and nevirapine have larger molecular size than ibuprofen, it is harder for the molecules to access the adsorbent material pores, which accounts for their lower Q_{max}. Hence, the order of adsorption was

Ibuprofen>sulfamethoxazole>nevirapine. Notably, surface diffusion is therefore primarily responsible for driving the adsorption (Varela et al., 2024).

Table 5.3: Linear isotherms data for the adsorption of the selected pharmaceuticals onto MO/PL-AgNPs and MO/PL-nanoMIPs

Isotherm	Parameters	Sulfamethoxazole				Nevirapine				Ibuprofen			
		MO-AgNPs	MO-nanoMIP	PL-AgNPs	PL-nanoMIP	MO-AgNPs	MO-nanoMIP	PL-AgNPs	PL-nanoMIP	MO-AgNPs	MO-nanoMIP	PL-AgNPs	PL-nanoMIP
Freundlich	K_F (L/mg)	2.89	4.25	0.093	2.94	0.29	8.28	0.65	2.99	1.40	1.08	2.02	2.94
	1/n	2.39	0.69	6.99	0.96	4.28	1.08	3.23	0.94	2.05	1.68	1.13	0.95
	R^2	0.9902	0.9917	0.9969	0.9965	0.9898	0.9797	0.9943	0.9971	0.9952	0.9720	0.9966	0.9924
Langmuir	Q_{max}	10.18	32.50	20.83	94.34	9.46	16.91	13.39	27.24	12.39	97.74	22.96	110.1
	K_L (L/mg)	0.51	0.63	0.41	0.12	1.39	0.088	0.49	0.075	0.20	1.00	0.19	0.061
	R_L	0.020	0.61	0.323	1.13	0.078	0.92	0.26	1.01	1.02	0.50	0.34	0.94
	R^2	0.9946	0.9987	0.9879	0.9996	0.9866	0.9988	0.9966	0.9998	0.9979	0.9990	0.9878	0.9986

Table 5.4: Non-linear isotherms data for the adsorption of the selected pharmaceuticals onto MO/PL-AgNPs and MO/PL-nanoMIPs

Isotherm	Parameters	Sulfamethoxazole				Nevirapine				Ibuprofen			
		MO-AgNPs	MO-nanoMIP	PL-AgNPs	PL-nanoMIP	MO-AgNPs	MO-nanoMIP	PL-AgNPs	PL-nanoMIP	MO-AgNPs	MO-nanoMIP	PL-AgNPs	PL-nanoMIP
Freundlich	K_F (L/mg)	1.99	4.02	0.093	2.33	0.23	8.03	0.60	1.98	1.40	1.08	2.02	2.94
	1/n	1.89	0.55	6.20	0.78	4.03	1.01	3.11	0.90	2.05	1.68	1.13	0.95
	R^2	0.9830	0.9877	0.9705	0.9955	0.9855	0.9886	0.9899	0.9906	0.9865	0.9830	0.9876	0.9904
Langmuir	Q_{max}	10.02	32.01	19.90	94.12	9.22	16.31	11.44	27.14	11.22	92.33	22.42	100.3
	K_L (L/mg)	0.21	0.43	0.31	0.095	1.11	0.068	0.22	0.036	0.11	0.98	0.10	0.044
	R_L	0.011	0.43	0.23	1.08	0.058	0.68	0.22	1.01	0.98	0.38	0.22	0.75
	R^2	0.9877	0.9905	0.9777	0.9956	0.9822	0.9955	0.9897	0.9988	0.9982	0.9991	0.9789	0.9869

5.12.6 Thermodynamics

Based on the slope and intercept of the plot of ln qe/ce and 1/T in **Figure S5.3**, the values of ΔG°, ΔH°, and ΔS° in **Table 5.5** were determined. The results indicate that for both MO/PL-nanoMIPs, the value of ΔG° was found to be negative at all temperatures. which shows that the adsorption of sulfamethoxazole. nevirapine and ibuprofen onto the MO/PL-nanoMIPs exhibit favourable and spontaneous adsorption. suggesting a high level of affinity between the pharmaceuticals and the adsorbent. Additionally, the Gibbs free energy variation was seen to decrease as temperature increased. suggesting that higher temperatures facilitate the adsorption process of the targeted pharmaceuticals with MO/PL-AgNPs and MO/PL-nanoMIPs. The reason for this could be that the adsorbent's pores expand at a higher temperature, creating larger pores that facilitate a greater diffusion of sulfamethoxazole. nevirapine and ibuprofen within the MO/PL-AgNPs and MO/PL-nanoMIP adsorbents (Haro et al., 2021). The value of ΔH° is positive for MO/PL-AgNPs and MO/PL-nanoMIPs, indicating that the adsorption is endothermic, as rising temperatures drive the rate of adsorbate diffusion on the adsorbent surface to also increase. However, the values of ΔH° for the MO/PL-AgNPs were less than 40 kJ/mol and more than 40 kJ/mol for the MO/PL-nanoMIPs. This therefore confirmed that the MO/AgNPs was dominated by physical adsorption whereas the MO/PL-nanoMIPs was dominated by chemical adsorption. Additionally, this suggests that physisorption (weak Van der Waals forces and π–π dispersion interactions) was the mode of adsorption for the MO/PL-AgNPs (Heidari et al., 2023). Hence, the forces holding physisorbed pharmaceutical molecules on the MO/PL-AgNPs surface are insufficient to disrupt the chemical bonds within the adsorbed molecule. Whereas the adsorption of the target pharmaceuticals by MO/PL-nanoMIP was through chemisorption due to strong bonds (ionic or covalent interaction) between the pharmaceuticals and MO/PL-nanoMIPs. Moreover, the positive value of ΔS° suggests that there is an increase in disorder in the solid/solute interface when sulfamethoxazole, nevirapine, and ibuprofen are adsorbed on MO/PL-nanoMIPs (Sadia et al., 2023).

Table 5.5: Thermodynamics data for the adsorption of the selected pharmaceuticals onto MO/PL-AgNPs and MO/PL-nanoMIPs

Compounds	**ΔG° (kJ/mol)**						**ΔH° (kJ/mol)**	**ΔS° (J/mol/K)**	**R^2**
	298 K	**303 K**	**313 K**	**323 K**	**333 K**	**343 K**			
MO-AgNPs									
Sulfamethoxazole	-12.37	-13.10	-14.10	-15.00	-15.86	-16.63	15.34	93.962	0.9731
Nevirapine	-5.51	-5.66	-6.04	-6.40	-6.76	-7.00	4.75	34.43	0.9812
Ibuprofen	-9.73	-9.95	-10.37	-10.82	-11.26	-11.62	2.92	42.49	0.9837
MO-nanoMIPs									
Sulfamethoxazole	-18.03	-18.48	-19.26	-20.59	-26.07	-27.71	86.86	20.39	0.8427
Nevirapine	-2.76	-4.49	-5.88	-6.64	-6.33	-6.13	42.22	5.24	0.6882
Ibuprofen	-3.82	-3.88	-4.41	-4.64	-4.75	-5.57	96.94	35.15	0.8263
PL-AgNPs									
Sulfamethoxazole	-10.53	-12.06	-13.04	-14.77	-15.56	-16.88	29.14	134.7	0.9531
Nevirapine	-6.01	-6.13	-6.35	-6.56	-6.77	-8.00	4.44	12.68	0.9445
Ibuprofen	-10.10	-11.07	-11.07	-11.52	-12.12	-12.79	7.71	59.67	0.9721
PL-nanoMIPs									
Sulfamethoxazole	-5.56	-5.62	-5.78	-5.90	-6.02	-6.19	44.65	13.80	0.9826
Nevirapine	-4.42	-4.50	-4.61	-4.99	-5.08	-6.19	54.91	19.97	0.9022
Ibuprofen	-10.12	-10.75	-11.22	-12.01	-12.47	-13.57	101.4	69.45	0.9319

5.12.7 Selectivity

To verify the formation of specific cavities in MO/PL nanoMIPs, competitive adsorption analysis was conducted in the presence of fenoprofen which has similar physicochemical properties as the target pharmaceuticals (sulfamethoxazole, nevirapine and ibuprofen). It was noted from the results in **Figure 5.13 (a)** that the MO-nanoMIP adsorbed 89% sulfamethoxazole, 79.6% nevirapine, 95.7% ibuprofen and 41.8% fenoprofen, whereas the PL-nanoMIP (**Figure 5.13 (b)**) adsorbed 96.9% sulfamethoxazole, 89.2% nevirapine, 99.4% ibuprofen and 55.9% fenoprofen. Because of the MO/PL-nanoMIPs' enhanced molecular recognition selectivity toward sulfamethoxazole, nevirapine, and ibuprofen, it implies that the imprinting cavities were formed effectively during the polymerization process due to the interaction of the target molecules size, shape, and functionality. The target pharmaceutical's firm molecular structure and specific positions are most likely to be responsible for the binding site interaction, which explains the MO/PL-nanoMIPs selectivity (Chiarello et al., 2021). Nonetheless, the fenoprofen competitor's poor adsorption effectiveness in contrast to the targeted pharmaceutical indicates that conformation memory is mostly reliant on the memory of the particular functional group. Thus, the distribution of the functional groups themselves was important for MO/PL-nanoMIPs molecular recognition, in addition to the molecule's size. Further, PL-nanoMIP had high adsorption efficiency in contrast to MO-nanoMIP. It can be therefore concluded that the PL-nanoMIP has a more superior surface for the target pharmaceuticals than MO-nanoMIP.

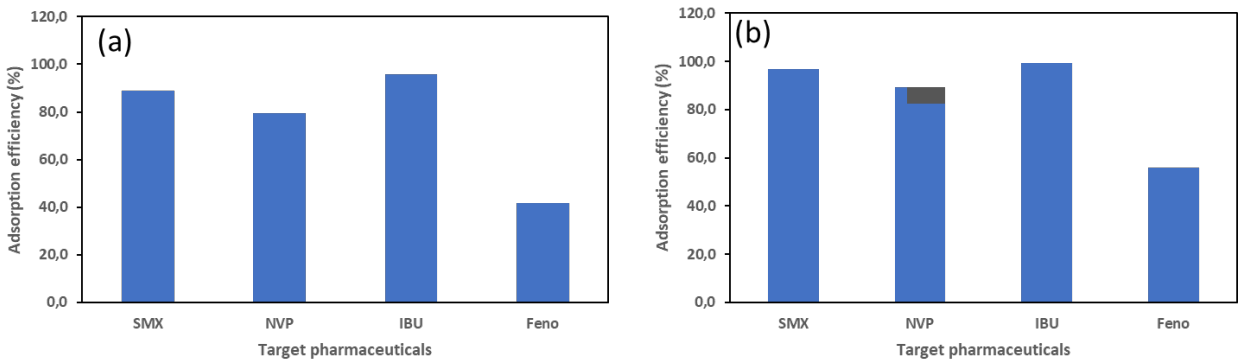

Figure 5.13: selectivity of the targeted pharmaceuticals for (a) MO-nanoMIP and (b) PL-nanoMIP

The selectivity of each compound on MO/PL-nanoMIPs is summarised by the K_d and k values in **Table 5.6**. Notably. The distribution ratio (KD) of ibuprofen, nevirapine, and sulfamethoxazole for both the MO and PL-nanoMIPs was notably higher than that of the

competitive compound fenoprofen. This is because the molecules of sulfamethoxazole, nevirapine, and ibuprofen match specific binding sites found in MO/PL-nanoMIPs. This indicates that MO/PL-nanoMIPs are well suited to recognize and bind to the targeted pharmaceutical compound. Accordingly. the order of the K_d values for the MO/PL-nanoMIP selectivity was ibuprofen > sulfamethoxazole > nevirapine. This indicates that the compounds' imprinting cavities formed in accordance with the interaction between the pharmaceuticals' functionality and their size, shape, and amount of hydrogen bonding (S'busiso et al., 2022). Additionally, the value of the specific selectivity coefficient (k) obtained was greater than 1 indicated that the synthesized MO/PL-nanoMIPs showed a good performance as remarkably successful molecular recognition (Roland et al., 2023). This is because, in contrast to the competing compound (fenoprofen), the synthesized MO/PL-nanoMIPs has binding sites that correspond to its template molecule (sulfamethoxazole, nevirapine, and ibuprofen).

Table 5.6: Selectivity of MO/PL-nanoMIPs

Pharmaceuticals	**MO-nanoMIP**		**PL-nanoMIP**	
	K_d (mg/g)	***k***	**K_d (mg/g)**	***k***
Sulfamethoxazole	0.89	1.62	0.84	1.38
Nevirapine	0.67	1.22	0.78	1.29
Ibuprofen	0.91	1.67	0.89	1.46
Fenoprofen	0.55	-	0.61	-

5.12.8 Reusability of MO/PL-nanoMIPs

The reusability of MO/PL-nanoMIPs was explored by investigating the adsorption efficiency in a number of adsorption-desorption cycles. The recyclability of MO-nanoMIP and PL-nanoMIP for the removal of ibuprofen, nevirapine, and sulfamethoxazole is depicted in **Figure 5.14 (a)** and **(b)**. Upon recycling the adsorbents for five cycles, it was noted that the MO-nanoMIP adsorbent was effective continued to remove 86.7-88.8% and 97-98% for PL-nanoMIP even in the fifth cycle. This suggests that the MO/PL-nanoMIPs can be efficiently reused over extended periods as they preserve the adsorption capacity. Nevertheless, the effectiveness of adsorbents slightly decreased after each cycle of adsorption/desorption, presumably as a result of a reduction in the number of available

active sites caused by blocking of the adsorbent surface's micropores and due to mass loss from handling or reusability of adsorbent surface as a result of repeated cycles. It is also possible that the ageing effect decreased the adsorbent's capacity for adsorption (Chakraborty et al., 2020, Bhattacharya et al., 2020). Overall, the findings point to the use of MO/PL-nanoMIPs as an inexpensive, efficient, reusable and sustainable adsorbent that shows a reasonably good capacity for adsorption of sulfamethoxazole, nevirapine, and ibuprofen. As such, their application in wastewater treatment should be taken into consideration as a strategy for environmental sustainability.

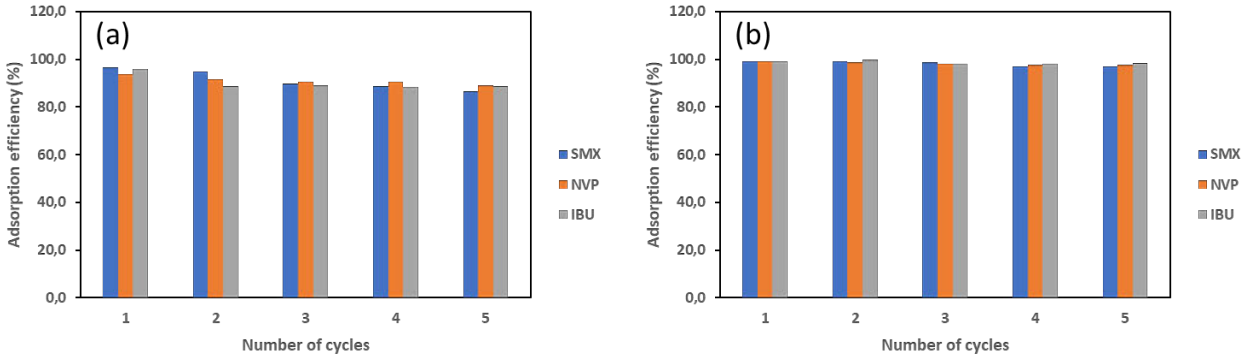

Figure 5.14: Reusability cycles for (a) MO-nanoMIP and (b) PL-nanoMIP

5.12.9 Application in wastewater

Adsorptive removal of sulfamethoxazole. nevirapine. and ibuprofen from influents and effluents of Darvill, Northern, and Amanzimtoti wastewater treatment plants (WWTPs) located in KwaZulu-Natal was conducted in order to assess the applicability of MO/PL-nanoMIP in wastewater samples. **Table 5.7** displays the adsorption capacities and removal efficiency percentages of the target pharmaceutical compounds by MO/PL-nanoMIPs in each of the three WWTPs. The adsorption capacities of MO-nanoMIP for the influent and effluent. varied from 61.0-96.9 mg/g and 45.0-89.8 mg/g, respectively. On the other hand, the PL-nanoMIP exhibited adsorption capacities ranging from 98.7-148.8 mg/g for the influent and 62.3-99.9 mg/g for the effluent, respectively. Notably, the MO/PL-nanoMIPs demonstrated remarkable promise as superior adsorbents with strong adsorption capacity for the removal of sulfamethoxazole, nevirapine and ibuprofen. Notably, in the Darvill and Amanzimtoti WWTPs, nevirapine and ibuprofen showed the highest adsorption capacity on both MO-nanoMIP and PL-nanoMIP. The log Kow may serve as a preliminary measure for the high adsorption capacity obtained for ibuprofen and nevirapine. Consequently, ibuprofen and nevirapine have a higher log Kow (3.97 and 3.89) than sulfamethoxazole (0.89) as depicted in **Table S5.1**. This may be the result of hydrophobic interactions being

more prominent during competitive adsorption for nevirapine and ibuprofen (Sekulic et al., 2019). Moreover, nevirapine and ibuprofen are highly consumed pharmaceuticals. Nevirapine is widely used to treat HIV and prevent mother-to-child transmission, while ibuprofen is commonly prescribed to treat fever and headaches, hence their high detection frequency in the environment. Furthermore, the adsorption of sulfamethoxazole, nevirapine, and ibuprofen by MO/PL-nanoMIPs yielded the highest removal efficiencies in all wastewater samples, ranging from 70.2 to 98%. This indicates that the target compounds were effectively removed from the wastewater by the applied MO/PL-nanoMIPs. This further demonstrates that MO/PL-nanoMIPs can be applied in the removal of pharmaceuticals in different wastewater systems.

Table 5.7: Adsorption capacities of selected pharmaceuticals in WWTPs by MO/PL-nanoMIPs

WWTP	**Sampling point**	**MO-nanoMIP**						**PL-nanoMIP**					
		Sulfamethoxazole		**Nevirapine**		**Ibuprofen**		**Sulfamethoxazole**		**Nevirapine**		**Ibuprofen**	
		Qe (mg/g)	**RE %**	**Qe (mg/g)**	**RE %**	**Qe (mg/g)**	**RE %**	**Qe (mg/g)**	**RE %**	**Qe (mg/g)**	**RE %**	**Qe (mg/g)**	**RE %**
Darvill	Influent	87.6	81	96.9	98	96.8	89	114.1	98	131.4	96	121.2	97
	Effluent	45.0	58	89.8	99	81.1	82	88.8	90	92.8	90	96.6	95
Northen	Influent	82.7	77	90.9	82	70.4	79	102.0	80	111.5	92	110.4	93
	Effluent	66.3	60	69.7	77	77.8	80	79.9	77	89.6	89	89.9	80
Amanzimtoti	Influent	79.6	61	93.6	89	88.7	78	98.7	89	125.3	94	148.8	98
	Effluent	55.1	45	70.2	78	62.5	70	62.3	78	98.4	86	99.9	88

Qe = adsorption capacity

RE= removal efficiency

5.13 Conclusion

The synthesized adsorbent was characterized by UV-spectroscopy, SEM, TGA, XRD, Raman spectroscopy, and FTIR. It was found that MO/PL-nanoMIPs showed enhanced surface properties and had high thermal stability in contrast to MO/PL-AgNPs. Moreover, the F-test and ANOVA statistical analysis demonstrated that the effects of contact time, concentration, temperature, adsorbent dosage, and pH were statistically significant. The best fitting model for the adsorption process was the linear pseudo second order model, as demonstrated by the adsorption kinetics. The linear Langmuir isotherm proved to be the most appropriate adsorption isotherm, indicating that the MO/PL-nanoMIPs adsorption occurs through chemisorption and monolayer. These results demonstrate that, in comparison to the non-linear approach, the linear method was more effective to consider the adsorption process. The maximum adsorption capacity (Qmax) obtained from the linear Langmuir model was in the order of ibuprofen > sulfamethoxazole > nevirapine. Comparative adsorption demonstrated the relationship between adsorption and the pharmaceutical's molecular size and log Kow. The MO/PL-nanoMIPs showed fast adsorption rate and high adsorption capacities when compared to MO/PL-AgNPs. Thus, MO/PL-nanoMIPs have larger surface area and are highly selective, which indicate that the incorporation of MIP and AgNPs favours enhancement in adsorption capacity. The thermodynamic analysis demonstrated that the adsorption process for MO/PL-AgNPs and MO/PL-nanoMIPs is endothermic in nature, favourable, and spontaneous. Further, regeneration study confirmed potential of synthesized MO/PL-nanoMIP adsorbents in five cycles to remove pharmaceuticals from wastewater, thereby sustaining cost-efficiency. Accordingly, the MO/PL-nanoMIPs showed high selectivity (>90%) for the target pharmaceutical compounds in the presence of a competitor. When applied to remove the presence of these pharmaceuticals in wastewater samples, the method showed removal efficiency of >61% in influent water samples and >45% in effluent water samples. The lower removal efficiency may be attributed to the presence of other material present in both water samples, thus further studies reporting on the impact of physicochemical parameters in water are recommended. The obtained results confirmed the efficiency and applicability of nanoMIPs in pharmaceuticals removal in wastewater. Notably, the nanoMIPs for pharmaceutical removal can effectively replace traditional methods due to their various advantages, which include excellent selectivity, reusability, low cost, and stability.

5.14 References

AHMADI, S., IGWEGBE, C. A., RAHDAR, S. & ASADI, Z. 2019. The survey of application of the linear and nonlinear kinetic models for the adsorption of nickel (II) by modified multi-walled carbon nanotubes. *Applied water science,* 9**,** 1-7.

ALNAJRANI, M. N. & ALSAGER, O. A. 2020. Removal of antibiotics from water by polymer of intrinsic microporosity: Isotherms, kinetics, thermodynamics, and adsorption mechanism. *Scientific reports,* 10**,** 794.

ALTAF, S., ZAFAR, R., ZAMAN, W. Q., AHMAD, S., YAQOOB, K., SYED, A., KHAN, A. J., BILAL, M. & ARSHAD, M. 2021. Removal of levofloxacin from aqueous solution by green synthesized magnetite (Fe3O4) nanoparticles using Moringa olifera: Kinetics and reaction mechanism analysis. *Ecotoxicology and Environmental Safety,* 226**,** 112826.

AZEEZ, L., LATEEF, A., ADEJUMO, A. L., ADELEKE, J. T., ADETORO, R. O. & MUSTAPHA, Z. 2020. Adsorption behaviour of rhodamine B on hen feather and corn starch functionalized with green synthesized silver nanoparticles (AgNPs) mediated with cocoa pods extracts. *Chemistry Africa,* 3**,** 237-250.

BANKOLE, D. T., OLUYORI, A. P. & INYINBOR, A. A. 2023. The removal of pharmaceutical pollutants from aqueous solution by Agro-waste. *Arabian Journal of Chemistry,* 16**,** 104699.

BHATTACHARYA, S., BANERJEE, P., DAS, P., BHOWAL, A., MAJUMDER, S. K. & GHOSH, P. 2020. Removal of aqueous carbamazepine using graphene oxide nanoplatelets: process modelling and optimization. *Sustainable Environment Research,* 30**,** 1-12.

BINDHU, M., UMADEVI, M., ESMAIL, G. A., AL-DHABI, N. A. & ARASU, M. V. 2020. Green synthesis and characterization of silver nanoparticles from Moringa oleifera flower and assessment of antimicrobial and sensing properties. *Journal of Photochemistry and Photobiology B: Biology,* 205**,** 111836.

BIRNIWA, A. H., ALI, U., KUTTY, S. R. M., JAGABA, A. H. & NOOR, A. 2023. Innovative and eco-friendly technologies for the upgradation of pharmaceutical wastewater treatment processes. *The Treatment of Pharmaceutical Wastewater.* Elsevier.

CHAKRABORTY, P., SINGH, S. D., GORAI, I., SINGH, D., RAHMAN, W.-U. & HALDER, G. 2020. Explication of physically and chemically treated date stone biochar for sorptive remotion of ibuprofen from aqueous solution. *Journal of Water Process Engineering,* 33**,** 101022.

CHIARELLO, M., ANFOSSI, L., CAVALERA, S., DI NARDO, F., SERRA, T. & BAGGIANI, C. 2021. NanoMIP-based solid phase extraction of fluoroquinolones from human urine: a proof-of-concept study. *Separations,* 8**,** 226.

DAVID, L. & MOLDOVAN, B. 2020. Green synthesis of biogenic silver nanoparticles for efficient catalytic removal of harmful organic dyes. *Nanomaterials,* 10**,** 202.

ESPINOZA-TORRES, S., LÓPEZ, R., SOTOMAYOR, M. D., TUESTA, J. C., PICASSO, G. & KHAN, S. 2023. Synthesis, Characterization, and Evaluation of a Novel Molecularly Imprinted Polymer (MIP) for Selective Quantification of Curcumin in Real Food Sample by UV-Vis Spectrophotometry. *Polymers,* 15**,** 3332.

EZEUKO, A. S., OJEMAYE, M. O., OKOH, O. O. & OKOH, A. I. 2022. The effectiveness of silver nanoparticles as a clean-up material for water polluted with bacteria DNA conveying antibiotics resistance genes: Effect of different molar concentrations and competing ions. *OpenNano***,** 100060.

GABR, S. S., MUBARAK, M. F., KESHAWY, M., EL SAYED, I. E. T. & ABDEL MOGHNY, T. 2023. Linear and nonlinear regression analysis of phenol and P-

nitrophenol adsorption on a hybrid nanocarbon of ACTF: kinetics, isotherm, and thermodynamic modeling. *Applied Water Science,* 13**,** 230.

GERAVI, H. A. & GHAEMY, M. 2024. Preparation of molecularly imprinted polymer nanoparticles for selective adsorption of caffeine using dual-functionalized Ag2S quantum dots. *Colloids and Surfaces A: Physicochemical and Engineering Aspects,* 680**,** 132735.

GKIKA, D. A., TOLKOU, A. K., LAMBROPOULOU, D. A., BIKIARIS, D. N., KOKKINOS, P., KALAVROUZIOTIS, I. K. & KYZAS, G. Z. 2024. Application of molecularly imprinted polymers (MIPs) as environmental separation tools. *RSC Applied Polymers*.

HAMAD, M. T. M. H. & EL-SESY, M. E. 2023. Adsorptive removal of levofloxacin and antibiotic resistance genes from hospital wastewater by nano-zero-valent iron and nano-copper using kinetic studies and response surface methodology. *Bioresources and Bioprocessing,* 10**,** 1.

HARO, N. K., DÁVILA, I. V. J., NUNES, K. G. P., DE FRANCO, M. A. E., MARCILIO, N. R. & FÉRIS, L. A. 2021. Kinetic, equilibrium and thermodynamic studies of the adsorption of paracetamol in activated carbon in batch model and fixed-bed column. *Applied Water Science,* 11**,** 1-9.

HEIDARI, G., AFRUZI, F. H. & ZARE, E. N. 2023. Molecularly imprinted magnetic nanocomposite based on carboxymethyl dextrin for removal of ciprofloxacin antibiotic from contaminated water. *Nanomaterials,* 13**,** 489.

HLENGWA, N. & MAHLAMBI, P. 2020. SPE-LC-PDA method development and application for the analysis of selected pharmaceuticals in river and wastewater samples from South Africa. *Water SA,* 46**,** 514-522.

JAIN, N., JAIN, P., RAJPUT, D. & PATIL, U. K. 2021. Green synthesized plant-based silver nanoparticles: Therapeutic prospective for anticancer and antiviral activity. *Micro and Nano Systems Letters,* 9**,** 5.

JIANG, G.-Y., LIU, L., WAN, Y.-Q., LI, J.-K. & PI, F.-W. 2023. Surface-enhanced Raman scattering based determination on sulfamethazine using molecularly imprinted polymers decorated with silver nanoparticles. *Microchimica Acta,* 190**,** 169.

KEBEDE, T., SEROTO, M., CHOKWE, R., DUBE, S. & NINDI, M. 2020. Adsorption of antiretroviral (ARVs) and related drugs from environmental wastewaters using nanofibers. *Journal of Environmental Chemical Engineering,* 8**,** 104049.

KHANE, Y., BENOUIS, K., ALBUKHATY, S., SULAIMAN, G. M., ABOMUGHAID, M. M., AL ALI, A., AOUF, D., FENNICHE, F., KHANE, S. & CHAIBI, W. 2022. Green synthesis of silver nanoparticles using aqueous Citrus limon zest extract: Characterization and evaluation of their antioxidant and antimicrobial properties. *Nanomaterials,* 12**,** 2013.

KRYUCHKOVA, M., BATASHEVA, S., AKHATOVA, F., BABAEV, V., BUZYUROVA, D., VIKULINA, A., VOLODKIN, D., FAKHRULLIN, R. & ROZHINA, E. 2021. Pharmaceuticals removal by adsorption with montmorillonite nanoclay. *International Journal of Molecular Sciences,* 22**,** 9670.

KUHN, J., AYLAZ, G., SARI, E., MARCO, M., YIU, H. H. & DUMAN, M. 2020. Selective binding of antibiotics using magnetic molecular imprint polymer (MMIP) networks prepared from vinyl-functionalized magnetic nanoparticles. *Journal of hazardous materials,* 387**,** 121709.

LIU, P., LIU, R., GUAN, G., JIANG, C., WANG, S. & ZHANG, Z. 2011. Surface-enhanced Raman scattering sensor for theophylline determination by molecular imprinting on silver nanoparticles. *Analyst,* 136**,** 4152-4158.

MADIKIZELA, L. M. & CHIMUKA, L. 2016. Determination of ibuprofen, naproxen and diclofenac in aqueous samples using a multi-template molecularly imprinted polymer

as selective adsorbent for solid-phase extraction. *Journal of pharmaceutical and biomedical analysis,* 128**,** 210-215.
MANKAR, J. S., SHARMA, M. D. & KRUPADAM, R. J. 2020. Molecularly imprinted nanoparticles (nanoMIPs): an efficient new adsorbent for removal of arsenic from water. *Journal of Materials Science,* 55**,** 6810-6825.
MELÉNDEZ-MARMOLEJO, J., DÍAZ DE LEÓN-MARTÍNEZ, L., GALVÁN-ROMERO, V., VILLARREAL-LUCIO, S., OCAMPO-PÉREZ, R., MEDELLÍN-CASTILLO, N. A., PADILLA-ORTEGA, E., RODRÍGUEZ-TORRES, I. & FLORES-RAMÍREZ, R. 2022. Design and application of molecularly imprinted polymers for adsorption and environmental assessment of anti-inflammatory drugs in wastewater samples. *Environmental Science and Pollution Research,* 29**,** 45885-45902.
MOODLEY, J. S., KRISHNA, S. B. N., PILLAY, K., SERSHEN, F. & GOVENDER, P. 2018. Green synthesis of silver nanoparticles from Moringa oleifera leaf extracts and its antimicrobial potential. *Advances in Natural Sciences: Nanoscience and Nanotechnology,* 9**,** 015011.
MORADI, A., KHAMFOROUSH, M., RAHMANI, F. & AJAMEIN, H. 2023. Synthesis of 0D/1D electrospun titania nanofibers incorporating CuO nanoparticles for tetracycline photodegradation and modeling and optimization of the removal process. *Materials Science and Engineering: B,* 297**,** 116711.
NAKHAEITAZREJI, S., HADI, N., TAGHIZADEH, S.-M., MORADI, N., KAKIAN, F., HASHEMIZADEH, Z., BERENJIAN, A. & EBRAHIMINEZHAD, A. 2023. Green Synthesized Iron-Coated Silver Nanoparticles: Economic Bimetallic Nanoparticles Potential Against Methicillin-Resistance Staphylococcus aureus. *Molecular Biotechnology***,** 1-11.
NASRAOUI, C., JAOUED-GRAYAA, N., VANOYE, L., CHEVALIER, Y. & HBAIEB, S. 2022. Development of molecularly imprinted polymer for the selective recognition of the weakly interacting fenamiphos molecule. *European Polymer Journal,* 177**,** 111441.
NATARAJAN, R., BANERJEE, K., KUMAR, P. S., SOMANNA, T., TANNANI, D., ARVIND, V., RAJ, R. I., VO, D.-V. N., SAIKIA, K. & VAIDYANATHAN, V. K. 2021. Performance study on adsorptive removal of acetaminophen from wastewater using silica microspheres: Kinetic and isotherm studies. *Chemosphere,* 272**,** 129896.
NGQWALA, N. P. & MUCHESA, P. 2020. Occurrence of pharmaceuticals in aquatic environments: A review and potential impacts in South Africa. *South African Journal of Science,* 116**,** 1-7.
NURHAYATI, T. & ROYANI, I. Synthesis and characterization of MAA-based molecularly-imprinted polymer (MIP) with D-glucose template. Journal of Physics: Conference Series, 2016. IOP Publishing, 012143.
OKAIYETO, K., HOPPE, H. & OKOH, A. I. 2021. Plant-based synthesis of silver nanoparticles using aqueous leaf extract of Salvia officinalis: characterization and its antiplasmodial activity. *Journal of Cluster Science,* 32**,** 101-109.
PARANJAPE, P. & SADGIR, P. 2023. Linear and nonlinear regression methods for isotherm and kinetic modelling of iron ions bioadsorption using Ocimum sanctum Linn. leaves from aqueous solution. *Water Practice & Technology,* 18**,** 1807-1827.
QIU, B., SHAO, Q., SHI, J., YANG, C. & CHU, H. 2022. Application of biochar for the adsorption of organic pollutants from wastewater: Modification strategies, mechanisms and challenges. *Separation and Purification Technology***,** 121925.
RATAN, Z. A., HAIDERE, M. F., NURUNNABI, M., SHAHRIAR, S. M., AHAMMAD, A. S., SHIM, Y. Y., REANEY, M. J. & CHO, J. Y. 2020. Green chemistry synthesis of silver nanoparticles and their potential anticancer effects. *Cancers,* 12**,** 855.

RAVI, S., CHOI, Y. & CHOE, J. K. 2020. Novel phenyl-phosphate-based porous organic polymers for removal of pharmaceutical contaminants in water. *Chemical Engineering Journal,* 379**,** 122290.

ROLAND, R. M., BHAWANI, S. A. & IBRAHIM, M. N. M. 2023. Synthesis of molecularly imprinted polymer by precipitation polymerization for the removal of ametryn. *BMC chemistry,* 17**,** 165.

S'BUSISO, M. N., MAHLAMBI, P. N. & CHIMUKA, L. 2022. Synthesis, characterisation and optimisation of bulk molecularly imprinted polymers from nonsteroidal anti-inflammatory drugs. *South African Journal of Chemistry,* 76**,** 56–64-56–64.

SADIA, M., AHMAD, I., UL-SALEHEEN, Z., ZUBAIR, M., ZAHOOR, M., ULLAH, R., BARI, A. & ZEKKER, I. 2023. Synthesis and Characterization of MIPs for Selective Removal of Textile Dye Acid Black-234 from Wastewater Sample. *Molecules,* 28**,** 1555.

SAHANI, S., HANSA, SHARMA, Y. C. & KIM, T. Y. 2022. Emerging contaminants in wastewater and surface water. *New Trends in Emerging Environmental Contaminants***,** 9-30.

SAMAL, K., MAHAPATRA, S. & ALI, M. H. 2022. Pharmaceutical wastewater as Emerging Contaminants (EC): Treatment technologies, impact on environment and human health. *Energy Nexus***,** 100076.

SEKULIC, M. T., BOSKOVIC, N., MILANOVIC, M., LETIC, N. G., GLIGORIC, E. & PAP, S. 2019. An insight into the adsorption of three emerging pharmaceutical contaminants on multifunctional carbonous adsorbent: Mechanisms, modelling and metal coadsorption. *Journal of Molecular Liquids,* 284**,** 372-382.

SHALABY, E. A., SHANAB, S. M., EL-RAHEEM, W. M. A. & HANAFY, E. A. 2022. Biological activities and antioxidant potential of different biosynthesized nanoparticles of Moringa oleifera. *Scientific reports,* 12**,** 18400.

SHENDE, S., JOSHI, K., KULKARNI, A., CHAROLKAR, C., SHINDE, V., PARIHAR, V., KITTURE, R., BANERJEE, K., KAMBLE, N. & BELLARE, J. 2018. Platanus orientalis leaf mediated rapid synthesis of catalytic gold and silver nanoparticles. *J Nanomed Nanotechnol,* 9**,** 494.

SHOW, S., KARMAKAR, B. & HALDER, G. 2020. Sorptive uptake of anti-inflammatory drug ibuprofen by waste biomass–derived biochar: experimental and statistical analysis. *Biomass Conversion and Biorefinery***,** 1-19.

SONI, V., RAIZADA, P., SINGH, P., CUONG, H. N., RANGABHASHIYAM, S., SAINI, A., SAINI, R. V., VAN LE, Q., NADDA, A. K. & LE, T.-T. 2021. Sustainable and green trends in using plant extracts for the synthesis of biogenic metal nanoparticles toward environmental and pharmaceutical advances: A review. *Environmental Research,* 202**,** 111622.

SPILAREWICZ-STANEK, K., KISIELEWSKA, A., GINTER, J., BAŁUSZYŃSKA, K. & PIWOŃSKI, I. 2016. Elucidation of the function of oxygen moieties on graphene oxide and reduced graphene oxide in the nucleation and growth of silver nanoparticles. *RSC advances,* 6**,** 60056-60067.

THACH, U. D., NGUYEN THI, H. H., PHAM, T. D., MAI, H. D. & NHU-TRANG, T.-T. 2021. Synergetic effect of dual functional monomers in molecularly imprinted polymer preparation for selective solid phase extraction of ciprofloxacin. *Polymers,* 13**,** 2788.

VARELA, C. F., MORENO-ALDANA, L. & AGÁMEZ-PERTUZ, Y. Y. 2024. Adsorption of pharmaceutical pollutants on ZnCl2-activated biochar from corn cob: Efficiency, selectivity and mechanism. *Journal of Bioresources and Bioproducts,* 9**,** 58-73.

WAHAB, S., KHAN, T., ADIL, M. & KHAN, A. 2021. Mechanistic aspects of plant-based silver nanoparticles against multi-drug resistant bacteria. *Heliyon,* 7.

WALENG, N. J. & NOMNGONGO, P. N. 2022. Occurrence of pharmaceuticals in the environmental waters: African and Asian perspectives. *Environmental Chemistry and Ecotoxicology,* 4**,** 50-66.

WANG, L., YU, J., WANG, X., LI, J. & CHEN, L. 2023. Molecular imprinting-based nanocomposite adsorbents for typical pollutants removal. *Journal of Hazardous Materials Letters,* 4**,** 100073.

YING, S., GUAN, Z., OFOEGBU, P. C., CLUBB, P., RICO, C., HE, F. & HONG, J. 2022. Green synthesis of nanoparticles: Current developments and limitations. *Environmental Technology & Innovation,* 26**,** 102336.

ZHANG, Y., WANG, Q., ZHAO, X., MA, Y., ZHANG, H. & PAN, G. 2023. Molecularly imprinted nanomaterials with stimuli responsiveness for applications in biomedicine. *Molecules,* 28**,** 918.

ZHAO, C., LI, J. & ZUO, Z. 2023. Molecularly imprinted polymers with ionic liquid as the functional monomer for selective solid-phase extraction of gastrodin.

ZULKIFLI, N. I., MUHAMAD, M., MOHAMAD ZAIN, N. N., TAN, W.-N., YAHAYA, N., BUSTAMI, Y., ABDUL AZIZ, A. & NIK MOHAMED KAMAL, N. N. S. 2020. A bottom-up synthesis approach to silver nanoparticles induces anti-proliferative and apoptotic activities against MCF-7, MCF-7/TAMR-1 and MCF-10A human breast cell lines. *Molecules,* 25**,** 4332.

Chapter 6

6.1 Conclusion

In industry, effluents rarely contain a single component; hence adsorption systems design must be based on multi-component removal, making multi-component adsorption data a necessity. This study revealed for the first time the potential of a multi-template MIPs synthesized by bulk polymerization for the selective removal of sulfamethoxazole, nevirapine and ibuprofen simultaneously from wastewater. According to the results of the optimization of parameters affecting adsorption efficiency, it was observed that the synthesized MIP can simultaneously adsorb sulfamethoxazole, ibuprofen and nevirapine selectively. This indicates the potential application of the MIP for selective removal of pharmaceuticals in water or wastewater treatment. Additionally, kinetic studies and adsorption isotherms showed that the adsorption of the chosen pharmaceuticals adsorption onto the MIP cavities followed both a pseudo-second order kinetic model and a Langmuir adsorption isotherm. This demonstrated the homogeneity of the binding surface energies on the MIP, which led to numerous chemisorption interactions. In contrast to adsorbents that are sold commercially and cannot be reused, MIP demonstrated that it can be recycled five times by being cleaned with acetonitrile/acetic acid (9:1 v/v) prior their re-usage. As a result, less solid waste was produced, and the MIP sorbent costs are reduced.

On the other hand, the synthesized AgNPs and MIP showed the capability of adsorbing the selected pharmaceuticals, however, AgNPs are not selective but have high surface area and MIP is highly selective but bulky. Therefore, this work's results showed that the incorporation of AgNPs with MIP enhances the selectivity and reliability of molecular recognition while providing a material that is highly specific and has a high surface area for pharmaceuticals to be adsorbed. Accordingly, nanoMIPs were synthesized for the selective removal of three classes of pharmaceuticals from wastewater samples. These include antibiotics (sulfamethoxazole), antiretrovirals (nevirapine) and non-steroidal anti-inflammatory drugs (ibuprofen).

In this study starch, macadamia nut shells, platanus acerifolia and moringa oleifera were selected as stabilizing and reducing agents for the synthesis of silver nanoparticles. This was due to their including accessibility, ease of use, environmental friendliness and affinity for target analytes. These silver nanoparticles were then each incorporated with MIP for the

enhancement of adsorption capability. It was observed from the result that the nanoMIPs had much better adsorption performance for the targeted pharmaceuticals than MIP and AgNPs alone. Consequently, this was in line with the enhanced adsorption caused by larger surface and porosity of the nanoMIPs. In comparison of starch and macadamia nanoMIPs, it was observed that the adsorption of the chosen pharmaceuticals onto the St/MCD-nanoMIP cavities followed a linear pseudo-second order adsorption model and a non-linear Freundlich adsorption isotherm, according to kinetics and isotherms studies. This demonstrated that the binding surface energies on the St/MCD-nanoMIP were heterogeneous, leading to a variety of chemisorption interactions. The adsorption isotherms fitted on the linear Langmuir model and the kinetics model fitted on the linear pseudo-second order for the MO/PL-nanoMIPs. Moreover, adsorbent regeneration is required to remove the pharmaceuticals and recover the adsorbent; otherwise, disposing of the adsorbents loaded with pharmaceuticals causes a secondary pollution issue. Hence, the regeneration of St/MCD-nanoMIPs and MO/PL-nanoMIPs was conducted over five consecutive adsorption-regeneration cycles. Accordingly, the adsorption efficiency results over these cycles indicated that the nanoMIPs can be regenerated efficiently without obvious loss of performance, therefore, minimising secondary pollution problem. In addition, the developed analytical method was applied in the analysis of wastewater samples collected from three WWTPs. Even with complex species present in influent and effluent water, the use of nanoMIPs for the removal of sulfamethoxazole, nevirapine, and ibuprofen demonstrated outstanding adsorption affinity. The selected pharmaceuticals were detected in the wastewater samples with nevirapine being the most prominent. The results indicated that St/MCD-nanoMIPs and MO/PL-nanoMIPs were indeed effective adsorbent material for the removal of selected pharmaceuticals in wastewater, However, St-nanoMIP showed high adsorption capacities for the targeted pharmaceuticals compared to the MCD-nanoMIP. Whereas in comparison to MO-nanoMIP and PL-nanoMIP, the PL-nanoMIP had fairly higher adsorption capacities for the targeted pharmaceuticals than MO-nanoMIP. Higher adsorption capacities are due to the large surface area, and porosity of the St-nanoMIP and PL-nanoMIPs. When comparing the studied adsorbents, the PL-nanoMIP exhibited the highest adsorption capacity and well as faster equilibrium time for the targeted pharmaceuticals. This was due to the porous structure, many functional groups structural stability, and high specific surface area of PL-nanoMIP, which makes the targeted pharmaceuticals more readily adsorbed onto its surface. Moreover, Platanus acerifolia has been rarely employed as pollutants nano-adsorbent. Therefore, the application of PL-nanoMIPs may encourage more research in this field. Additionally, the application of PL-nanoMIPs reduces

environmental solid waste discharge by addressing the problem of disposing of unused platanus acerifolia leaves. Henceforth, applying platanus acerifolia as a nano-adsorbents can help accomplish sustainable development goals. Herein, the use of nanoMIPs as an adsorbent to remove pollutants from wastewater shows great potential for cost reduction of water treatment. Moreover, the study was able to demonstrate that pharmaceuticals remained in wastewater samples even after treatment procedures, demonstrating their persistence in wastewater. However, with the proposed effective nanoMIP adsorbent materials, the selected pharmaceuticals were effectively removed from the complex WWTPs matrices. As a result, these adsorbents may be used in wastewater treatment to remove a wide range of pharmaceuticals.

6.2 Recommendations

The findings of this study lead to the following recommendations for further research:

- This work demonstrated a higher level of efficiency in the simultaneous determination of multiclass pharmaceuticals in complex wastewater samples through the use of combination adsorption material (AgNPs and MIP). Consequently, research into using a combination of adsorption materials rather than just one could improve the efficiency of pharmaceuticals detection and removal in WWTPs.
- In order to lessen the impact of pharmaceuticals on aquatic species and the environment, additional regulations and standards pertaining to prescription, consumption, production, and importation of products containing these compounds are needed. The aquatic environment should be the primary focus of in-depth research on river waters that receive treated effluent. In South Africa, there is very little of this kind of information.
- Although the primary focus of this study was wastewater matrices, it is advised to also examine other environmental matrices, such as river water, sediments, tap water, surface waters, and ground waters, in order to comprehend the presence and distribution of these pollutants in the environment. This will confirm this study with regards to the St/MCD-nanoMIPs and MO/PL-nanoMIPs ability and performance in removing pharmaceuticals as well as to determine upscale methods for its application for industrial use.
- To further clarify the applicability of nanoMIPs, investigation of other WWTPs outside of KZN is required.

- Furthermore, there is a need to improve the collaboration between university research laboratories and WWTP laboratories. This would enable laboratories to create model plants that integrate newly developed adsorption material and pretreatment methods in order to evaluate their viability and efficacy without raising costs.

6.3 Supplementary data

6.3.1 Chapter 4

6.3.1.1 List of figures

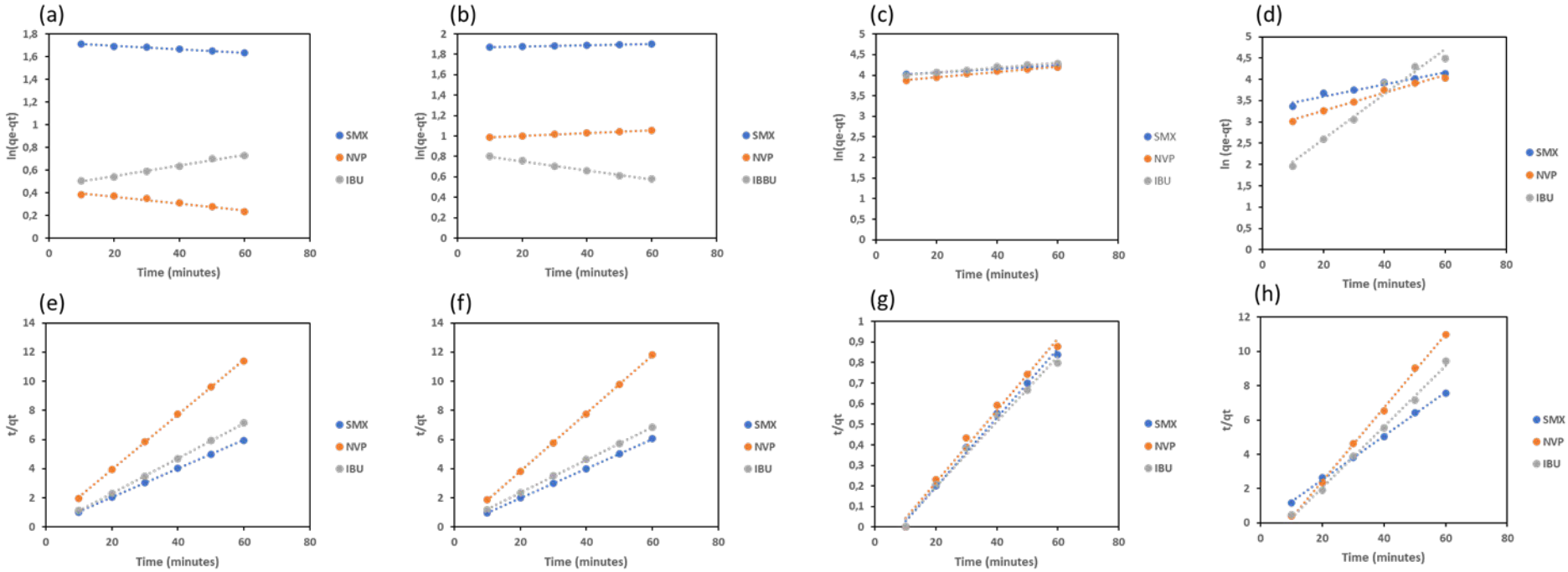

Figure S4.1: Linear pseudo-first order plots for (a)St-AgNPs, (b)MCD-AgNPs, (c)St-nanoMIP, (d)MCD-nanoMIP and linear pseudo-second order for (e)St-AgNPs, (f)MCD-AgNPs, (g)St-nanoMIP, (h)MCD-nanoMIP.

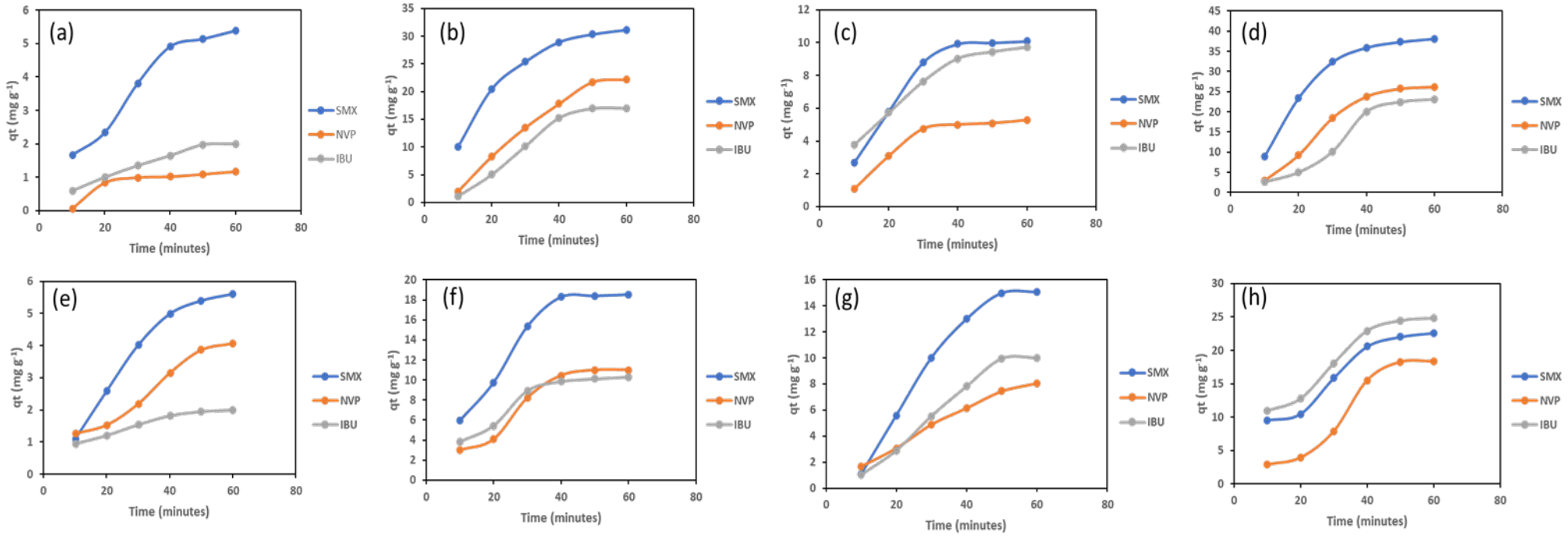

Figure S4.2: Non-linear Pseudo-first-order plots for (a)St-AgNPs, (b)MCD-AgNPs, (c)St-nanoMIP, (d)MCD-nanoMIP and Non-linear pseudo-second-order for (e)St-AgNPs, (f)MCD-AgNPs, (g)St-nanoMIP, (h)MCD-nanoMIP.

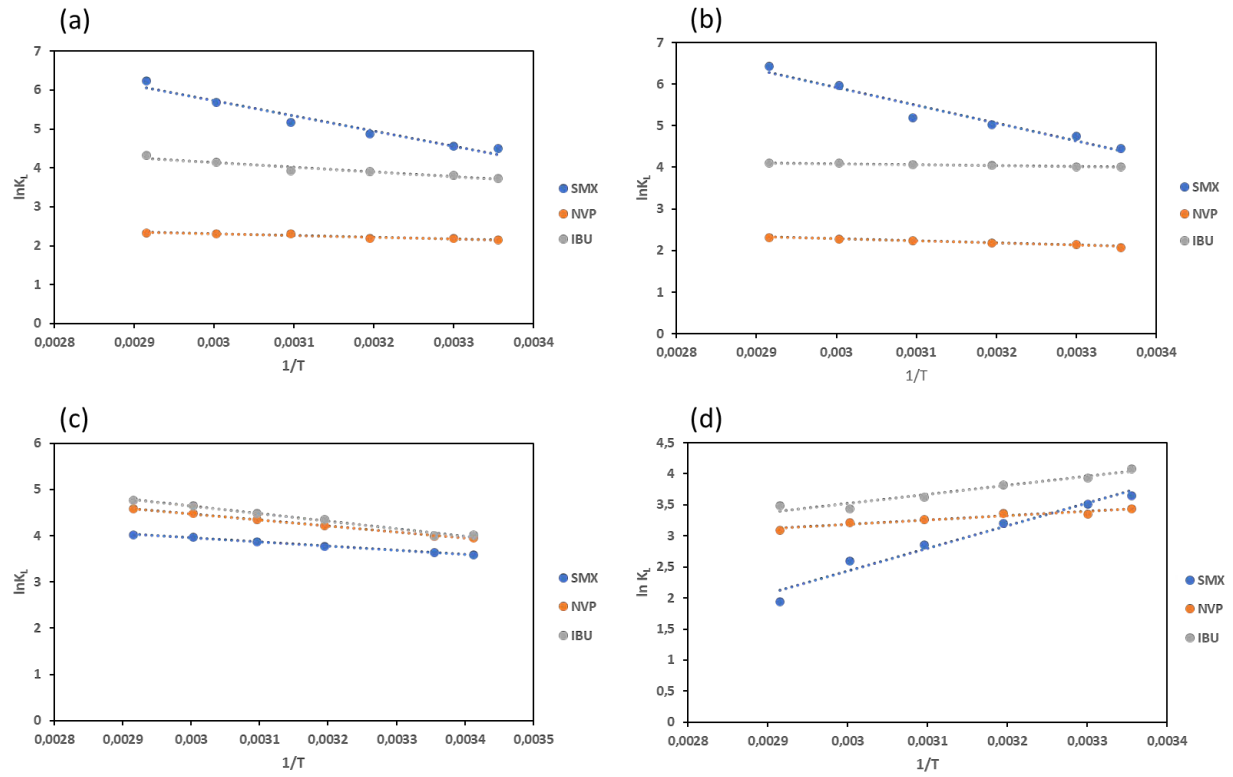

Figure S4.3: Plot of $\ln K_L$ and 1/T for the (a)St-AgNps (b)MCD-AgNps, (c)St-nanoMIP and (d)MCD-nanoMIP.

6.3.1.2 List of Tables

Table S4.1: Physicochemical properties of the selected pharmaceuticals

Pharmaceutical	**Class**	**Chemical structure**	**Molecular weight (g/mol)**	**pKa**	**Log K_{ow}**
Nevirapine	ARVDs	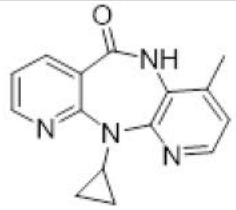	266.30	2.8	3.89
Sulfamethoxazole	Antibiotics	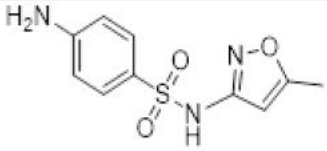	253.28	1.6, 5.6	0.89
Ibuprofen	NSAIDs	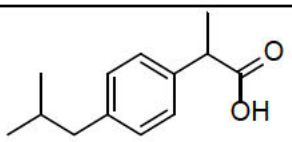	206.29	4.85	3.97
Fenoprofen	NSAIDs	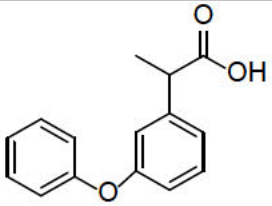	242.27	4.50	3.65

Table S4.2: Analysis of variance (ANOVA) and optimization parameters

Parameters		**St-nanoMIP**				
	Sum of square	**Df**	**Mean square**	**F value**	**F crit**	**P value**
Model	5540	4	1108	98.20	2.71	4×10^{-3}
pH	1985	4	496	56.90	3.84	6.46×10^{-6}
Mass dosage	4490	4	1123	30.83	3.84	6.55×10^{-5}
Concentration	1746	5	349	63.14	3.33	3.08×10^{-8}
Contact time	496	5	99	11.90	3.33	6.63×10^{-4}
Temperature	2423	5	85	9.47	3.33	1.5×10^{-3}
Residual	1803	20	388			
Pure error	2.41	6	11.92			
Total	7343	24				
		MCD-nanoMIP				
Model	1141	4	1228	75.32	2.71	3×10^{-3}
pH	461	4	115	77.36	3.84	1.98×10^{-6}
Mass dosage	801	4	200	44.28	3.84	1.68×10^{-5}

Concentration	707	5	361	121	3.33	1.25×10^{-8}
Contact time	290	5	158	51.12	3.33	8.46×10^{-7}
Temperature	964	5	193	630	3.33	3.7×10^{-12}
Residual	1611	20	450			
Pure error	3.39	6	8.37			
Total	7752	24				

P-value = probability of error,

df = degrees of freedom,

F value= Fischer's exact test

Table S4.3: Parameters contribution percentage

Parameter	**Contribution factor (%)**	
	St-nanoMIP	**MCD-nanoMIP**
pH	35.83	40.40
Mass dosage	81.05	70.20
Concentration	31.52	61.96
Contact time	8.95	24.42
Temperature	43.74	84.49

6.3.2 Chapter 5

6.3.2.1 List of figures

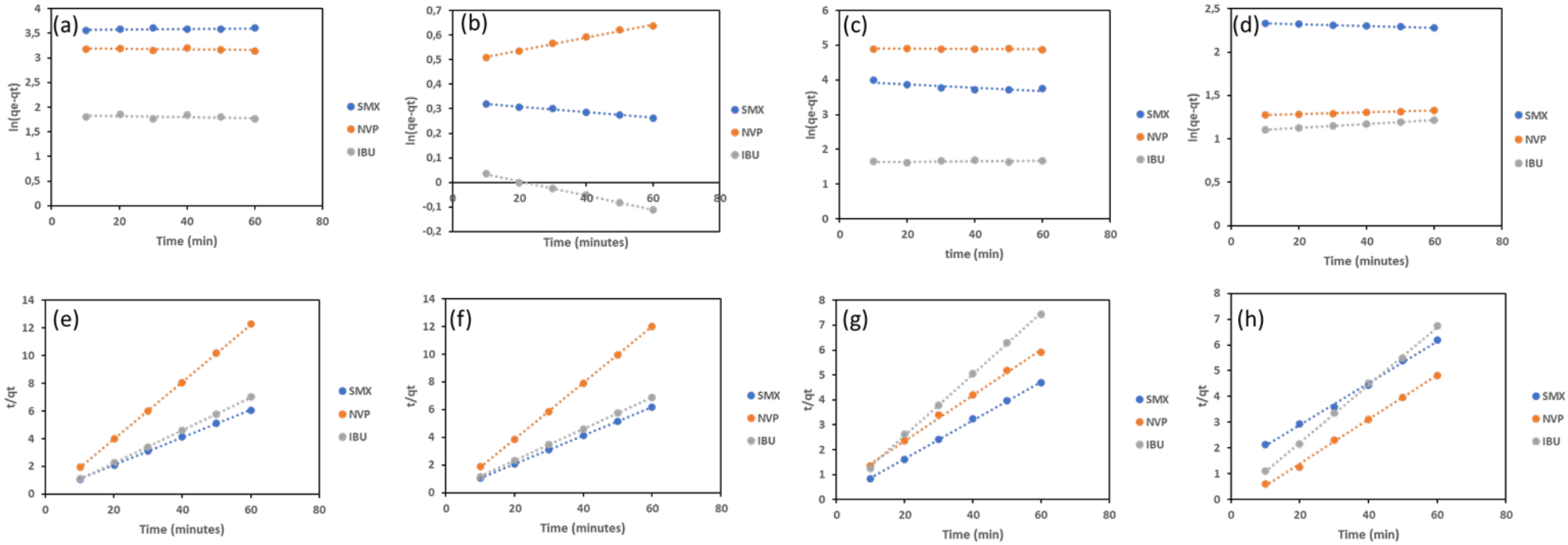

Figure S5.1: Linear Pseudo-first-order plots for (a) MO-AgNPs, (b) PL-AgNPs, (c) MO-nanoMIP, (d) PL-nanoMIP and Linear pseudo-second-order for (e) MO-AgNPs, (f) PL-AgNPs, (g) MO-nanoMIP, (h) PL-nanoMIP

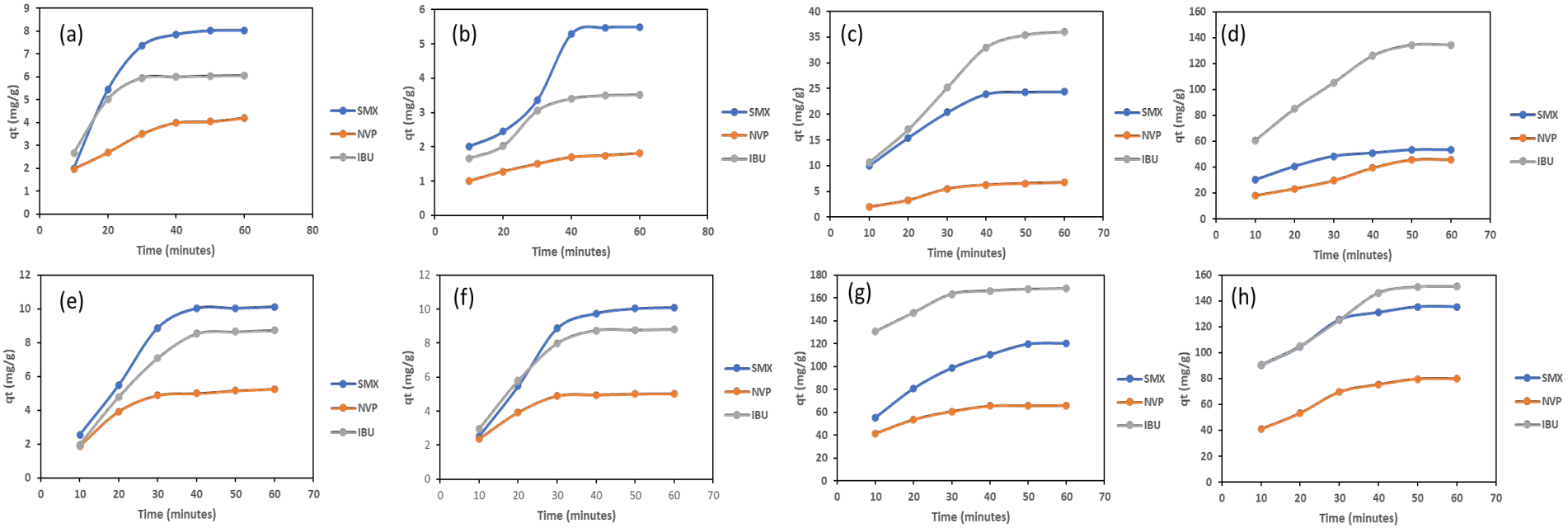

Figure S5.2: Non-linear Pseudo-first-order plots for (a) MO-AgNPs, (b) PL-AgNPs, (c) MO-nanoMIP, (d) PL-nanoMIP and Non-linear pseudo-second-order for (e) MO-AgNPs, (f) PL-AgNPs, (g) MO-nanoMIP, (h) PL-nanoMIP

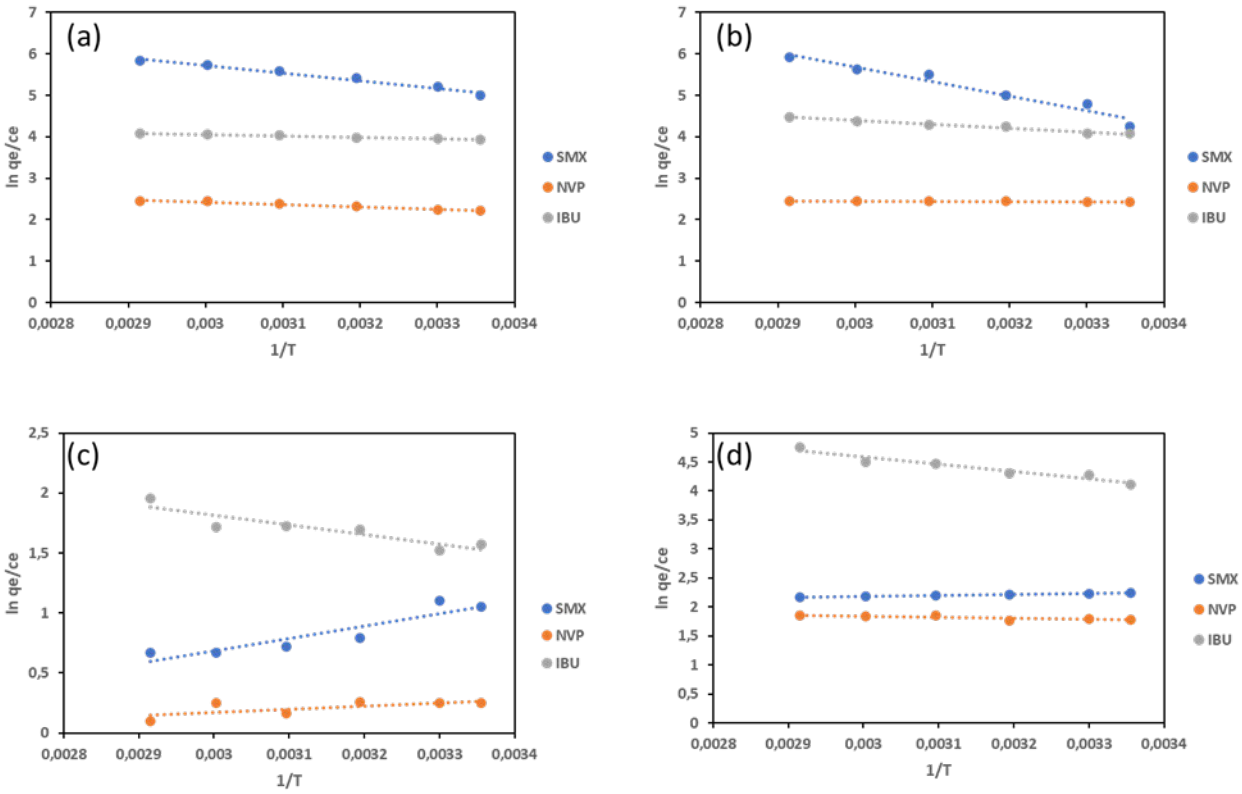

Figure S5.3: Plot of ln qe/ce and 1/T for the (a) MO-AgNPs (b) PL-AgNPs, (c) MO-nanoMIP and (d)PL-nanoMIP.

6.3.2.2 List of Tables

Table S5.1: Physicochemical properties of the selected pharmaceuticals

Pharmaceutical	**Class**	**Chemical structure**	**Molecular weight (g/mol)**	**pKa**	**Log K_{ow}**
Nevirapine	ARVDs	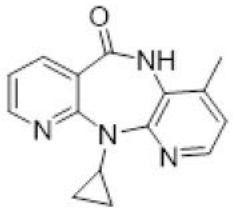	266.30	2.8	3.89
Sulfamethoxazole	Antibiotics	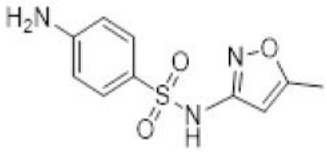	253.28	1.6, 5.6	0.89
Ibuprofen	NSAIDs	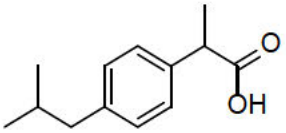	206.29	4.85	3.97
Fenoprofen	NSAIDs	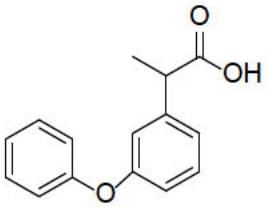	242.27	4.50	3.65

Table S5.2: Analysis of variance (ANOVA) and optimization parameters

Parameters		**MO-nanoMIP**				
	Sum of square	**Df**	**Mean square**	**F value**	**F crit**	**P value**
Model	7029	4	1405.82	3.53	2.71	0.02
pH	358	4	89.57	26.74	3.84	1.11×10^{-4}
Mass dosage	440	4	110.18	17.60	3.84	4.97×10^{-4}
Concentration	2522	5	505.44	102.86	3.33	2.98×10^{-8}
Contact time	1.35	5	0.269	1.19	3.33	0.38
Temperature	171	5	34.21	22.28	3.33	4×10^{-5}
Residual	2556	20	398			
Pure error	2.98	6	17.6			
Total	9585	24				
		PL-nanoMIP				
Model	6884	4	1376.87	3.51	2.71	0.02
pH	435	4	108.52	139.46	3.84	1.98×10^{-7}
Mass dosage	696	4	173.98	35.60	3.84	3.83×10^{-5}

Concentration	530	5	66.65	125.11	3.33	1.11×10^{-8}
Contact time	17.28	5	3.46	4.29	3.33	0.02
Temperature	340	5	68.02	34.37	3.33	5.5×10^{-6}
Residual	2609	20	392			
Pure error	1.76	6	17.40			
Total	9493	24				

P-value = probability of error,

df = degrees of freedom,

F value= Fischer's exact test

Table S5.3: Parameters contribution percentage

Parameter	**Contribution factor (%)**	
	MO-nanoMIP	**PL-nanoMIP**
Ph	5.09	6.31
Mass dosage	6.26	10.11
Concentration	35.88	7.70
Contact time	0.019	0.25
Temperature	2.43	4.94